量子系の時間発展と場の理論

(課題番号 14540280)

2002年度～2005年度 科学研究費補助金 (基盤研究(C)) 研究成果報告書

2006年4月

研究代表者　中里 弘道
(早稲田大学・理工学術院・教授)

はしがき

閉じた微視系を記述する理論として量子論ほど成功した理論はないが，現実には対象微視系もその周囲の多自由度系 (一般には開放系) と常に相互作用しており，実験技術の進展とあいまって，今日ではこのような状況をきちんと考慮することが不可欠となっている．巨視的測定器系と相互作用する量子系のコヒーレンスの消失やエネルギー散逸機構，不安定量子系の指数関数的崩壊現象などはその典型であり，そこでは対象量子系と多 (無限) 自由度系との相互作用の存在が決定的な意味を持っている．本研究の究極的な目的は，多自由度系による対象量子系の散乱現象を場の量子論の枠組み内で可能な限り忠実に記述するとともに，解析に当たって保持されるべき自由度と消去されるべき自由度の峻別とその規準を明らかにして当該の散乱過程のより根本的な理解を目指すこと，さらにはこれらの解析を通して量子論の枠組みの再吟味を行うことにある．4年間の本研究期間においては，量子系の時間発展，特に測定操作が量子系に及ぼす本質的影響に関して，従来の研究成果を格段に発展させることができたと感じている．

測定操作が量子系に及ぼす効果の例としては，いわゆる量子ゼノン効果が古くから知られるが，実験技術の進展に伴なうその実証可能性の高まりにつれ，改めて近年活発に議論されている．これは，量子力学では，測定操作によって系の状態が確率振幅の重ね合わせ状態から測定に対応した状態に移行する (これは，誤解を招きやすい表現ではあるが,「波束の収縮」と呼ばれる) とされること，その一方で，量子系の時間発展はユニタリー的であることに起因している．同じ測定を繰り返すことで対象系の時間発展が遅くなる量子ゼノン効果に関しては多くの理論的，実験的議論がなされている．

本研究ではまず，可解なモデルに基づいた量子系の時間発展の異なる三様式—時間発展初期のガウス型時間発展，続いて現れる指数関数型崩壊形式，長時間領域での冪型崩壊形式—の詳細な解析結果をまとめた．

続いて，測定操作の及ぼす効果のうち，これまで見過ごされてきた別の側面として，全体系の一部にのみ繰り返された測定操作によって，系の残りの部分が，その初期状態とは関係なく，一定の純粋状態へと移行する機構 (状態の「純化」機構) が存在することを明らかにした．近年注目を集めている量子計算や量子情報といった分野では，量子コヒーレンスの存在が決定的重要性を持っており，その維持あるいは回復ということがアイデアを実現させる上で緊急の課題となっている．既に様々な方法が提案されているが，我々が提案した方法は，他の手法では両立することが困難となることの多かった高い信頼性 (fidelity) と有限の収率 (yield) を同時に実現可能としているだけでなく，枠組み自体が簡単で様々な状況に柔軟に適用できるという特徴を備えている．その基本的アイデアは，量子系 A と相互作用しているもう一つの量子系 X を一定の時間間隔で測定し X が特定の状態にあることの確認を繰り返すと，A の状態は，それが最初どのような状態 (一般には混合状態) にあったとしても，ある純粋状態に導かれるというものである．この方法では純化したい系を直接測定するわけではないので，純粋状態として量子絡み合い状態を実現させる枠組みとしても利用することができる．そこでこの枠組みをいくつかの簡単な量子系に適用し，最適な純化が実現できるための条件を明らかにした．具体的には

- 複数の 2 準位系 (qubit) から成る複合量子系では，一つの qubit の状態確認によってこれと相互作用している他の qubit 系が確かにある純粋状態に導かれることを明らかにした．
- 量子絡み合い状態としてよく知られた Bell 状態の抽出が可能であること，さらにその最適条件を明らかにした．
- 空間的に離れた二つの量子系間に絡み合った状態を抽出する方法を提案し，量子ゼノンダイナミクスと組み合わせることでこれまで以上に多様な量子状態がこの枠組みを通して実現可能であることを明らかにした．
- 離れた 2 qubit 間に量子絡み合い状態を抽出するための (測定回数を可能な限り抑制したという意味において) 最適な手続きを提案した．
- 半導体積層量子ドット系を用いて実際の実験室でこの枠組みを実証するための提案を行った．

一方，現実の物理系に以上のような枠組みを適用しようとした際には様々な非理想的状況を考慮する必要に迫られる．その直接的反映が量子コヒーレンスの喪失 (デコヒーレンス) であり，散逸やデコヒーレンスを伴うダイナミクスを取り扱わなければならない．これに関連して本研究ではまず，量子コヒーレンスの回復，維持の方法として提唱されている三つの手法，すなわち，いわゆる量子ゼノン効果，Bang-Bang コントロール，そして連続的相互作用の手法を比較し，これらの手法が良く機能するためには十分頻繁な測定あるいはパルスの照射，あるいは十分強い結合が必要であることを定量的に明らかにした．次に，散逸的ダイナミクスを記述するマスター方程式としてよく用いられる Lindblad 型方程式に対して新たな解法を考案した．この解法では，従来のようにマスター方程式を行列要素間の連立方程式に書き下すことなく，行列 (演算子) の形で解が与えられるため，物理的意味や内容が理解しやすく，応用的な観点からも有用である．実際，この解法を用いて上記の量子状態純化法の散逸的環境下での有効性を検討している．さらに，マスター方程式自体に対しても，これまで見過ごされてきた暗黙の仮定に焦点を当てて再吟味した．

以上が 4 年間の本研究の主な成果である．より詳細な研究成果に関しては，この後に添付する公表済み論文を参照してもらいたい．もちろんこれで当初の目的が完全に達成された訳ではなく，引き続き目標に向かって研究を進展させなければならない．理論物理学の研究においては，その究極的目標を一直線に達成することは余程のことがない限り不可能である．むしろ，紆余曲折の中にこそ新たな研究の萌芽が見出せるのではなかろうか．

最後に，本研究を遂行するに当たって，有形無形のご支援をいただいた方々，ご協力いただいた方々に深くお礼申し上げます．特に，大場一郎 早稲田大学理工学術院教授をはじめとする研究室の皆さんとの議論ならびにご協力，早稲田大学 21 世紀 COE プログラム「多元要素からなる自己組織系の物理」(代表：石渡信一 早稲田大学理工学術院教授) からのご支援に深く感謝いたします．

2006 年 4 月

中里 弘道　(早稲田大学・理工学術院・教授)

研 究 組 織

研究代表者 ：	中里 弘道	(早稲田大学・理工学術院・教授)
研究分担者 ：	湯浅 一哉	(早稲田大学・理工学術院・助手)
(海外研究協力者 ：	Pascazio, Saverio	(イタリア Bari 大学)
(海外研究協力者 ：	Facchi, Paolo	(イタリア Bari 大学)
(海外研究協力者 ：	Messina, Antonino	(イタリア Palermo 大学)
(海外研究協力者 ：	Militello, Danielle	(イタリア Palermo 大学)

交付決定額 (配分額)　　(金額単位：千円)

	直接経費	間接経費	合 計
2002 年度	700	0	700
2003 年度	500	0	500
2004 年度	500	0	500
2005 年度	500	0	500
総 計	2,200	0	2,200

研 究 発 表

学術論文

1) H. Nakazato, T. Takazawa and K. Yuasa, Purification through Zeno–like measurements, Phys. Rev. Lett. **90** No. 6 (2003, February) 060401

2) H. Nakazato, To decay or not to decay? Temporal behavior of a quantum system —Analysis based on a solvable model—, in Fundamental Aspects of Quantum Physics (World Sci. Pub., Singapore) (2003, February) pp.267–283

3) P. Facchi, Y. Nakaguro, H. Nakazato, S. Pascazio, M. Unoki and K. Yuasa, Optimization of a neutron–spin test of the quantum Zeno effect, Phys. Rev. A **68** No. 1 (2003, July) 012107

4) H. Nakazato, K. Yuasa and T. Takazawa, Purification of quantum state through Zeno–like measurements, J. Phys. Soc. Jpn. **72** Suppl. C (2003, November) pp.34–37

5) K. Yuasa, H. Nakazato and M. Unoki, Entanglement purification through Zeno–like measurements, J. Mod. Opt. (Taylor & Francis) **51** No. 6–7 (2004, April) pp.1005–1009

6) H. Nakazato, K. Yuasa and M. Unoki, Preparation and entanglement purification of qubits through Zeno–like measurements, Phys. Rev. A **70** No. 1 (2004, July) 012303 (12 pages)

7) G. Compagno, A. Messina, H. Nakazato, A. Napoli, M. Unoki and K. Yuasa, Distillation of

entanglement between distant systems by repeated measurements on entanglement mediator, Phys. Rev. A **70** No. 5 (2004, November) 052316 (10 pages)

8) P. Facchi, S. Tasaki, S. Pascazio, H. Nakazato, A. Tokuse and D.A. Lidar, Control of decoherence: Analysis and comparison of three different strategies, Phys. Rev. A **71** No. 2 (2005, February) 022302 (22 pages)
9) B. Militello, H. Nakazato and A. Messina, Steering distillation processes through quantum Zeno dynamics, Phys. Rev. A **71** No. 3 (2005, March) 032102 (7 pages)
10) B. Militello, A. Messina and H. Nakazato, Governing survival probability to distill quantum states, Optics and Spectroscopy **99** No. 3 (2005, September) pp.438–442
11) K. Yuasa and H. Nakazato, A simple scheme to entangle distant qubits from a mixed state via an entanglement mediator, Prog. Theor. Phys. **114** No. 3 (2005, September) pp.523–531
12) K. Yoh, K. Yuasa and H. Nakazato, Quantum entanglement formation by repeated spin blockade measurements in a spin field–effect transistor structure embedded with quantum dots, Physica E **29** No. 3-4 (2005, November) pp.674–678

国際会議講演

1) K. Yuasa, Purification of quantum state through Zeno–like measurements, Waseda International Symposium on Fundamental Physics, Tokyo, Japan (2002, November)
2) K. Yuasa, Purification and entanglement through Zeno–like measurements, Gargnano, Italy (2003, September)
3) H. Nakazato, A purification scheme and entanglement distillation, ICQI03WU, Tokyo, Japan (2003, October)
4) H. Nakazato, Purification and entanglement distillations, ICQI03TU, Tokyo, Japan (2003, November)
5) K. Yuasa, Distillation of entanglement between distant systems by repeated measurements on an entanglement mediator, Vietri sul Mare, Italy (2005, March)
6) K. Yuasa, Derivation of master equation in van Hove's limit in the presence of initial correlation with reservoir: Projection method revisited, TQMFA 2005, Palermo, Italy (2005, November)
7) K. Yuasa, Projection operator method for open quantum systems revisited, YITP Workshop, Kyoto, Japan (2005, December)

国際会議ポスター発表

1) K. Yuasa, Distillation of qubits through Zeno–like easurements, Quantum Information and Quantum Control Conference, Toronto, Canada (2004, July)
2) K. Yuasa, Preparation of quantum state through Zeno–like measurements, The Third 21COE Symposium at Waseda University "Astrophysics as Interdisciplinary Science," Tokyo, Japan (2005, September)

共編

1) I. Ohba, Y. Aizawa, T. Daishido, S. Kurihara, K.-I. Maeda, H. Nakazato, S. Tasaki and K. Yuasa, Proceedings of Waseda International Symposium on Fundamental Physics —New Perspectives in Quantum Physics— (The Physical Society of Japan) (2003, November)

研究成果による工業所有権の出願・取得 なし

VOLUME 90, NUMBER 6 PHYSICAL REVIEW LETTERS week ending 14 FEBRUARY 2003

Purification through Zeno-Like Measurements

Hiromichi Nakazato,* Tomoko Takazawa, and Kazuya Yuasa†
Department of Physics, Waseda University, Tokyo 169–8555, Japan
(Received 13 May 2002; published 10 February 2003)

A series of frequent measurements on a quantum system (Zeno-like measurements) is shown to result in the "purification" of another quantum system in interaction with the former. Even though the measurements are performed on the former system, their effect drives the latter into a pure state, irrespectively of its initial (mixed) state, provided certain conditions are satisfied.

DOI: 10.1103/PhysRevLett.90.060401 PACS numbers: 03.65.Xp

It is well known that unstable particles or quantum states display a peculiar behavior at short and long times [1]. Phenomenologically, they are known to decay exponentially and this is well confirmed experimentally [2]. Short-time deviations were observed only very recently [3]. The deviations from the familiar exponential decay law are unavoidable consequences of the quantum dynamics both at short and long times, and the derivation of the exponential decay law itself is not a trivial matter in quantum mechanics. These deviations reflect the unitarity of the time-evolution operator or the time reversal symmetry of the Schrödinger equation at short times and the lower boundedness of the Hamiltonian or the stability of the vacuum at long times. See, e.g., Ref. [1] for a review.

The quantum behavior of unstable states at short times has been one of the central issues of investigation and discussion in recent years, since it is closely connected to the so-called quantum Zeno effect (QZE) [4,5], where the act of measurement [6] (usually represented by the von Neumann projection or the generalized spectral decomposition [7]) affects in an essential way the dynamics of the measured system and results in a hindrance of the decay process. The first attempt at the experimental observation of the QZE in an atomic transition process [8], following Cook's theoretical work [9], has triggered heated discussions on this subject. Furthermore, another exciting experiment has been reported very recently: the observation of the QZE (and also of the inverse QZE [10]) in an atomic tunneling process [11], which is the first experimental observation of the (inverse) QZE in a truly unstable quantum system, unlike in the previous experiment [8] performed on an oscillating system.

In this Letter, we will shed new light on another (and so far not well explored) feature of the quantum dynamics with measurements, closely related to the QZE. Notice first that the system under consideration cannot be considered completely isolated and usually interacts with other systems. Therefore, it would be interesting and maybe more realistic to consider the case where the measurement, represented by a von Neumann projection for simplicity, is *not performed on the total system, but only on the system of interest.* Here, we consider such measurements and address the following point: *How does a series of frequent measurements on a system affect the dynamics of another system in interaction with the former?* Under frequent measurements performed only on the former system, the latter evolves away from its initial state. We shall show that such measurements can result in a purification phenomenon. That is, a series of frequent measurements on system A, represented by projections on a given (usually pure) state of A, makes the state of system B, which interacts with A and is initially in *any* (mixed) state, approach a pure state, if certain conditions prescribed below are satisfied.

Let a total quantum system A + B be described by a Hamiltonian H of the form

$$H = H_{\mathrm{A}} + H_{\mathrm{B}} + H_{\mathrm{int}}, \tag{1}$$

where $H_{\mathrm{A(B)}}$ stands for a free Hamiltonian of system A(B) and H_{int} for an interaction. We prepare system A in its initial (pure) state $|\phi\rangle\langle\phi|$ at time $t = 0$. The initial state of system B, denoted by ρ_{B}, can be arbitrary. The initial state of the total system is

$$\rho_0 = |\phi\rangle\langle\phi| \otimes \rho_{\mathrm{B}} \tag{2}$$

and its dynamics is governed by the Hamiltonian (1) unless it is interrupted by a series of measurements on system A, each of which is represented by a projection operator $\mathcal{O} = |\phi\rangle\langle\phi| \otimes \mathbb{1}$, performed at time intervals τ. Notice that this operator, even if it is a *bona fide* projection operator (we assume that $|\phi\rangle$ is normalized), does not return the time-evolved total system to its initial state. The projection is partial, in the sense that only the state of system A is set back to its initial state and that of system B is not initialized, even though the dynamics of B is certainly affected.

After N such measurements have been done, the survival probability of finding system A still in its initial state is represented by

$$\begin{aligned} P^{(\tau)}(N) &= \mathrm{Tr}[(\mathcal{O}e^{-iH\tau}\mathcal{O})^N \rho_0 (\mathcal{O}e^{iH\tau}\mathcal{O})^N] \\ &= \mathrm{Tr}_{\mathrm{B}}[(V_\phi(\tau))^N \rho_{\mathrm{B}} (V_\phi^\dagger(\tau))^N]. \end{aligned} \tag{3}$$

Notice that the quantity $V_\phi(\tau) \equiv \langle\phi|e^{-iH\tau}|\phi\rangle$ is an operator acting on the Hilbert space of system B. The density operators of the total and B systems read

$$\rho^{(\tau)}(N) = (\mathcal{O}e^{-iH\tau}\mathcal{O})^N \rho_0 (\mathcal{O}e^{iH\tau}\mathcal{O})^N / P^{(\tau)}(N)$$
$$= |\phi\rangle\langle\phi| \otimes \rho_{\mathrm{B}}^{(\tau)}(N), \tag{4a}$$
$$\rho_{\mathrm{B}}^{(\tau)}(N) = (V_\phi(\tau))^N \rho_{\mathrm{B}} (V_\phi^\dagger(\tau))^N / P^{(\tau)}(N), \tag{4b}$$

respectively. We collect only the right outcomes of measurements: this is implicit in the normalization factors in (4). Experimentally, this means that after each measurement, only those events will be retained in which system A has been found in its initial state.

In the ordinary situation, one performs infinitely frequent measurements by taking $N \to \infty$ and $\tau \to 0$, keeping $N\tau = T$, a finite nontrivial value; one easily checks that the ordinary QZE [1] appears in this case and the survival probability $P^{(\tau)}(N)$ increases as N becomes large, approaching unity in the $N \to \infty$ limit [5]. At the same time, the dynamics of system B becomes unitary in this limit, and this is an example of the so-called "quantum Zeno dynamics" [12]. However, we stress that our interest lies in a different situation: we keep the time interval τ between measurements finite and nonvanishing. If N were taken to be ∞, the survival probability $P^{(\tau)}(N)$ would decay out completely for such $\tau \neq 0$, but we are interested in the asymptotic behavior of the state of system B for large but *finite* values of N. We expect that the effect of repeated measurements on system A would modify the dynamics of system B through its interaction with the measured system A, even if B has never been directly measured. To examine this idea, we need to clarify the asymptotic behavior of the state of system B, $\rho_{\mathrm{B}}^{(\tau)}(N)$, for large N.

It is clear that the behavior of $\rho_{\mathrm{B}}^{(\tau)}(N)$ is governed by the operator $V_\phi(\tau)$ in (4). Let us consider its eigenvalue problem. Since this operator is *not Hermitian*, $V_\phi^\dagger(\tau) \neq V_\phi(\tau)$, in general, we need to set up both the right- and left-eigenvalue problems

$$V_\phi(\tau)|u_n) = \lambda_n |u_n), \qquad (v_n|V_\phi(\tau) = \lambda_n (v_n|. \tag{5}$$

The eigenvalue λ_n is in general complex valued. Let us assume that the spectrum of the operator $V_\phi(\tau)$ is discrete and nondegenerate, and its eigenvectors form an orthonormal complete set in the following sense:

$$\sum_n |u_n)(v_n| = \mathbb{1}, \qquad (v_n|u_m) = \delta_{nm}. \tag{6}$$

[It will soon become clear that the assumption of the nondegenerate spectrum is not essential for the following discussion except for that of the largest (in magnitude) eigenvalue $\lambda_{\max}$.] The operator itself is expanded in terms of its eigenvectors

$$V_\phi(\tau) = \sum_n \lambda_n |u_n)(v_n|, \tag{7}$$

and we obtain

$$(V_\phi(\tau))^N = \sum_n \lambda_n^N |u_n)(v_n|. \tag{8}$$

One can show [13] that the absolute value of the eigenvalue λ_n satisfies the inequality $0 \leq |\lambda_n| \leq 1$, $\forall n$, which reflects the unitarity of the time-evolution operator. It is now evident that, in the large N limit, the operator (8) is dominated by a single term

$$(V_\phi(\tau))^N \xrightarrow{\text{large } N} \lambda_{\max}^N |u_{\max})(v_{\max}|, \tag{9}$$

where $|u_{\max})$ and $(v_{\max}|$ are the eigenvectors belonging to $\lambda_{\max}$, provided the largest (in magnitude) eigenvalue $\lambda_{\max}$ is unique, discrete, and nondegenerate.

Thus we reach the conclusion, under the assumption of unique, discrete, and nondegenerate $\lambda_{\max}$, that, in the large N limit with a nonvanishing τ, the state of system B in interaction with system A, on which N measurements are performed at time intervals τ, asymptotically approaches the pure state $|u_{\max})$

$$\rho_{\mathrm{B}}^{(\tau)}(N) \xrightarrow{\text{large } N} |u_{\max})(u_{\max}|/(u_{\max}|u_{\max}), \tag{10}$$

with probability

$$P^{(\tau)}(N) \xrightarrow{\text{large } N} |\lambda_{\max}|^{2N} (u_{\max}|u_{\max})(v_{\max}|\rho_{\mathrm{B}}|v_{\max}). \tag{11}$$

Notice that the final pure state $|u_{\max})$ is independent of the choice of the initial state of system B, i.e., any initial (mixed) state shall be driven to the unique pure state $|u_{\max})$ by repeated measurements performed on the other system A. Since the asymptotic state $|u_{\max})$ is one of the eigenstates of the operator $V_\phi(\tau)$, we have the possibility of adjusting the interaction strength and the measurement interval and of choosing an appropriate initial state $|\phi\rangle$ for system A so that a desired pure state $|u_{\max})$ is realized in system B after a large number of measurements on A [as long as the probability $P^{(\tau)}(N)$ does not become meaninglessly small]. This discloses another feature of the Zeno phenomenon: the action of the quantum Zeno-like measurements dramatically affects the dynamics of system B of interest.

A few comments are in order. First, the existence of a unique, discrete, and nondegenerate $\lambda_{\max}$ of the operator $V_\phi(\tau)$, which has been assumed here, is essential for this purification mechanism. Even though this condition is satisfied for some systems with a discrete spectrum as will be shown in the examples below, some definite mathematical criteria for its validity have yet to be clarified. In particular, it remains open if the present purification mechanism can be applied to systems with continuous spectra. Nevertheless at the same time, it would be worth stressing that not a few discrete quantum systems, including two- or three-level systems which play important roles in the field of quantum information and computation, certainly fall into the category of systems with unique, discrete, and nondegenerate $\lambda_{\max}$.

Second, it is easy to see that the approach to the final pure state $|u_{\max})$ is governed by the ratio between the largest and the second largest (in magnitude) eigenvalues of the operator $V_\phi(\tau)$. It is possible that as the number of degrees of freedom increases, the eigenvalues λ_n distribute more closely to each other, which would make the present purification process less effective. Last, even though the measurements are repeated many times, as in the *bona fide* Zeno case, the present scheme does not explicitly rely on the peculiar quadratic behavior of quantum systems at short times. As far as the essential assumption on the spectrum of the operator $V_\phi(\tau)$ is satisfied, there will be no limit on the time interval τ. Notice that the repetition of one and the same quantum measurement is crucial here.

Let us illustrate the above conclusion in a simple but still nontrivial model. We consider two single-mode harmonic oscillators a and b, in interaction in the rotating-wave approximation. The total Hamiltonian reads

$$H = \Omega a^\dagger a + \omega b^\dagger b + ig(a^\dagger b - ab^\dagger), \tag{12}$$

where the frequencies Ω and ω and the coupling constant g are real parameters. The spectrum is discrete. We prepare system A (oscillator a) in some definite pure state $|\phi\rangle$ (typically a number state $|n_a\rangle$ or a coherent state $|\alpha\rangle$) at time $t = 0$ and let it evolve under the above Hamiltonian. Then the initial state of system A starts to evolve towards other states owing to the coupling to system B (oscillator b), the initial state of which can be arbitrary. The state of oscillator a is projected onto its initial state $|\phi\rangle$ at each measurement, and the interval between measurements τ is taken small, compared with the typical time scales of the system, e.g., $2\pi/\delta$ in (14) below.

The eigenvalue problem (5) of the relevant operator $V_\phi(\tau)$ is solved exactly in this case. Indeed, since the time-evolution operator $e^{-iH\tau}$ can be factorized as

$$e^{-iH\tau} = e^{Aa^\dagger b} e^{Ba^\dagger a} e^{Cb^\dagger b} e^{-Aab^\dagger}, \tag{13}$$

in terms of the τ-dependent functions

$$A = \frac{(g/\delta)\sin\delta\tau}{\cos\delta\tau + i[(\Omega-\omega)/2\delta]\sin\delta\tau}, \tag{14a}$$

$$B = -\frac{i}{2}(\Omega+\omega)\tau - \ln\left[\cos\delta\tau + i\frac{\Omega-\omega}{2\delta}\sin\delta\tau\right], \tag{14b}$$

$$C = -\frac{i}{2}(\Omega+\omega)\tau + \ln\left[\cos\delta\tau + i\frac{\Omega-\omega}{2\delta}\sin\delta\tau\right], \tag{14c}$$

where $\delta = \sqrt{g^2 + (\Omega-\omega)^2/4}$, we easily find the eigenvectors $|u_n)$ and $(v_n|$ of the operator $V_\phi(\tau)$, once the initial state $|\phi\rangle$ of oscillator a is specified.

If we prepare oscillator a in the number state $|n_a\rangle$ at $t = 0$, the relevant operator is calculated to be

$$V_{n_a}(\tau) = \sum_{k=0}^{n_a} \frac{n_a!}{[(n_a-k)!]^2 k!} e^{kB}(-A^2 e^C)^{n_a-k} \times e^{Cb^\dagger b} \prod_{\ell=1}^{n_a-k} (b^\dagger b + \ell), \tag{15}$$

from which we understand that the number states $|n_b)$ of oscillator b constitute the set of eigenvectors of the operator (15). Therefore the state of oscillator b is driven to a number state *irrespectively* of its initial state, when the coupled oscillator a is repeatedly confirmed to be in the number state $|n_a\rangle$. The state of system B is *purified* into a number state.

On the other hand, when oscillator a is prepared in a coherent state $|\alpha\rangle$ and found to be in this state at every τ, the relevant operator is rearranged to be

$$V_\alpha(\tau) = e^{-[1-e^B - A^2/(1-e^{-C})]|\alpha|^2} e^{D(b^\dagger, b)}, \tag{16}$$

where the operator $D(b^\dagger, b)$ is expressed as

$$D(b^\dagger, b) = C\left[b^\dagger + \frac{A\alpha^*}{1-e^{-C}}\right]\left[b - \frac{A\alpha}{1-e^{-C}}\right]. \tag{17}$$

It is easily understood that the state of oscillator b approaches a coherent state $b|\beta) = \beta|\beta)$ with $\beta = A\alpha/(1-e^{-C})$, since this is the right eigenvector of $D(b^\dagger, b)$ belonging to zero eigenvalue and therefore that of $V_\alpha(\tau)$ belonging to the largest (in magnitude) eigenvalue [14]. The state of system B is again *purified* into (another) pure state $|\beta)$.

In Fig. 1, the survival probability $P^{(\tau)}(N)$ and the so-called fidelity

$$F^{(\tau)}(N) = (u_{\max}|\rho_{\rm B}^{(\tau)}(N)|u_{\max})/(u_{\max}|u_{\max}) \tag{18}$$

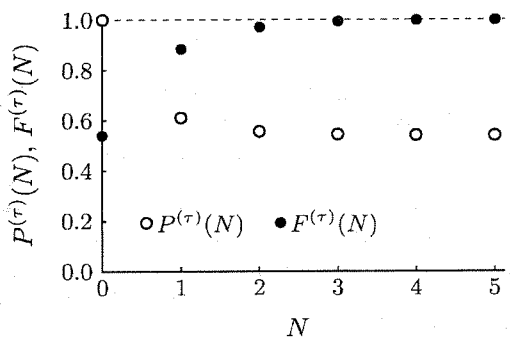

FIG. 1. Probability $P^{(\tau)}(N)$ and fidelity $F^{(\tau)}(N)$ for the model (12) when the initial state of system A, onto which N measurements are performed, is a coherent state $|\alpha\rangle$ and that of system B is $\rho_{\rm B} \propto e^{-\omega b^\dagger b/k_{\rm B}T}$ (thermal, i.e., maximally mixed). The parameters are taken to be $\omega = 1$, $g = 0.2$, $T = 1$, $\alpha = 0.5$, and $\tau = 2\pi/[(\Omega+\omega)/2 + \delta] \simeq 5.24$ in units such that $\hbar = k_{\rm B} = \Omega = 1$. τ is tuned so as to satisfy the condition $|\lambda_{\max}| = 1$ [13], and the ratio of the second largest (in magnitude) eigenvalue to the largest one $\lambda_{\max}$ is $|e^C| = \sqrt{1-(g/\delta)^2\sin^2\delta\tau} \simeq 0.37$ [14].

are shown as functions of the number of measurements N for the case (16) and (17) with a particular choice of parameters. In order to make the purification procedure more effective, it is preferable that (i) the magnitude of the largest eigenvalue of the operator $V_\phi(\tau)$ be close to 1, $|\lambda_{\max}| \simeq 1$, which maintains the probability $P^{(\tau)}(N)$ large enough even for large N [see (11)], and (ii) the other eigenvalues be all small (in magnitude) compared with $|\lambda_{\max}|$, in order to realize a faster approach to the final pure state $|u_{\max}\rangle$. For this purpose, one may adjust the relevant parameters, such as the interval between measurements τ, the strength of the interaction g, and the state $|\alpha\rangle$ onto which system A is projected. The condition $|\lambda_{\max}| \simeq 1$ is satisfied in general if the interval τ is taken to be small enough as in the ordinary Zeno measurements, but one can optimize this procedure and find better values of τ, not necessarily very small [13], that satisfy both conditions (i) and (ii). See Fig. 1 and its caption, where τ is tuned so as to satisfy the conditions (i) and (ii) for the case (16) and (17), and the purification mechanism becomes very effective after only $N = 2$ steps.

The above arguments clearly and explicitly show how the action of repeated measurements (projections) on one system A can affect the dynamics of the other system B in interaction with A. Interestingly enough, even though the effect of the measurement on the latter system B is indirect, its influence is far reaching if the measurement is repeated many times: irrespectively of its initial (mixed) state, the state of system B is *purified* towards a pure state, provided the conditions on the spectrum of $V_\phi(\tau)$ are satisfied. The final state of system B is prescribed by the total Hamiltonian, the pure state (usually taken to be the initial state) onto which system A is projected by the measurement, and the time interval between successive measurements. This opens a new possibility on how to control the state of a quantum system on which we have no direct access. If another system under our control can be coupled to the former system, we would only have to decide which state has to be measured on the controllable system. After such measurements are performed many times at the prescribed time intervals, the desired pure state would be realized with some probability in the system beyond our control.

Purification of quantum states is now considered to be one of the key technologies for quantum information and computation, and is being widely explored [15] (especially in the context of "entanglement purification"). Compared to some other procedures, the idea here is rather simple: one has only to repeat the same measurements. The objects to which the present method is applicable are general and not restricted to "qubits." Furthermore, it is worth emphasizing the versatility of this procedure, i.e., the possibility to adjust the target pure state, the balance between fidelity and probability yield, and so on. These issues would deserve further study, for example, in the context of quantum information and computation.

The authors acknowledge useful and helpful discussions with Professor Ohba, Professor Accardi, and Dr. Imafuku. This work is partly supported by a Grant-in-Aid for Priority Areas Research (B) from the Ministry of Education, Culture, Sports, Science and Technology, Japan (No. 13135221), and by a Waseda University Grant for Special Research Projects (No. 2002A-567).

Note added.—We thank Professor M. B. Plenio for pointing out that a similar idea, which falls into a special case of our general framework, was employed by him and his collaborators [16], though the motivation was different.

*Electronic address: hiromici@waseda.jp
†Electronic address: yuasa@hep.phys.waseda.ac.jp

[1] H. Nakazato, M. Namiki, and S. Pascazio, Int. J. Mod. Phys. B **10**, 247 (1996).
[2] G.-C. Cho, H. Kasari, and Y. Yamaguchi, Prog. Theor. Phys. **90**, 803 (1993); **91**, 1259 (1994).
[3] S. R. Wilkinson *et al.*, Nature (London) **387**, 575 (1997).
[4] A. Beskow and J. Nilsson, Ark. Fys. **34**, 561 (1967); L. A. Khalfin, JETP Lett. **8**, 65 (1968); see also D. Home and M. A. B. Whitaker, Ann. Phys. (N.Y.) **258**, 237 (1997).
[5] B. Misra and E. C. G. Sudarshan, J. Math. Phys. (N.Y.) **18**, 756 (1977).
[6] *Quantum Theory and Measurement*, edited by J. A. Wheeler and W. H. Zurek (Princeton University Press, Princeton, 1993).
[7] S. Pascazio and M. Namiki, Phys. Rev. A **50**, 4582 (1994).
[8] W. M. Itano *et al.*, Phys. Rev. A **41**, 2295 (1990).
[9] R. J. Cook, Phys. Scr. **T21**, 49 (1988).
[10] P. Facchi, H. Nakazato, and S. Pascazio, Phys. Rev. Lett. **86**, 2699 (2001), and references therein.
[11] M. C. Fischer, B. Gutiérrez-Medina, and M. G. Raizen, Phys. Rev. Lett. **87**, 040402 (2001).
[12] P. Facchi *et al.*, Phys. Lett. A **257**, 232 (1999); P. Facchi *et al.*, *ibid.* **275**, 12 (2000); P. Facchi *et al.*, Phys. Rev. A **65**, 012108 (2001); P. Facchi and S. Pascazio, Phys. Rev. Lett. **89**, 080401 (2002). Also see, K. Machida *et al.*, Phys. Rev. A **60**, 3448 (1999).
[13] H. Nakazato, T. Takazawa, and K. Yuasa (to be published).
[14] The eigenvalues of the operator $V_\alpha(\tau)$ in (16) are given by $\lambda_n = e^{-[1-e^B-A^2/(1-e^{-C})]|\alpha|^2} e^{nC}$ $(n = 0, 1, 2, \ldots)$, and $\lambda_{\max} = \lambda_0$ as long as $\mathrm{Re}C \neq 0$.
[15] C. H. Bennett *et al.*, Phys. Rev. Lett. **76**, 722 (1996); **78**, 2031(E) (1997); C. H. Bennett *et al.*, Phys. Rev. A **54**, 3824 (1996); J. I. Cirac, A. K. Ekert, and C. Macchiavello, Phys. Rev. Lett. **82**, 4344 (1999); *The Physics of Quantum Information*, edited by D. Bouwmeester, A. Ekert, and A. Zeilinger (Springer-Verlag, Heidelberg, 2000), and references therein.
[16] M. B. Plenio *et al.*, Phys. Rev. A **59**, 2468 (1999).

TO DECAY OR NOT TO DECAY? TEMPORAL BEHAVIOR OF A QUANTUM SYSTEM —ANALYSIS BASED ON A SOLVABLE MODEL—

H. NAKAZATO

Department of Physics, Waseda University
3-4-1 Okubo, Shinjuku, Tokyo 169-8555, Japan
E-mail: hiromici@waseda.jp

The exact expression of the survival amplitude of a model system, which may describe photodetachment of a negative ion, is derived and analyzed in detail with an attention on its behavior as a function of time. The latter is governed by the location of poles of the amplitude in the complex energy plane. Poles located on the real energy axis can prevent the system from decay (known as plasmon poles), while other poles on the second Riemannian sheet give rise to exponentially decaying terms. The solvability of the model enables us to see explicitly the analytic structure of the amplitude, e.g., the movement of the poles in the complex energy plane as functions of parameters of the model. The behavior both at short and long times is also derived exactly and its peculiarity is pointed out and discussed.

1 Introduction

It is well known that a quantum system, interacting with another quantum system of (infinitely) many degrees of freedom and being supposed to be unstable, generally exhibits three different types of behavior for short, intermediate and long times.[1] The situation would be contrasted with our naive expectation: we naturally expect the familiar exponential decay form for unstable systems. The above behavior is most easily seen in the so-called survival probability, a probability of finding a system in its initial state at later times. Let $|\psi\rangle$ be the initial state of the system and H the total Hamiltonian which includes the interaction between the quantum system and its surrounding large quantum system (usually called environment). Then the survival probability $P(t)$ is nothing but the absolute value squared of the survival amplitude

$$P(t) \equiv \left|\langle\psi|e^{-iHt}|\psi\rangle\right|^2 . \tag{1}$$

The temporal behavior of $P(t)$ is characterized in each of the three different time regions in the following way.

1) "Short" times: If the system of interest is initially prepared not in an eigenstate of the total Hamiltonian, the transition to other states occurs at a rate of order Δt for the amplitude, while the change of probability is of the order of $(\Delta t)^\alpha$. Here the exponent α is shown to be *greater than*

one, which implies that the system does not start to decay exponentially: The survival probability has a *flat derivative* at $t = 0$ and behaves like

$$P(t) \sim 1 + O(t^{\alpha}), \quad \alpha > 1. \tag{2}$$

This is considered to be rooted to the unitary evolution of quantum systems, reflecting the time-reversal symmetry at short times and this peculiar behavior of quantum systems leads to the so-called quantum Zeno effect (QZE)[2] (and sometimes also to the inverse quantum Zeno effect (IQZE)[3,4,5]), which states that repeated inspections of the system whether it is still in the initial state at later times would result in the dramatic changes of its evolution, i.e. hindrance for QZE and acceleration for IQZE of decay.[6]

2) "Intermediate" times: The *exponential decay*, familiar, e.g. for unstable radioactive atoms, is expected to show up at later times and the survival probability decays exponentially

$$P(t) \sim e^{-\Gamma t}, \quad \Gamma > 0. \tag{3}$$

Even though such a deviation from the exponential decay form at short times has never been observed experimentally until very recently,[7] we have to admit its existence: The deviation at short times is due to the finiteness of the energy expectation value in the initial state.[1] Furthermore, even though it would be rather difficult to observe experimentally, a theorem (the Paley–Wiener theorem[8]) strictly prescribes the behavior of the survival probability at very long times.

3) "Long" times: At very long times, the system decays more slowly than exponentially, usually like (*power decay*)

$$P(t) \sim t^{-b}, \quad b > 0, \tag{4}$$

only if the total Hamiltonian is bounded from below.

The temporal behavior of quantum systems stated above is understood in general on the basis of the analyticity of the survival amplitude in the complex energy plane: Possible poles on the second Riemannian sheet contribute to the exponentially decaying terms, while the contour integrals give dominant contributions both at short and long times.[1] It is, however, still not clear, for example, when the exponential decay manifests itself and is overridden by the power decay. Furthermore, it is known that there are cases where a system shows an oscillating behavior, even if it interacts with another system with infinitely many degrees of freedom, which actually prevents it from decay at

$t = \infty$. This behavior is due to a pole appearing on the real energy axis, known as a plasmon.[9]

These issues are surely related to a profound theme in quantum mechanics, that is, the reason why and the condition under which a system is destined to or not to decay. In order to find a clue to this question, a detailed and explicit study of a solvable model would be of great help and give us deeper understanding of the quantum dynamics. In this paper, according to this line of thought, the temporal behavior of a model system, which is sometimes used to describe the photodetachment phenomenon of a negative ion, is considered. The model is introduced and simplified[10,5] for later convenience in the next section, and then in Sec. 3, the survival amplitude is examined analytically and its explicit expression is given in a closed form. The locations of poles are explicitly written down as functions of the parameters in the model, that is, energy detuning, strength and energy scale of interaction in Sec. 4, through which we can see quantitatively a non-trivial and quite intriguing parameter dependence of the survival amplitude. On the basis of the exact expression, the typical behavior at short and long times is extracted and discussed in Sec. 5. Section 6 is devoted to discussions.

2 Model: *photodetachment of a negative ion*

Let us consider a system described by the total Hamiltonian H

$$H = \omega_0 |\psi\rangle\langle\psi| + \int_0^\infty d\omega\, \omega |\omega\rangle\langle\omega| + \Omega a^\dagger a + \int_0^\infty d\omega g(\omega) \left[|\omega\rangle\langle\psi| a + |\psi\rangle\langle\omega| a^\dagger \right]. \tag{5}$$

The Hamiltonian models a photodetachment process where a negative-ion (bound electron) state $|\psi\rangle$ with an energy $\omega_0 < 0$ can be ionized to the continuum (free electron state) $|\omega\rangle$ through the interaction with a single mode laser field a of frequency Ω, in the rotating-wave approximation. The form factor $g(\omega)$ characterizes the strength of the interaction responsible for bound-free transition of the electron. If the total system is initially prepared in the bound electron state with N single-mode photons $|\psi, N\rangle$, the system remains in the Tamm–Duncoff sector spanned by the initial state $|\psi, N\rangle$ and the continuum with $N-1$ photons $|\omega, N-1\rangle$.

As far as its dynamics is concerned, we can confine ourselves to this sector and consider a simpler Hamiltonian,[10,5]

$$H = \Delta |\psi\rangle\langle\psi| + \int_0^\infty d\omega \omega |\omega\rangle\langle\omega| + \int_0^\infty d\omega g(\omega) \left[|\omega\rangle\langle\psi| + |\psi\rangle\langle\omega| \right], \tag{6}$$

by suppressing the photon degrees of freedom. Clearly, parameters here are

properly modified from the original ones:

$$\Delta = \omega_0 + \Omega, \quad \sqrt{N} g(\omega) \to g(\omega). \tag{7}$$

The discrete level $|\psi\rangle$ and continuous ones $|\omega\rangle$ are mutually orthogonal and normalized. Two parameters Δ and $g(\omega)$ represent the energy level of $|\psi\rangle$ relative to the continuum (i.e., the detuning parameter) and the strength of interaction, respectively. Notice that the value of parameter Δ is controlled by the frequency of the laser field and takes both signs.

3 Survival amplitude

We prepare the system in the discrete level $|\psi\rangle$ at time $t = 0$ and let it evolve. The dynamics is governed by the above Hamiltonian (6) and we are interested in the temporal behavior of the system, which can be read off from the behavior of the survival amplitude, an amplitude of the system to be in the initial state,

$$\langle\psi|e^{-iHt}|\psi\rangle \equiv x(t), \qquad (t \geq 0). \tag{8}$$

The standard manipulation[4] yields the following expression of $x(t)$:

$$x(t) = \int_C \frac{dE}{2\pi} \frac{ie^{-iEt}}{E - \Delta - \Sigma(E)}, \tag{9}$$

where the contour C runs from $-\infty$ to ∞, just above the real E-axis. The self-energy part

$$\Sigma(E) \equiv \int_0^\infty d\omega \frac{g^2(\omega)}{E - \omega} \tag{10}$$

usually has a branch point at $E = 0$, a cut and possible poles on the second Riemannian sheet.

It is known that a specific choice of the form factor,[5]

$$g^2(\omega) = \frac{A}{\pi} \frac{\sqrt{\beta\omega}}{\omega + \beta}, \qquad (\omega \geq 0), \tag{11}$$

where positive parameters A and β represent the strength of interaction (proportional to the laser intensity), and the peak position and width of $g^2(\omega)$, respectively, enables us to calculate explicitly the self-energy part, leading to a closed form of the survival amplitude $x(t)$. It is actually an elementary task to integrate (10) to obtain

$$\Sigma(E) = -\frac{iA\sqrt{\beta}}{\sqrt{E} + i\sqrt{\beta}}, \qquad E \equiv |E|e^{i\varphi}, \tag{12}$$

with $\sqrt{E}$ being defined as $\sqrt{|E|}e^{i\varphi/2}$. It is manifest that the self-energy part has a cut from the origin $E = 0$ and we need two Riemannian sheets. There is no logarithmic branch point and no infinite number of sheets is needed either in this case. By inserting the above expression of $\Sigma(E)$ into (9) and changing the integration variable $E \to \zeta = \sqrt{E}$, $x(t)$ is now expressed as

$$x(t) = \int\limits_{C_1+C_2} \frac{\zeta d\zeta}{\pi} \frac{i(\zeta + i\sqrt{\beta})e^{-i\zeta^2 t}}{(\zeta^2 - \Delta)(\zeta + i\sqrt{\beta}) + iA\sqrt{\beta}}. \tag{13}$$

The contour $C_1 + C_2$ is composed of two segments C_1 and C_2: the former (C_1) runs infinitesimally right of the imaginary ζ-axis from $+i\infty$ to 0, while the latter (C_2) just above the positive real ζ-axis from 0 to $+\infty$. These contours C_1 and C_2 are rotated around the origin by angles $\pi/4$ and $-\pi/4$, respectively, to form a straight-line contour C_3: $[-\infty e^{-i\pi/4}, +\infty e^{-i\pi/4}]$. In this way, we arrive at the following expression of $x(t)$,

$$x(t) = -i \int_{-\infty}^{+\infty} \frac{dy}{\pi} \frac{y(y + e^{-i\pi/4}\sqrt{\beta})e^{-y^2 t}}{(y^2 - i\Delta)(y + e^{-i\pi/4}\sqrt{\beta}) + iAe^{-i\pi/4}\sqrt{\beta}} - 2\pi i \,\mathrm{Res}, \tag{14}$$

where the last term represents residues of the integrant in (13) at poles located in the region between the two contours $C_1 + C_2$ and C_3. Notice that this region, subdivided into two regions with $\mathrm{Re}\,\zeta \gtrless 0$, just corresponds, in the original complex E-plane, to the region with $\mathrm{Im}E < 0$, and therefore the last term in (14) represents the exponential decay if it exists, while the first term corresponds to the contour integration along the cut in the complex E-plane. It will be shown later that poles contributing exponential decay only appear in one of the above two regions, i.e. in the region between C_2 and C_3 where $\mathrm{Re}\,\zeta > 0$ and this region does correspond to that on the second Riemannian sheet with $\mathrm{Im}E < 0$.

The evaluation of each term in (14) is not difficult, only if one notices that the denominator of the integrant is the third-order polynomial function. Indeed, if we put

$$\xi = e^{i\pi/4}y, \qquad \text{or} \qquad \xi = -i\zeta, \tag{15}$$

the denominators in (14) and (13) are written respectively as

$$(y^2 - i\Delta)(y + e^{-i\pi/4}\sqrt{\beta}) + iAe^{-i\pi/4}\sqrt{\beta} = e^{-3i\pi/4}f(\xi),$$

and

$$(\zeta^2 - \Delta)(\zeta + i\sqrt{\beta}) + iA\sqrt{\beta} = -if(\xi),$$

with

$$f(\xi) = \xi^3 + \sqrt{\beta}\xi^2 + \Delta\xi + \sqrt{\beta}(\Delta - A). \tag{16}$$

Let the three roots of this function be ξ_0, ξ_1 and ξ_2. They satisfy

$$\xi_0 + \xi_1 + \xi_2 = -\sqrt{\beta}, \qquad \xi_0\xi_1 + \xi_1\xi_2 + \xi_2\xi_0 = \Delta, \qquad \xi_0\xi_1\xi_2 = -\sqrt{\beta}(\Delta - A). \tag{17}$$

It is now an easy exercise to evaluate the first term in (14), which is rewritten in the following form after a simple manipulation:

$$-i \sum_{k=0,1,2} \left[\frac{\xi_k(\xi_k + \sqrt{\beta})}{3\xi_k^2 + 2\sqrt{\beta}\xi_k + \Delta} \int_{-\infty}^{\infty} \frac{dy}{\pi} \frac{e^{-y^2 t}}{y - e^{-i\pi/4}\xi_k} \right]. \tag{18}$$

This type of integration can be performed with the help of the integral formula for the Error function

$$\int_{-\infty}^{\infty} \frac{dy}{\pi} \frac{e^{-y^2 t}}{y - z} = i\epsilon(z_{\mathrm{I}})\mathrm{erfc}(-i\sqrt{t}z\epsilon(z_{\mathrm{I}}))e^{-z^2 t}, \qquad z_{\mathrm{I}} \equiv \mathrm{Im}z. \tag{19}$$

On the other hand, the integrant in (13) is easily rearranged to be

$$\frac{i}{\pi} \sum_{k=0,1,2} \left[\frac{\xi_k(\xi_k + \sqrt{\beta})}{3\xi_k^2 + 2\sqrt{\beta}\xi_k + \Delta} \frac{e^{-i\zeta^2 t}}{\zeta - i\xi_k} \right] \tag{20}$$

and we finally arrive at the analytic expression of the survival amplitude

$$\begin{aligned} x(t) = & \sum_{k=0,1,2} \left[\frac{\xi_k(\xi_k + \sqrt{\beta})}{3\xi_k^2 + 2\sqrt{\beta}\xi_k + \Delta} \epsilon(\mathrm{Im}y_k)\mathrm{erfc}(-i\sqrt{t}y_k\epsilon(\mathrm{Im}y_k))e^{it\xi_k^2} \right] \\ & + 2\mathrm{Res} \sum_k \left[\frac{\xi_k(\xi_k + \sqrt{\beta})}{3\xi_k^2 + 2\sqrt{\beta}\xi_k + \Delta} \frac{e^{-i\zeta^2 t}}{\zeta - i\xi_k} \right], \quad y_k \equiv e^{-i\pi/4}\xi_k, \end{aligned} \tag{21}$$

where, as already stated, the residues are evaluated at those poles located in the region between two contours $\mathrm{C}_1 + \mathrm{C}_2$ and C_3, i.e. at such poles satisfying $0 \leq \mathrm{Arg}(\xi_k) < \pi/4$ or $5\pi/4 < \mathrm{Arg}(\xi_k) \leq 3\pi/2$.

4 Behavior of survival amplitude

In order to clarify the behavior of the survival amplitude, especially the existence or absence of the exponential decay, we have only to investigate the second term in (21), responsible for it. That is, we need to know the three roots ξ_k explicitly. For later convenience, let us introduce c by

$$c \equiv \sqrt{\beta}\left|\Delta - \frac{\beta}{3}\right|^{-\frac{3}{2}} \left(\frac{2\beta}{27} + \frac{2\Delta}{3} - A\right). \tag{22}$$

It is a tedious but elementary task to write down the three roots ξ_k. Notice that when the condition $\Delta > \beta/3$ is satisfied or both conditions $\Delta < \beta/3$ and $|c| > \sqrt{4/27}$ are satisfied, we have one real (ξ_0) and two complex ($\xi_1 = \xi_2^*$) roots conjugate to each other, and otherwise, we have three real roots.

4.1 Dependence on the interaction strength A

Let us first investigate the behavior of the survival amplitude as a function of the strength of interaction A, with the remaining parameters Δ and β being fixed.

Case I: $\Delta > \beta/3$

We have one real root ξ_0 and two complex roots $\xi_1 = \xi_2^*$ in this case and their explicit expressions read (see (22) above)

$$\xi_k \equiv -\frac{\sqrt{\beta}}{3} + \left|\Delta - \frac{\beta}{3}\right|^{\frac{1}{2}} z_k, \qquad (k = 0, 1, 2),$$

$$z_0 = \left[\frac{1}{2}\left(\sqrt{\frac{4}{27} + c^2} - c\right)\right]^{\frac{1}{3}} - \left[\frac{1}{2}\left(\sqrt{\frac{4}{27} + c^2} + c\right)\right]^{\frac{1}{3}},$$

$$z_1 = -\frac{z_0}{2} + i\sqrt{1 + \frac{3}{4}z_0^2} = z_2^*. \tag{23}$$

Observe that (a) when the interaction is weak, i.e. $0 < A < 2\beta/27 + 2\Delta/3$, c is positive and $z_0 < 0$, while for strong interaction $2\beta/27 + 2\Delta/3 < A$, $c < 0$ and $z_0 > 0$ and (b) the complex quantities z_1 and z_2 lie on a hyperbola $y^2 - 3x^2 = 1$.

It is not difficult to find the locations of these poles as functions of A. As A is increased from zero (free case), the real pole ξ_0 shifts right from $-\sqrt{\beta}$ along the real ξ-axis, crosses the origin at $A = \Delta$ and becomes large indefinitely. This pole can contribute only when it appears on the positive real ξ- axis, for it is then included in the area $0 \leq \mathrm{Arg}(\xi_k) < \pi/4$. Remark that this pole is responsible for an oscillating behavior of the survival amplitude and if it appears, the system ceases to decay out completely even for $t \to \infty$. Two poles ξ_1 and ξ_2 locate at $i\sqrt{\Delta}$ and $-i\sqrt{\Delta}$ when $A = 0$, representing free oscillation of state $|\psi\rangle$, and start to move on each leaf of a hyperbola $y^2 - 3(x + \sqrt{\beta}/3)^2 = \Delta - \beta/3 > 0$ toward its center $(-\sqrt{\beta}/3, 0)$ and move away it as A becomes stronger. Since only one of the hyperbola's asymptotic lines $y = \sqrt{3}(x + \sqrt{\beta}/3)$ can have intersections with the boundary of the area $5\pi/4 < \mathrm{Arg}(\xi_k) \leq 3\pi/2$, that is, with the straight line $y = x$, only ξ_2 can contribute to give the residue in (21) when it stays in this area, while ξ_1 has no contribution at all.

Thus we have the following classification of the behavior of the survival amplitude: (i) In the perturbative regime, no matter how small the interaction is, the exponentially decaying pole is always present and the system exhibits exponential decay together with the power behavior arising from cut contribution (the first term in (21)) and dominating the former both at short and long times. (ii) When the interaction becomes strong and $(\beta/3 <)\Delta < \beta/2$ is satisfied (then the hyperbola has intersections with the boundary line $y = x$), this pole suddenly disappears at a critical value of A and reappears for even stronger A, while for the system with $\Delta > \beta/2$, the decaying pole is always present for any value of A. (iii) If the value of A exceeds the threshold Δ, the system never decays completely and the oscillating behavior survives at $t = \infty$. See Fig. 1.

Case II: $0 < \Delta < \beta/3$

In this case, we obtain the following expressions of ξ_k: for weak and strong interaction, where $|c| > \sqrt{4/27}$, one real pole ξ_0 and two complex poles $\xi_1 = \xi_2^*$ exist. That is, for $0 < A < 2\beta/27 + 2\Delta/3 - \sqrt{4/27\beta}\sqrt{\beta/3 - \Delta}^3$ or $2\beta/27 + 2\Delta/3 + \sqrt{4/27\beta}\sqrt{\beta/3 - \Delta}^3 < A$,

$$\xi_k \equiv -\frac{\sqrt{\beta}}{3} + \sqrt{\frac{\beta}{3} - \Delta} z_k, \qquad (k = 0, 1, 2),$$

$$z_0 = \left[\frac{1}{2}\left(\sqrt{c^2 - \frac{4}{27}} - c\right)\right]^{\frac{1}{3}} - \left[\frac{1}{2}\left(\sqrt{c^2 - \frac{4}{27}} + c\right)\right]^{\frac{1}{3}},$$

$$z_1 = -\frac{z_0}{2} + i\sqrt{\frac{3}{4}z_0^2 - 1} = z_2^*. \tag{24}$$

On the other hand, for intermediate cases, $|c|$ is less than $\sqrt{4/27}$ and we have three real roots; for $2\beta/27 + 2\Delta/3 - \sqrt{4/27\beta}\sqrt{\beta/3 - \Delta}^3 < A < 2\beta/27 + 2\Delta/3 + \sqrt{4/27\beta}\sqrt{\beta/3 - \Delta}^3$,

$$\xi_k \equiv -\frac{\sqrt{\beta}}{3} + \sqrt{\frac{\beta}{3} - \Delta} z_k, \qquad (k = 0, 1, 2),$$

$$z_0 = \frac{2}{\sqrt{3}}\cos\left(\frac{\theta}{3} - \pi\right), \quad z_1 = \frac{2}{\sqrt{3}}\cos\left(\frac{\theta}{3} + \frac{\pi}{3}\right), \quad z_2 = \frac{2}{\sqrt{3}}\cos\left(\frac{\theta}{3} - \frac{\pi}{3}\right),$$

$$\theta \equiv \tan^{-1}\left[\frac{1}{c}\sqrt{\frac{4}{27} - c^2}\right]. \tag{25}$$

Notice that if the interaction is sufficiently weak or strong, the two complex poles ξ_1 and ξ_2 lie on a hyperbola $3(x + \sqrt{\beta}/3)^2 - y^2 = \beta/3 - \Delta > 0$.

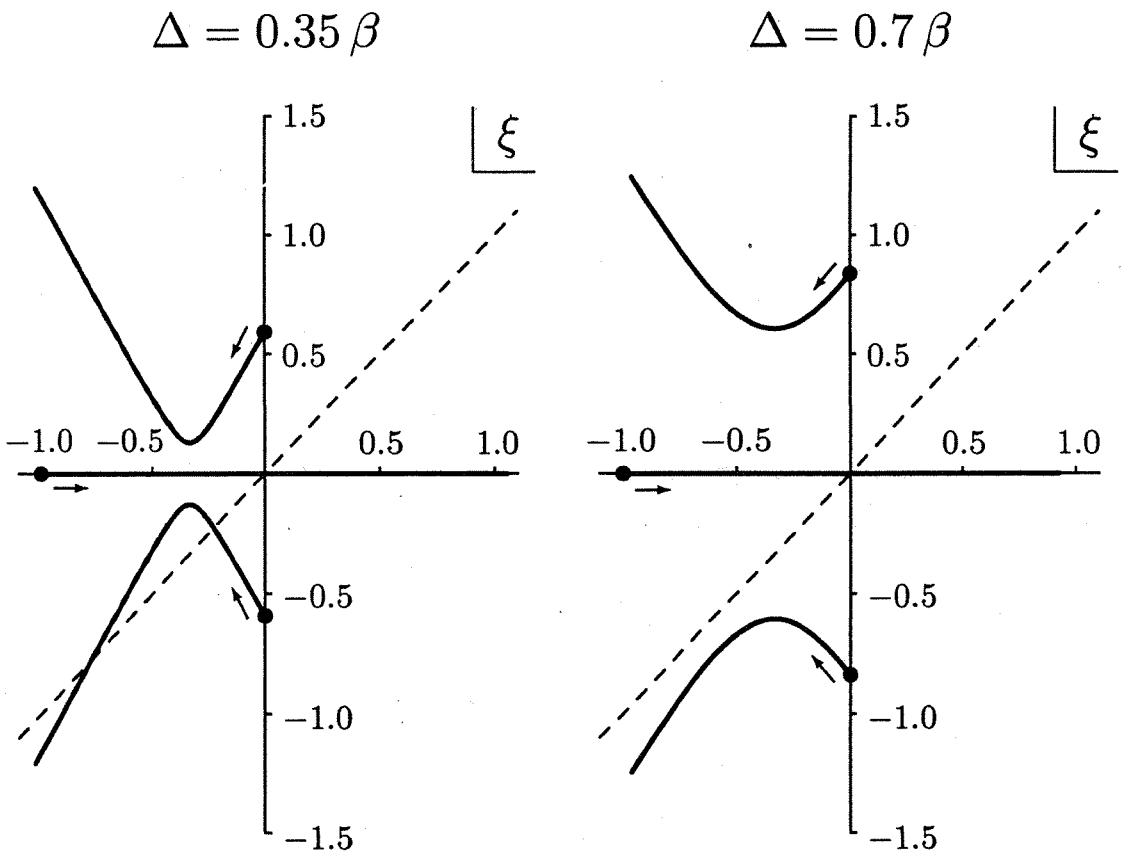

Figure 1. Locations of poles as functions of the coupling constant A, in cases of $\beta/3 < \Delta = 0.35\beta < \beta/2$ (left) and $\beta/2 < \Delta = 0.70\beta$ (right). There are one real pole ξ_0 and two complex poles $\xi_1 = \xi_2^*$. The complex poles lie on each leaf of hyperbola $y^2 - 3(x + \sqrt{\beta}/3)^2 = \Delta - \beta/3$ in the left-half plane $x < 0$. Notice that at $A = 0$ (free case), $\xi_0 = -\sqrt{\beta}$ and $\xi_{1(2)} = +(-)i\sqrt{\Delta}$. As the coupling A is increased, ξ_0 moves right on the real axis to become a plasmon pole when it crosses the origin, which occurs at $A = \Delta$, while the two complex poles $\xi_{1(2)}$ move left on the hyperbola. The poles contribute to $x(t)$ if they locate in the two regions which are both below the line $y = x$ (broken line) and either above the positive x-axis or left of the negative y-axis. When $\beta/3 < \Delta < \beta/2$ is satisfied, there are two critical values of A between which the exponentially decaying term does not exist. If Δ is greater than $\beta/2$, the exponentially decaying term is always present, irrespectively of the value of A. Here the poles ξ_k are measured in units of $\sqrt{\beta}$.

We summarize the behavior of the survival amplitude in this case: (i) In the perturbative regime, the system always exhibits the exponential decay (at intermediate times). (ii) When A exceeds a critical value, it shows no exponential decay and the behavior is governed solely by the cut contribution. (iii) When the interaction reaches and exceeds the threshold $A = \Delta$, an oscillating behavior appears. (iv) If the interaction becomes even stronger, the

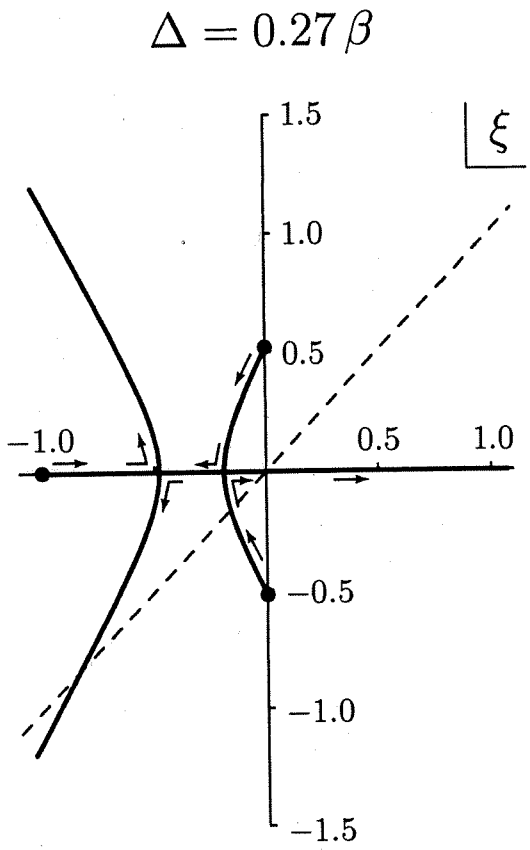

Figure 2. Locations of poles as functions of A, same as in Fig. 1, but in the case of $0 < \Delta = 0.27\beta < \beta/3$. Both for small and large couplings, two complex poles are present on each leaf of the hyperbola $3(x+\sqrt{\beta}/3)^2 - y^2 = \beta/3 - \Delta > 0$, one of which can contribute to give the exponential decay if it lies below $y = x$ (broken line), while at intermediate couplings, they are both real and have no contributions to $x(t)$. The exponentially decaying term appears both at small coupling and at very large coupling. The oscillation pole is present for large coupling, i.e., $A \geq \Delta$.

exponentially decaying term appears again, however, the system's behavior is dominated by the above oscillation and it never decays out. See Fig. 2.

Case III: $\Delta < 0$

Since Δ is negative, there are three real roots existing for small A. For sufficiently large A, c becomes less than $-\sqrt{4/27}$ and only one root remains to be real and two others become complex. Though the actual critical values of A are different depending on whether Δ is bigger or smaller than $-\beta/9$, the expressions of the poles are the same as in (25) for small A and in (24) for A exceeding the critical value, respectively. See Fig. 3.

We can conclude, in this case, that the exponentially decaying term is

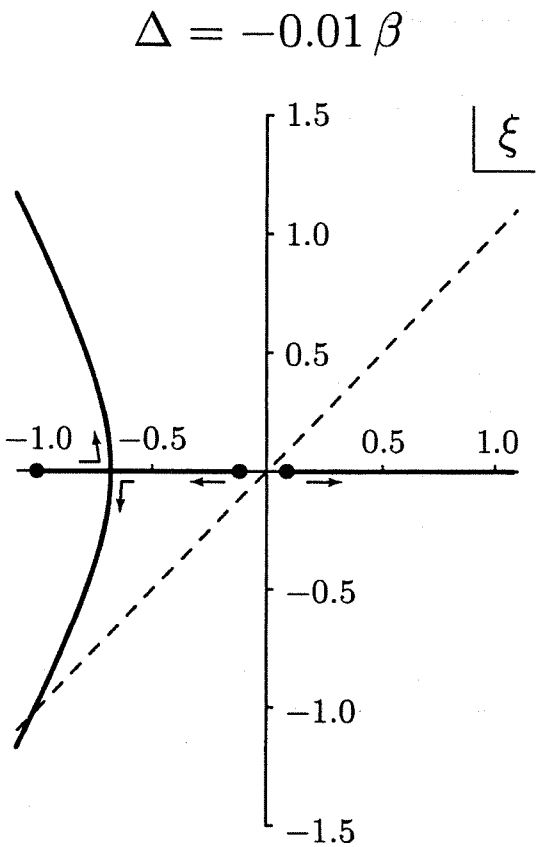

Figure 3. Locations of poles as functions of A, same as in Fig. 1, but in the case of $\Delta = -0.01\beta < 0$. At $A = 0$ (free case), all three poles are real, $\xi_0 = -\sqrt{\beta}$, $\xi_{1(2)} = \pm\sqrt{|\Delta|}$. The hyperbola is the same as in Fig. 2. For a sufficiently large coupling, an exponentially decaying term appears, while an oscillation pole is always present and the system never decays out.

present if the interaction is weak, disappears for stronger interaction and reappears for even stronger interaction, however, an oscillating term is always present and the system never decays completely.

4.2 Dependence on the detuning parameter Δ

So far, we have treated Δ as a given, fixed parameter and examined the behavior of the survival amplitude (actually, the locations of poles) as a function of parameter A, the strength of interaction. Since we can also change the value of Δ by adjusting the frequency of the laser field Ω (see (7)), the locations of the poles ξ_k can be seen as functions of Δ, given the strength of the laser field $A > 0$. It turns out that (i) the complex poles are allowed to exist only for those Δ larger than a critical value and if they exist, they lie on each leaf of a

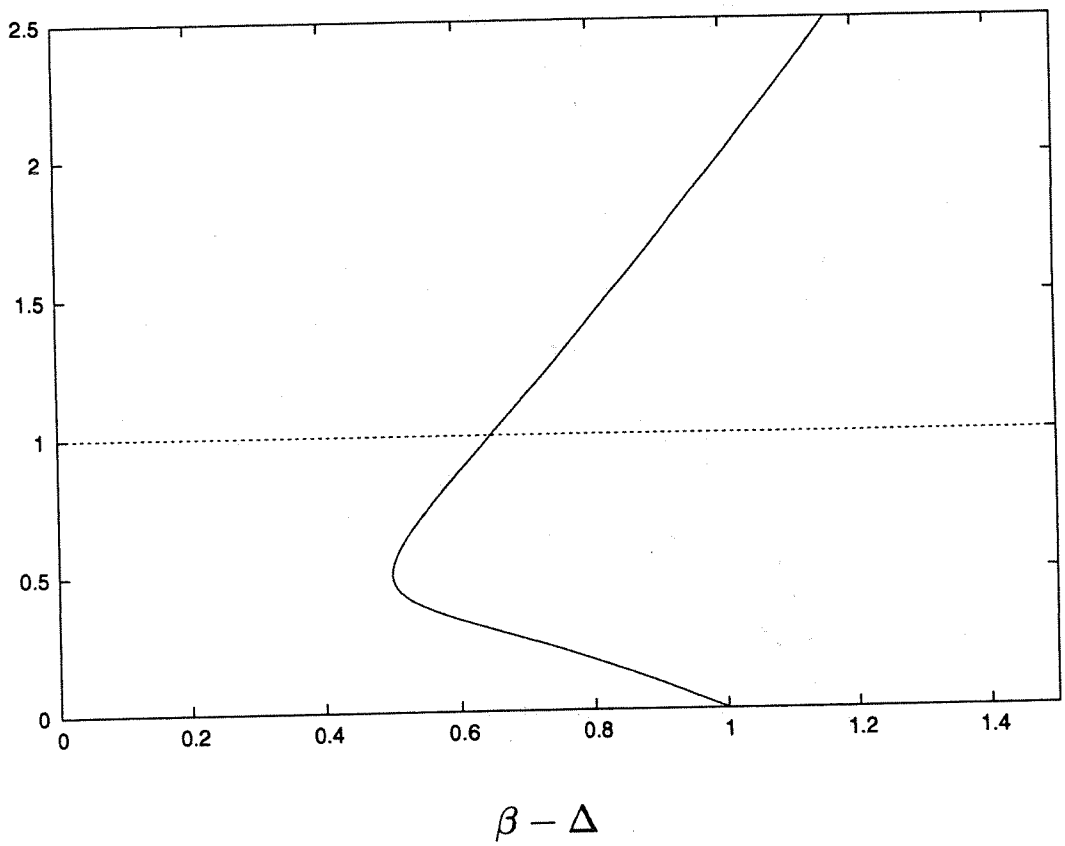

Figure 4. The curve $y = (\beta - \Delta)(1 \pm \sqrt{1 - 2\Delta/\beta})$ as a function of $\beta - \Delta$. The intersection with $y = A$ gives the critical value of Δ below which no exponentially decaying term is present. Both axes are in units of β and the case $A = \beta(= 1)$ is drawn here.

curve $y^2 = -(x + \sqrt{\beta})^2 - \sqrt{\beta}A/x$, $(x < 0)$, and (ii) an exponentially decaying term appears only if Δ exceeds a threshold value $\Delta_c(< \beta/2)$, given by

$$A = (\beta - \Delta_c)\left(1 \pm \sqrt{1 - \frac{2\Delta_c}{\beta}}\right). \tag{26}$$

In other words, if Δ is smaller than Δ_c, no exponential decay can be realized, while for those Δ greater than $\beta/2(> \Delta_c)$, (26) has no solution and the exponential decay appears for all values of $A > 0$ and $\beta > 0$. See Fig. 4.

5 Behavior at short and long times

We can draw the survival probability $P(t) = |x(t)|^2$ as a function of time for various cases, some of which are seen in Fig. 5, and extract the behavior of $x(t)$ both at short and long times from its exact and explicit expression (21).

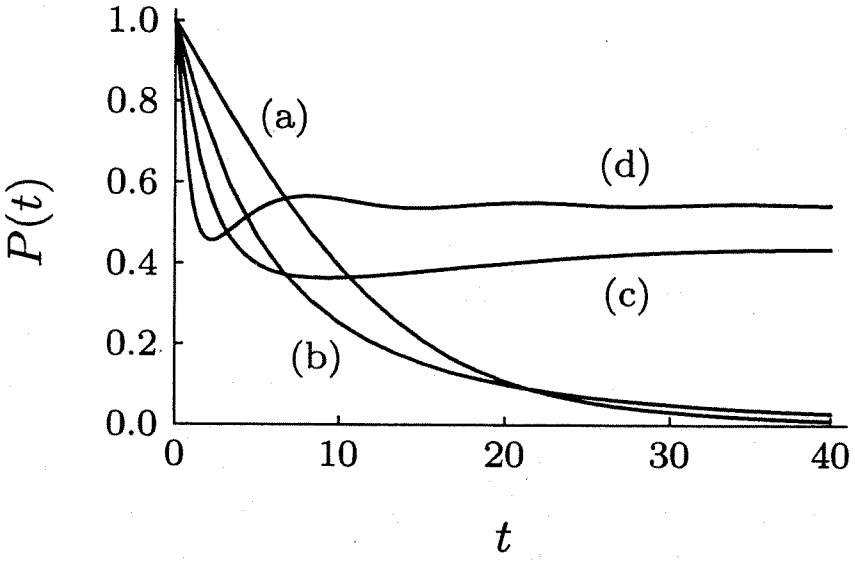

Figure 5. The survival probability $P(t)$ in *Case I* ($\Delta = 0.35\beta > \beta/3$). Here time t is measured in units of β^{-1}. The four curves (a)~(d) represent the typical cases: (a) $A = 0.4\Delta$ (weak coupling and exponentially decaying pole present), (b) $A = 0.9\Delta$ (no pole contribution present), (c) $A = 1.7\Delta$ (only plasmon pole present) and (d) $A = 4.0\Delta$ (both plasmon pole and exponentially decaying pole present). Every curve has been confirmed to have a flat derivative at $t = 0$.

5.1 Short-time behavior

First, remember the following expansion of the Error function $\mathrm{erfc}(\epsilon)$ for small ϵ

$$\mathrm{erfc}(\epsilon) = 1 - \frac{2}{\sqrt{\pi}} \sum_{n=0}^{\infty} \frac{(-1)^n \epsilon^{2n+1}}{(2n+1)n!} = 1 - \frac{2}{\sqrt{\pi}} \left(\epsilon - \frac{\epsilon^3}{3} + \cdots \right). \tag{27}$$

It is then easy to see that, independently of the presence or absence of pole contributions, the short-time behavior of the survival amplitude always reads

$$\begin{aligned} x(t) = & \sum_{k=0,1,2} \frac{\xi_k(\xi_k + \sqrt{\beta})}{3\xi_k^3 + 2\sqrt{\beta}\xi_k + \Delta} \\ & \times \left(1 + \frac{2e^{\pi i/4}}{\sqrt{\pi}} \xi_k \sqrt{t} + i\xi_k^2 t - \frac{4e^{-\pi i/4}}{3\sqrt{\pi}} \xi_k^3 \sqrt{t}^3 - \frac{1}{2}\xi_k^4 t^2 + \cdots \right), \end{aligned} \tag{28}$$

which, after some manipulation, is reduced to

$$x(t) = 1 - \frac{5\Delta}{3} it - \frac{4e^{-\pi i/4}}{3\sqrt{\pi}} \sqrt{\beta} A \sqrt{t}^3 + O(t^2). \tag{29}$$

Notice that the term of order $\sqrt{t}$ has disappeared from the final expression (29), which is in accord with the finiteness of the derivative of the survival amplitude at the origin $|\dot{x}(0)| < \infty$ and that the linear (in t) term is purely imaginary. Therefore we arrive at the following short-time expansion of the survival probability

$$P(t) = |x(t)|^2 = 1 - \frac{4\sqrt{2}}{3\sqrt{\pi}}\sqrt{\beta}A\sqrt{t}^3 + O(t^2), \tag{30}$$

which is valid for all cases. Observe that there is no linear term and the first term is of order $\sqrt{t}^3$: The system does not start to decay exponentially. It does not start to decay quadratically either, however, the survival probability has a vanishing derivative at the origin $\dot{P}(0) = 0$. Deviation from the quadratic decay is due to the infiniteness of the variance of our interaction Hamiltonian in the initial state, which is a result of our choice of the form factor $g(\omega)$ in (11): The usual naive expansion of the evolution operator for small t is not meaningful in this case, however the flatness of the derivative of the survival probability is maintained even in such a case.

5.2 *Long-time behavior*

We know that the Error function has the following expansion for large value of its argument

$$\mathrm{erfc}(z) \sim \frac{1}{\sqrt{\pi}}e^{-z^2}\left(\frac{1}{z} - \frac{1}{2z^3} + \cdots\right), \qquad \text{for } z \to \infty,\ |\mathrm{Arg}(z)| < \frac{3\pi}{4}. \tag{31}$$

We understand that for large t, the exponentially decaying term, if it exists, is to be overwhelmed by other terms decaying more slowly like an inverse power of t, which come from the above expansion of the Error function originated from the contour integrals. Inserting the above expansion (31) into $x(t)$ in (21), we find that the leading term is, not of order $1/\sqrt{t}$, but of order $1/\sqrt{t}^3$

$$\begin{aligned} x(t) &\overset{t\to\infty}{\longrightarrow} \frac{1}{\sqrt{t}^3}\frac{-e^{\pi i/4}}{2\sqrt{\pi}}\sum_{k=1,2,3}\frac{\xi_k + \sqrt{\beta}}{\xi_k^2(3\xi_k^2 + 2\sqrt{\beta}\xi_k + \Delta)} + \cdots \\ &= \frac{1}{\sqrt{t}^3}\frac{-e^{\pi i/4}}{2\sqrt{\pi}}\frac{A}{\sqrt{\beta}(\Delta - A)^2} + \cdots, \end{aligned} \tag{32}$$

irrespectively of the presence or absence of the exponentially decaying term.

There are exceptional cases, for which the above expression is not valid. Such an exception occurs for the threshold case $A = \Delta$. In this case, the

amplitude decays much more slowly[5]

$$x(t) \xrightarrow{t\to\infty} \frac{1}{\sqrt{t}} \frac{ie^{\pi i/4}}{\sqrt{\pi}} \left(-\frac{\sqrt{\beta}}{A}\right) + \cdots, \qquad A = \Delta. \tag{33}$$

The exception also occurs if the coupling A exceeds the threshold value Δ and we have a plasmon pole. Let ξ_0 be positive and responsible for the plasmon. Then the survival amplitude never decays out even at $t = \infty$, instead it keeps to oscillate:

$$x(t) \xrightarrow{t\to\infty} \frac{2\xi_0(\xi_0 + \sqrt{\beta})}{3\xi_0^2 + 2\sqrt{\beta}\xi_0 + \Delta} e^{i\xi_0^2 t} + \frac{1}{\sqrt{t}^3} \frac{-e^{\pi i/4}}{2\sqrt{\pi}} \frac{A}{\sqrt{\beta}(\Delta - A)^2} + \cdots. \tag{34}$$

It is interesting to see that, while $\xi_0 \to \infty$ as the coupling A goes to infinity, the survival probability remains at a value of 4/9, and never becomes unity.

6 Discussions

The behavior of a quantum system which is in interaction with another large quantum system and is therefore supposed to be unstable, is not simple and is characterized by different functions in each time region, as stated in 1)~3) in Introduction. The present analysis of a solvable model explicitly shows that there is more: In some cases, a system which is supposed to be unstable owing to its coupling to the environmental degrees of freedom can survive and never decays out completely even in the $t \to \infty$ limit. This is due to the presence of an oscillation pole, known as a plasmon and the existence of such a pole implies that the spectrum of the total Hamiltonian includes a discrete level, represented by a delta-function. It is easily understood that if the spectrum of the total Hamiltonian is continuous and has no discrete levels, the system has to vanish in the $t \to \infty$ limit: More precisely, the survival amplitude (and therefore the survival probability) decays to 0 as $t \to \infty$, since

$$\begin{aligned} \left|\langle\psi|e^{-iHt}|\psi\rangle\right| &= \left|\int_0^\infty dE\rho(E)e^{-iEt}\right| \\ &\le \frac{1}{t}\int_0^\infty dE|\rho'(E)| = \frac{2}{t}\sum_i \left[\rho(E^{(i)}_{\max}) - \rho(E^{(i)}_{\min})\right], \end{aligned} \tag{35}$$

where the energy density of the initial state $\rho(E) \equiv |\langle E|\psi\rangle|^2$ vanishes at the boundaries of the spectrum $\rho(0) = \rho(\infty) = 0$ and is assumed to have ith local maximum (minimum) at $E^{(i)}_{\max(\min)}$. As long as the left most quantity is finite, survival amplitude decays to 0 as $t \to \infty$. It is also evident that if the

spectrum contains a discrete level, represented by a delta-function, then the above estimation loses its meaning, for $\rho(E)$ is not bounded any longer.

It would easily be understood that for a quantum system of finite degrees of freedom to decay out, it is necessary that it is coupled to another system of infinitely many degrees of freedom (environment) and that the energy spectrum of the total system is continuous and does not contain any discrete levels. It is, however, still not clear, at least for the present author, the physical reason why and the condition under which most of possible process are to be overwhelmed by a certain decay process, even though the dynamics is governed by a Hamiltonian which is hermitian. The issue clearly needs much deeper analysis of temporal behaviors of quantum systems, which would result in better understanding of quantum dynamics.

Acknowledgments

The author would like to thank those participants of Japan–Italy Joint Waseda Workshop 2001 who contributed to the discussion during and after his talk, according to which the manuscript has been improved. In particular, helpful discussions with Paolo Facchi, Dr. K. Imafuku, Saverio Pascazio, Antonello Scardicchio and Dr. K. Yuasa are greatly appreciated.

References

1. H. Nakazato, M. Namiki and S. Pascazio, *Int. J. Mod. Phys.* B **10**, 247 (1996) and references therein.
2. A. Beskow and J. Nilsson, *Arkiv für Fysik* **34**, 561 (1967); L.A. Khalfin, *Zh. Eksp. Teor. Fiz. Pis. Red.* **8**, 106 (1968) [*JETP Letters* **8**, 65 (1968)]; B. Misra and E. C. G. Sudarshan, *J. Math. Phys.* **18**, 758 (1977); D. Home and M.A.B. Whitaker, *Ann. Phys.* **258**, 237 (1997).
3. A.G. Kofman and G. Kurizki, *Acta Physica Slovaca* **49**, 541 (1999); S. Pascazio and P. Facchi, *Acta Physica Slovaca* **49**, 557 (1999); A.G. Kofman and G. Kurizki, *Nature* **405**, 546 (2000); P. Facchi and S. Pascazio, *Phys. Rev.* A **62**, 023804 (2000).
4. P. Facchi, H. Nakazato and S. Pascazio, *Phys. Rev. Lett.* **86**, 2699 (2001).
5. M. Lewenstein and K. Rzążewski, *Phys. Rev.* A **61**, 022105 (2000).
6. M.C. Fischer, B. Gutiérrez-Medina and M.G. Raizen, *Phys. Rev. Lett.* **87**, 040402 (2001).
7. S.R. Wilkinson *et al*, *Nature* **387**, 575 (1997).

8. R.E.A.C. Paley and N. Wiener, *Fourier Transforms in the Complex Domain* (American Mathematical Society Colloquium Pub. **XIX**, New York, 1934).
9. G. Gaveau and L.S. Schulamn, *J. Phys.* A **28**, 7359 (1995).
10. K. Rzążewski, M. Lewenstein and J.H. Eberly, *J. Phys.* B **15**, L661 (1982); J. Javanainen, *J. Phys.* B **16**, 1343 (1983); J. Javanainen, *Optics Comm.* **46**, 175 (1983); S.L. Haan and J. Cooper, *J. Phys.* B **17**, 3481 (1984).

PHYSICAL REVIEW A **68**, 012107 (2003)

Optimization of a neutron-spin test of the quantum Zeno effect

Paolo Facchi,[1,*] Yoichi Nakaguro,[2] Hiromichi Nakazato,[2,†] Saverio Pascazio,[1,‡] Makoto Unoki,[2] and Kazuya Yuasa[2,§]
[1]*Dipartimento di Fisica, Università di Bari and Istituto Nazionale di Fisica Nucleare, Sezione di Bari, I-70126 Bari, Italy*
[2]*Department of Physics, Waseda University, Tokyo 169-8555, Japan*
(Received 14 January 2003; published 22 July 2003)

A neutron-spin experimental test of the quantum Zeno effect (QZE) is discussed from a practical point of view, where the nonideal efficiency of the magnetic mirrors, used for filtering the spin state, is taken into account. In the idealized case, the number N of (ideal) mirrors can be indefinitely increased, yielding an increasingly better QZE. In contrast, in a practical situation with imperfect mirrors, there is an optimal number of mirrors, $N_{\rm opt}$, at which the QZE becomes maximum: more frequent measurements would deteriorate the performance. However, a quantitative analysis shows that a good experimental test of the QZE is still feasible. These conclusions are of general validity: in a realistic experiment, the presence of losses and imperfections leads to an optimal frequency $N_{\rm opt}$, which is in general finite. One should not increase N beyond $N_{\rm opt}$. A convenient formula for $N_{\rm opt}$, valid in a broad framework, is derived as a function of the parameters characterizing the experimental setup.

DOI: 10.1103/PhysRevA.68.012107 PACS number(s): 03.65.Xp

I. INTRODUCTION

If very frequent measurements are made on a quantum system in order to ascertain whether it is still in the initial state, its evolution is slowed down and eventually totally hindered in the limit of infinite frequency. This is the quantum Zeno effect (QZE) [1–3], which was considered little more than a curiosity until the experimental confirmations by Itano *et al.* [4] (which followed a theoretical proposal by Cook [5]) and by Raizen and co-workers in Texas [6]. This last experiment proved the existence of the QZE for bona fide unstable systems and the occurrence of the inverse QZE, i.e., acceleration of decay by repeated (not extremely frequent) measurements [7]. The temporal behavior of quantum-mechanical systems and, in particular, the nonexponential features at short times, on which QZE and inverse QZE hinge, are reviewed in Ref. [3].

We are now going through a phase of experimental verification of the QZE. It is therefore important to understand the physical meaning of "infinitely" frequent measurements, focusing on practical applications, imperfections of the apparatus, experimental losses, as well as theoretical bounds. Some of these problems were tackled in Ref. [8]. In this paper, we reconsider the proposal of an experimental test of the QZE, which makes use of neutron spin [9]. In view of the recent progress in the perfect-crystal neutron-storage technology [10,11], it is necessary to investigate the physical properties of a Zeno setup, focusing, in particular, on practical limits.

In this paper, we will study the practical *imperfections in the spectral decomposition*. In a few words, a "spectral decomposition" in Wigner's sense [12] is a unitary process that associates additional degrees of freedom to different values of the observable to be measured. In this sense, it yields no wave-function collapse. It is known, and will be reviewed in Sec. II, that a frequent series of spectral decompositions is sufficient for obtaining a QZE [3,9,13].

In the proposed neutron-spin experimental test of the QZE [9], the spectral decomposition is realized by a magnetic mirror, with its inevitable imperfections, leading to nonideal efficiency. The main purpose of this paper is to quantitatively analyze the consequences of these imperfections: clearly, they tend to deteriorate the performance of the experimental setup; yet, for reasonable values of the experimental parameters [10,11], a good test is still clearly feasible with high efficiency. This will be shown in Sec. III, where we will determine an *optimum* value $N_{\rm opt}$ of the frequency of measurements: more frequent measurements would simply deteriorate the overall performance of the setup, masking the QZE. These conclusions are of general validity: the presence of losses and imperfections always leads to an optimal frequency, which is in general finite. Our analysis will be extended and generalized in Sec. IV to an arbitrary lossy quantum Zeno experiment, and a convenient formula for $N_{\rm opt}$ will be derived. We summarize our results in Sec. V.

II. NEUTRON-SPIN TEST OF THE QZE WITH IDEAL MIRRORS

Let us first briefly review the original proposal of the neutron-spin test of the QZE [9]. The basic setup is shown in Fig. 1(a). We prepare, equally spaced along the y axis, N identical regions in each of which a static magnetic field B is applied in the x direction. A neutron wave packet, whose initial spin is oriented in the z direction, travels along the y axis and undergoes a spin rotation at each interaction with the magnetic field, according to the Hamiltonian

$$H=\mu B\sigma_x, \tag{2.1}$$

μ being the neutron magnetic moment and σ_i $(i=x,y,z)$ the Pauli matrices. The initial state of the incident neutron is

*Electronic address: paolo.facchi@ba.infn.it
†Electronic address: hiromici@waseda.jp
‡Electronic address: saverio.pascazio@ba.infn.it
§Electronic address: yuasa@hep.phys.waseda.ac.jp

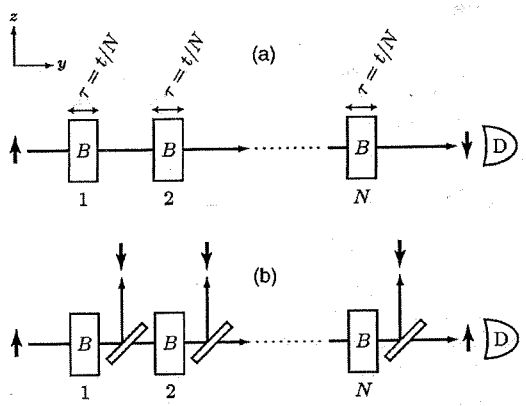

FIG. 1. (a) Basic setup for the neutron-spin test of QZE. We set $t/\tau_Z = \pi/2$, so that $2\theta = \pi$. (b) Neutron-spin test of QZE with ideal mirrors.

$|S_0\rangle = |\uparrow\rangle$ (spin up along the z direction). The final state, after crossing the N regions with the magnetic fields, reads

$$|S(t)\rangle = e^{-iHt/\hbar}|\uparrow\rangle = \cos\frac{\mu Bt}{\hbar}|\uparrow\rangle - i\sin\frac{\mu Bt}{\hbar}|\downarrow\rangle, \quad (2.2)$$

where t is the total time spent in the magnetic field and we have ignored, for simplicity, the spatial degrees of freedom of the neutron. By defining

$$\theta = \frac{\mu Bt}{\hbar} = \frac{t}{\tau_Z}, \quad (2.3)$$

where τ_Z $(=\hbar\langle\uparrow|H^2|\uparrow\rangle^{-1/2}$ in this case) is the so-called Zeno time and 2θ the classical precession angle of the spin, the survival probability of the initial state $|\uparrow\rangle$ reads

$$P(\theta) = |\langle\uparrow|e^{-iHt/\hbar}|\uparrow\rangle|^2 = \cos^2\theta. \quad (2.4)$$

Note that if Bt is adjusted so as to satisfy

$$\theta = \frac{\pi}{2}, \quad (2.5)$$

the spin is completely flipped

$$|S(t)\rangle = e^{-iHt/\hbar}|\uparrow\rangle = -i|\downarrow\rangle. \quad (2.6)$$

In this case the survival probability of the initial state $|\uparrow\rangle$ vanishes:

$$P(\theta) = 0. \quad (2.7)$$

This situation, shown in Fig. 1(a), is the one usually considered in the literature. However, the whole analysis that follows identically applies to the general case (2.3) and (2.4).

Let us now check, at every step, whether the spin remains in the initial state $|\uparrow\rangle$ despite the spin rotation in the B field. To this end, we insert N magnetic mirrors after every B region, as in Fig. 1(b). The incident neutron undergoes N "spin-measurements" until it reaches the detector D. At each step, if the spin state remains up, the neutron is transmitted through the mirror and keeps traveling right, otherwise it is reflected out by the mirror. Detector D counts those neutrons that have "survived" at each of these N measurements, so that the detection probability at D is nothing but the survival probability of the initial state $|\uparrow\rangle$.

As clarified in Refs. [3] and [9], the insertion of a mirror does not represent a measurement of the spin state; it just constitutes a generalized spectral decomposition (GSD) in Wigner's sense [12], namely, a (unitary) physical process that associates an "external" degree of freedom (whose role is played here by the wave packet of the neutron) to different values of the observable to be measured (the neutron spin): a frequent sequence of GSD is sufficient for the occurrence of a QZE. In a magnetic field, the spin state of the incident neutron is changed from the initial one $|\uparrow\rangle$ to $e^{-iHt/N\hbar}|\uparrow\rangle$ and the neutron is then *decomposed* by the mirror into two branch waves: the spin-up component going rightward and the spin-down one going upward in Fig. 1(b). The state of the neutron just after the first mirror is hence given by

$$|\psi_1\rangle = \mathcal{T}e^{-iHt/N\hbar}|\uparrow\rangle\otimes|t_1\rangle + \mathcal{R}e^{-iHt/N\hbar}|\uparrow\rangle\otimes|r_1\rangle, \quad (2.8)$$

where the spectral decomposition with respect to the spin state is expressed in terms of the projection operators

$$\mathcal{T} = |\uparrow\rangle\langle\uparrow|, \quad \mathcal{R} = |\downarrow\rangle\langle\downarrow|, \quad (2.9)$$

and $|t_n\rangle$ and $|r_n\rangle$ are the transmitted and reflected wave packets after the nth mirror [and before the $(n+1)$th magnetic field], representing the spatial degrees of freedom of the neutron. Repeating these operations N times, we obtain the final state of the neutron

$$|\psi_N\rangle = (\mathcal{T}e^{-iHt/N\hbar})^N|\uparrow\rangle\otimes|t_N\rangle + \sum_{n=1}^{N}\mathcal{R}e^{-iHt/N\hbar}(\mathcal{T}e^{-iHt/N\hbar})^{n-1}|\uparrow\rangle\otimes|r_n\rangle, \quad (2.10)$$

so that the probability for the neutron to be detected at detector D, i.e., the survival probability of the initial spin state $|\uparrow\rangle$, reads

$$\begin{aligned} P^{(N)}(\theta) &= |\{\langle\uparrow|\otimes\langle t_N|\}|\psi_N\rangle|^2 \\ &= |\langle\uparrow|(\mathcal{T}e^{-iHt/N\hbar})^N|\uparrow\rangle|^2 \\ &= |\langle\uparrow|e^{-iHt/N\hbar}|\uparrow\rangle|^{2N} \\ &= \left(\cos\frac{\theta}{N}\right)^{2N}, \end{aligned} \quad (2.11)$$

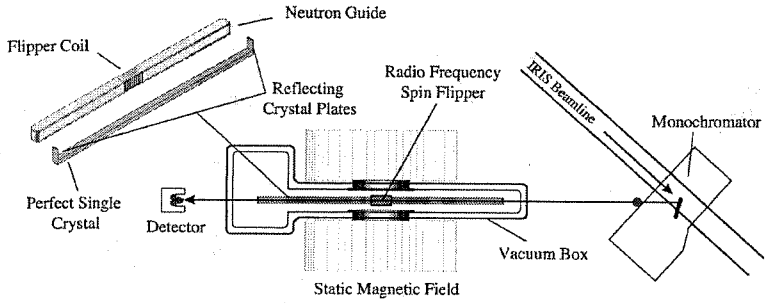

FIG. 2. Schematic setup of the VESTA (Viennese neutron storage apparatus) experiment. (Courtesy: the Vienna group.) Neutrons are fed from the right and bounce back and forth in the guide between the reflecting plates. Their spin is rotated when they go through the B field in the rf spin flipper. The neutrons are finally extracted from the storage apparatus and detected at the left.

where we have made use of Eq. (2.3) (within our approximations, the total duration of the experiment is t, with or without magnetic mirrors). Under condition (2.5) (and, in general, for $\theta < \pi/2$), this is nonvanishing for any $N \geqslant 2$ and is an increasing function of N. Frequent "checks" of the spin state slow down the evolution of the initial state $|\uparrow\rangle$: the survival probability $P^{(N)}(\theta)$ increases with the frequency of measurements. This is a QZE. Furthermore, in the limit of infinite frequency,

$$\lim_{N\to\infty} P^{(N)}(\theta) = 1 \quad (\theta \text{ fixed}), \tag{2.12}$$

i.e., the spin is frozen and ceases to evolve, in agreement with the theorem by Misra and Sudarshan [2].

An experiment is at present being performed [11] by making use of a recently developed neutron-storage technique [10]. Neutrons with a well-defined energy and in a given spin state are stored in a 1-m-long perfect-crystal resonator (see Fig. 2). The neutrons, at the given energy, satisfy the Bragg reflection condition and bounce back and forth between the two reflecting crystal plates at both ends of the silicon crystal. A neutron guide is inserted between the crystal plates in order to minimize the lateral losses. In this way, at present, neutrons can be reflected a few thousand times, traveling for a few kilometers in the resonator [10,11]. In the central part of the resonator, a spin-rotating radio frequency (rf) field can be applied, playing the role of the magnetic field in Fig. 1.

The Zeno effect can be obtained as follows. A neutron traveling in the guide, whose wavelength satisfies the Bragg condition at the crystal plate, is reflected back inside the guide. However, if a static magnetic field is applied at one of the crystal plates, yielding different potentials for different spin states of the neutron, the neutrons are selected according to their spin state: if, say, a spin-up neutron satisfies the Bragg condition at a plate, the neutron is reflected back and kept inside the resonator; if, on the other hand, the spin is flipped by the spin-rotating rf field, the neutron is transmitted out of the resonator. The crystal plates with the magnetic fields play therefore the role of the "magnetic mirrors" in Fig. 1(b), performing the GSDs. Hence, in this experimental setup, the probability for the neutron to remain in the perfect single crystal is the survival probability of the initial spin state. In the most recent setup, displayed in Fig. 2, a static magnetic field has been added in the central part of the perfect-crystal resonator, in order to minimize the mechanical vibrations due to the on-off switching of the magnetic fields at the plates, thereby making the whole apparatus less sensitive to depolarization effects.

It should be clear by now that it is of primary importance to analyze the effect of losses and imperfections, in order to understand whether the experiment is still meaningful in a realistic situation. Note that the number N of traverses and interactions should be very large, in order to get a good manifestation of the QZE. This, on the other hand, entails a dramatic (exponential) propagation of "errors." This will be investigated in the following two sections.

III. NEUTRON-SPIN TEST OF THE QZE WITH NONIDEAL MIRRORS

Losses are unavoidable in real experiments and must be duly taken into account. A magnetic mirror, for example, is not ideal, as tacitly assumed in the preceding section. It has a nonvanishing probability of failing to correctly decompose the spin state. Assume that the magnetic mirror has transmission $T_{\uparrow(\downarrow)}$ and reflection $R_{\uparrow(\downarrow)}$ coefficients for a spin-up (spin-down) neutron (Fig. 3). (They are in general complex valued and constrained by $|T_{\uparrow(\downarrow)}|^2 + |R_{\uparrow(\downarrow)}|^2 = 1$.) We assumed in the preceding section that $|T_\uparrow| = |R_\downarrow| = 1$ and $R_\uparrow = T_\downarrow = 0$, but this is not the case for actual magnetic mirrors. So the question arises as to whether (and to which extent) it is possible to observe the QZE with nonideal mirrors. In other words, whether the QZE still takes place if the measurements (i.e., the spectral decompositions) are *imperfect*.

At the nth (nonideal) mirror, the spin-up component of a neutron, $|\uparrow\rangle \otimes |t_{n-1}\rangle$, is split into two waves

$$|\uparrow\rangle \otimes |t_{n-1}\rangle \to |\uparrow\rangle \otimes (T_\uparrow |t_n\rangle + R_\uparrow |r_n\rangle) \tag{3.1a}$$

and a similar expression holds for the spin-down component

$$|\downarrow\rangle \otimes |t_{n-1}\rangle \to |\downarrow\rangle \otimes (T_\downarrow |t_n\rangle + R_\downarrow |r_n\rangle). \tag{3.1b}$$

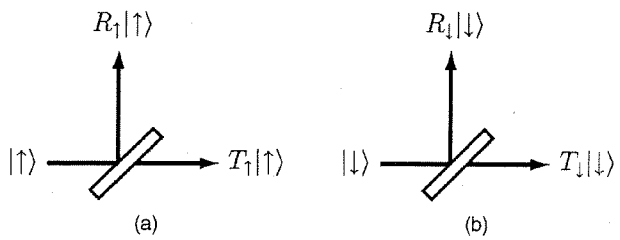

FIG. 3. Transmission and reflection coefficients for (a) a spin-up neutron and (b) a spin-down neutron.

(No spin flip is assumed to occur at the magnetic mirror. The most general case, where such spin flips take place, is investigated in the Appendix.) The right arrows in Eqs. (3.1) and in the following stand for the (unitary) physical processes that are responsible for the spectral decomposition. Hence for a neutron in a general spin state $|S\rangle$, the magnetic mirror provokes the following spectral decomposition:

$$\begin{aligned}|S\rangle\otimes|t_{n-1}\rangle &\equiv (c_\uparrow|\uparrow\rangle+c_\downarrow|\downarrow\rangle)\otimes|t_{n-1}\rangle\\ &\to (c_\uparrow T_\uparrow|\uparrow\rangle+c_\downarrow T_\downarrow|\downarrow\rangle)\otimes|t_n\rangle\\ &\quad+(c_\uparrow R_\uparrow|\uparrow\rangle+c_\downarrow R_\downarrow|\downarrow\rangle)\otimes|r_n\rangle\\ &=\tilde{\mathcal{T}}|S\rangle\otimes|t_n\rangle+\tilde{\mathcal{R}}|S\rangle\otimes|r_n\rangle,\end{aligned}\tag{3.2}$$

where the operators

$$\tilde{\mathcal{T}}=|\uparrow\rangle T_\uparrow\langle\uparrow|+|\downarrow\rangle T_\downarrow\langle\downarrow|,\quad \tilde{\mathcal{R}}=|\uparrow\rangle R_\uparrow\langle\uparrow|+|\downarrow\rangle R_\downarrow\langle\downarrow|\tag{3.3}$$

incorporate the effects due to the imperfections of the mirror. These operators $\tilde{\mathcal{T}}$ and $\tilde{\mathcal{R}}$, even though they are no longer projection operators, play the same role as the projection operators $\mathcal{T}$ and $\mathcal{R}$ in the ideal case (2.8) and (2.9). The final state of the neutron after the final (Nth) magnetic mirror is given by

$$\begin{aligned}|\tilde{\psi}_N\rangle &=(\tilde{\mathcal{T}}e^{-iHt/N\hbar})^N|\uparrow\rangle\otimes|t_N\rangle\\ &\quad+\sum_{n=1}^{N}\tilde{\mathcal{R}}e^{-iHt/N\hbar}(\tilde{\mathcal{T}}e^{-iHt/N\hbar})^{n-1}|\uparrow\rangle\otimes|r_n\rangle\end{aligned}\tag{3.4}$$

and the probability for the neutron to be detected at detector D reads

$$\begin{aligned}\tilde{P}^{(N)}(\theta)&=\|\langle t_N|\tilde{\psi}_N\rangle\|^2\\ &=\mathrm{tr}[(\tilde{\mathcal{T}}e^{-iHt/N\hbar})^N\rho_0(e^{iHt/N\hbar}\tilde{\mathcal{T}}^\dagger)^N],\end{aligned}\tag{3.5}$$

where $\rho_0=|\uparrow\rangle\langle\uparrow|$ is the initial density operator of the neutron spin. [The spin state observed at the detector is not necessarily $|\uparrow\rangle$; it is probability (3.5) that one measures in the actual experiment.]

Let us evaluate probability (3.5). The eigenvalues $\xi_\pm(N)$ of the operator

$$\begin{aligned}\tilde{\mathcal{T}}e^{-iHt/N\hbar}&=\frac{1}{2}(T_\uparrow+T_\downarrow)\cos\frac{\theta}{N}-\sigma_x\frac{i}{2}(T_\uparrow+T_\downarrow)\sin\frac{\theta}{N}\\ &\quad+\sigma_y\frac{1}{2}(T_\uparrow-T_\downarrow)\sin\frac{\theta}{N}+\sigma_z\frac{1}{2}(T_\uparrow-T_\downarrow)\cos\frac{\theta}{N}\end{aligned}\tag{3.6}$$

are given by

$$\begin{aligned}\xi_\pm(N)=\frac{1}{2}\Bigg[&(T_\uparrow+T_\downarrow)\cos\frac{\theta}{N}\\ &\pm\sqrt{(T_\uparrow+T_\downarrow)^2\cos^2\frac{\theta}{N}-4T_\uparrow T_\downarrow}\Bigg].\end{aligned}\tag{3.7}$$

[The eigenvalues $\xi_\pm(N)$ will henceforth be written $\xi_\pm$, unless confusion arises.] By rewriting operator (3.6) as

$$\tilde{\mathcal{T}}e^{-iHt/N\hbar}=\tfrac{1}{2}(\xi_++\xi_-)+\tfrac{1}{2}(\xi_+-\xi_-)\sigma_n,\tag{3.8}$$

where $\sigma_n=\boldsymbol{n}\cdot\boldsymbol{\sigma}$, $\boldsymbol{n}$ being a complex-valued vector satisfying $\boldsymbol{n}^2=n_x^2+n_y^2+n_z^2=1$, we readily obtain

$$(\tilde{\mathcal{T}}e^{-iHt/N\hbar})^N=\tfrac{1}{2}(\xi_+^N+\xi_-^N)+\tfrac{1}{2}(\xi_+^N-\xi_-^N)\sigma_n.\tag{3.9}$$

A series of elementary calculations yields the following exact expression for the probability:

$$\tilde{P}^{(N)}(\theta)=\left|A(N)-B(N)T_\downarrow\cos\frac{\theta}{N}\right|^2+\left|B(N)T_\downarrow\sin\frac{\theta}{N}\right|^2,\tag{3.10}$$

with

$$A(N)=\frac{\xi_+^{N+1}(N)-\xi_-^{N+1}(N)}{\xi_+(N)-\xi_-(N)},\tag{3.11a}$$

$$B(N)=\frac{\xi_+^{N}(N)-\xi_-^{N}(N)}{\xi_+(N)-\xi_-(N)}.\tag{3.11b}$$

We are now in a position to see whether it is possible to observe the QZE with nonideal mirrors. In order to analyze its N dependence, let us expand probability (3.10) as a function of $|T_\downarrow/T_\uparrow|\ll 1$. (In the experiment [10], $|T_\downarrow/T_\uparrow|^2\lesssim 10^{-4}$.) For any $N\geqslant 2$, the eigenvalues in Eq. (3.7) are expanded as

$$\xi_+\simeq T_\uparrow\cos\frac{\theta}{N}\left[1-\frac{T_\downarrow}{T_\uparrow}\tan^2\frac{\theta}{N}+O(T_\downarrow^2/T_\uparrow^2)\right],\tag{3.12a}$$

$$\xi_-\simeq\xi_+\left[\frac{T_\downarrow}{T_\uparrow}\left(1+\tan^2\frac{\theta}{N}\right)+O(T_\downarrow^2/T_\uparrow^2)\right],\tag{3.12b}$$

from which one obtains

$$\begin{aligned}A(N)&=\xi_+^N\left[1+\frac{\xi_-}{\xi_+}+\cdots+\left(\frac{\xi_-}{\xi_+}\right)^N\right]\\ &\simeq\left(T_\uparrow\cos\frac{\theta}{N}\right)^N\left[1-\frac{T_\downarrow}{T_\uparrow}\left((N-1)\tan^2\frac{\theta}{N}-1\right)+\cdots\right]\end{aligned}\tag{3.13}$$

and a similar expansion holds for $B(N)$. We thus easily obtain an approximate expression for probability (3.10)

$$\begin{aligned}\tilde{P}^{(N)}(\theta)&\simeq|T_\uparrow|^{2N}\left(\cos\frac{\theta}{N}\right)^{2N}\\ &\quad\times\left[1-2\,\mathrm{Re}\left(\frac{T_\downarrow}{T_\uparrow}\right)(N-1)\tan^2\frac{\theta}{N}+\cdots\right],\end{aligned}\tag{3.14}$$

valid for $N\geqslant 2$. [For $N=1$, $\tilde{P}^{(1)}(\theta)=\sin^2\theta\,H|T_\downarrow|^2+\cos^2\theta\,H|T_\uparrow|^2$ exactly.] It is clear from formula (3.14) that the probability $\tilde{P}^{(N)}(\theta)$ is well approximated by

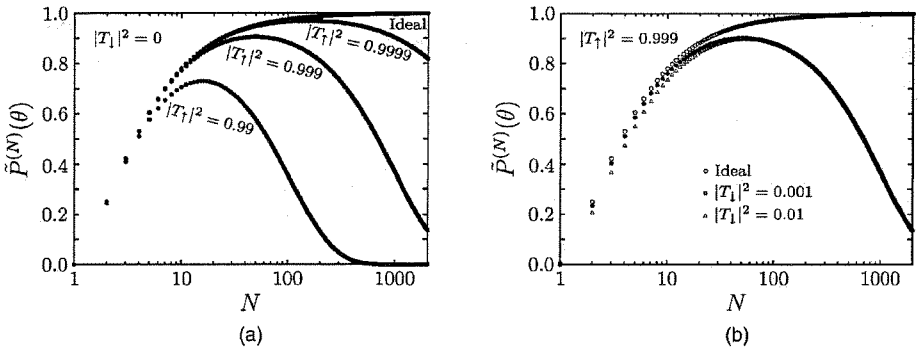

FIG. 4. (a) $T_\uparrow$ dependence and (b) $T_\downarrow$ dependence of the probability $\tilde{P}^{(N)}(\theta)$ in Eq. (3.10). In both figures, $\arg T_\uparrow = \arg T_\downarrow = 0$.

$$\tilde{P}^{(N)}(\theta) \simeq |T_\uparrow|^{2N}\left(\cos\frac{\theta}{N}\right)^{2N}. \tag{3.15}$$

This shows that neither the transmission coefficient $T_\downarrow$ for a spin-down neutron, nor the phases of $T_\uparrow$ and $T_\downarrow$ bear any important influence on the probability $\tilde{P}^{(N)}(\theta)$; the only relevant quantity is the transmission probability $|T_\uparrow|^2$. Since $|T_\uparrow|^2 \simeq 1$, for N not too large the factor $|T_\uparrow|^{2N}$ is almost unity and the probability $\tilde{P}^{(N)}(\theta)$ behaves like

$$\tilde{P}^{(N)}(\theta) \simeq \left(\cos\frac{\theta}{N}\right)^{2N} \quad (N \text{ not too large}). \tag{3.16}$$

This is the same as the survival probability with ideal mirrors given in Eq. (2.11), and is an increasing function of N. However, for larger N, the factor $[\cos(\theta/N)]^{2N}$ is almost unity, and the probability behaves like

$$\tilde{P}^{(N)}(\theta) \simeq |T_\uparrow|^{2N} \quad (\text{larger } N), \tag{3.17}$$

decreasing exponentially to zero as $N \to \infty$: as the number of mirrors, N, is increased, the mirror imperfections ($|T_\uparrow|^{2N} < 1$) dominate over the increasing factor $[\cos(\theta/N)]^{2N}$, suppressing the QZE for very large N. (Clearly, the meaning of "large" N in the two previous equations must be precisely defined. This will be done in the following.)

There must be therefore an optimal number of mirrors, $N_{\rm opt}$, in order to observe the QZE if the losses in the measurement processes (spectral decompositions) are taken into account. In Fig. 4, the probability $\tilde{P}^{(N)}(\theta)$, computed according to the exact expression (3.10), is plotted as a function of N for a few values of the transmission coefficients $T_\uparrow$ and $T_\downarrow$. The figures corroborate the previous discussion. The QZE can be observed even with nonideal mirrors, if N is not too large, namely if one does not check the system's state too frequently: this is good news from an experimental point of view, since one need not and should not attempt to indefinitely increase the number of mirrors (or reflections in the neutron resonator experiment) in order to achieve an optimal QZE. Notice also that the probability $\tilde{P}^{(N)}(\theta)$ significantly depends on $T_\uparrow$, but displays almost no dependence on $T_\downarrow$.

It is possible to estimate the optimal number of measurements, $N_{\rm opt}$, yielding the maximum probability $\tilde{P}^{(N_{\rm opt})}(\theta)$. This can be done from the approximate formula (3.15) as follows. For actual magnetic mirrors, $|T_\uparrow|^2$ is almost unity (a reasonable value of $1-|T_\uparrow|^2$ is of order 10^{-4} [10]) and $N_{\rm opt}$ is expected to be large. The maximum of the function $f(x) = a^x \cos^x(2\theta/x)$, with $a \lesssim 1$, is given by one of the solutions of the equation $a\cos(2\theta/x) = \exp[-(2\theta/x)\tan(2\theta/x)]$ and is approximately $x_{\rm opt} \simeq 2\theta/\sqrt{\ln a^{-2}}$. Applying this result to the probability (3.15) one obtains

$$N_{\rm opt} \simeq \left[\frac{\theta}{\sqrt{1-|T_\uparrow|^2}}\right] \quad (|T_\uparrow|^2 \simeq 1), \tag{3.18}$$

where $[x]$ is the closest integer to x. The maximum is then readily evaluated as

$$\tilde{P}^{(N_{\rm opt})}(\theta) \simeq 1 - \frac{2\theta^2}{N_{\rm opt}} \quad (N_{\rm opt} \gg 1) \tag{3.19a}$$

$$\simeq 1 - 2\theta\sqrt{1-|T_\uparrow|^2} \quad (|T_\uparrow|^2 \simeq 1). \tag{3.19b}$$

Some values of $N_{\rm opt}$ and $\tilde{P}^{(N_{\rm opt})}(\theta)$ estimated from Eqs. (3.18) and (3.19a), respectively, are listed in Table I for some $|T_\uparrow|^2$. The agreement with the numerical results shown in Fig. 4, based on the exact formula (3.10), is excellent [except for $|T_\uparrow|^2 = 0.99$, where $\tilde{P}^{(N_{\rm opt})}(\theta)$ differs by about 5%].

Notice that for $1-|T_\uparrow|^2 \sim 10^{-4}$ [10], the estimated optimal number is $N_{\rm opt} = 157$, which is much smaller than the so-far achievable number of traverses $N_{\rm max} \sim 4000$ in the experiment [10,11]; yet the survival probability $\tilde{P}^{(N_{\rm opt})}(\theta) \simeq 0.97$ is already very close to unity. This estimate shows that a good test of the QZE can be performed in this case.

Of course, actual experiments suffer from other losses than those considered here. However, such additional losses can be taken into account (to a large extent) by duly renormalizing the transmission probability $|T_\uparrow|^2$. We therefore expect that the present analysis essentially maintains its valid-

TABLE I. $N_{\rm opt}$ from Eq. (3.18) and $\tilde{P}^{(N_{\rm opt})}(\theta)$ from Eq. (3.19a) versus $|T_\uparrow|^2$. The exact values, obtained from Eq. (3.10) with $|T_\downarrow|^2 = 0$, are indicated in parentheses.

$\lvert T_\uparrow\rvert^2$	$N_{\rm opt}$	$\tilde{P}^{(N_{\rm opt})}(\theta)$
0.99	16 (16)	0.69 (0.73)
0.999	50 (50)	0.90 (0.91)
0.9999	157 (157)	0.97 (0.97)

ity. For example, if the maximum number of traverses in a neutron-spin test of the QZE is of order $N_{\max}\simeq 4000$, one can roughly estimate that $1-|T_{\uparrow}|^2\sim \text{losses}\simeq 1/4000$. This yields $N_{\text{opt}}\simeq 99$ and $\tilde{P}^{(N_{\text{opt}})}(\theta)\simeq 0.95$, a very reasonable value.

IV. QZE WITH NONIDEAL MEASUREMENTS: GENERAL FRAMEWORK

It is possible to extend the conclusions of the preceding section to a broader framework, by making use of the well-known characteristics of the QZE (short-time behavior of the evolved wave function) and of some sensible assumptions regarding the GSD. Assume that N is large and the losses are small, so that the quantum Zeno survival probability be given by an expression of the types (3.14) and (3.15),

$$\tilde{P}^{(N)}(\theta)\simeq[L(t_1/N)]^N[p(t_2/N)]^N \quad (t_1+t_2=t=\tau_Z\theta), \tag{4.1}$$

where the factor L represents losses (due to imperfect transmission, measurements, and so on), while p is the survival probability of the quantum system in its initial state. We require that

$$0\leq L(t), \quad p(t)\leq 1. \tag{4.2}$$

Equations (4.1) and (4.2) describe the Zeno survival probability in an experiment in which a quantum evolution followed by a lossy spectral decomposition is repeated N times. In short, the system spends a time t_2 evolving under the action of a given Hamiltonian H and a time t_1 in GSDs. (We note that t_2 plays the same role as t of the preceding section, where the GSD time t_1 was neglected.) We will write

$$t_j=\alpha_j t, \quad \alpha_j>0 \ (j=1,2), \quad \alpha_1+\alpha_2=1. \tag{4.3}$$

The quantum-mechanical survival probability has the following short-time expansion [3]:

$$p(t)\sim 1-\frac{t^2}{\tau_Z^2} \quad (t<\tau_Z), \tag{4.4}$$

where τ_Z is the Zeno time. Note that, in general (and, in particular, for bona fide unstable systems), the above equation is valid on a (much) *shorter* time scale than τ_Z, but this will not be discussed here: see Ref. [14] and the last paper in Ref. [7].

We assume, in general, that

$$L(t)\sim a+bt+ct^2, \quad 0\leq a\leq 1 \ (\text{small } t). \tag{4.5}$$

When $a=1$, the GSD is very effective and losses appear on a time scale of the order of $|b|^{-1}$. In contrast, when $a<1$, losses are "instantaneous" and have serious consequences on a realistic test of the QZE. (Note that the above formula includes the case in which L is independent of t when $b=c=0$.)

The strategy is to maximize $\ln\tilde{P}^{(N)}(\theta)$ in Eq. (4.1) as a function of N, at fixed t_1 and t_2. We get

$$\frac{d}{dN}\ln\tilde{P}^{(N)}(\theta)=\ln L(t_1/N)+\ln p(t_2/N)-\frac{t_1L'(t_1/N)}{NL(t_1/N)}-\frac{t_2p'(t_2/N)}{Np(t_2/N)}=0, \tag{4.6}$$

where the prime denotes derivative with respect to the whole argument. By expanding for large N, according to Eqs. (4.4) and (4.5), this yields

$$\tau_{\text{opt}}^{-1}\equiv\frac{N_{\text{opt}}}{t}\simeq\frac{\alpha_2}{\tau_Z\sqrt{\ln a^{-1}}}\sqrt{1-\tau_Z^2\left(\frac{\alpha_1}{\alpha_2}\right)^2\left(\frac{c}{a}-\frac{b^2}{2a^2}\right)}. \tag{4.7}$$

Plugging this result into Eqs. (4.4), (4.5), and (4.1), we obtain

$$\begin{aligned}\tilde{P}^{(N_{\text{opt}})}(\theta)&\sim\left[a+b\frac{t_1}{N_{\text{opt}}}+c\left(\frac{t_1}{N_{\text{opt}}}\right)^2\right]^{N_{\text{opt}}}\left[1-\left(\frac{t_2}{\tau_Z N_{\text{opt}}}\right)^2\right]^{N_{\text{opt}}}\\&\simeq a^{N_{\text{opt}}}\exp\left(\frac{b}{a}t_1+\frac{c}{a}\frac{t_1^2}{N_{\text{opt}}}-\frac{1}{2}\frac{b^2}{a^2}\frac{t_1^2}{N_{\text{opt}}}-\frac{t_2^2}{\tau_Z^2N_{\text{opt}}}\right)\\&\simeq a^{2N_{\text{opt}}}\exp\left(\frac{b}{a}t_1\right),\end{aligned} \tag{4.8}$$

where we used Eq. (4.7) in the last equality. The factor $a^{2N_{\text{opt}}}$ is due to the two (almost equal) terms L and p in Eq. (4.1), each contributing $a^{N_{\text{opt}}}$. Equations (4.7) and (4.8) are the main results of this section and express the optimal frequency of GSDs, τ_{opt}^{-1}, and the maximal survival probability $\tilde{P}^{(N_{\text{opt}})}(\theta)$ as a function of the parameters characterizing the system and the apparatus.

Let us look at some particular cases. If $a\to 1$ (and $\forall b,c$), corresponding to (almost) lossless GSDs, $\tau_{\text{opt}}\to 0$ and one gets the usual QZE, with no limitations on the frequency of GSDs: infinitely frequent GSDs slow down the evolution away from the initial quantum state. However, due to the presence of losses, the survival probability is not unity, even in the limit of infinitely frequent GSDs:

$$\begin{aligned}\tilde{P}^{(N_{\text{opt}})}(\theta)&=\tilde{P}^{(\infty)}(\theta)\\&=\exp(-|b|t_1) \quad (a\to 1),\end{aligned} \tag{4.9}$$

where we took into account the fact that $b<0$ due to Eq. (4.2) and $a=1$. This result is intuitively clear: due to the presence of linear losses in t in Eq. (4.5), one cannot hope that the Zeno mechanism can work better than Eq. (4.9). It is worth noticing that there are analogies between this approach and the interesting work by Berry and Klein on twisted stacks of light polarizers [15]. It should be emphasized that the practical limitations one has to face in the case of very frequent "pulsed" measurements (N large) are encompassed when one considers "continuous" measurement processes, due to a Hamiltonian interaction with an external system playing the role of the apparatus. This is relevant in the light of the physical equivalence between the pulsed and continuous formulations of the QZE [16].

If, on the other hand, $a \lesssim 1$, corresponding to instantaneous losses, occurring on a GSD time scale (which we assume to be much shorter than any other time scale: $t_1 \ll t_2 \simeq t$, or $\alpha_1 \ll \alpha_2 \simeq 1$), Eq. (4.7) yields

$$N_{\rm opt} \simeq \frac{t}{\tau_Z \sqrt{\ln a^{-1}}} \simeq \frac{t}{\tau_Z \sqrt{1-a}}. \tag{4.10}$$

This is the case considered in the preceding section: if one recalls the definition of θ in Eq. (2.3) and identifies $a = |T_\uparrow|^2$, one recovers Eq. (3.18). In this case the survival probability (4.8) reduces to Eq. (3.19a).

Equations (4.7) and (4.8) enable one to look at the "lossy" Zeno phenomenon from a more general perspective. Clearly, in *any* physical situation, the optimal frequency (4.7) to obtain a QZE is smaller than ∞ and the optimal survival probability (4.8) is smaller than 1.

V. SUMMARY

We have discussed a neutron-spin experimental test of the QZE from a practical point of view, taking account of the inevitable imperfection in the GSD at the magnetic mirror. We endeavored to clarify that losses are important, but do not make an experimental test of the QZE unrealistic. This is probably somewhat at variance with expectation, for losses *exponentially* propagate in a Zeno setup, involving N repetitions of one and the same GSD. However, we have seen that, if duly taken into account, the disruptive effect of losses can be controlled and an interesting test is still feasible for rather large values of N. This is a positive conclusion, from an experimental perspective. Our conclusions are of general validity for any practical test of the QZE.

ACKNOWLEDGMENTS

We acknowledge fruitful discussions and a useful exchange of ideas with I. Ohba. K.Y. thanks L. Accardi and K. Imafuku for enlightening comments and discussions. We also thank H. Rauch and his collaborators for useful discussions and for kindly giving us detailed information about their VESTA apparatus, realized within the TMR European Network on "Perfect Crystal Neutron Optics" (Grant No. ERB-FMRX-CT96-0057). Figure 2 is reproduced with their permission. This work was partly supported by Grants-in-Aid for Scientific Research (C) from the Japan Society for the Promotion of Science (Grant No. 14540280) and Priority Areas Research (B) from the Ministry of Education, Culture, Sports, Science and Technology, Japan (Grant No. 13135221), by a Waseda University Grant for Special Research Projects (Grant No. 2002A-567), and by the bilateral Italian-Japanese project 15C1 on "Quantum Information and Computation" of the Italian Ministry for Foreign Affairs.

APPENDIX: SPIN-FLIP EFFECTS AT THE MAGNETIC MIRRORS

In practice, one cannot exclude the possibility that a spin flip occurs at the magnetic mirrors. This effect introduces additional mistakes and was neglected in Sec. III. In this appendix, we take it into account and clarify its role in the QZE.

The effects of the nth magnetic mirror on a spin-up and a spin-down neutron read

$$|\uparrow\rangle \otimes |t_{n-1}\rangle \to (T_{\uparrow\uparrow}|\uparrow\rangle + T_{\downarrow\uparrow}|\downarrow\rangle) \otimes |t_n\rangle + (R_{\uparrow\uparrow}|\uparrow\rangle + R_{\downarrow\uparrow}|\downarrow\rangle) \otimes |r_n\rangle \tag{A1}$$

and

$$|\downarrow\rangle \otimes |t_{n-1}\rangle \to (T_{\downarrow\downarrow}|\downarrow\rangle + T_{\uparrow\downarrow}|\uparrow\rangle) \otimes |t_n\rangle + (R_{\downarrow\downarrow}|\downarrow\rangle + R_{\uparrow\downarrow}|\uparrow\rangle) \otimes |r_n\rangle, \tag{A2}$$

respectively, where $T_{\downarrow\uparrow}$, $T_{\uparrow\downarrow}$ ($R_{\downarrow\uparrow}$, $R_{\uparrow\downarrow}$) are the probability amplitudes for spin-flips when the neutron is transmitted (reflected), and the two constraints $|T_{\uparrow\uparrow}|^2 + |T_{\downarrow\uparrow}|^2 + |R_{\uparrow\uparrow}|^2 + |R_{\downarrow\uparrow}|^2 = 1$ and $|T_{\downarrow\downarrow}|^2 + |T_{\uparrow\downarrow}|^2 + |R_{\downarrow\downarrow}|^2 + |R_{\uparrow\downarrow}|^2 = 1$ hold. Hence the action of the magnetic mirror on a neutron in a general spin state $|S\rangle$ reads

$$\begin{aligned} |S\rangle \otimes |t_{n-1}\rangle &\equiv (c_\uparrow|\uparrow\rangle + c_\downarrow|\downarrow\rangle) \otimes |t_{n-1}\rangle \\ &\to [c_\uparrow(T_{\uparrow\uparrow}|\uparrow\rangle + T_{\downarrow\uparrow}|\downarrow\rangle) \\ &\quad + c_\downarrow(T_{\downarrow\downarrow}|\downarrow\rangle + T_{\uparrow\downarrow}|\uparrow\rangle)] \otimes |t_n\rangle \\ &\quad + [c_\uparrow(R_{\uparrow\uparrow}|\uparrow\rangle + R_{\downarrow\uparrow}|\downarrow\rangle) \\ &\quad + c_\downarrow(R_{\downarrow\downarrow}|\downarrow\rangle + R_{\uparrow\downarrow}|\uparrow\rangle)] \otimes |r_n\rangle \\ &= \tilde{\mathcal{T}}|S\rangle \otimes |t_n\rangle + \tilde{\mathcal{R}}|S\rangle \otimes |r_n\rangle, \end{aligned} \tag{A3}$$

where

$$\tilde{\mathcal{T}} = |\uparrow\rangle T_{\uparrow\uparrow}\langle\uparrow| + |\uparrow\rangle T_{\uparrow\downarrow}\langle\downarrow| + |\downarrow\rangle T_{\downarrow\uparrow}\langle\uparrow| + |\downarrow\rangle T_{\downarrow\downarrow}\langle\downarrow|, \tag{A4a}$$

$$\tilde{\mathcal{R}} = |\uparrow\rangle R_{\uparrow\uparrow}\langle\uparrow| + |\uparrow\rangle R_{\uparrow\downarrow}\langle\downarrow| + |\downarrow\rangle R_{\downarrow\uparrow}\langle\uparrow| + |\downarrow\rangle R_{\downarrow\downarrow}\langle\downarrow|. \tag{A4b}$$

Compare with Eq. (3.3). The operator $\tilde{\mathcal{T}} e^{-iHt/N\hbar}$ now reads

$$\begin{aligned} \tilde{\mathcal{T}} e^{-iHt/N\hbar} &= \frac{1}{2}\left[(T_{\uparrow\uparrow} + T_{\downarrow\downarrow})\cos\frac{\theta}{N} - i(T_{\uparrow\downarrow} + T_{\downarrow\uparrow})\sin\frac{\theta}{N}\right] \\ &\quad + \sigma_x \frac{1}{2}\left[(T_{\uparrow\downarrow} + T_{\downarrow\uparrow})\cos\frac{\theta}{N} - i(T_{\uparrow\uparrow} + T_{\downarrow\downarrow})\sin\frac{\theta}{N}\right] \\ &\quad + \sigma_y \frac{i}{2}\left[(T_{\uparrow\downarrow} - T_{\downarrow\uparrow})\cos\frac{\theta}{N} - i(T_{\uparrow\uparrow} - T_{\downarrow\downarrow})\sin\frac{\theta}{N}\right] \\ &\quad + \sigma_z \frac{1}{2}\left[(T_{\uparrow\uparrow} - T_{\downarrow\downarrow})\cos\frac{\theta}{N} - i(T_{\uparrow\downarrow} - T_{\downarrow\uparrow})\sin\frac{\theta}{N}\right] \end{aligned} \tag{A5}$$

and its eigenvalues $\xi_\pm(N)$ are given by

$$\xi_\pm(N) = C \pm \sqrt{C^2 - (T_{\uparrow\uparrow}T_{\downarrow\downarrow} - T_{\uparrow\downarrow}T_{\downarrow\uparrow})}, \tag{A6a}$$

with

$$C=\frac{1}{2}\left[(T_{\uparrow\uparrow}+T_{\downarrow\downarrow})\cos\frac{\theta}{N}-i(T_{\uparrow\downarrow}+T_{\downarrow\uparrow})\sin\frac{\theta}{N}\right]. \quad \text{(A6b)}$$

A calculation similar to that in Sec. III yields the survival probability

$$\tilde{P}^{(N)}(\theta)=\left|A(N)-B(N)\left(T_{\downarrow\downarrow}\cos\frac{\theta}{N}-iT_{\downarrow\uparrow}\sin\frac{\theta}{N}\right)\right|^2 + \left|B(N)\left(T_{\downarrow\downarrow}\sin\frac{\theta}{N}+iT_{\downarrow\uparrow}\cos\frac{\theta}{N}\right)\right|^2, \quad \text{(A7)}$$

where $A(N)$ and $B(N)$ are defined as in Eqs. (3.11a) and (3.11b), respectively, but with the eigenvalues $\xi_{\pm}(N)$ in Eq. (A6). For $|T_{\downarrow\downarrow}|$, $|T_{\uparrow\downarrow}|$, $|T_{\downarrow\uparrow}|\ll|T_{\uparrow\uparrow}|$, probability (A7) is readily evaluated as

$$\tilde{P}^{(N)}(\theta)\simeq|T_{\uparrow\uparrow}|^{2N}\left(\cos\frac{\theta}{N}\right)^{2N} \times\left[1-2\,\mathrm{Re}\left(\frac{T_{\downarrow\downarrow}}{T_{\uparrow\uparrow}}\right)(N-1)\tan^2\frac{\theta}{N} +2\,\mathrm{Im}\left(\frac{T_{\uparrow\downarrow}}{T_{\uparrow\uparrow}}\right)N\tan\frac{\theta}{N} +2\,\mathrm{Im}\left(\frac{T_{\downarrow\uparrow}}{T_{\uparrow\uparrow}}\right)(N-1)\tan\frac{\theta}{N}+\cdots\right], \quad \text{(A8)}$$

which shows that the probability $\tilde{P}^{(N)}(\theta)$ is again dominated by factor (3.15) (with $|T_{\uparrow}|$ replaced by $|T_{\uparrow\uparrow}|$), and the spin flips at the mirrors yield only a first-order correction.

[1] A. Beskow and J. Nilsson, Ark. Fys. **34**, 561 (1967); L.A. Khalfin, Pis'ma Zh. Eksp. Teor. Fiz. **8**, 106 (1968) [JETP Lett. **8**, 65 (1968)].

[2] B. Misra and E.C.G. Sudarshan, J. Math. Phys. **18**, 756 (1977).

[3] For reviews, see H. Nakazato, M. Namiki, and S. Pascazio, Int. J. Mod. Phys. B **10**, 247 (1996); D. Home and M.A.B. Whitaker, Ann. Phys. (N.Y.) **258**, 237 (1997); P. Facchi and S. Pascazio, *Progress in Optics*, edited by E. Wolf (Elsevier, Amsterdam, 2001), Vol. 42, p. 147.

[4] W.H. Itano, D.J. Heinzen, J.J. Bollinger, and D.J. Wineland, Phys. Rev. A **41**, 2295 (1990).

[5] R.J. Cook, Phys. Scr. **T21**, 49 (1988).

[6] S.R. Wilkinson, C.F. Bharucha, M.C. Fischer, K.W. Madison, P.R. Morrow, Q. Nu, B. Sundaram, and M.G. Raizen, Nature (London) **387**, 575 (1997); M.C. Fischer, B. Gutiérrez-Medina, and M.G. Raizen, Phys. Rev. Lett. **87**, 040402 (2001).

[7] A.M. Lane, Phys. Lett. A **99**, 359 (1983); W.C. Schieve, L.P. Horwitz, and J. Levitan, *ibid.* **136**, 264 (1989); S.A. Gurvitz, Phys. Rev. B **56**, 15215 (1997); A.G. Kofman and G. Kurizki, Nature (London) **405**, 546 (2000); P. Facchi, H. Nakazato, and S. Pascazio, Phys. Rev. Lett. **86**, 2699 (2001).

[8] H. Nakazato, M. Namiki, S. Pascazio, and H. Rauch, Phys. Lett. A **199**, 27 (1995); Z. Hradil, H. Nakazato, M. Namiki, S. Pascazio, and H. Rauch, *ibid.* **239**, 333 (1998); K. Machida, H. Nakazato, S. Pascazio, H. Rauch, and S. Yu, Phys. Rev. A **60**, 3448 (1999).

[9] S. Pascazio, M. Namiki, G. Badurek, and H. Rauch, Phys. Lett. A **179**, 155 (1993); S. Pascazio and M. Namiki, Phys. Rev. A **50**, 4582 (1994).

[10] M. Schuster, C.J. Carlile, and H. Rauch, Z. Phys. B: Condens. Matter **85**, 49 (1991); E. Jericha, C.J. Carlile, M. Jäkel, and H. Rauch, Physica B **234-236**, 1066 (1997); E. Jericha, D.E. Schwab, M.R. Jäkel, C.J. Carlile, and H. Rauch, *ibid.* **283**, 414 (2000).

[11] H. Rauch, Physica B **297**, 299 (2001).

[12] E.P. Wigner, Am. J. Phys. **31**, 6 (1963).

[13] T. Petrosky, S. Tasaki, and I. Prigogine, Phys. Lett. A **151**, 109 (1990); Physica A **170**, 306 (1991).

[14] I. Antoniou, E. Karpov, G. Pronko, and E. Yarevsky, Phys. Rev. A **63**, 062110 (2001); T. Petrosky and V. Barsegov, Phys. Rev. E **65**, 046102 (2002).

[15] M.V. Berry and S. Klein, J. Mod. Opt. **43**, 165 (1996); P. Facchi, A.G. Klein, S. Pascazio, and L.S. Schulman, Phys. Lett. A **257**, 232 (1999).

[16] L.S. Schulman, Phys. Rev. A **57**, 1509 (1998).

Proc. Waseda Int. Sympo. on Fundamental Physics —New Perspectives in Quantum Physics—
J. Phys. Soc. Jpn. Vol. 72 (2003) Suppl. C pp. 34–37

Purification of Quantum State through Zeno-like Measurements

Kazuya YUASA,* Hiromichi NAKAZATO† and Tomoko TAKAZAWA

Department of Physics, Waseda University, Tokyo 169-8555, Japan

(Received February 14, 2003)

We present a novel procedure to purify quantum states, i.e., purification through Zeno-like measurements. By simply repeating one and the same measurement on a quantum system, one can purify another system in interaction with the former. The conditions for the (efficient) purification are specified on a rather general setting, and the framework of the method possesses wide applicability. It is explicitly demonstrated on a specific setup that the purification becomes very efficient by tuning relevant parameters.

KEYWORDS: purification of quantum states, quantum Zeno effect, repeated measurement

One cannot observe a quantum system without any disturbance on the object, and the dynamics of the quantum system is affected by the measurement. An interesting manifestation of this effect is the "quantum Zeno effect" (QZE):[1–3] if one repeats measurement very frequently in order to ascertain whether a system remains in the initial state, the evolution of the system is slowed down and totally hindered in the limit of infinite frequency. Or conversely, one can also accelerate the decay of an unstable state by repeating the measurement less frequently than a critical frequency (inverse QZE).[4] These are typical examples of the effects of measurement on quantum dynamics.

In this article, we present another interesting effect of measurement on quantum dynamics when the measurement is repeated as in the case of the (inverse) QZE: *purification of quantum state through Zeno-like measurements.*[5] We show in the following that a series of measurements on a quantum system indirectly affects the dynamics of another system in interaction with the former, and the latter (initially in any mixed state) is driven into a *pure* state, provided certain conditions are satisfied. The state of the latter system is purified through the repeated measurement on the former.

In the ideas of quantum information and computation, quantum coherence plays crucial roles.[6,7] It is hence one of the important issues to be addressed how to maintain and/or recover quantum coherence, and various schemes have been proposed attacking this subject.[6–14] The work presented here contributes to this issue and provides a novel method to purify quantum states (i.e., to recover quantum coherence), which is simple compared to the standard purification techniques[6,9,10] and the framework is rather general.

Let a total system A+B be described by a Hamiltonian of the form

$$H = H_{\rm A} + H_{\rm B} + H_{\rm int}, \tag{1}$$

where $H_{\rm A(B)}$ is a free Hamiltonian of system A(B) and $H_{\rm int}$ is an interaction between A and B. We prepare system A in a pure state $|\phi\rangle$ at time $t = 0$, while the initial state of system B, denoted by $\rho_{\rm B}$, can be arbitrary (a mixed state). The total system starts to evolve from the initial state

$$\rho_0 = |\phi\rangle\langle\phi| \otimes \rho_{\rm B} \tag{2}$$

with the Hamiltonian (1), and we check the state of system A at time $t = \tau$. If it is confirmed that system A remains in its initial state $|\phi\rangle$, the state of the total system is projected by a projection operator

$$\mathcal{O} = |\phi\rangle\langle\phi| \otimes \mathbb{1} \tag{3}$$

and restarts to evolve. We repeat such a measurement regularly at time intervals τ (Zeno-like measurement) as long as system A is found in the state $|\phi\rangle$ at every step.

Notice that we do not check the state of system B and the projection operator (3) does not return the time-evolved total system to its initial state: system A is set back to its initial state $|\phi\rangle$ but system B is not. System B evolves away from its initial state under the sequence of measurements on system A. We are interested in such evolution of system B, which is indirectly affected by the measurement repeated on system A through the interaction $H_{\rm int}$. We shall show in the following that such evolution can result in a purification phenomenon: system B evolves into a *pure* state irrespectively of its initial (mixed) state $\rho_{\rm B}$, if certain conditions specified below are satisfied.

System A is confirmed to be in the state $|\phi\rangle$ successively N times with the probability

$$\begin{aligned} P^{(\tau)}(N) &= {\rm Tr}[(\mathcal{O}e^{-iH\tau}\mathcal{O})^N \rho_0 (\mathcal{O}e^{iH\tau}\mathcal{O})^N] \\ &= {\rm Tr}_{\rm B}[(V_\phi(\tau))^N \rho_{\rm B} (V_\phi^\dagger(\tau))^N], \end{aligned} \tag{4}$$

where the operator $V_\phi(\tau) \equiv \langle\phi|e^{-iH\tau}|\phi\rangle$ is an operator acting on the Hilbert space of system B. (Once system A is found in a different state from $|\phi\rangle$, we stop proceeding to the next step, failing to purify the state of system B.) After the N successful confirmations, the total and B systems are in the states

$$\rho^{(\tau)}(N) = |\phi\rangle\langle\phi| \otimes \rho_{\rm B}^{(\tau)}(N), \tag{5}$$

$$\rho_{\rm B}^{(\tau)}(N) = (V_\phi(\tau))^N \rho_{\rm B} (V_\phi^\dagger(\tau))^N / P^{(\tau)}(N), \tag{6}$$

respectively.

* E-mail address: yuasa@hep.phys.waseda.ac.jp
† E-mail address: hiromici@waseda.jp

In the ordinary situation where the measurement is repeated at an infinite frequency by taking the limit $N \to \infty$ keeping $T = N\tau$ finite, the probability $P^{(\tau)}(N)$ in (4) increases as N becomes large, approaching unity $P^{(\tau)}(N) \to 1$ and the ordinary QZE[2] appears. At the same time, the dynamics of system B in (6) becomes unitary $(V_\phi(T/N))^N \to \mathcal{V}_\phi(T)$ (a unitary operator) in this limit. This is an example of the so-called "quantum Zeno dynamics."[12,14,15] We are however interested in a different situation: we repeat the measurement with a nonvanishing (not necessarily small) τ. The probability $P^{(\tau)}(N)$ would decay out completely for such a finite τ, but we are interested in the asymptotic behavior of the state of system B, $\rho_{\rm B}^{(\tau)}(N)$, for large (but finite) values of N.

In order to clarify the evolution of system B under the Zeno-like measurement on system A, let us consider the eigenvalue problem of the projected time-evolution operator $V_\phi(\tau)$. Since the operator $V_\phi(\tau)$ is not Hermitian, we need to set up both the right- and left-eigenvalue problems

$$V_\phi(\tau)|u_n) = \lambda_n|u_n), \quad (v_n|V_\phi(\tau) = \lambda_n(v_n|. \tag{7}$$

The eigenvalue λ_n is in general complex valued and satisfies $0 \le |\lambda_n| \le 1$, $\forall n$, which reflects the unitarity of the time-evolution operator. Let us assume for the moment that the spectrum of the operator $V_\phi(\tau)$ is discrete and nondegenerate. The eigenvectors then form an orthonormal complete set in the following sense:

$$\sum_n |u_n)(v_n| = \mathbb{1}, \quad (v_m|u_n) = \delta_{mn}. \tag{8}$$

The operator $V_\phi(\tau)$ itself is expanded in terms of the eigenvectors

$$V_\phi(\tau) = \sum_n \lambda_n |u_n)(v_n|, \tag{9}$$

and we obtain

$$(V_\phi(\tau))^N = \sum_n \lambda_n^N |u_n)(v_n|, \tag{10}$$

which asymptotically behaves for large N as

$$(V_\phi(\tau))^N \xrightarrow{\text{large } N} \lambda_0^N |u_0)(v_0| \tag{11}$$

if the largest (in magnitude) eigenvalue λ_0 is unique, discrete, and nondegenerate. It is now evident that the state of system B, $\rho_{\rm B}^{(\tau)}(N)$ given in (6), asymptotically approaches a pure state

$$\rho_{\rm B}^{(\tau)}(N) \xrightarrow{\text{large } N} |u_0)(u_0|/(u_0|u_0), \tag{12}$$

i.e., as we repeat the confirmation that system A is in the state $|\phi\rangle$ at regular intervals τ, system B is driven into the pure state $|u_0)$. This is what we call "purification through Zeno-like measurements."

Notice that the final pure state $|u_0)$ is independent of the initial state of system B, $\rho_{\rm B}$, i.e., any initial (mixed) state is purified into the unique pure state $|u_0)$ through the Zeno-like measurement on system A. The pure state $|u_0)$ is the eigenstate belonging to the largest (in magnitude) eigenvalue λ_0 of the projected time-evolution operator $V_\phi(\tau)$ and is prescribed by the Hamiltonian H, the measurement interval τ, and the state $|\phi\rangle$ onto which system A is repeatedly projected. We therefore have the possibility to purify system B into a *desired* pure state by adjusting τ, $|\phi\rangle$, and H.

But one cannot always purify system B successfully. System A should be found in the state $|\phi\rangle$ at *every* measurement for the purification to be accomplished, but the probability for this to occur, which is nothing but the probability $P^{(\tau)}(N)$ given in (4), is less than 1, unfortunately. It decays asymptotically as

$$P^{(\tau)}(N) \xrightarrow{\text{large } N} |\lambda_0|^{2N}(u_0|u_0)(v_0|\rho_{\rm B}|v_0), \tag{13}$$

which gives the yield of the purification protocol presented here. For an efficient purification with high yield $P^{(\tau)}(N)$, you can adjust parameters again to satisfy $|\lambda_0| = 1$, which prevents the yield $P^{(\tau)}(N)$ from decaying out completely. We will come back to this point below.

Before going on, let us recapitulate the conditions for the purification. The heart of the mechanism of the purification is the asymptotic behavior of the operator $(V_\phi(\tau))^N$ in (11), which is true *if the largest (in magnitude) eigenvalue λ_0 is unique, discrete, and nondegenerate.* Although we assumed above for concreteness that the spectrum of the operator $V_\phi(\tau)$ is discrete and nondegenerate, these assumptions on the spectrum is not essential for the purification except for the conditions on the largest (in magnitude) eigenvalue λ_0. One has only to check the largest (in magnitude) eigenvalue λ_0, which should be *unique, discrete, and nondegenerate.* In the field of quantum information and computation, for example, finite level (two- or three-level) systems play important roles, and we can easily expect that such systems with discrete spectra fulfill these conditions.

Let us illustrate the purification described above with a model Hamiltonian

$$H = \Omega a^\dagger a + \omega b^\dagger b + ig(a^\dagger b - ab^\dagger), \tag{14}$$

i.e., two single-mode harmonic oscillators a and b in interaction with the rotating-wave approximation. The frequencies Ω and ω and the coupling constant g are real parameters. At time $t = 0$, we prepare oscillator a in a coherent state $|\alpha\rangle$ specified by a complex parameter α, while the state of oscillator b is arbitrary. We let the total system evolve with the Hamiltonian (14) and confirm repeatedly at regular intervals τ that oscillator a is in the coherent state $|\alpha\rangle$. The time-evolution operator (between adjacent measurements), $e^{-iH\tau}$, is calculated exactly to be

$$e^{-iH\tau} = e^{Aa^\dagger b} e^{Ba^\dagger a} e^{Cb^\dagger b} e^{-Aab^\dagger} \tag{15}$$

in terms of the τ-dependent functions

$$A = \frac{(g/\delta)\sin\delta\tau}{\cos\delta\tau + i[(\Omega-\omega)/2\delta]\sin\delta\tau}, \tag{16a}$$

$$B = -\frac{i}{2}(\Omega+\omega)\tau - \ln\left(\cos\delta\tau + i\frac{\Omega-\omega}{2\delta}\sin\delta\tau\right), \tag{16b}$$

$$C = -\frac{i}{2}(\Omega+\omega)\tau + \ln\left(\cos\delta\tau + i\frac{\Omega-\omega}{2\delta}\sin\delta\tau\right), \quad (16c)$$

where $\delta = \sqrt{g^2+(\Omega-\omega)^2/4}$, and the projected time-evolution operator $V_\alpha(\tau) \equiv \langle\alpha|e^{-iH\tau}|\alpha\rangle$ reads

$$V_\alpha(\tau) = e^{-|\alpha|^2[1-e^B-A^2/(1-e^{-C})]}e^{D(b^\dagger,b)}, \quad (17a)$$

$$D(b^\dagger,b) = C\left(b^\dagger + \frac{A\alpha^*}{1-e^{-C}}\right)\left(b - \frac{A\alpha}{1-e^{-C}}\right), \quad (17b)$$

whose spectrum is given by

$$\lambda_n = e^{-|\alpha|^2[1-e^B-A^2/(1-e^{-C})]}e^{nC}, \quad (18a)$$

$$|u_n) = U|n), \quad (v_n| = (n|U^{-1}, \quad (18b)$$

$$U = \exp\left[\frac{A}{1-e^{-C}}(\alpha^* b + \alpha b^\dagger)\right], \quad (18c)$$

where $n = 0,1,2,\ldots$ and $\{|n)\}$ are the number states of oscillator b. Since the absolute value of e^C is $|e^C| = \sqrt{1-(g/\delta)^2\sin^2\delta\tau} \leq 1$, the largest (in magnitude) eigenvalue of the relevant operator $V_\alpha(\tau)$ is λ_0 unless $|e^C| = 1$, which is explicitly given by

$$\begin{aligned}\lambda_0 &= e^{-|\alpha|^2[1-e^B-A^2/(1-e^{-C})]} \\ &= \exp\left[-2|\alpha|^2\left\{1 - \frac{i}{2}\left[\left(1+\frac{\Omega-\omega}{2\delta}\right)\cot\frac{\Omega_+\tau}{2} \right.\right.\right. \\ &\qquad \left.\left.\left. + \left(1-\frac{\Omega-\omega}{2\delta}\right)\cot\frac{\Omega_-\tau}{2}\right]\right\}^{-1}\right],\end{aligned} \quad (19)$$

where $\Omega_\pm = (\Omega+\omega)/2 \pm \delta$, and is discrete and nondegenerate, satisfying the conditions for the purification. We see therefore that oscillator b, initially in any (mixed) state, is purified into the pure state $|u_0)$, i.e., into a coherent state

$$|u_0) = U|0) = \left|\frac{A\alpha}{1-e^{-C}}\right), \quad (20)$$

as we repeatedly confirm at time intervals τ that oscillator a is in the coherent state $|\alpha\rangle$, provided $\delta\tau \neq m\pi$ $(m = 0,1,2,\ldots)$.

In fact, for an initial state $\rho_B \propto e^{-\beta\omega b^\dagger b}$ (β is a positive parameter), the state of oscillator b under the Zeno-like measurement, $\rho_B^{(\tau)}(N)$, is explicitly evaluated to be

$$\begin{aligned}\rho_B^{(\tau)}(N) &= (1-|e^C|^{2N}e^{-\beta\omega}) \\ &\quad \times D(N)e^{-(\beta\omega-2N\,\mathrm{Re}\,C)b^\dagger b}D^\dagger(N),\end{aligned} \quad (21a)$$

$$D(N) = \exp\left(-\frac{\alpha\Theta(N)b^\dagger - \alpha^*\Theta^*(N)b}{1-|e^C|^{2N}e^{-\beta\omega}}\right), \quad (21b)$$

$$\Theta(N) = \frac{1-e^{NC}}{1-e^{-C}}A - \left(\frac{1-e^{NC}}{1-e^{-C}}A\right)^* e^{NC}e^{-\beta\omega}, \quad (21c)$$

which indeed approaches the coherent state (20)

$$\rho_B^{(\tau)}(N) \xrightarrow{N\to\infty} D(\infty)|0)(0|D^\dagger(\infty) = \left|\frac{A\alpha}{1-e^{-C}}\right) \quad (22)$$

if $\mathrm{Re}\,C \neq 0$. [$|0)$ here is normalized to unity, i.e., $(0|0) = 1$.]

Let us finally discuss the efficiency of the purification. For this purpose, we introduce the so-called fidelity $F^{(\tau)}(N)$ for the target pure state $|u_0)$:

$$F^{(\tau)}(N) \equiv (u_0|\rho_B^{(\tau)}(N)|u_0). \quad (23)$$

We want to achieve high fidelity $F^{(\tau)}(N)$ close to 1 with high yield $P^{(\tau)}(N)$ after a small number of measurements, N. We can make the fidelity $F^{(\tau)}(N)$ as high as we want by indefinitely increasing the number of measurements, N, while the yield $P^{(\tau)}(N)$ would keep decaying asymptotically as (13). It is however possible to prevent the decay of the yield $P^{(\tau)}(N)$ in (13) by adjusting relevant parameters to satisfy the condition

$$|\lambda_0| = 1. \quad (24)$$

If, at the same time, the absolute values of the other eigenvalues λ_n $(\forall n \neq 0)$ are much smaller than that of λ_0, i.e.,

$$|\lambda_n/\lambda_0| \ll 1 \quad (\forall n \neq 0), \quad (25)$$

we can purify a quantum state quickly. Equations (24) and (25) are the conditions for an efficient purification.

For the above oscillator model, we can indeed achieve these conditions: by tuning the time interval between measurements as $\tau = 2m\pi/|\Omega_\pm|$ $(m = 0,1,2,\ldots)$, we have $\lambda_0 = 1$. [See (19).] The fidelity $F^{(\tau)}(N)$ and the yield $P^{(\tau)}(N)$ for the oscillator model are shown in Fig. 1, where τ is tuned to be $\tau = 2\pi/\Omega_+$. The decay of the yield $P^{(\tau)}(N)$ is suppressed due to this tuning, and a very high fidelity is achieved after only $N = 2$ steps since the ratio of the second largest (in magnitude) eigenvalue λ_1 to the largest one λ_0, i.e., $|\lambda_1/\lambda_0| = |e^C|$, is well less than 1.

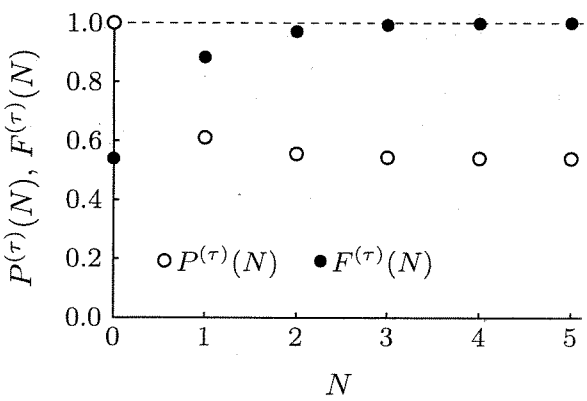

Fig. 1. Fidelity $F^{(\tau)}(N)$ and yield $P^{(\tau)}(N)$ for the oscillator model (14) when the initial state of oscillator a, onto which N measurements are performed, is a coherent state $|\alpha\rangle$ and that of oscillator b is $\rho_B \propto e^{-\beta\omega}$. The parameters are taken to be $\omega = 1$, $g = 0.2$, $\beta = 1$, $\alpha = 0.5$, and $\tau = 2\pi/\Omega_+ \simeq 5.24$ in units such that $\hbar = \Omega = 1$. τ is tuned so as to satisfy the condition (24) and the ratio of the second largest (in magnitude) eigenvalue λ_1 to the largest one λ_0 is $|\lambda_1/\lambda_0| = |e^C| \simeq 0.37$.

(See the caption of Fig. 1.)

The above discussions clearly reveal that repeated measurements on a quantum system dramatically affect the dynamics of another system in interaction with the former and the latter is driven into a pure state irrespectively of its initial (mixed) state. One can purify quantum states through Zeno-like measurements. This procedure is very simple compared to the other standard techniques:[6,9,10] we have only to repeat the same measurement. One can prescribe the final pure state by tuning the measurement interval τ, the state $|\phi\rangle$ onto which the former (controlled) system is repeatedly projected, and the Hamiltonian H.

Since we have clarified the mechanism of the purification under a rather general setup, without specifying the Hamiltonian, it possesses wide applicability. The only conditions for the purification one should check is that the largest (in magnitude) eigenvalue λ_0 of the projected time-evolution operator $V_\phi(\tau)$ be unique, discrete, and nondegenerate. Furthermore, careful control of this eigenvalue λ_0 leads us to an efficient purification, the conditions for which are given in (24) and (25).

In the field of quantum information and computation, entangled states play important roles, and many people are involved with the issue of "entanglement purification/distillation."[6,9] Our general framework of the purification also applies to this issue, and one can purify quantum entanglement through Zeno-like measurements discussed here, details of which will be reported elsewhere.[16] Further studies, e.g., to clarify the optimality of this method,[10] to propose some realistic physical setups, and so on, would provide us with deeper understandings on the present method.

The authors acknowledge fruitful discussions with Professor I. Ohba. K.Y. thanks Professors S. Tasaki and I. Ojima for comments and encouragements, and Professor T. Petrosky for discussions at the symposium. This work is partly supported by Grants-in-Aid for Scientific Research (C) from the Japan Society for the Promotion of Science (No. 14540280) and Priority Areas Research (B) from the Ministry of Education, Culture, Sports, Science and Technology, Japan (No. 13135221), and by a Waseda University Grant for Special Research Projects (No. 2002A-567).

1) A. Beskow and J. Nilsson: Ark. Fys. **34** (1967) 561; L. A. Khalfin: JETP Lett. **8** (1968) 65.
2) B. Misra and E. C. G. Sudarshan: J. Math. Phys. **18** (1977) 756.
3) H. Nakazato, M. Namiki and S. Pascazio: Int. J. Mod. Phys. B **10** (1996) 247; D. Home and M. A. B. Whitaker: Ann. Phys. **258** (1997) 237; P. Facchi and S. Pascazio: Progress in Optics **42**, ed. E. Wolf (Elsevier, Amsterdam, 2001) p. 147.
4) A. M. Lane: Phys. Lett. A **99** (1983) 359; W. C. Schieve, L. P. Horwitz and J. Levitan: *ibid.* **136** (1989) 264; S. A. Gurvitz: Phys. Rev. B **56** (1997) 15215; A. G. Kofman and G. Kurizki: Nature **405** (2000) 546; P. Facchi, H. Nakazato and S. Pascazio: Phys. Rev. Lett. **86** (2001) 2699.
5) H. Nakazato, T. Takazawa and K. Yuasa: Phys. Rev. Lett. **90** (2003) 060401.
6) *The Physics of Quantum Information*, ed. D. Bouwmeester, A. Ekert and A. Zeilinger (Springer-Verlag, Heidelberg, 2000), and references therein.
7) M. A. Nielsen and I. L. Chuang: *Quantum Computation and Quantum Information* (Cambridge University Press, Cambridge, 2000), and references therein.
8) P. W. Shor: Phys. Rev. A **52** (1995) 2493; A. R. Calderbank and P. W. Shor: *ibid.* **54** (1996) 1098; A. Steane: Proc. Roy. Soc. London A **452** (1996) 2551; Phys. Rev. Lett. **77** (1996) 793.
9) C. H. Bennett, G. Brassard, S. Popescu, B. Schumacher, J. A. Smolin and W. K. Wootters: Phys. Rev. Lett. **76** (1996) 722; **78** (1997) 2031(E); C. H. Bennett, D. P. DiVincenzo, J. A. Smolin and W. K. Wootters: Phys. Rev. A **54** (1996) 3824.
10) J. I. Cirac, A. K. Ekert and C. Macchiavello: Phys. Rev. Lett. **82** (1999) 4344.
11) G. M. Palma, K. A. Suominen and A. K. Ekert: Proc. Roy. Soc. London A **452** (1996) 567; L. M. Duan and G. C. Guo: Phys. Rev. Lett. **79** (1997) 1953; P. Zanardi and M. Rasetti: *ibid.* **79** (1997) 3306; D. A. Lidar, I. L. Chuang and K. B. Whaley: *ibid.* **81** (1998) 2594; A. Beige, D. Braun, B. Tregenna and P. L. Knight: *ibid.* **85** (2000) 1762; B. Tregenna, A. Beige and P. L. Knight: Phys. Rev. A **65** (2002) 032305.
12) P. Facchi and S. Pascazio: Phys. Rev. Lett. **89** (2002) 080401.
13) L. Viola and S. Lloyd: Phys. Rev. A **58** (1998) 2733; L. Viola, E. Knill and S. Lloyd: Phys. Rev. Lett. **82** (1999) 2417.
14) S. Tasaki, A. Tokuse, P. Facchi and S. Pascazio: quant-ph/0210129 (2002).
15) P. Facchi, A. G. Klein, S. Pascazio and L. S. Schulman: Phys. Lett. A **257** (1999) 232; P. Facchi, V. Gorini, G. Marmo, S. Pascazio and E. C. G. Sudarshan: *ibid.* **275** (2000) 12; P. Facchi, S. Pascazio, A. Scardicchio and L. S. Schulman: Phys. Rev. A **65** (2001) 012108; Also see, K. Machida, H. Nakazato, S. Pascazio, H. Rauch and S. Yu: Phys. Rev. A **60** (1999) 3448.
16) A similar mechanism to the one discussed here was employed for an entanglement generation in, M. B. Plenio, S. F. Huelga, A. Beige and P. L. Knight: Phys. Rev. A **59** (1999) 2468. In contrast to the method there, which utilizes dissipation and can create entanglement only from a limited class of initial states, our method can purify entanglement of any initial (decohered) states.

論文 5)

JOURNAL OF MODERN OPTICS, 15 APRIL–10 MAY 2004
VOL. 51, NO. 6–7, 1005–1009

Entanglement purification through Zeno-like measurements

K. YUASA, H. NAKAZATO and M. UNOKI
Department of Physics, Waseda University, Tokyo 169–8555, Japan

(*Received 3 November 2003; revision received 16 December 2003*)

Abstract. We present a novel method for purifying quantum states, i.e. *purification through Zeno-like measurements*, and show an application to *entanglement purification*.

1. Introduction

One of the main obstacles to the experimental realization of the ideas of quantum computation and quantum information is 'decoherence' [1, 2]. There are many attempts to overcome this problem, and several approaches have been proposed. Among these are the 'purification/distillation' technologies [2, 3], i.e. methods for extracting pure states, especially entanglements, from general mixed states recovering/preparing quantum coherence. Contributing to this subject, we have recently proposed a novel method for purifying quantum states, i.e. purification through Zeno-like measurements [4]. Here we show that it is possible to apply it for extracting *entanglement*, which is the key resource to the fundamentals of quantum computation and information.

2. Purification through Zeno-like measurements

Let us recapitulate the framework of our purification [4]. We consider two quantum systems X and A interacting with each other. The total system is initially in a general *mixed* state $\varrho_{\rm tot}$, from which we try to extract a pure state in A. We first make a measurement on X *to confirm that it is in a given state* $|\phi\rangle_{\rm X}$. If it is found in the state $|\phi\rangle_{\rm X}$, the state of the total system is projected by the projection operator

$$\mathcal{O} = |\phi\rangle_{\rm X}\langle\phi| \otimes \mathbb{1}_{\rm A}. \tag{1}$$

We then let the total system start to evolve under the Hamiltonian $H_{\rm tot}$ and repeat the same measurement on X at time intervals τ. After N repetitions of successful confirmations, the state of the total system, $\varrho_{\rm tot}^{(\tau)}(N)$, is given by

$$\varrho_{\rm tot}^{(\tau)}(N) = (\mathcal{O}e^{-iH_{\rm tot}\tau}\mathcal{O})^N \varrho_{\rm tot}(\mathcal{O}e^{iH_{\rm tot}\tau}\mathcal{O})^N / P^{(\tau)}(N) = |\phi\rangle_{\rm X}\langle\phi| \otimes \varrho_{\rm A}^{(\tau)}(N), \tag{2}$$

$$\varrho_{\rm A}^{(\tau)}(N) = [V_\phi(\tau)]^N \varrho_{\rm A} [V_\phi^\dagger(\tau)]^N / P^{(\tau)}(N), \tag{3}$$

where $\varrho_{\rm A} = {}_{\rm X}\langle\phi|\varrho_{\rm tot}|\phi\rangle_{\rm X}$ is the state of A after the zeroth confirmation,

$$V_\phi(\tau) \equiv {}_{\rm X}\langle\phi|e^{-iH_{\rm tot}\tau}|\phi\rangle_{\rm X} \tag{4}$$

Journal of Modern Optics ISSN 0950–0340 print/ISSN 1362–3044 online © 2004 Taylor & Francis Ltd
http://www.tandf.co.uk/journals
DOI: 10.1080/09500340410001664304

is a projected time-evolution operator, and $P^{(\tau)}(N)$ is the normalization factor,

$$P^{(\tau)}(N) = \mathrm{Tr}[(\mathcal{O}e^{-iH_{\mathrm{tot}}\tau}\mathcal{O})^N \varrho_{\mathrm{tot}}(\mathcal{O}e^{iH_{\mathrm{tot}}\tau}\mathcal{O})^N] = \mathrm{Tr}_{\mathrm{A}}\{[V_\phi(\tau)]^N \varrho_{\mathrm{A}}[V_\phi^\dagger(\tau)]^N\}. \tag{5}$$

Note that we retain only the events where X is found in the state $|\phi\rangle_{\mathrm{X}}$ at *every* measurement; other events, resulting in failure to purify A, are discarded. The normalization factor $P^{(\tau)}(N)$ in (5) is nothing but the probability for the *successful events* and is the probability of obtaining the state given in (2) and (3).

Let us assume for simplicity that the eigenvalues λ_n of $V_\phi(\tau)$, which are complex-valued in general, are discrete and $V_\phi(\tau)$ is decomposed (diagonalized) as

$$V_\phi(\tau) = \sum_n \lambda_n |u_n\rangle_{\mathrm{A}}\langle v_n|, \tag{6}$$

where $|u_n\rangle_{\mathrm{A}}$ and ${}_{\mathrm{A}}\langle v_n|$ are the right and left eigenvectors of $V_\phi(\tau)$, respectively, belonging to the eigenvalue λ_n and satisfy ${}_{\mathrm{A}}\langle v_n|u_m\rangle_{\mathrm{A}} = \delta_{mn}$. (The right eigenvectors are normalized as ${}_{\mathrm{A}}\langle u_n|u_n\rangle_{\mathrm{A}} = 1$ in the following.) It is now easy to observe the asymptotic behaviour of the state of A in (3). Since the eigenvalues λ_n are bounded as $0 \le |\lambda_n| \le 1$, each term in the expansion of $[V_\phi(\tau)]^N$ decays away and a single term dominates asymptotically as the number of measurements, N, increases,

$$[V_\phi(\tau)]^N = \sum_n \lambda_n^N |u_n\rangle_{\mathrm{A}}\langle v_n| \to \lambda_0^N |u_0\rangle_{\mathrm{A}}\langle v_0| \quad \text{as } N \text{ increases}, \tag{7}$$

provided the largest (in magnitude) eigenvalue λ_0 *is unique, discrete and nondegenerate.* Then, the state of A in (3) accordingly approaches the pure state $|u_0\rangle_{\mathrm{A}}$,

$$\varrho_{\mathrm{A}}^{(\tau)}(N) \to |u_0\rangle_{\mathrm{A}}\langle u_0| \quad \text{as } N \text{ increases}. \tag{8}$$

This is the purification we have found recently [4]: extraction of a pure state $|u_0\rangle_{\mathrm{A}}$ from an *arbitrary* mixed state ϱ_{A} through repeated measurements on X. Since we repeat measurements (on X) as in the case of the quantum Zeno effect [5], we call such measurements 'Zeno-like measurements'.[1]

The above observation shows that the assumption of the 'spectral decomposition' (6) is not essential but the existence of the *unique, discrete and nondegenerate largest eigenvalue* λ_0 is crucial for the purification. Furthermore, note the asymptotic behaviour of the 'success probability' $P^{(\tau)}(N)$: it decays asymptotically as

$$P^{(\tau)}(N) \to |\lambda_0|^{2N}\,{}_{\mathrm{A}}\langle v_0|\varrho_{\mathrm{A}}|v_0\rangle_{\mathrm{A}} \quad \text{as } N \text{ increases}, \tag{9}$$

which is dominated by the eigenvalue λ_0. Efficient purification is possible if it satisfies the condition $|\lambda_0| = 1$, which suppresses the decay in (9). At the same time, if the other eigenvalues are much smaller than λ_0 in magnitude, purification is achieved faster. Hence,

$$|\lambda_0| = 1, \qquad |\lambda_n/\lambda_0| \ll 1 \quad \text{for} \quad n \neq 0, \tag{10}$$

are the conditions for the *efficient purification*, which we try to achieve by adjusting parameters such as τ, $|\phi\rangle_{\mathrm{X}}$ and those in the Hamiltonian H_{tot}.

[1] It should be noted however that the time interval τ in this scheme is not necessarily small as in the ordinary Zeno measurements, and the purification (8) is not due to the quantum Zeno effect.

3. Application to entanglement purification

Now we show an interesting application of the above scheme: application to *entanglement purification*. Let us consider, for example, a three-qubit system with the Hamiltonian

$$H_{\rm tot} = \Omega\frac{1+\sigma_3^{\rm X}}{2} + \Omega\frac{1+\sigma_3^{\rm A}}{2} + \Omega\frac{1+\sigma_3^{\rm B}}{2} + g(\sigma_+^{\rm X}\sigma_-^{\rm A} + \sigma_-^{\rm X}\sigma_+^{\rm A}) + g(\sigma_+^{\rm X}\sigma_-^{\rm B} + \sigma_-^{\rm X}\sigma_+^{\rm B}), \tag{11}$$

where $\sigma_i\,(i = 1, 2, 3)$ are the Pauli operators and $\sigma_\pm = (\sigma_1 \pm i\sigma_2)/2$ are the ladder operators. Qubit X is coupled to qubits A and B. We confirm X to be in the state $|\phi\rangle_{\rm X}$ repeatedly at time intervals τ and end up with an extraction of an entanglement between A and B, which are initially in a general mixed state $\varrho_{\rm tot}$.

The projected time-evolution operator $V_\phi(\tau)$ is given, in this case, by

$$\begin{aligned} V_\phi(\tau) = {} & |\Psi^-\rangle_{\rm AB}\langle\Psi^-|\left(|\beta|^2 + |\alpha|^2 e^{-i\Omega\tau}\right)e^{-i\Omega\tau} \\ & + |\downarrow\downarrow\rangle_{\rm AB}\langle\downarrow\downarrow|\left(|\beta|^2 + |\alpha|^2 e^{-i\Omega\tau}\cos\sqrt{2}g\tau\right) \\ & + |\Psi^+\rangle_{\rm AB}\langle\Psi^+|\left(|\beta|^2 + |\alpha|^2 e^{-i\Omega\tau}\right)e^{-i\Omega\tau}\cos\sqrt{2}g\tau \\ & + |\uparrow\uparrow\rangle_{\rm AB}\langle\uparrow\uparrow|\left(|\beta|^2\cos\sqrt{2}g\tau + |\alpha|^2 e^{-i\Omega\tau}\right)e^{-i2\Omega\tau} \\ & - i\left(\alpha^*\beta|\downarrow\downarrow\rangle_{\rm AB}\langle\Psi^+| + \alpha\beta^*|\Psi^+\rangle_{\rm AB}\langle\downarrow\downarrow|\right)e^{-i\Omega\tau}\sin\sqrt{2}g\tau \\ & - i\left(\alpha\beta^*|\uparrow\uparrow\rangle_{\rm AB}\langle\Psi^+| + \alpha^*\beta|\Psi^+\rangle_{\rm AB}\langle\uparrow\uparrow|\right)e^{-i2\Omega\tau}\sin\sqrt{2}g\tau, \end{aligned} \tag{12}$$

where $|\Psi^\pm\rangle_{\rm AB} = (|\uparrow\downarrow\rangle_{\rm AB} \pm |\downarrow\uparrow\rangle_{\rm AB})/\sqrt{2}$ and $|\phi\rangle_{\rm X} = \alpha|\uparrow\rangle_{\rm X} + \beta|\downarrow\rangle_{\rm X}$, with $|\uparrow(\downarrow)\rangle$ the eigenstates of σ_3 belonging to the eigenvalues $+1\,(-1)$. Since the Hamiltonian (11) is symmetric under the exchange between A and B, $V_\phi(\tau)$ splits into the singlet and triplet sectors, and the singlet state $|\Psi^-\rangle_{\rm AB}$ is one of the four eigenstates of $V_\phi(\tau)$. It is hence possible to extract a Bell state $|\Psi^-\rangle_{\rm AB}$ provided (i) the corresponding eigenvalue

$$\lambda_{\Psi^-} = e^{-i\Omega\tau}\left(|\beta|^2 + |\alpha|^2 e^{-i\Omega\tau}\right) \tag{13}$$

is larger (in magnitude) than any other eigenvalue, and the extraction is efficient if the conditions (10), i.e. (ii) $|\lambda_{\Psi^-}| = 1$ and (iii) $|\lambda_n/\lambda_{\Psi^-}| \ll 1\,(n \neq \Psi^-)$, are fulfilled.

Condition (ii) is achieved by tuning τ such as

$$|\Omega|\tau = 2n\pi \quad (n = 0, 1, 2, \ldots), \tag{14}$$

and condition (i) is possible unless $|\phi\rangle_{\rm X} = |\uparrow\rangle_{\rm X}$ or $|\downarrow\rangle_{\rm X}$. Let us hence consider, under the condition (14), the case where

$$\alpha = \beta = 1/\sqrt{2}, \quad \text{i.e.} \quad |\phi\rangle_{\rm X} = |\rightarrow\rangle_{\rm X} \equiv \left(|\uparrow\rangle_{\rm X} + |\downarrow\rangle_{\rm X}\right)/\sqrt{2}. \tag{15}$$

In this case, three other eigenvalues than λ_{Ψ^-} are given by

$$\lambda_{\Phi^-} = \cos^2\frac{g\tau}{\sqrt{2}}, \quad \lambda_\pm = 1 - \frac{1}{2}\sin\frac{g\tau}{\sqrt{2}}\left(3\sin\frac{g\tau}{\sqrt{2}} \pm \sqrt{1 - 9\cos^2\frac{g\tau}{\sqrt{2}}}\right), \tag{16}$$

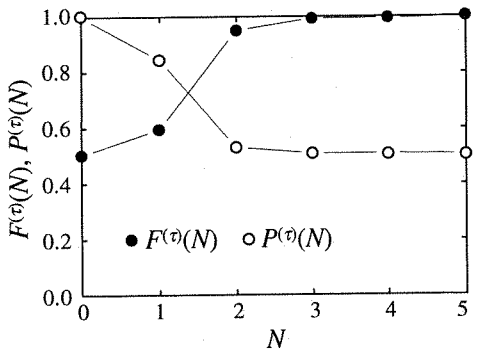

Figure 1. Extraction of a Bell state $|\Psi^-\rangle_{AB}$ from a product state $\varrho_{tot} = |\rightarrow\rangle_X\langle\rightarrow| \otimes |\uparrow\rangle_A\langle\uparrow| \otimes |\downarrow\rangle_B\langle\downarrow|$ [or from a mixed state $\varrho_{tot} = |\rightarrow\rangle_X\langle\rightarrow| \otimes (|\uparrow\downarrow\rangle_{AB}\langle\uparrow\downarrow| + |\downarrow\uparrow\rangle_{AB}\langle\downarrow\uparrow|)/2$]. Parameters are $\tau = 2\pi/\Omega$, $|\phi\rangle_X = |\rightarrow\rangle_X$ and $g = 0.25\Omega$ ($\Omega > 0$).

whose magnitudes are less than 1, fulfilling condition (i), when

$$|g|\tau/\sqrt{2} \neq m\pi/2 \quad (m = 0, 1, 2, \ldots). \tag{17}$$

Therefore, the set of such parameters as (14), (15) and (17) enables us to extract the Bell state $|\Psi^-\rangle_{AB}$ from a general mixed state ϱ_{tot}.

The extraction of the Bell state $|\Psi^-\rangle_{AB}$ is demonstrated in figure 1, where the fidelity to the target state $|\Psi^-\rangle_{AB}$, defined by $F^{(\tau)}(N) \equiv {}_{AB}\langle\Psi^-|\varrho_{AB}^{(\tau)}(N)|\Psi^-\rangle_{AB}$, and the success probability $P^{(\tau)}(N)$ versus the number of measurements, N, are shown for the initial state $\varrho_{tot} = |\rightarrow\rangle_X\langle\rightarrow| \otimes |\uparrow\rangle_A\langle\uparrow| \otimes |\downarrow\rangle_B\langle\downarrow|$, a (pure but) product state [or for a mixed state $\varrho_{tot} = |\rightarrow\rangle_X\langle\rightarrow| \otimes (|\uparrow\downarrow\rangle_{AB}\langle\uparrow\downarrow| + |\downarrow\uparrow\rangle_{AB}\langle\downarrow\uparrow|)/2$]. It is clear that the Bell state $|\Psi^-\rangle_{AB}$ is extracted after only four or five measurements (in this case, $|\lambda_{\Phi^-}| \simeq 0.20$ and $|\lambda_\pm| \simeq 0.44$). Since condition (ii) is fulfilled, the decay of the success probability $P^{(\tau)}(N)$ is suppressed, yielding $P^{(\tau)}(N) \rightarrow {}_{AB}\langle\Psi^-|\varrho_{AB}|\Psi^-\rangle_{AB}$ ($= 1/2$ in figure 1), which means that the $|\Psi^-\rangle_{AB}$ component contained in the initial state ϱ_{AB} (after the zeroth measurement on ϱ_{tot}) is fully extracted. In this sense, the extraction is *optimal*.

4. Concluding remarks

The above example clearly and explicitly shows that our purification scheme works for entanglement purification. It is quite simple: one has simply to repeat one and the same measurement. At the same time, the purification can be made optimal: the optimal success probability is attainable as in the above example. Since the basic framework presented in section 2 is general, it possesses wide potential applicabilities in various settings for quantum computation and quantum information.

Acknowledgements

This work is partly supported by Grants-in-Aid for Scientific Research (C) from the Japan Society for the Promotion of Science (No. 14540280) and Priority Areas Research (B) from the Ministry of Education, Culture, Sports, Science and Technology, Japan (No. 13135221), by a Waseda University Grant for Special Research Projects (No. 2002A–567), and by the bilateral Italian–Japanese project

15C1 on 'Quantum Information and Computation' of the Italian Ministry for Foreign Affairs.

References

[1] NIELSEN, M. A., and CHUANG, I. L., 2000, *Quantum Computation and Quantum Information* (Cambridge: Cambridge University Press), and references therein.

[2] BOUWMEESTER, D., EKERT, A., and ZEILINGER, A., 2000, *The Physics of Quantum Information* (Heidelberg: Springer-Verlag), and references therein.

[3] BENNETT, C. H., BRASSARD, G., POPESCU, S., SCHUMACHER, B., SMOLIN, J. A., and WOOTTERS, W. K., 1996, *Phys. Rev. Lett.*, **76,** 722; BENNETT, C. H., DIVINCENZO, D. P., SMOLIN, J. A., and WOOTTERS, W. K., 1996, *Phys. Rev.* A, **54,** 3824.

[4] NAKAZATO, H., TAKAZAWA, T., and YUASA, K., 2003, *Phys. Rev. Lett.*, **90,** 060401.

[5] For reviews, see: NAKAZATO, H., NAMIKI, M., and PASCAZIO, S., 1996, *Int. J. Mod. Phys.* B, **10,** 247; HOME, D., and WHITAKER, M. A. B., 1997, *Ann. Phys.* (N.Y.), **258,** 237; FACCHI, P., and PASCAZIO, S., 2001, in *Progress in Optics*, edited by E. Wolf (Amsterdam: Elsevier), Vol. 42, p. 147.

PHYSICAL REVIEW A **70**, 012303 (2004)

Preparation and entanglement purification of qubits through Zeno-like measurements

Hiromichi Nakazato,* Makoto Unoki, and Kazuya Yuasa†
Department of Physics, Waseda University, Tokyo 169-8555, Japan
(Received 25 February 2004; published 2 July 2004)

A method of purification, purification through Zeno-like measurements [H. Nakazato, T. Takazawa, and K. Yuasa, Phys. Rev. Lett. **90**, 060401 (2003)], is discussed extensively and applied to a few simple qubit systems. It is explicitly demonstrated how it works and how it is optimized. As possible applications, schemes for initialization of multiple qubits and entanglement purification are presented, and their efficiency is investigated in detail. Simplicity and flexibility of the idea allow us to apply it to various kinds of settings in quantum information and computation, and would provide us with useful and practical methods of state preparation.

DOI: 10.1103/PhysRevA.70.012303 PACS number(s): 03.67.Mn, 03.65.Xp

I. INTRODUCTION

It is usually not seriously discussed in normal textbooks on quantum mechanics about how to prepare an initial state. It is, however, becoming an important subject not only from a viewpoint of foundation of quantum mechanics, but also from a practical point of view, since we are rushing towards experimental realizations of the ideas for quantum information and computation [1,2]. Without establishing particular initial states assumed in several algorithms, we cannot start any processes of the attractive ideas. State preparation is one of the key elements to quantum information processing [1,2], and there are several theoretical proposals [3–5] and experimental attempts [6–10].

In the ideas for quantum information and computation, quantum states with high coherence, especially entangled states, play significant and essential roles. But such "clean" states required for quantum information technologies are not easily found in nature, since many of them are fragile against environmental perturbations and suffer from decoherence. Therefore, there would often be a demand for preparing a desired pure state out of an arbitrary mixed state. Several schemes have been proposed for it, which are called "purification," "distillation," "concentration," "extraction," etc. [2,11,12].

One of the simplest and easiest ways of state preparation is to resort to a projective measurement: a quantum system shall be in a pure state $|\phi\rangle$ after it is measured and confirmed to be in the state $|\phi\rangle$. Such a strategy is not possible, however, in cases where the desired state $|\phi\rangle$ cannot be directly measured or where the relevant system is not available after the confirmation. This is often the case for entangled states, which are the key resources to quantum information and computation. This is why more elaborate purification protocols are required and several schemes of entanglement purification/preparation have been proposed [2,11,12].

Recently, a mechanism to purify quantum states has been found and reported: purification through Zeno-like measurements [13]. A pure state is extracted in a quantum system through a series of repeated measurements (Zeno-like measurements) on another quantum system in interaction with the former. Since the relevant system to be purified is not directly measured in this scheme, it would be suitable for such situations mentioned above. In this paper, we discuss this scheme in detail and explore, on a heuristic basis, its potential as a useful and effective method of purification of qubits. The examples considered here are quite simple but still possess potential and practical applicability.

This paper is organized as follows. First, the basic framework of the purification is described in a general setting, and the conditions for the purification and its optimization are summarized in Sec. II, where some details which are not discussed in the first report [13] are included. It is then demonstrated in Sec. III how it works and how it can be made optimal in a simplest example, i.e., single-qubit purification, and a generalization to a multiqubit case is considered in Sec. IV, which would afford us a useful method of initialization of multiple qubits. One of the interesting applications of the present scheme is entanglement purification, which is discussed in Sec. V and shown to be actually possible. Concluding remarks are given in Sec. VI with some comments on possible extensions and future subjects. Appendixes A–E are supplied in order to demonstrate detailed calculations and proofs, that are not described in the text.

II. FRAMEWORK

Let us recapitulate the framework of the purification reported in Ref. [13]. We consider two quantum systems X and A interacting with each other (Fig. 1). The total system X +A is initially in a mixed state $\varrho_{\rm tot}$, from which we try to extract a pure state in A by controlling X. We first perform a measurement on X (the zeroth measurement) to confirm that

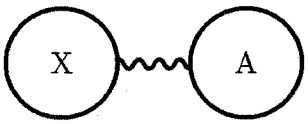

FIG. 1. We repeat measurements on X and purify A.

*Electronic address: hiromici@waseda.jp
†Electronic address: yuasa@hep.phys.waseda.ac.jp

it is in a state $|\phi\rangle_X$. If it is found in the state $|\phi\rangle_X$, the state of the total system is projected by the projection operator

$$\mathcal{O} = |\phi\rangle_X\langle\phi| \otimes 1_A \tag{1}$$

to yield

$$\varrho_{tot} \to \tilde{\varrho}_{tot} = \frac{\mathcal{O}\varrho_{tot}\mathcal{O}}{\mathrm{Tr}(\mathcal{O}\varrho_{tot}\mathcal{O})} = |\phi\rangle_X\langle\phi| \otimes \varrho_A, \tag{2}$$

where $\varrho_A \equiv {}_X\langle\phi|\varrho_{tot}|\phi\rangle_X / P_0$ is the state of A after this zeroth confirmation and $P_0 \equiv \mathrm{Tr}(\mathcal{O}\varrho_{tot}\mathcal{O})$ is the probability for this to happen. We then let the total system start to evolve under a total Hamiltonian H_{tot} and repeat the same measurement on X at regular time intervals τ. After N repetitions of successful confirmations, i.e., after X is confirmed to be in the state $|\phi\rangle_X$ successively N times, the state of the total system, $\varrho_{tot}^{(\tau)}(N)$, is cast into the following form:

$$\begin{aligned}\varrho_{tot}^{(\tau)}(N) &= (\mathcal{O}e^{-iH_{tot}\tau})^N \tilde{\varrho}_{tot}(e^{iH_{tot}\tau}\mathcal{O})^N / \tilde{P}^{(\tau)}(N) \\ &= |\phi\rangle_X\langle\phi| \otimes \varrho_A^{(\tau)}(N),\end{aligned} \tag{3a}$$

$$\varrho_A^{(\tau)}(N) = [V_\phi(\tau)]^N \varrho_A [V_\phi^\dagger(\tau)]^N / \tilde{P}^{(\tau)}(N), \tag{3b}$$

where $V_\phi(\tau)$, defined by

$$V_\phi(\tau) \equiv {}_X\langle\phi|e^{-iH_{tot}\tau}|\phi\rangle_X, \tag{4}$$

is a projected time-evolution operator acting on the Hilbert space of A, and $\tilde{P}^{(\tau)}(N)$ is the normalization factor,

$$\begin{aligned}\tilde{P}^{(\tau)}(N) &= \mathrm{Tr}[(\mathcal{O}e^{-iH_{tot}\tau})^N \tilde{\varrho}_{tot}(e^{iH_{tot}\tau}\mathcal{O})^N] \\ &= \mathrm{Tr}_A\{[V_\phi(\tau)]^N \varrho_A [V_\phi^\dagger(\tau)]^N\}.\end{aligned} \tag{5}$$

Note that we retain only those events where X is found in the state $|\phi\rangle_X$ at every measurement (including the zeroth one); other events, resulting in failure to purify A, are discarded. The normalization factor $\tilde{P}^{(\tau)}(N)$ multiplied by P_0, i.e., $P^{(\tau)}(N) \equiv \tilde{P}^{(\tau)}(N)P_0$ is nothing but the probability for the successful events and is the probability of obtaining the state given in (3).

For definiteness, let us restrict ourselves on finite-dimensional systems throughout this paper and consider the spectral decomposition of the operator $V_\phi(\tau)$. Since the operator $V_\phi(\tau)$ is not a Hermitian operator, we should set up both right and left eigenvalue equations,

$$V_\phi(\tau)|u_n\rangle_A = \lambda_n|u_n\rangle_A, \tag{6a}$$

$${}_A\langle v_n|V_\phi(\tau) = \lambda_n\, {}_A\langle v_n|. \tag{6b}$$

The eigenvalues λ_n are complex in general and bounded as

$$0 \leq |\lambda_n| \leq 1 \tag{7}$$

(see Appendix A). Here we assume for simplicity that the spectrum of the operator $V_\phi(\tau)$ is not degenerate. In such a case, the eigenvectors are orthogonal to each other in the sense

$${}_A\langle v_m|u_n\rangle_A = \delta_{mn} \tag{8a}$$

and form a complete set in the Hilbert space of system A,

$$\sum_n |u_n\rangle_A\langle v_n| = 1_A, \tag{8b}$$

which readily leads to the spectral decomposition of the operator $V_\phi(\tau)$,

$$V_\phi(\tau) = \sum_n \lambda_n |u_n\rangle_A\langle v_n|. \tag{9}$$

(In the following, we also normalize the right eigenvectors as ${}_A\langle u_n|u_n\rangle_A = 1$.)

Even in a general situation where the spectrum of the operator $V_\phi(\tau)$ is degenerate, the diagonalization (9) is possible when and only when all the right eigenvectors $|u_n\rangle_A$ are linearly independent of each other and form a complete basis [14]. Otherwise, the spectral decomposition is not like (9), but in the "Jordan canonical form" [14]. The diagonalizability of the operator $V_\phi(\tau)$ is, however, not an essential assumption as clarified in Appendix B.

It is now easy to observe the asymptotic behavior of the state of A, $\varrho_A^{(\tau)}(N)$ in (3b). Since the eigenvalues λ_n are bounded like (7), each term in the expansion

$$[V_\phi(\tau)]^N = \sum_n \lambda_n^N |u_n\rangle_A\langle v_n| \tag{10}$$

decays out and a single term dominates asymptotically as the number of measurements, N, increases,

$$[V_\phi(\tau)]^N \to \lambda_0^N |u_0\rangle_A\langle v_0| \text{ as } N \text{ increases}, \tag{11}$$

provided

the largest (in magnitude) eigenvalue λ_0 is unique, discrete, and nondegenerate. (12)

[The word "unique" means that there is only one eigenvalue that has the maximum modulus, and "nondegenerate" means that there is only one right eigenvector (and a corresponding left eigenvector) belonging to that maximal (in magnitude) eigenvalue.] Thus, the state of A in (3b) approaches a pure state $|u_0\rangle_A$,

$$\varrho_A^{(\tau)}(N) \to |u_0\rangle_A\langle u_0| \text{ as } N \to \infty. \tag{13}$$

This is the purification scheme proposed recently [13]: extraction of a pure state $|u_0\rangle_A$ through a series of repeated measurements on X. Since we repeat measurements (on X) as in the case of the quantum Zeno effect [15], we call such measurements "Zeno-like measurements" [16,17]. The final pure state $|u_0\rangle_A$ is the eigenstate of the projected time-evolution operator $V_\phi(\tau)$ belonging to the largest (in magnitude) eigenvalue λ_0 and depends on the parameters τ, $|\phi\rangle_X$, and those in the Hamiltonian H_{tot}. It is, however, independent of the initial state ϱ_{tot}. The pure state $|u_0\rangle_A$ is extracted from an arbitrary mixed state ϱ_{tot} through the Zeno-like measurements. By tuning such parameters mentioned above, we have a possibility of extracting a desired pure state $|u_0\rangle_A$.

The above observation shows that the assumption of the diagonalizability in (9) is not essential but condition (12), i.e., the existence of the unique, discrete, and nondegenerate largest (in magnitude) eigenvalue λ_0, is crucial to the purification. For our purification mechanism to work, it is crucial

that a single state is extracted and this is accomplished when these qualifications, i.e., the uniqueness of the largest eigenvalue and the nondegeneracy of the eigenvector, are both met. The diagonalizability of $V_\phi(\tau)$ is not relevant to these conditions and is not essential to the purification. This point is clarified in Appendix B.

Furthermore, note the asymptotic behavior of the success probability $P^{(\tau)}(N)$: it decays asymptotically as

$$P^{(\tau)}(N) \to |\lambda_0|^{2N} P_{0A}\langle v_0|\varrho_A|v_0\rangle_A = |\lambda_0|^{2N}{}_{XA}\langle \phi v_0|\varrho_{tot}|\phi v_0\rangle_{XA} \text{ as } N \text{ increases}, \tag{14}$$

where $|\phi v_0\rangle_{XA}$ stands for $|\phi\rangle_X \otimes |v_0\rangle_A$ and ${}_{XA}\langle \phi v_0| = {}_X\langle\phi| \otimes {}_A\langle v_0|$. The decay is governed by the eigenvalue λ_0, and therefore, an efficient purification is possible if λ_0 satisfies the condition

$$|\lambda_0| = 1, \tag{15}$$

which suppresses the decay in (14) to give the final (nonvanishing) success probability

$$P^{(\tau)}(N) \to {}_{XA}\langle \phi v_0|\varrho_{tot}|\phi v_0\rangle_{XA}. \tag{16}$$

It is worth stressing that the condition (15) allows us to repeat the measurement as many times as we wish without running the risk of losing the success probability $P^{(\tau)}(N)$. In other words, high fidelity to the target state and nonvanishing success probability do not contradict each other in this scheme, but rather they can be achieved simultaneously. At the same time, if the other eigenvalues are much smaller than λ_0 in magnitude,

$$|\lambda_n/\lambda_0| \ll 1 \quad \text{for } n \neq 0, \tag{17}$$

purification is achieved quickly. Equations (15) and (17) are the conditions for the optimal purification, which we try to accomplish by adjusting parameters τ, $|\phi\rangle_X$, and those in the Hamiltonian H_{tot}.

In the following sections, we discuss the above purification scheme in more detail addressing a few specific examples, which are so simple but still possess potential and practical applications in quantum information and computation.

III. SINGLE-QUBIT PURIFICATION

Let us first observe how the above mechanism works in the simplest example: we consider two qubits (two two-level systems) X and A interacting with each other, whose total Hamiltonian is given by

$$H_{tot} = \Omega_X \frac{1+\sigma_3^X}{2} + \Omega_A \frac{1+\sigma_3^A}{2} + g(\sigma_+^X\sigma_-^A + \sigma_-^X\sigma_+^A), \tag{18}$$

where σ_i $(i=1,2,3)$ are the Pauli operators, $\sigma_\pm = (\sigma_1 \pm i\sigma_2)/2$ are the ladder operators, and the frequencies $\Omega_{X(A)}$ and the coupling constant $g(\neq 0)$ are real parameters. We repeatedly confirm the state of X and purify qubit A, i.e., we discuss a purification of a single qubit.

The four eigenvalues of the total Hamiltonian H_{tot} in (18) are given by

$$E^{(0)} = 0, \tag{19a}$$

$$E_\pm^{(1)} = (\Omega_X + \Omega_A)/2 \pm \delta, \tag{19b}$$

$$E^{(2)} = \Omega_X + \Omega_A, \tag{19c}$$

and the corresponding eigenstates are

$$|E^{(0)}\rangle_{XA} = |\downarrow\downarrow\rangle_{XA}, \tag{20a}$$

$$|E_\pm^{(1)}\rangle_{XA} = \frac{1}{\sqrt{2}}\left(\epsilon(g)\sqrt{1 \pm \frac{\Omega_X - \Omega_A}{2\delta}}|\uparrow\downarrow\rangle_{XA} \pm \sqrt{1 \mp \frac{\Omega_X - \Omega_A}{2\delta}}|\downarrow\uparrow\rangle_{XA}\right), \tag{20b}$$

$$|E^{(2)}\rangle_{XA} = |\uparrow\uparrow\rangle_{XA}, \tag{20c}$$

where

$$\delta = \sqrt{(\Omega_X - \Omega_A)^2/4 + g^2}, \tag{21}$$

$\epsilon(g)$ is the sign function, and $|\uparrow(\downarrow)\rangle$ is the eigenstate of the operator σ_3 belonging to the eigenvalue $+1(-1)$ with the phase convention $|\uparrow\rangle = \sigma_+|\downarrow\rangle$. Hence, when the state of X, $|\phi\rangle_X$, is confirmed repeatedly at time intervals τ, the relevant operator to be investigated, the projected time-evolution operator $V_\phi(\tau)$, reads

$$\begin{aligned} V_\phi(\tau) &\equiv {}_X\langle\phi|e^{-iH_{tot}\tau}|\phi\rangle_X \\ &= |\uparrow\rangle_A\langle\uparrow|e^{-i(\Omega_X+\Omega_A)\tau}\left[\cos^2\frac{\theta}{2} + e^{i(\Omega_X+\Omega_A)\tau/2}\left(\cos\delta\tau + i\frac{\Omega_X-\Omega_A}{2\delta}\sin\delta\tau\right)\sin^2\frac{\theta}{2}\right] \\ &\quad + |\downarrow\rangle_A\langle\downarrow|\left[\sin^2\frac{\theta}{2} + e^{-i(\Omega_X+\Omega_A)\tau/2}\left(\cos\delta\tau - i\frac{\Omega_X-\Omega_A}{2\delta}\sin\delta\tau\right)\cos^2\frac{\theta}{2}\right] \\ &\quad - i(|\uparrow\rangle_A\langle\downarrow|e^{-i\varphi} + |\downarrow\rangle_A\langle\uparrow|e^{i\varphi})\frac{g}{\delta}e^{-i(\Omega_X+\Omega_A)\tau/2}\sin\delta\tau\sin\frac{\theta}{2}\cos\frac{\theta}{2}, \end{aligned} \tag{22}$$

where the state $|\phi\rangle_X$ is parametrized as

$$|\phi\rangle_X = e^{-i\varphi/2}\cos\frac{\theta}{2}|\uparrow\rangle_X + e^{i\varphi/2}\sin\frac{\theta}{2}|\downarrow\rangle_X \tag{23}$$

and the set of angles (θ,φ) characterizes the "direction of spin X."

If one of the two eigenvalues of the operator (22) is larger in magnitude than the other, the condition for purification (12) is fulfilled, and qubit A is purified into the eigenstate $|u_0\rangle_A$ belonging to the larger (in magnitude) eigenvalue λ_0. Furthermore, if condition (15), $|\lambda_0|=1$, is satisfied, we can purify with a nonvanishing success probability $P^{(\tau)}(N) \to {}_{XA}\langle\phi v_0|\varrho_{tot}|\phi v_0\rangle_{XA}$, and another condition (17), $|\lambda_1/\lambda_0| \ll 1$, enables us to accomplish quick purification. We try to achieve these conditions by tuning the parameters.

The first adjustment for the optimal purification is

$$\theta = 0 \text{ or } \pi, \text{ i.e., } |\phi\rangle_X = |\uparrow\rangle_X \text{ or } |\downarrow\rangle_X \tag{24}$$

(see Appendix C). Actually, if we choose $|\phi\rangle_X=|\uparrow\rangle_X$, the eigenvalues of the projected time-evolution operator $V_\phi(\tau)$ are given by

$$\lambda_0 = e^{-i(\Omega_X+\Omega_A)\tau},$$

$$\lambda_1 = e^{-i(\Omega_X+\Omega_A)\tau/2}\left(\cos\delta\tau - i\frac{\Omega_X-\Omega_A}{2\delta}\sin\delta\tau\right), \tag{25a}$$

and the eigenvectors belonging to them are

$$|u_0\rangle_A = |\uparrow\rangle_A,\quad {}_A\langle v_0| = {}_A\langle\uparrow|,$$

$$|u_1\rangle_A = |\downarrow\rangle_A,\quad {}_A\langle v_1| = {}_A\langle\downarrow|. \tag{25b}$$

It is clear that the magnitude of the eigenvalue λ_0 is unity and that of λ_1,

$$|\lambda_1| = \sqrt{1-\left(\frac{g}{\delta}\right)^2\sin^2\delta\tau}, \tag{26}$$

is less than unity provided

$$\delta\tau \neq n\pi \quad (n=1,2,\ldots). \tag{27}$$

Both conditions (12) and (15) are thus satisfied, and according to the theory presented in Sec. II, we have an optimal purification

$$\varrho_A^{(\tau)}(N) \to |\uparrow\rangle_A\langle\uparrow|,$$
$$P^{(\tau)}(N) \to {}_{XA}\langle\uparrow\uparrow|\varrho_{tot}|\uparrow\uparrow\rangle_{XA}, \qquad (N\to\infty). \tag{28}$$

After the repeated confirmations of the state $|\uparrow\rangle_X$, qubit A is purified into $|\uparrow\rangle_A$ with a nonvanishing probability ${}_{XA}\langle\uparrow\uparrow|\varrho_{tot}|\uparrow\uparrow\rangle_{XA}$. Similarly, another choice in (24), i.e., a series of repeated confirmations of the state $|\downarrow\rangle_X$, drives A into $|\downarrow\rangle_A$ with a nonvanishing probability ${}_{XA}\langle\downarrow\downarrow|\varrho_{tot}|\downarrow\downarrow\rangle_{XA}$:

$$\varrho_A^{(\tau)}(N) \to |\downarrow\rangle_A\langle\downarrow|,$$
$$P^{(\tau)}(N) \to {}_{XA}\langle\downarrow\downarrow|\varrho_{tot}|\downarrow\downarrow\rangle_{XA}. \qquad (N\to\infty). \tag{29}$$

The final success probability ${}_{XA}\langle\uparrow\uparrow|\varrho_{tot}|\uparrow\uparrow\rangle_{XA}$ for the former choice $|\phi\rangle_X=|\uparrow\rangle_X$ or ${}_{XA}\langle\downarrow\downarrow|\varrho_{tot}|\downarrow\downarrow\rangle_{XA}$ for the latter $|\phi\rangle_X=|\downarrow\rangle_X$ means that the target state $|\uparrow\uparrow\rangle_{XA}$ or $|\downarrow\downarrow\rangle_{XA}$ contained in the initial state ϱ_{tot} is fully extracted. In this sense, the purification is optimal.

The second adjustment is for the fastest purification, which is realized by the condition

$$\delta\tau = (n+1/2)\pi \quad (n=0,1,\ldots), \tag{30}$$

at which $|\lambda_1|$ in (26) is the smallest: $|\lambda_1|=|\Omega_X-\Omega_A|/2\delta$. We can achieve it by tuning the time interval τ, for instance.

To be more explicit, let us demonstrate the extraction of the pure state $|\uparrow\rangle_A$ from the initial mixed state

$$\varrho_{tot} = |\uparrow\rangle_X\langle\uparrow| \otimes \tfrac{1}{2}(|\uparrow\rangle_A\langle\uparrow| + |\downarrow\rangle_A\langle\downarrow|). \tag{31}$$

After X is confirmed to be in the state $|\uparrow\rangle_X$ successfully N times at time intervals τ, the state of qubit A and the probability for the successful confirmations read

$$\varrho_A^{(\tau)}(N) = \frac{|\uparrow\rangle_A\langle\uparrow| + [1-(g/\delta)^2\sin^2\delta\tau]^N|\downarrow\rangle_A\langle\downarrow|}{1+[1-(g/\delta)^2\sin^2\delta\tau]^N},$$

$$P^{(\tau)}(N) = \tfrac{1}{2}\{1+[1-(g/\delta)^2\sin^2\delta\tau]^N\}, \tag{32}$$

respectively, which clearly confirm the limits (28) unless $\delta\tau=n\pi$ $(n=1,2,\ldots)$, and the convergences are the fastest when the condition (30) is satisfied. (Note that ${}_{XA}\langle\uparrow\uparrow|\varrho_{tot}|\uparrow\uparrow\rangle_{XA}=1/2$ for the initial state considered here.)

In Fig. 2(a), the success probability $P^{(\tau)}(N)$ and the so-called fidelity to the target state $|u_0\rangle_A=|\uparrow\rangle_A$, defined by

$$F^{(\tau)}(N) \equiv {}_A\langle u_0|\varrho_A^{(\tau)}(N)|u_0\rangle_A = {}_A\langle\uparrow|\varrho_A^{(\tau)}(N)|\uparrow\rangle_A, \tag{33}$$

are shown as functions of the number of measurements, N, for the initial state (31), with the parameters $\Omega_X=5$, $\Omega_A=6$, $g=1$, $\tau=\pi/2\delta\simeq1.40$. Since the condition (15), $|\lambda_0|=1$, is fulfilled, the decay of the success probability $P^{(\tau)}(N)$ is suppressed to yield the finite value ${}_{XA}\langle\uparrow\uparrow|\varrho_{tot}|\uparrow\uparrow\rangle_{XA}=1/2$, and since the time interval τ is tuned so as to satisfy the condition for the fastest purification (30) ($|\lambda_1|\simeq0.45$), the pure state $|\uparrow\rangle_A$ is extracted after only $N=4$ or 5 measurements. In an extreme case where $|\lambda_1|=0$ is possible, the extraction is achieved just after one measurement. Such a situation is depicted in Fig. 2(b) for the same initial state as in Fig. 2(a) with the parameter set $\Omega_X=\Omega_A$, $g=1$, $\tau=\pi/2\simeq1.57$.

IV. INITIALIZATION OF MULTIPLE QUBITS

The single-qubit purification in the preceding section is too simple but is easily extended for multiqubit cases. In the above example, one may realize that the state $|\uparrow\uparrow\rangle_{XA}$ is an eigenstate of the total Hamiltonian (18) [see (20)] and this is why the optimization condition (15), $|\lambda_0|=1$, is achieved with $|\phi\rangle_X=|\uparrow\rangle_X$ and $|u_0\rangle_A=|\uparrow\rangle_A$ irrespectively of the choice

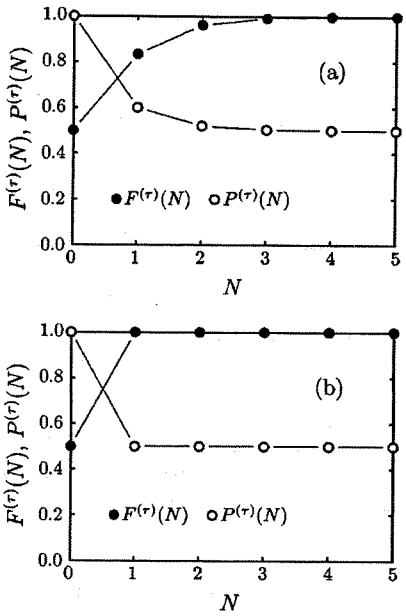

FIG. 2. Fidelity $F^{(\tau)}(N)$ and success probability $P^{(\tau)}(N)$ for single-qubit purification. The pure state $|\uparrow(\downarrow)\rangle_A$ is extracted from the initial mixed state $\varrho_{tot}=|\uparrow(\downarrow)\rangle_X\langle\uparrow(\downarrow)|\otimes(|\uparrow\rangle_A\langle\uparrow|+|\downarrow\rangle_A\langle\downarrow|)/2$ after repeated confirmations of the state $|\uparrow(\downarrow)\rangle_X$. Parameters are $\Omega_X=5$, $\Omega_A=6$, $\tau=\pi/2\delta\simeq 1.40$ for (a) and $\Omega_X=\Omega_A$, $\tau=\pi/2\delta\simeq 1.57$ for (b), in the unit such that $g=1$. The time interval τ is tuned so as to satisfy the condition for the fastest purification (30) in each case.

of the time interval τ. (The same argument applies to the case $|\phi\rangle_X=|\downarrow\rangle_X$ there.) In the case of a multiqubit system X+A+B+$\cdots$ in Fig. 3, with nearest-neighbor interactions,

$$H_{tot}=\Omega_X\frac{1+\sigma_3^X}{2}+\Omega_A\frac{1+\sigma_3^A}{2}+\Omega_B\frac{1+\sigma_3^B}{2}+\cdots + g_{XA}(\sigma_+^X\sigma_-^A+\sigma_-^X\sigma_+^A)+g_{AB}(\sigma_+^A\sigma_-^B+\sigma_-^A\sigma_+^B)+\cdots \tag{34}$$

($g_{XA}, g_{AB},\ldots\neq 0$), the state $|\uparrow\uparrow\uparrow\ldots\rangle_{XAB\ldots}$ is an eigenstate of this total Hamiltonian H_{tot}, and it is readily expected that the pure state $|\uparrow\uparrow\ldots\rangle_{AB\ldots}$ is extracted by repeated projections onto the state $|\uparrow\rangle_X$, with the optimal success probability. Similarly, repeated projections onto $|\downarrow\rangle_X$ set every qubit into $|\downarrow\rangle$ state, i.e., into $|\downarrow\downarrow\ldots\rangle_{AB\ldots}$, optimally. This would be useful for initialization of multiple qubits in a quantum computer.

In order to make this idea more concrete, let us discuss in detail with a three-qubit system X+A+B. The important point is whether the condition for the purification (12) is

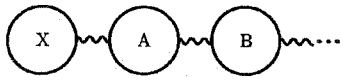

FIG. 3. A multiqubit system with nearest-neighbor interactions.

achievable, i.e., whether all the eigenvalues λ_n except for the relevant one λ_0, associated with the eigenstate $|\uparrow\uparrow\rangle_{AB}$ (or $|\downarrow\downarrow\rangle_{AB}$), can actually be less than unity in magnitude.

For simplicity, we consider the case where $\Omega_X=\Omega_A=\Omega_B=\Omega$. The eight eigenvalues of the total Hamiltonian H_{tot} are given by

$$E^{(0)}=0, \tag{35a}$$

$$E_0^{(1)}=\Omega,\ E_\pm^{(1)}=\Omega\pm\sqrt{2}\bar{g}, \tag{35b}$$

$$E_0^{(2)}=2\Omega,\ E_\pm^{(2)}=2\Omega\pm\sqrt{2}\bar{g}, \tag{35c}$$

$$E^{(3)}=3\Omega, \tag{35d}$$

and the corresponding eigenstates are

$$|E^{(0)}\rangle_{XAB}=|\downarrow\downarrow\downarrow\rangle_{XAB}, \tag{36a}$$

$$|E_0^{(1)}\rangle_{XAB}=\cos\chi|\downarrow\downarrow\uparrow\rangle_{XAB}-\sin\chi|\uparrow\downarrow\downarrow\rangle_{XAB}, \tag{36b}$$

$$|E_\pm^{(1)}\rangle_{XAB}=\frac{1}{\sqrt{2}}(\sin\chi|\downarrow\downarrow\uparrow\rangle_{XAB}+\cos\chi|\uparrow\downarrow\downarrow\rangle_{XAB}\pm|\downarrow\uparrow\downarrow\rangle_{XAB}), \tag{36c}$$

$$|E_0^{(2)}\rangle_{XAB}=\cos\chi|\uparrow\uparrow\downarrow\rangle_{XAB}-\sin\chi|\downarrow\uparrow\uparrow\rangle_{XAB}, \tag{36d}$$

$$|E_\pm^{(2)}\rangle_{XAB}=\frac{1}{\sqrt{2}}(\sin\chi|\uparrow\uparrow\downarrow\rangle_{XAB}+\cos\chi|\downarrow\uparrow\uparrow\rangle_{XAB}\pm|\uparrow\downarrow\uparrow\rangle_{XAB}), \tag{36e}$$

$$|E^{(3)}\rangle_{XAB}=|\uparrow\uparrow\uparrow\rangle_{XAB}, \tag{36f}$$

where

$$\sqrt{2}\bar{g}=\sqrt{g_{XA}^2+g_{AB}^2}, \tag{37}$$

$$\cos\chi=\frac{g_{XA}}{\sqrt{g_{XA}^2+g_{AB}^2}},\quad \sin\chi=\frac{g_{AB}}{\sqrt{g_{XA}^2+g_{AB}^2}}. \tag{38}$$

Aiming at initializing qubits A and B into $|\downarrow\downarrow\rangle_{AB}$, we repeatedly project X onto the state $|\downarrow\rangle_X$ at time intervals τ, and the relevant operator to be investigated reads

$$\begin{aligned}V_\downarrow(\tau)\equiv{}_X\langle\downarrow|e^{-iH_{tot}\tau}|\downarrow\rangle_X={}&|\downarrow\downarrow\rangle_{AB}\langle\downarrow\downarrow|+|\uparrow\downarrow\rangle_{AB}\langle\uparrow\downarrow|e^{-i\Omega\tau}\cos\sqrt{2}\bar{g}\tau+|\downarrow\uparrow\rangle_{AB}\langle\downarrow\uparrow|e^{-i\Omega\tau}(\cos^2\chi+\sin^2\chi\cos\sqrt{2}\bar{g}\tau)\\&-i|\uparrow\downarrow\rangle_{AB}\langle\downarrow\uparrow|e^{-i\Omega\tau}\sin\chi\sin\sqrt{2}\bar{g}\tau-i|\downarrow\uparrow\rangle_{AB}\langle\uparrow\downarrow|e^{-i\Omega\tau}\sin\chi\sin\sqrt{2}\bar{g}\tau\\&+|\uparrow\uparrow\rangle_{AB}\langle\uparrow\uparrow|e^{-2i\Omega\tau}(\sin^2\chi+\cos^2\chi\cos\sqrt{2}\bar{g}\tau).\end{aligned} \tag{39}$$

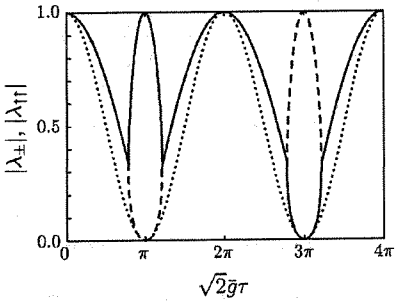

FIG. 4. Magnitudes of the eigenvalues λ_+ (solid line), λ_- (dashed line), and $\lambda_{\uparrow\uparrow}$ (dotted line) in (40), as functions of $\sqrt{2}\bar{g}\tau$. In this figure, we set $g_{XA}=g_{AB}$. Note that $|\lambda_+|=|\lambda_-|$ within each range $2n\pi-\zeta\leq\sqrt{2}\bar{g}\tau\leq 2n\pi+\zeta$ $(n=0,1,\ldots)$, where ζ $(0<\zeta<\pi)$ is defined by $\tan(\zeta/2)=2|\sin\chi|/\cos^2\chi$, and $\zeta\simeq 0.78\pi$ when $g_{XA}=g_{AB}$.

The target state $|\downarrow\downarrow\rangle_{AB}$ is an eigenstate of this operator belonging to the eigenvalue $\lambda_{\downarrow\downarrow}=1$, which satisfies the optimization condition (15), and the other three eigenvalues are given by

$$\lambda_\pm = e^{-i\Omega\tau}\left(\cos^2\frac{\bar{g}\tau}{\sqrt{2}} - \sin^2\chi\sin^2\frac{\bar{g}\tau}{\sqrt{2}} \mp \sin\frac{\bar{g}\tau}{\sqrt{2}}\sqrt{\cos^4\chi\sin^2\frac{\bar{g}\tau}{\sqrt{2}} - 4\sin^2\chi\cos^2\frac{\bar{g}\tau}{\sqrt{2}}}\right), \tag{40a}$$

$$\lambda_{\uparrow\uparrow} = e^{-2i\Omega\tau}\left(1-2\cos^2\chi\sin^2\frac{\bar{g}\tau}{\sqrt{2}}\right). \tag{40b}$$

If these three eigenvalues are all less than unity in magnitude, the condition for the purification (12) is satisfied, and the initialized state $|\downarrow\downarrow\rangle_{AB}$ is extracted from an arbitrary mixed state ϱ_{tot}, with a nonvanishing success probability $P^{(\tau)}(N)\to{}_{XAB}\langle\downarrow\downarrow\downarrow|\varrho_{tot}|\downarrow\downarrow\downarrow\rangle_{XAB}$. (Note that the left eigenvector belonging to the eigenvalue $\lambda_{\downarrow\downarrow}$ is ${}_{AB}\langle\downarrow\downarrow|$.) Such a situation is realized provided

$$\sqrt{2}\bar{g}\tau\neq n\pi \quad (n=1,2,\ldots), \tag{41}$$

which is clearly seen from Fig. 4 and a proof in Appendix D. The final success probability $P^{(\tau)}(N)\to{}_{XAB}\langle\downarrow\downarrow\downarrow|\varrho_{tot}|\downarrow\downarrow\downarrow\rangle_{XAB}$ is again optimal, in the sense that the target state $|\downarrow\downarrow\downarrow\rangle_{XAB}$ contained in the initial state ϱ_{tot} is fully extracted.

The above argument reveals the possibility of initialization at least for two qubits. Initialization of two qubits into $|\downarrow\downarrow\rangle_{AB}$ from the thermal equilibrium state of the total system at temperature T, i.e., $\varrho_{tot}\propto e^{-\beta H_{tot}}$ with $\beta=(k_BT)^{-1}$, is demonstrated in Fig. 5. Note that it is effective when $\Omega>\sqrt{2}\bar{g}$, since in such a case, $|\downarrow\downarrow\downarrow\rangle_{XAB}$ is the ground state of the total system. The analytic formula for the final success probability is $P^{(\tau)}(\infty)=[1+(e^{-\beta\Omega}+e^{-2\beta\Omega})(1+2\cosh\sqrt{2}\beta\bar{g})+e^{-3\beta\Omega}]^{-1}$.

It is natural to expect that the same mechanism also works for systems with more qubits as in Fig. 3. It is hard to imagine that the magnitudes of eigenvalues of $V_\downarrow(\tau)$ other than the relevant one $\lambda_{\downarrow\downarrow\ldots}$ (whose magnitude is unity) is also unity irrespectively of the values of parameters. Further detailed investigations on its efficiency, robustness, and so on, will certainly clarify the possibility of a new useful procedure for initializing multiple qubits.

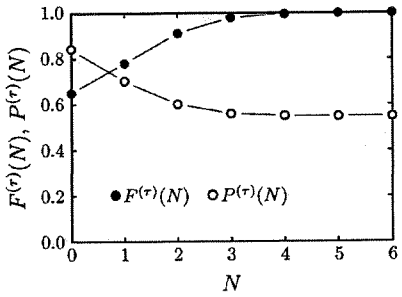

FIG. 5. Fidelity $F^{(\tau)}(N)$ and success probability $P^{(\tau)}(N)$ for two-qubit initialization. Through the repeated confirmations of the state $|\downarrow\rangle_X$, qubits A and B are initialized into $|\downarrow\downarrow\rangle_{AB}$ from the thermal equilibrium state of the total system at temperature T, i.e., $\varrho_{tot}\propto e^{-\beta H_{tot}}$ with $\beta=(k_BT)^{-1}$. Parameters are $g_{XA}=g_{AB}=1$, $\Omega=2$, $\tau=\zeta/\sqrt{2}\simeq 1.73$, $k_BT=\beta^{-1}=1$. The time interval τ is tuned so as to make $\max(|\lambda_+|,|\lambda_-|,|\lambda_{\uparrow\uparrow}|)$ the smallest, which is for the fastest initialization (see Fig. 4).

V. ENTANGLEMENT PURIFICATION

One of the most significant issues in the field of quantum information and computation is how to prepare entanglement, and therefore, it is interesting and important to examine whether the present scheme can realize entanglement purification/preparation. We show, in this section, that it is actually possible. In order to demonstrate it explicitly, let us discuss a simple Hamiltonian

$$H_{tot}=\Omega\frac{1+\sigma_3^X}{2}+\Omega\frac{1+\sigma_3^A}{2}+\Omega\frac{1+\sigma_3^B}{2} + g(\sigma_+^X\sigma_-^A+\sigma_-^X\sigma_+^A)+g(\sigma_+^X\sigma_-^B+\sigma_-^X\sigma_+^B). \tag{42}$$

The control qubit X is coupled to qubits A and B as in Fig. 6. We confirm X to be in the state $|\phi\rangle_X$ repeatedly at time intervals τ and end up with an extraction of an entanglement between A and B, which are initially in a mixed state ϱ_{tot}.

The spectrum of the total Hamiltonian H_{tot} is already given in (35) with $\bar{g}$ replaced by g, and the eigenstates are

$$|E^{(0)}\rangle_{XAB}=|\downarrow\downarrow\downarrow\rangle_{XAB}, \tag{43a}$$

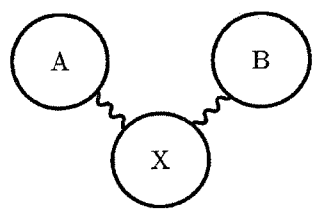

FIG. 6. We repeat measurements on qubit X and extract one of the Bell states, $|\Psi^-\rangle_{AB}\equiv(|\uparrow\downarrow\rangle_{AB}-|\downarrow\uparrow\rangle_{AB})/\sqrt{2}$, in qubits A and B.

$$|E_0^{(1)}\rangle_{\mathrm{XAB}} = |\downarrow\Psi^-\rangle_{\mathrm{XAB}}, \tag{43b}$$

$$|E_\pm^{(1)}\rangle_{\mathrm{XAB}} = \frac{1}{\sqrt{2}}[|\downarrow\Psi^+\rangle_{\mathrm{XAB}} \pm \epsilon(g)|\uparrow\downarrow\downarrow\rangle_{\mathrm{XAB}}], \tag{43c}$$

$$|E_0^{(2)}\rangle_{\mathrm{XAB}} = |\uparrow\Psi^-\rangle_{\mathrm{XAB}}, \tag{43d}$$

$$|E_\pm^{(2)}\rangle_{\mathrm{XAB}} = \frac{1}{\sqrt{2}}[|\uparrow\Psi^+\rangle_{\mathrm{XAB}} \pm \epsilon(g)|\downarrow\uparrow\uparrow\rangle_{\mathrm{XAB}}], \tag{43e}$$

$$|E^{(3)}\rangle_{\mathrm{XAB}} = |\uparrow\uparrow\uparrow\rangle_{\mathrm{XAB}}. \tag{43f}$$

The relevant projected time-evolution operator is given, in this case, by

$$\begin{aligned}
V_\phi(\tau) &\equiv {}_{\mathrm{X}}\langle\phi|e^{-iH_{\mathrm{tot}}\tau}|\phi\rangle_{\mathrm{X}} \\
&= |\Psi^-\rangle_{\mathrm{AB}}\langle\Psi^-|e^{-i\Omega\tau}\left(\sin^2\frac{\theta}{2} + e^{-i\Omega\tau}\cos^2\frac{\theta}{2}\right) + |\downarrow\downarrow\rangle_{\mathrm{AB}}\langle\downarrow\downarrow|\left(\sin^2\frac{\theta}{2} + e^{-i\Omega\tau}\cos\sqrt{2}g\tau\cos^2\frac{\theta}{2}\right) \\
&\quad + |\Psi^+\rangle_{\mathrm{AB}}\langle\Psi^+|e^{-i\Omega\tau}\cos\sqrt{2}g\tau\left(\sin^2\frac{\theta}{2} + e^{-i\Omega\tau}\cos^2\frac{\theta}{2}\right) + |\uparrow\uparrow\rangle_{\mathrm{AB}}\langle\uparrow\uparrow|e^{-2i\Omega\tau}\left(\cos\sqrt{2}g\tau\sin^2\frac{\theta}{2} + e^{-i\Omega\tau}\cos^2\frac{\theta}{2}\right) \\
&\quad - i(|\downarrow\downarrow\rangle_{\mathrm{AB}}\langle\Psi^+|e^{i\varphi} + |\Psi^+\rangle_{\mathrm{AB}}\langle\downarrow\downarrow|e^{-i\varphi})e^{-i\Omega\tau}\sin\sqrt{2}g\tau\sin\frac{\theta}{2}\cos\frac{\theta}{2} \\
&\quad - i(|\uparrow\uparrow\rangle_{\mathrm{AB}}\langle\Psi^+|e^{-i\varphi} + |\Psi^+\rangle_{\mathrm{AB}}\langle\uparrow\uparrow|e^{i\varphi})e^{-2i\Omega\tau}\sin\sqrt{2}g\tau\sin\frac{\theta}{2}\cos\frac{\theta}{2},
\end{aligned} \tag{44}$$

where $|\Psi^\pm\rangle_{\mathrm{AB}}$ are the two of the four Bell states $|\Psi^\pm\rangle_{\mathrm{AB}} = (|\uparrow\downarrow\rangle_{\mathrm{AB}} \pm |\downarrow\uparrow\rangle_{\mathrm{AB}})/\sqrt{2}$, $|\Phi^\pm\rangle_{\mathrm{AB}} = (|\uparrow\uparrow\rangle_{\mathrm{AB}} \pm |\downarrow\downarrow\rangle_{\mathrm{AB}})/\sqrt{2}$, and $|\phi\rangle_{\mathrm{X}}$ is parametrized as in (23). Since the Hamiltonian (42) is symmetric under the exchange between A and B, $V_\phi(\tau)$ splits into two sectors: the singlet sector and the triplet one. The singlet state $|\Psi^-\rangle_{\mathrm{AB}}$ is apparently one of the four eigenstates of $V_\phi(\tau)$ belonging to the eigenvalue

$$\lambda_{\Psi^-} = e^{-i\Omega\tau}\left(\sin^2\frac{\theta}{2} + e^{-i\Omega\tau}\cos^2\frac{\theta}{2}\right), \tag{45}$$

and hence, we can extract an entangled state, i.e., the Bell state $|\Psi^-\rangle_{\mathrm{AB}}$, after a number of measurements on X, provided (i) the eigenvalue λ_{Ψ^-} is larger in magnitude than any other eigenvalues. Furthermore, if (ii) condition (15), i.e., $|\lambda_{\Psi^-}| = 1$, is achieved, $|\Psi^-\rangle_{\mathrm{AB}}$ is extracted with an optimal probability $P^{(\tau)}(N) \to {}_{\mathrm{XAB}}\langle\phi\Psi^-|\varrho_{\mathrm{tot}}|\phi\Psi^-\rangle_{\mathrm{XAB}}$, which is again optimal in the same sense as in the preceding examples, i.e., the target entangled state $|\Psi^-\rangle_{\mathrm{AB}}$ contained in the initial state ϱ_{tot} has been fully extracted.

Requirement (ii) is fulfilled by the choice of the parameters as $|\Omega|\tau = 2n\pi$ $(n=0,1,\ldots)$ or $\sin\theta = 0$, but the latter choice violates requirement (i). It is, therefore, necessary that

$$|\Omega|\tau = 2n\pi \quad (n=0,1,\ldots) \text{ and } |\phi\rangle_{\mathrm{X}} \neq |\uparrow\rangle_{\mathrm{X}}, |\downarrow\rangle_{\mathrm{X}}. \tag{46a}$$

(Note that the first condition is automatically satisfied without tuning the time interval τ, when $\Omega = 0$.) Furthermore, one can prove as in Appendix E that requirement (i) is met, under the condition (46a), provided

$$|g|\tau/\sqrt{2} \neq m\pi/2 \quad (m=1,2,\ldots). \tag{46b}$$

The existence of such a parameter set satisfying (46) explicitly discloses the possibility of extracting entanglement through Zeno-like measurements.

In the case of the choice

$$|\phi\rangle_{\mathrm{X}} = |\rightarrow\rangle_{\mathrm{X}} \equiv \frac{1}{\sqrt{2}}(|\uparrow\rangle_{\mathrm{X}} + |\downarrow\rangle_{\mathrm{X}}), \tag{47}$$

for example, the four eigenvalues are given by

$$\lambda_{\Psi^-} = 1, \quad \lambda_{\Phi^-} = \cos^2\frac{g\tau}{\sqrt{2}}, \tag{48a}$$

$$\lambda_\pm = 1 - \frac{1}{2}\sin\frac{g\tau}{\sqrt{2}}\left(3\sin\frac{g\tau}{\sqrt{2}} \pm \epsilon(g)\sqrt{1 - 9\cos^2\frac{g\tau}{\sqrt{2}}}\right), \tag{48b}$$

whose magnitudes behave as in Fig. 4 but with $\lambda_{\uparrow\uparrow}$ replaced by λ_{Φ^-}.

The extraction of the entangled state $|\Psi^-\rangle_{\mathrm{AB}}$ is demonstrated in Fig. 7, from a product state $\varrho_{\mathrm{tot}} = |\rightarrow\rangle_{\mathrm{X}}\langle\rightarrow|\otimes|\uparrow\rangle_{\mathrm{A}}\langle\uparrow|\otimes|\downarrow\rangle_{\mathrm{B}}\langle\downarrow|$ and from the thermal equilibrium state $\varrho_{\mathrm{tot}} \propto e^{-\beta H_{\mathrm{tot}}}$ at temperature $T = (k_{\mathrm{B}}\beta)^{-1}$.

VI. CONCLUDING REMARKS

The examples presented in this paper demonstrate how the present purification scheme works, and suggest a few potential applications, even though the analyses are heuristically based and no general "optimization" theory or strategy

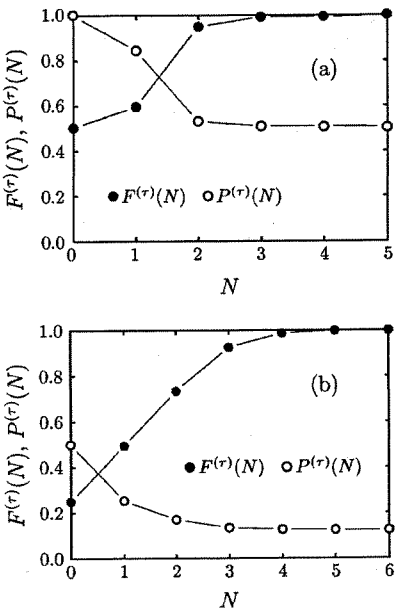

FIG. 7. Fidelity $F^{(\tau)}(N)$ and success probability $P^{(\tau)}(N)$ for entanglement purification. The entangled state $|\Psi^-\rangle_{AB}$ is extracted from (a) a product state $\varrho_{tot}=|\rightarrow\rangle_X\langle\rightarrow|\otimes|\uparrow\rangle_A\langle\uparrow|\otimes|\downarrow\rangle_B\langle\downarrow|$ and (b) the thermal state $\varrho_{tot}\propto e^{-\beta H_{tot}}$ at temperature $T=(k_B\beta)^{-1}$, through repeated confirmations of the state $|\rightarrow\rangle_X$. Parameters are $\Omega=0$, $\tau=0.5\pi\simeq 1.57$ for (a), and $\Omega=0$, $\tau=\zeta/\sqrt{2}\simeq 1.73$, $k_BT=\beta^{-1}=\infty$ for (b), in the unit such that $g=1$, where ζ is defined in the caption of Fig. 4. For the initial thermal state in (b) with $\Omega=0$, the success probability for the zeroth confirmation is given by $P^{(\tau)}(0)=1/2$ for any set of parameters (θ,φ,g,T), and the final value $P^{(\tau)}(\infty)=[8\cosh^2(\beta g/\sqrt{2})]^{-1}$ becomes largest at $k_BT/|g|=(\beta|g|)^{-1}=\infty$.

has been given. Remarkable features of the scheme are summarized as follows. (i) The first point is the simplicity. Many of the other proposed procedures are composed of several steps with different operations, such as rotation, CNOT operation, and measurement [2,11]. In the present scheme, on the other hand, one has only to repeat one and the same measurement. (ii) Furthermore, the "optimal" success probability is possible in the sense that the target state contained in the initial state is fully extracted. In several other methods [2,11], on the contrary, it decays to zero as the fidelity approaches unity [18]. (iii) The number of measurements required for purification is considerably reduced by appropriate choices of parameters, and purification is attainable after only a few steps.

Another point to be stressed is the flexibility. While many of the other schemes [2,11] are designed for specific systems, the framework is presented in Sec. II on a general setting, and there are diverse systems and purposes which fit the present scheme. We have already observed, in this paper, two different applications on the same idea: initialization and entanglement purification. Additional ideas or slight modifications to the basic scheme would provide us with various methods of state preparation. An interesting extension of the present scheme is for extraction of entanglement between two spatially separated qubits [2,5,11,12], which is often necessary for quantum communication, quantum teleportation, and so on. (The original protocols for entanglement purification [2,11] are aimed at this purpose.) It is actually possible and will be reported elsewhere [19]. One of the other possible extensions is to go beyond a method of extracting quantum state. It would be interesting, for example, if we could find a novel method of *transferring* quantum state [20,21] rather than extracting it.

In this paper, only qubit systems, i.e., finite-dimensional systems, have been discussed. One has to keep in mind that the condition (12) plays a crucial role in the present purification scheme. If this condition is met, it works for infinite dimensional ones as well. In fact, a harmonic oscillator, which has an infinite number of energy levels, can be purified through the present method, which is explicitly demonstrated in Ref. [13]. This also shows the broad range of applicability of the scheme. It is not obvious, however, whether one can purify systems with continuous spectra, since they seem, at first sight, unlikely to satisfy the condition for purification (12), especially the discreteness of the eigenvalues. This point is one of the interesting future subjects, since it would be required in some cases to purify quantum states in the presence of environmental systems, namely, under dissipation and/or dephasing.

The simplicity and the efficiency mentioned above would facilitate practical experimental applications of the present scheme. The flexibility allows one to apply it to various kinds of systems intended for quantum information and computation, such as optical setups [12], ion-trap systems [7,8], solid-state quantum computers [9], and so on. In practice, one should face many unwanted factors, and robustness of the method against them is crucial. In the present scheme, it is often required to tune certain parameters in order to extract a desired pure state, and it is an important subject to clarify how precise the tuning should be and how much error the method suffers from when the parameters are mistuned. It is also a remained issue to explore how ideal projective measurements are realized in actual experiments. Investigations on these points are now in progress.

Note added in proof. Recently, a related work [22] has been reported.

ACKNOWLEDGMENTS

The authors acknowledge useful and helpful discussions with Professor I. Ohba. This work is partly supported by the Grant for The 21st Century COE Program (Physics of Self-Organization Systems) at Waseda University and Grant-in-Aid for Priority Areas Research (B) (No. 13135221) from the Ministry of Education, Culture, Sports, Science and Technology, Japan, by Grant-in-Aid for Scientific Research (C) (No. 14540280) from the Japan Society for the Promotion of Science, by a Waseda University Grant for Special Research Projects (No. 2002A-567), and by the bilateral Italian-Japanese Project 15C1 on "Quantum Information and Computation" of the Italian Ministry for Foreign Affairs.

APPENDIX A: BOUND ON THE EIGENVALUES OF $V_\phi(\tau)$

Let us prove that the eigenvalues λ_n of the projected time-evolution operator $V_\phi(\tau)$ are bounded as in (7).

For an arbitrary state of A, say $|\psi\rangle_A$,

$$\begin{aligned} 0 &\leq \|V_\phi(\tau)|\psi\rangle_A\|^2 \\ &= \|{}_X\langle\phi|e^{-iH_{tot}\tau}|\phi\rangle_X|\psi\rangle_A\|^2 \\ &\leq \|e^{-iH_{tot}\tau}|\phi\rangle_X|\psi\rangle_A\|^2 \\ &= 1. \end{aligned} \tag{A1}$$

Hence, by setting $|\psi\rangle_A = |u_n\rangle_A$ [a right eigenvector of the operator $V_\phi(\tau)$] and noting $\|V_\phi(\tau)|u_n\rangle_A\|^2 = |\lambda_n|^2$, we obtain the inequality (7). As is clear from this proof, the bound (7) reflects unitarity of the time-evolution operator $e^{-iH_{tot}\tau}$.

APPENDIX B: A NONDIAGONALIZABLE $V_\phi(\tau)$ CASE

It is assumed in Sec. II that the projected time-evolution operator $V_\phi(\tau)$ is diagonalized like (9), but it is not the case if some of its eigenvalues are degenerated. Here we show, however, that the assumption of the diagonalizability is not essential to the purification.

When an eigenvalue λ_n of the (finite-dimensional) operator $V_\phi(\tau)$ is M_n-fold degenerate, there do not always exist M_n linearly independent eigenvectors. This fact spoils the diagonalizability of the operator $V_\phi(\tau)$. There exist d_n ($\leq M_n$) linearly independent right eigenvectors $|u_n^{(k)}\rangle_A$ ($k=1,\ldots,d_n$) belonging to the eigenvalue λ_n (d_n is called "dimension of the eigenspace"), and one can find $M_n - d_n$ linearly independent "generalized eigenvectors" $|u_n^{(k)}\rangle_A$ ($k=d_n+1,\ldots,M_n$) which are subjected to the conditions

$$V_\phi(\tau)|u_n^{(k)}\rangle_A = \lambda_n|u_n^{(k)}\rangle_A + |u_n^{(k-1)}\rangle_A \quad (k = d_n+1,\ldots,M_n) \tag{B1}$$

and linearly independent of the eigenvectors $|u_n^{(k)}\rangle_A$ ($k=1,\ldots,d_n$) [14]. The right vectors $|u_n^{(k)}\rangle_A$ ($k=1,\ldots,M_n$) then form a complete set within the subspace associated with the eigenvalue λ_n, and there exist corresponding left vectors ${}_A\langle v_n^{(k)}|$ ($k=1,\ldots,M_n$), which satisfy the orthonormality

$${}_A\langle v_m^{(k)}|u_n^{(\ell)}\rangle_A = \delta_{mn}\delta_{k\ell} \tag{B2a}$$

and completeness conditions

$$\sum_n \mathcal{P}_n = \mathbb{1}_A, \quad \mathcal{P}_n = \sum_{k=1}^{M_n} |u_n^{(k)}\rangle_A\langle v_n^{(k)}|.$$

The operator $V_\phi(\tau)$ is now expanded as

$$V_\phi(\tau) = \sum_n (\lambda_n\mathcal{P}_n + \mathcal{D}_n) \tag{B3a}$$

with

$$\mathcal{D}_n = \sum_{k=d_n+1}^{M_n} |u_n^{(k-1)}\rangle_A\langle v_n^{(k)}|, \tag{B3b}$$

which is the most general form of spectral decomposition and is called "Jordan canonical form" [14]. Note the relations

$$\mathcal{P}_m\mathcal{P}_n = \delta_{mn}\mathcal{P}_n, \tag{B4a}$$

$$\mathcal{D}_m\mathcal{P}_n = \mathcal{P}_n\mathcal{D}_m = \mathcal{D}_m\delta_{mn}, \tag{B4b}$$

$$\mathcal{D}_m\mathcal{D}_n = 0 \quad (m \neq n), \tag{B4c}$$

and

$$\mathcal{D}_n^{M_n-d_n+1} = 0. \tag{B4d}$$

From the spectral decomposition (B3), it is easily deduced that

$$[V_\phi(\tau)]^N = \sum_n \left(\lambda_n^N\mathcal{P}_n + \sum_{r=1}^{\min(N,M_n-d_n)} {}_NC_r\lambda_n^{N-r}\mathcal{D}_n^r\right), \tag{B5a}$$

where

$$\mathcal{D}_n^r = \sum_{k=d_n+r}^{M_n} |u_n^{(k-r)}\rangle_A\langle v_n^{(k)}|. \tag{B5b}$$

Therefore, if the largest (in magnitude) eigenvalue is unique, which is denoted by λ_0, and nondegenerate (i.e., $M_0=1$, $d_0=1$), the single term in the expansion (B5a) again dominates asymptotically like (11) (note that ${}_NC_r \sim N^r/r!$ for large N), which leads to the same conclusion as (13). The purification does not suffer from degeneracy in the other eigenvalues than the largest (in magnitude) one λ_0. The crucial condition to the purification is (12).

APPENDIX C: OPTIMIZATION OF THE SINGLE-QUBIT PURIFICATION

We show here that the condition (24) together with (27) is the necessary and sufficient condition for the optimal purification with both (12) and (15) for model (18).

First, we try to achieve the upper bound in the inequality (A1), i.e., $\|V_\phi(\tau)|\psi\rangle_A\| = 1$, in model (18). If such a state $|\psi\rangle_A$ is found and is an eigenstate of the operator $V_\phi(\tau)$, say $|u_n\rangle_A$, we have $|\lambda_n| = 1$. As is easily seen from (A1), the equality holds only when

$${}_X\langle\phi_\perp|e^{-iH_{tot}\tau}|\phi\rangle_X|\psi\rangle_A = 0 \tag{C1}$$

is satisfied, where $|\phi_\perp\rangle_X$ is a vector perpendicular to $|\phi\rangle_X$ in (23), i.e.,

$$|\phi_\perp\rangle_X = e^{-i\varphi/2}\sin\frac{\theta}{2}|\uparrow\rangle_X - e^{i\varphi/2}\cos\frac{\theta}{2}|\downarrow\rangle_X. \tag{C2}$$

Equation (C1) means that the operator $V_\phi^\perp(\tau) \equiv {}_X\langle\phi_\perp| \times e^{-iH_{tot}\tau}|\phi\rangle_X$ should have a zero eigenvalue, and hence

$$\det V_{\phi}^{\perp}(\tau)=0. \tag{C3}$$

For model (18), the operator $V_{\phi}^{\perp}(\tau)$ reads

$$\begin{aligned} V_{\phi}^{\perp}(\tau)=&|\uparrow\rangle_{\mathrm{A}}\langle\uparrow|e^{-i(\Omega_{\mathrm{X}}+\Omega_{\mathrm{A}})\tau}\left[1-e^{i(\Omega_{\mathrm{X}}+\Omega_{\mathrm{A}})\pi/2}\left(\cos\delta\tau+i\frac{\Omega_{\mathrm{X}}-\Omega_{\mathrm{A}}}{2\delta}\sin\delta\tau\right)\right]\sin\frac{\theta}{2}\cos\frac{\theta}{2}\\ &-|\downarrow\rangle_{\mathrm{A}}\langle\downarrow|\left[1-e^{-i(\Omega_{\mathrm{X}}+\Omega_{\mathrm{A}})\pi/2}\left(\cos\delta\tau-i\frac{\Omega_{\mathrm{X}}-\Omega_{\mathrm{A}}}{2\delta}\sin\delta\tau\right)\right]\sin\frac{\theta}{2}\cos\frac{\theta}{2}\\ &+i|\uparrow\rangle_{\mathrm{A}}\langle\downarrow|\frac{g}{\delta}e^{-i\varphi}e^{-i(\Omega_{\mathrm{X}}+\Omega_{\mathrm{A}})\pi/2}\sin\delta\tau\cos^2\frac{\theta}{2}-i|\downarrow\rangle_{\mathrm{A}}\langle\uparrow|\frac{g}{\delta}e^{i\varphi}e^{-i(\Omega_{\mathrm{X}}+\Omega_{\mathrm{A}})\pi/2}\sin\delta\tau\sin^2\frac{\theta}{2}, \end{aligned} \tag{C4}$$

and

$$\det V_{\phi}^{\perp}(\tau)=-\frac{1}{4}e^{-i(\Omega_{\mathrm{X}}+\Omega_{\mathrm{A}})\tau}\left[\left|1-e^{i(\Omega_{\mathrm{X}}+\Omega_{\mathrm{A}})\pi/2}\left(\cos\delta\tau+i\frac{\Omega_{\mathrm{X}}-\Omega_{\mathrm{A}}}{2\delta}\sin\delta\tau\right)\right|^2+\left(\frac{g}{\delta}\right)^2\sin^2\delta\tau\right]\sin^2\theta. \tag{C5}$$

Condition (C1), namely (C3), is hence reduced to

$$\sin\theta=0 \tag{C6a}$$

or

$$\cos\delta\tau=\pm1 \text{ and } e^{i(\Omega_{\mathrm{X}}+\Omega_{\mathrm{A}})\pi/2}=\pm1. \tag{C6b}$$

In the first case (C6a), both conditions (12) and (15) are satisfied unless $\delta\tau=n\pi$ $(n=1,2,\ldots)$ as is explained around (24)–(27). In the second case (C6b), on the other hand, the projected time-evolution operator reads $V_{\phi}(\tau)=\mathbb{1}_{\mathrm{A}}$ and the eigenvalue $\lambda_0=1$ is degenerated, i.e., condition (12) is not fulfilled. Therefore, the necessary and sufficient condition for the optimal purification in model (18) is given by the first choice (C6a) [i.e., (24)] with (27).

APPENDIX D: CONDITION FOR THE TWO-QUBIT INITIALIZATION

We here outline the proof of the necessary and sufficient condition for the optimal two-qubit initialization, Eq. (41), in Sec. IV. What we have to show is how to make the eigenvalues $\lambda_{\pm}$ and $\lambda_{\uparrow\uparrow}$ in (40) all less than unity in magnitude.

The eigenvalues $\lambda_{\pm}$ are the solutions to an eigenvalue equation

$$(\lambda e^{i\Omega\tau})^2-2\left(\cos^2\frac{\bar{g}\tau}{\sqrt{2}}-\sin^2\chi\sin^2\frac{\bar{g}\tau}{\sqrt{2}}\right)(\lambda e^{i\Omega\tau})+1-2\cos^2\chi\sin^2\frac{\bar{g}\tau}{\sqrt{2}}=0. \tag{D1}$$

We clarify when this equation has a solution whose magnitude is unity. Seeking such a solution, we insert $\lambda=e^{-i\Omega\tau}e^{i\Theta}$ into (D1) to obtain the conditions

$$\sin\Theta\left(\cos\Theta-\cos^2\frac{\bar{g}\tau}{\sqrt{2}}+\sin^2\chi\sin^2\frac{\bar{g}\tau}{\sqrt{2}}\right)=0, \tag{D2a}$$

$$\cos\Theta\left(\cos\Theta-\cos^2\frac{\bar{g}\tau}{\sqrt{2}}+\sin^2\chi\sin^2\frac{\bar{g}\tau}{\sqrt{2}}\right)-\cos^2\chi\sin^2\frac{\bar{g}\tau}{\sqrt{2}}=0, \tag{D2b}$$

which are reduced to

$$\sin\frac{\bar{g}\tau}{\sqrt{2}}=0 \text{ and } \cos\Theta=1 \tag{D3a}$$

or

$$\cos\frac{\bar{g}\tau}{\sqrt{2}}=0 \text{ and } \cos\Theta=-1. \tag{D3b}$$

(Note that $\cos\chi\neq0$ and $\sin\chi\neq0$, since it is assumed that g_{XA}, $g_{\mathrm{AB}}\neq0$.) It is easy to see from (40b) that we have $|\lambda_{\uparrow\uparrow}|=1$ when $\sin(\bar{g}\tau/\sqrt{2})=0$, and in summary, the magnitude of one of the eigenvalues $\lambda_{\pm}$ and $\lambda_{\uparrow\uparrow}$ becomes unity only when

$$\sqrt{2}\bar{g}\tau=n\pi \quad (n=1,2,\ldots). \tag{D4}$$

The condition for the initialization in Sec. IV is thus proved to be (41). See also Fig. 4.

APPENDIX E: CONDITION FOR THE ENTANGLEMENT PURIFICATION

The necessary and sufficient condition (46) for the entanglement purification in Sec. V is proved in a similar manner to that in Appendix D.

The eigenvalues $\lambda_{\pm}$ and λ_{Φ^-} under the condition (46a) are the solutions to an eigenvalue equation

$$\left(\kappa-\sin\frac{g\tau}{\sqrt{2}}\right)\left(\kappa-\cos^2\frac{\theta}{2}\sin\frac{g\tau}{\sqrt{2}}\right)\left(\kappa-\sin^2\frac{\theta}{2}\sin\frac{g\tau}{\sqrt{2}}\right)+2\sin^2\frac{\theta}{2}\cos^2\frac{\theta}{2}\cos^2\frac{g\tau}{\sqrt{2}}\left(\kappa-\frac{1}{2}\sin\frac{g\tau}{\sqrt{2}}\right)=0 \tag{E1}$$

with $\kappa=(1-\lambda)/[2\sin(g\tau/\sqrt{2})]$. Seeking a solution λ with unit magnitude, we insert $\lambda=e^{i\Theta}$ into this equation to obtain

$$\sin\Theta\left[2\cos^2\Theta-\left(3-4\sin^2\frac{g\tau}{\sqrt{2}}\right)\cos\Theta+1-\left(2-\frac{1}{2}\sin^2\theta\right)\sin^2\frac{g\tau}{\sqrt{2}}\left(2-\sin^2\frac{g\tau}{\sqrt{2}}\right)\right]=0, \tag{E2a}$$

$$\cos\Theta\left[2\cos^2\Theta-\left(3-4\sin^2\frac{g\tau}{\sqrt{2}}\right)\cos\Theta-\left(2-\frac{1}{2}\sin^2\theta\right)\sin^2\frac{g\tau}{\sqrt{2}}\left(2-\sin^2\frac{g\tau}{\sqrt{2}}\right)\right]$$
$$+1-2\sin^4\frac{g\tau}{\sqrt{2}}-\frac{1}{2}\sin^2\theta\sin^2\frac{g\tau}{\sqrt{2}}\left(2-3\sin^2\frac{g\tau}{\sqrt{2}}\right)=0, \tag{E2b}$$

which are reduced to

$$\sin\frac{g\tau}{\sqrt{2}}=0 \text{ and } \cos\Theta=1 \tag{E3a}$$

or

$$\cos\frac{g\tau}{\sqrt{2}}=0 \text{ and } \cos\Theta=-1. \tag{E3b}$$

Extraction of entanglement is not possible when (E3a) or (E3b) is satisfied, and therefore, the condition for the entanglement purification in Sec. V is given by (46).

[1] M. A. Nielsen and I. L. Chuang, *Quantum Computation and Quantum Information* (Cambridge University Press, Cambridge, 2000).

[2] *The Physics of Quantum Information*, edited by D. Bouwmeester, A. Ekert, and A. Zeilinger (Springer-Verlag, Heidelberg, 2000).

[3] K. Vogel, V. M. Akulin, and W. P. Schleich, Phys. Rev. Lett. **71**, 1816 (1993); A. S. Parkins, P. Marte, P. Zoller, and H. J. Kimble, *ibid.* **71**, 3095 (1993); B. M. Garraway, B. Sherman, H. Moya-Cessa, P. L. Knight, and G. Kurizki, Phys. Rev. A **49**, 535 (1994); C. K. Law and J. H. Eberly, Phys. Rev. Lett. **76**, 1055 (1996); B. Kneer and C. K. Law, Phys. Rev. A **57**, 2096 (1998), and references therein.

[4] J. I. Cirac and P. Zoller, Phys. Rev. A **50**, R2799 (1994); M. Freyberger, P. K. Aravind, M. A. Horne, and A. Shimony, *ibid.* **53**, 1232 (1996); M. B. Plenio, S. F. Huelga, A. Beige, and P. L. Knight, *ibid.* **59**, 2468 (1999); J. Hong and H.-W. Lee, Phys. Rev. Lett. **89**, 237901 (2002); C. Marr, A. Beige, and G. Rempe, Phys. Rev. A **68**, 033817 (2003).

[5] C. Cabrillo, J. I. Cirac, P. García-Fernández, and P. Zoller, Phys. Rev. A **59**, 1025 (1999); L.-M. Duan, M. D. Lukin, J. I. Cirac, and P. Zoller, Nature (London) **414**, 413 (2001); A. Messina, Eur. Phys. J. D **18**, 379 (2002); D. E. Browne and M. B. Plenio, Phys. Rev. A **67**, 012325 (2003); X.-L. Feng, Z.-M. Zhang, X.-D. Li, S.-Q. Gong, and Z.-Z. Xu, Phys. Rev. Lett. **90**, 217902 (2003); L.-M. Duan and H. J. Kimble, *ibid.* **90**, 253601 (2003); D. E. Browne, M. B. Plenio, and S. F. Huelga, *ibid.* **91**, 067901 (2003).

[6] E. Hagley, X. Maître, G. Nogues, C. Wunderlich, M. Brune, J. M. Raimond, and S. Haroche, Phys. Rev. Lett. **79**, 1 (1997).

[7] B. DeMarco, A. Ben-Kish, D. Leibfried, V. Meyer, M. Rowe, B. M. Jelenković, W. M. Itano, J. Britton, C. Langer, T. Rosenband, and D. J. Wineland, Phys. Rev. Lett. **89**, 267901 (2002); A. Ben-Kish, B. DeMarco, V. Meyer, M. Rowe, J. Britton, W. M. Itano, B. M. Jelenković, C. Langer, D. Leibfried, T. Rosenband, and D. J. Wineland, *ibid.* **90**, 037902 (2003), and references therein.

[8] F. Schmidt-Kaler, H. Häffner, M. Riebe, S. Gulde, G. P. T. Lancaster, T. Deuschle, C. Becher, C. F. Roos, J. Eschner, and R. Blatt, Nature (London) **422**, 408 (2003); F. Schmidt-Kaler, H. Häffner, S. Gulde, M. Riebe, G. P. T. Lancaster, T. Deuschle, C. Becher, W. Hänsel, J. Eschner, C. F. Roos, and R. Blatt, Appl. Phys. B: Lasers Opt. **B77**, 789 (2003), and references therein.

[9] Y. Nakamura, Yu. A. Pashkin, and J. S. Tsai, Nature (London) **398**, 786 (1999); T. Yamamoto, Yu. A. Pashkin, O. Astafiev, Y. Nakamura, and J. S. Tsai, *ibid.* **425**, 941 (2003), and references therein.

[10] E. Waks, E. Diamanti, and Y. Yamamoto, e-print quant-ph/0308055.

[11] C. H. Bennett, G. Brassard, S. Popescu, B. Schumacher, J. A. Smolin, and W. K. Wootters, Phys. Rev. Lett. **76**, 722 (1996), **78**, 2031(E) (1997); C. H. Bennett, D. P. DiVincenzo, J. A. Smolin, and W. K. Wootters, Phys. Rev. A **54**, 3824 (1996).

[12] T. Yamamoto, M. Koashi, Ş. K. Özdemir, and N. Imoto, Nature (London) **421**, 343 (2003); Z. Zhao, T. Yang, Y.-A. Chen, A.-N. Zhang, and J.-W. Pan, Phys. Rev. Lett. **90**, 207901 (2003); A. Vaziri, J.-W. Pan, T. Jennewein, G. Weihs, and A.

Zeilinger, *ibid.* **91**, 227902 (2003).

[13] H. Nakazato, T. Takazawa, and K. Yuasa, Phys. Rev. Lett. **90**, 060401 (2003); K. Yuasa, H. Nakazato, and T. Takazawa, J. Phys. Soc. Jpn. **72** Suppl. C, 34 (2003).

[14] T. Kato, *Perturbation Theory for Linear Operators*, 2nd ed. (Springer-Verlag, Berlin, 1984).

[15] For reviews, see H. Nakazato, M. Namiki, and S. Pascazio, Int. J. Mod. Phys. B **10**, 247 (1996); D. Home and M. A. B. Whitaker, Ann. Phys. (N.Y.) **258**, 237 (1997); P. Facchi and S. Pascazio, in *Progress in Optics*, edited by E. Wolf (Elsevier, Amsterdam, 2001), Vol. 42, p. 147.

[16] It should be noted, however, that the time interval τ in this scheme is not necessarily small as in the ordinary Zeno measurements, and the purification (13) is not due to the quantum Zeno effect. If the ordinary Zeno limit $N \to \infty$ and $\tau \to 0$ ($N\tau = T$ fixed) [15] is taken in the present scheme, a quantum Zeno effect appears yielding the so-called "quantum Zeno dynamics" [17], which is unitary and provides us with a quite different effect from the one discussed in this paper.

[17] P. Facchi, A. G. Klein, S. Pascazio, and L. S. Schulman, Phys. Lett. A **257**, 232 (1999); P. Facchi, V. Gorini, G. Marmo, S. Pascazio, and E. C. G. Sudarshan, *ibid.* **275**, 12 (2000); P. Facchi, S. Pascazio, A. Scardicchio, and L. S. Schulman, Phys. Rev. A **65**, 012108 (2001); P. Facchi and S. Pascazio, Phys. Rev. Lett. **89**, 080401 (2002).

[18] One should keep in mind, however, that some other schemes [2,11] are discussed in more severe situations.

[19] H. Nakazato, M. Unoki, and K. Yuasa, e-print quant-ph/0403009; G. Compagno, A. Messina, H. Nakazato, A. Napoli, M. Unoki, and K. Yuasa, e-print quant-ph/0405074.

[20] S. Bose, Phys. Rev. Lett. **91**, 207901 (2003); L. Amico, A. Osterloh, F. Plastina, R. Fazio, and G. M. Palma, Phys. Rev. A **69**, 022304 (2004); V. Subrahmanyam, *ibid.* **69**, 034304 (2004); M. Christandl, N. Datta, A. Ekert, and A. J. Landahl, Phys. Rev. Lett. **92**, 187902 (2004).

[21] For a review, see C. H. Bennett and D. P. DiVincenzo, Nature (London) **404**, 247 (2000).

[22] L.-A. Wu, D. A. Lidar, and S. Schneider, e-print quant-ph/0402209.

PHYSICAL REVIEW A **70**, 052316 (2004)

Distillation of entanglement between distant systems by repeated measurements on an entanglement mediator

G. Compagno,[1,*] A. Messina,[1,†] Hiromichi Nakazato,[2,‡] A. Napoli,[1,§] Makoto Unoki,[2] and Kazuya Yuasa[2,‖]
[1]*INFM, MURST, and Dipartimento di Scienze Fisiche ed Astronomiche dell'Università di Palermo, Via Archirafi 36, 90123 Palermo, Italy*
[2]*Department of Physics, Waseda University, Tokyo 169-8555, Japan*
(Received 12 May 2004; published 18 November 2004)

A recently proposed purification method, in which Zeno-like measurements of a subsystem can bring about a distillation of another subsystem in interaction with the former, is utilized to yield entangled states between distant systems. It is shown that measurements of a two-level system, locally interacting with two other spatially separated uncoupled subsystems, can distill entangled states from the latter irrespective of the initial states of the two subsystems.

DOI: 10.1103/PhysRevA.70.052316 PACS number(s): 03.67.Mn, 03.65.Xp

I. INTRODUCTION

One of the key technologies for quantum information and computation is purification/distillation of quantum states [1,2]. Particular pure states, such as entangled states, often play significant roles there, but it is not easy to find such "clean" states in nature. It is therefore required to prepare them out of mixed states; otherwise, we cannot carry out any interesting ideas of quantum information and computation.

A different purification mechanism has recently been proposed [3]. It is shown that repeated measurements on a system, say A, result in a purification of another system, say B, in interaction with A [4]. That is, the state of B is driven to a pure state irrespective of its (generally mixed) initial state, if certain conditions are satisfied. Remarkably, if appropriate adjustment of the relevant parameters is possible, the maximal yield, which is prescribed by the initial mixed state of B and its target pure state, can be attained, while keeping the maximal fidelity, by a finite number of measurements on A (an "optimal purification"). This constitutes a remarkable contrast to the standard purification protocol [1,2], in which it is generally difficult to realize both a nonvanishing yield and the maximal fidelity at the same time.

Since an entangled state is one of the pure states of two quantum systems, say A and B, one can think of the possibility of extracting the entangled state between A and B by repeatedly performing measurements on X which interacts with both A and B. This possibility has already been pointed out [5,6] and explored to show that one of the Bell states can be extracted when this mechanism is applied to a three-qubit system, where qubits A and B always interact with the other qubit X on which one and the same measurement is repeatedly performed. Notice that in this case the two systems A and B are not spatially separated, because they are supposed to locally interact with X. On the other hand, it is often required, e.g., in the ideas of quantum teleportation and communication [2,7], to establish an entanglement between two quantum systems that are located at or at least can be sent to, without losing the entanglement, distant places. In this respect, it would be worth remembering that interesting ideas of generating an entanglement between two cavities [8] and of transferring an entanglement between two modes in a cavity to that between two other modes in different cavities [9] have been proposed. In the former a two-level atom is sent to interact successively with the two cavities resulting in the generation of an entanglement between the two, and in the latter the entanglement is shown to be transferred by a two-level atom which passes through the two cavities and interacts with the relevant cavity modes. In this paper, this kind of successive interaction with two quantum systems is incorporated within the framework of the recent purification mechanism [3,5,6] to show that an entanglement can be established between the states of two systems spatially separated (or that can be separated). Notice that the entangled state is distilled from an arbitrary initial state that is in general mixed, while in the generation of entanglement in Ref. [8] the initial state should be prepared in an appropriate pure state and in the transfer of entanglement in Ref. [9] the state is assumed to be initially entangled.

After a brief review of the purification mechanism in Sec. II, a scheme of successive interaction is introduced in a three-qubit system, $A+B+X$, in which system X is assumed to interact first with system A and then with B, in Sec. III. System X is prepared in an initial pure state and is measured after it has interacted with A and B. Then only those events in which system X is found in the initial state are kept. This process is repeated many times. It is shown that an optimal entanglement purification is actually realizable for a particular choice of interaction and by properly adjusting interaction times and strengths between A and X and B and X. In Sec. IV, another example of an entanglement purification is examined in a physical system where a two-level atom X is injected successively to the two cavities A and B "back and forth," interacts with their cavity modes under the rotating-wave approximation, and the state of X is repeatedly mea-

*Electronic address: compagno@fisica.unipa.it
†Electronic address: messina@fisica.unipa.it
‡Electronic address: hiromici@waseda.jp
§Electronic address: napoli@fisica.unipa.it
‖Electronic address: yuasa@hep.phys.waseda.ac.jp

sured in a prescribed way. It is explicitly shown that, under certain conditions, a particular entangled state between the lowest two modes of each cavity is extracted, irrespective of the initial cavity states. Finally, we summarize the results obtained and give future perspectives in Sec. V.

II. PURIFICATION VIA REPEATED MEASUREMENTS

Let the total system consist of two parts, system A and system B, and the dynamics be described by the total Hamiltonian

$$H = H_A + H_B + H_{\text{int}}, \tag{2.1}$$

where H_{int} stands for the interaction between the two (sub)-systems. We initially prepare the system in a product state

$$\rho_0 = |\phi\rangle\langle\phi| \otimes \rho_B(0) \tag{2.2}$$

at $t=0$. Notice that system B can be in an *arbitrary mixed* state $\rho_B(0)$. We perform measurements on A at regular intervals τ to confirm that it is still in the state $|\phi\rangle$ [4], while the total system $A+B$ during the time τ evolves unitarily in terms of the total Hamiltonian H. Since the measurement is performed only on system A, the action of such a (projective, for simplicity) measurement can be conveniently described by the following projection operator:

$$\mathcal{O} \equiv |\phi\rangle\langle\phi| \otimes \hat{1}_B. \tag{2.3}$$

Thus the state of system A is set back to $|\phi\rangle$ every after τ, while that of B just evolves dynamically on the basis of the total Hamiltonian H. We repeat the same measurement, represented by Eq. (2.3) N times and collect only those events in which system A has been found in the state $|\phi\rangle$ consecutively N times; other events are discarded. The state of system B is then described by the density matrix

$$\rho_B^{(\tau)}(N) = [V_\phi(\tau)]^N \rho_B(0) [V_\phi^\dagger(\tau)]^N / P^{(\tau)}(N), \tag{2.4}$$

where

$$V_\phi(\tau) \equiv \langle\phi|e^{-iH\tau}|\phi\rangle \tag{2.5}$$

is an operator acting on B and

$$\begin{aligned} P^{(\tau)}(N) &= \mathrm{Tr}[(\mathcal{O}e^{-iH\tau}\mathcal{O})^N \rho_0 (\mathcal{O}e^{iH\tau}\mathcal{O})^N] \\ &= \mathrm{Tr}_B\{[V_\phi(\tau)]^N \rho_B(0) [V_\phi^\dagger(\tau)]^N\} \end{aligned} \tag{2.6}$$

is the probability for these events to occur (yield). This normalization factor appearing in Eq. (2.4) reflects the fact that only the right outcomes are collected in this process.

In order to examine the asymptotic state of system B for large N, consider, assuming its existence, the spectral decomposition of the operator $V_\phi(\tau)$, which is not Hermitian, $V_\phi(\tau) \neq V_\phi^\dagger(\tau)$. We therefore need to set up both the right- and left-eigenvalue problems

$$V_\phi(\tau)|u_n\rangle = \lambda_n|u_n\rangle, \ \langle v_n|V_\phi(\tau) = \lambda_n\langle v_n|. \tag{2.7}$$

The eigenvalue λ_n is complex valued in general, but its absolute value is bounded [5]

$$0 \leqslant |\lambda_n| \leqslant 1. \tag{2.8}$$

This reflects the unitarity of the time evolution operator $e^{-iH\tau}$. These eigenvectors are assumed to form a complete orthonormal set in the following sense

$$\sum_n |u_n\rangle\langle v_n| = \hat{1}_B, \ \langle v_n|u_m\rangle = \delta_{nm}. \tag{2.9}$$

(We normalize $|u_n\rangle$ as $\langle u_n|u_n\rangle = 1$, while the norm of $\langle v_n|$ has been fixed by the above relations and is not necessarily unity.) The operator $V_\phi(\tau)$ itself is now expanded in terms of these eigenvectors

$$V_\phi(\tau) = \sum_n \lambda_n |u_n\rangle\langle v_n|. \tag{2.10}$$

It is now easy to see that the Nth power of this operator is expressed as

$$[V_\phi(\tau)]^N = \sum_n \lambda_n^N |u_n\rangle\langle v_n| \tag{2.11}$$

and therefore it is dominated by a single term for large N,

$$[V_\phi(\tau)]^N \xrightarrow{\text{large } N} \lambda_0^N |u_0\rangle\langle v_0|, \tag{2.12}$$

provided the largest (in magnitude) eigenvalue λ_0 is *discrete, nondegenerate, and unique*. If these conditions are satisfied, the density operator of system B is driven to a pure state

$$\rho_B^{(\tau)}(N) \xrightarrow{\text{large } N} |u_0\rangle\langle u_0| \tag{2.13}$$

with the probability

$$P^{(\tau)}(N) \xrightarrow{\text{large } N} |\lambda_0|^{2N} \langle v_0|\rho_B(0)|v_0\rangle. \tag{2.14}$$

The pure state $|u_0\rangle$, which is nothing but the right eigenvector of the operator $V_\phi(\tau)$ belonging to the largest (in magnitude) eigenvalue λ_0, is thus distilled in system B. This is the purification scheme proposed in [3].

A few comments are in order. First, the final pure state $|u_0\rangle$ toward which system B is to be driven is dependent on the choice of the state $|\phi\rangle$ on which system A is projected every after measurement, on the measurement interval τ, and on the Hamiltonian H, but does not depend on the initial state of system B at all. In this sense, the purification is accomplished irrespective of the initial (mixed) state $\rho_B(0)$. Second, as is clear in the above exposition, what is crucial in this purification scheme is the repetition of one and the same measurement (more appropriately, spectral decomposition) and the measurement interval τ need not be very small [4]. It instead remains an adjustable parameter. Third, if we can make other eigenvalues than λ_0 much smaller in magnitude

$$|\lambda_n/\lambda_0| \ll 1 \ \text{ for } n \neq 0, \tag{2.15}$$

by adjusting parameters, we will need fewer steps (i.e., smaller N) to purify system B.

It is now evident that the purification can be made *optimal*, if the conditions (2.15) and

$$|\lambda_0| = 1 \tag{2.16}$$

are satisfied. This condition (2.16) assures that we can repeat as many measurements as we wish without running the risk of losing the yield $P^{(\tau)}(N)$ in order to make the fidelity to the target state $|u_0\rangle$,

$$F^{(\tau)}(N) \equiv \mathrm{Tr}_B[\rho_B^{(\tau)}(N)|u_0\rangle\langle u_0|], \tag{2.17}$$

higher. Actually, the yield $P^{(\tau)}(N)$ decays like

$$P^{(\tau)}(N) = \sum_{n,m} \lambda_n^N \lambda_m^{*N} \langle v_n|\rho_B(0)|v_m\rangle\langle u_m|u_n\rangle \xrightarrow{\text{large } N} |\lambda_0|^{2N}\langle v_0|\rho_B(0)|v_0\rangle \tag{2.18}$$

and the condition (2.16) can bring us with the nonvanishing yield $\langle v_0|\rho_B(0)|v_0\rangle$ even in the $N\to\infty$ limit. Therefore the condition (2.16) makes the two (sometimes not compatible) demands, i.e., *higher fidelity and nonvanishing yield*, achievable, with fewer steps when the condition (2.15) is met. In this sense, the purification is considered to be optimal.

It would be desirable if an optimal purification can be realized by an appropriate choice of the state $|\phi\rangle$ and/or tuning of the measurement interval τ and parameters in a given Hamiltonian. A few simple systems have already been examined [3,5,6] to show how such optimal purifications are made possible.

III. ENTANGLEMENT DISTILLATION IN A TWO-QUBIT SYSTEM $A+B$ BY AN ENTANGLEMENT MEDIATOR X

Since an entangled state of system $A+B$ is one of the pure states, there is a possibility that we apply the purification mechanism described above to distill the initial (generally mixed) state of $A+B$ to a desired entangled state. This possibility has already been pointed out and it has been explicitly demonstrated that one of the Bell states $|\Psi^-\rangle$ of the two qubit systems $A+B$ can actually be extracted if we repeatedly measure one and the same state of another qubit system X, the interactions of which are symmetrical with respect to A and B, resulting in the maximal yield [5,6]. One of the limitations of this model is that the entanglement can be established only when the two systems A and B locally interact with the same system X at the same time and therefore it does not seem to allow to establish an entanglement between two systems that are spatially separated. A different scheme is certainly needed.

When the two systems A and B are spatially separated, their local interactions with the other system X cannot take place simultaneously. This means that the interactions are considered to become effective one by one, i.e., system X first interacts with, say, system A and then with B [8,9]. This kind of process can be conveniently described by a time-dependent total Hamiltonian. In this section, a total system composed of three qubits (or three spin-1/2 systems) A, B, and X is considered. The two qubits A and B interact with the other qubit X successively, the state of X, initially prepared in a particular state, say in an up state, is measured after the

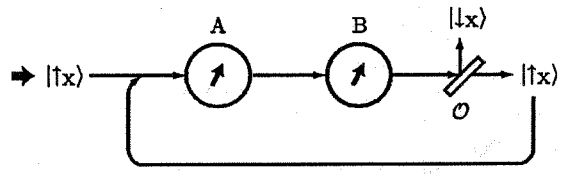

FIG. 1. Qubit X, prepared in $|\uparrow_X\rangle$, is brought to interaction with qubits A and B successively and then its state is measured. If it is found in $|\uparrow_X\rangle$, the whole process is repeated again; other events are discarded.

interactions with A and B, and only those events in which the state of X is found in the up state are retained and other events are just discarded. The process is repeated many times and we are interested in the resulting state of $A+B$.

Assume that the three-qubit system $A+B+X$ is described by a time-dependent total Hamiltonian $H(t)$. Qubit X, which is initially prepared in up state $|\uparrow_X\rangle$, is first brought to interaction with qubit A for time interval t_A. The Hamiltonian in this period is

$$H(t) = H_0 + H'_{XA}. \tag{3.1a}$$

Next, after a free time evolution under the free Hamiltonian H_0 for time duration τ_A, qubit X interacts with another qubit B, which has no direct interaction with A, for t_B. The Hamiltonian for this period reads

$$H(t) = H_0 + H'_{XB}. \tag{3.1b}$$

After another free time evolution for τ_B, the state of X is measured and only those cases in which qubit X is found in its initial up state $|\uparrow_X\rangle$ are retained. The whole process, i.e.,

$$\begin{aligned} &\text{interaction between } X \text{ and } A \text{ for } t_A \\ &\quad\to \text{free evolution for } \tau_A \\ &\quad\to \text{interaction between } X \text{ and } B \text{ for } t_B \\ &\quad\to \text{free evolution for } \tau_B \\ &\quad\to \text{projection to } |\uparrow_X\rangle, \end{aligned} \tag{3.2}$$

will be repeated many times and we are interested in the final state of $A+B$. See Fig. 1.

In order to describe the above process explicitly and to show the possibility of entanglement distillation by this process, we consider the following free and interaction Hamiltonians:

$$H_0 = \frac{\omega}{2}(1+\sigma_3^{(A)}) + \frac{\omega}{2}(1+\sigma_3^{(B)}) + \frac{\omega}{2}(1+\sigma_3^{(X)}), \tag{3.3a}$$

$$H'_{XA} = g_A\sigma_1^{(X)}\sigma_1^{(A)},\ H'_{XB} = g_B\sigma_1^{(X)}\sigma_1^{(B)}, \tag{3.3b}$$

where the $\sigma_i^{(A)}$'s are Pauli matrices acting on the Hilbert

space of system A and so on, and g_A and g_B are real (assumed, for definiteness, to be positive) coupling constants. The free Hamiltonians for A, B, and X are assumed to be the same for simplicity and are characterized solely by the common energy gap ω.

It is clear that the relevant evolution operator for the whole process (3.2) is given by

$$V \equiv \langle\uparrow_X| e^{-iH_0\tau_B} e^{-i(H_0+H'_{XB})t_B} e^{-iH_0\tau_A} e^{-i(H_0+H'_{XA})t_A} |\uparrow_X\rangle. \tag{3.4}$$

It is an elementary task to evaluate this operator, since each factor on the right-hand side is easily evaluated in terms of the eigenstates of the Hamiltonian in the exponent. Indeed, we have

$$\begin{aligned} e^{-i(H_0+H'_{XA})t_A}|\uparrow_X\rangle = e^{-i\omega t_A(1+\sigma_3^{(B)})/2-i\omega t_A}[&|\uparrow_X\rangle\{(\cos\varphi_A - i\sin\varphi_A\cos 2\theta_A)|\uparrow_A\rangle\langle\uparrow_A| + \cos(g_A t_A)|\downarrow_A\rangle\langle\downarrow_A|\} \\ &+ |\downarrow_X\rangle\{-i\sin\varphi_A\sin 2\theta_A|\downarrow_A\rangle\langle\uparrow_A| - i\sin(g_A t_A)|\uparrow_A\rangle\langle\downarrow_A|\}], \end{aligned} \tag{3.5a}$$

and similarly

$$\begin{aligned} \langle\uparrow_X| e^{-i(H_0+H'_{XB})t_B} = e^{-i\omega t_B(1+\sigma_3^{(A)})/2-i\omega t_B}[&\langle\uparrow_X|\{(\cos\varphi_B - i\sin\varphi_B\cos 2\theta_B)|\uparrow_B\rangle\langle\uparrow_B| + \cos(g_B t_B)|\downarrow_B\rangle\langle\downarrow_B|\} \\ &+ \langle\downarrow_X|\{-i\sin\varphi_B\sin 2\theta_B|\uparrow_B\rangle\langle\downarrow_B| - i\sin(g_B t_B)|\downarrow_B\rangle\langle\uparrow_B|\}], \end{aligned} \tag{3.5b}$$

where the angles $\varphi_{A(B)}$ and $\theta_{A(B)}$ are defined as

$$\varphi_{A(B)} = t_{A(B)}\sqrt{\omega^2 + g_{A(B)}^2}, \tag{3.6a}$$

$$\sin 2\theta_{A(B)} = \frac{g_{A(B)}}{\sqrt{\omega^2 + g_{A(B)}^2}}, \tag{3.6b}$$

$$\cos 2\theta_{A(B)} = \frac{\omega}{\sqrt{\omega^2 + g_{A(B)}^2}}. \tag{3.6c}$$

Let us introduce a parity operator $\mathcal{P} \equiv \sigma_3^{(A)}\sigma_3^{(B)}$ whose eigenvalues $+1$ and -1 single out two subspaces of the product Hilbert space $\mathcal{H}_A \otimes \mathcal{H}_B$ invariant under the action of the operator V. The two states $|\uparrow_A\uparrow_B\rangle$ and $|\downarrow_A\downarrow_B\rangle$ generate the even parity subspace and the following 2×2 matrix $\mathcal{M}$ with its elements

$$\begin{aligned} \mathcal{M}_{11} = e^{-i\omega(t_A+2\tau_A+t_B+2\tau_B)}&(\cos\varphi_A - i\sin\varphi_A\cos 2\theta_A) \\ &\times(\cos\varphi_B - i\sin\varphi_B\cos 2\theta_B), \end{aligned} \tag{3.7a}$$

$$\mathcal{M}_{12} = -e^{-i\omega t_A}\sin\varphi_A\sin 2\theta_A\sin(g_B t_B), \tag{3.7b}$$

$$\mathcal{M}_{21} = -e^{-i\omega(t_B+2\tau_B)}\sin(g_A t_A)\sin\varphi_B\sin 2\theta_B, \tag{3.7c}$$

$$\mathcal{M}_{22} = \cos(g_A t_A)\cos(g_B t_B) \tag{3.7d}$$

allows us to completely characterize the action of V in this subspace as follows:

$$V\begin{bmatrix} |\uparrow_A\uparrow_B\rangle \\ |\downarrow_A\downarrow_B\rangle \end{bmatrix} = e^{-i\omega(t_A+\tau_A+t_B+\tau_B)}\mathcal{M}\begin{bmatrix} |\uparrow_A\uparrow_B\rangle \\ |\downarrow_A\downarrow_B\rangle \end{bmatrix}. \tag{3.8}$$

We proceed in the same way for the odd parity subspace spanned by the states $|\uparrow_A\downarrow_B\rangle$ and $|\downarrow_A\uparrow_B\rangle$. To this end we define the 2×2 matrix $\mathcal{N}$ with its elements

$$\mathcal{N}_{11} = e^{-i\omega(2\tau_A+t_B)}(\cos\varphi_A - i\sin\varphi_A\cos 2\theta_A)\cos(g_B t_B), \tag{3.9a}$$

$$\mathcal{N}_{12} = -\sin\varphi_A\sin 2\theta_A\sin\varphi_B\sin 2\theta_B, \tag{3.9b}$$

$$\mathcal{N}_{21} = -e^{-i\omega(t_A+2\tau_A+t_B)}\sin(g_A t_A)\sin(g_B t_B), \tag{3.9c}$$

$$\mathcal{N}_{22} = e^{-i\omega(t_A+2\tau_A)}\cos(g_A t_A)(\cos\varphi_B - i\sin\varphi_B\cos 2\theta_B), \tag{3.9d}$$

so that the action of V is represented as

$$V\begin{bmatrix} |\uparrow_A\downarrow_B\rangle \\ |\downarrow_A\uparrow_B\rangle \end{bmatrix} = e^{-i\omega(t_A+t_B+2\tau_B)}\mathcal{N}\begin{bmatrix} |\uparrow_A\downarrow_B\rangle \\ |\downarrow_A\uparrow_B\rangle \end{bmatrix}. \tag{3.10}$$

In order to show explicitly that the process (3.2) with the particular choice of interaction (3.3b) admits an entanglement distillation for qubit system $A+B$, it turns out to be enough to consider a much simpler case. Let us treat systems A and B symmetrically, except for the ordering of their interactions with system X. We choose the same parameters for A and B, i.e., $g_A = g_B \equiv g$, $t_A = t_B \equiv t$, and $\tau_A = \tau_B \equiv \tau$ ($\varphi_{A(B)} \to \varphi$ and $\theta_{A(B)} \to \theta$). For the parity-odd states, the matrix $\mathcal{N}$ now is simplified to be

$$\mathcal{N}=\begin{pmatrix} e^{-i\omega(t+2\tau)}\cos(gt)(\cos\varphi - i\sin\varphi\cos 2\theta) & -\sin^2\varphi\sin^2 2\theta \\ -e^{-2i\omega(t+\tau)}\sin^2(gt) & e^{-i\omega(t+2\tau)}\cos(gt)(\cos\varphi - i\sin\varphi\cos 2\theta)\end{pmatrix}. \tag{3.11}$$

It is easy to find the condition under which an entangled state of the form

$$|\Psi\rangle \equiv \frac{1}{\sqrt{2}}(|\uparrow_A\downarrow_B\rangle + e^{i\chi}|\downarrow_A\uparrow_B\rangle), \tag{3.12}$$

where χ is a real parameter, is an eigenstate of this matrix $\mathcal{N}$ (and therefore of the operator V). A straightforward calculation shows that if the parameters g, t, and τ are so chosen that the relation

$$\cos\varphi - i\sin\varphi\cos 2\theta = -e^{i\omega\tau}\cos(gt) \tag{3.13}$$

is satisfied, the state $|\Psi\rangle$ with $\chi=\omega(t+\tau)$ is indeed an eigenstate of V belonging to the eigenvalue $\lambda_0=-e^{-3i\omega(t+\tau)}$. [There is another possibility of optimal distillation of the above entangled state (3.12), but with a different χ, i.e., $\chi=\omega(t+\tau)+\pi$. This case is realized under the condition (3.13) with the replacement $\omega\tau\to\omega\tau+\pi$; the corresponding eigenvalue is also given by the shifted one, i.e., $e^{-3i\omega(t+\tau)}$.]

Notice that we are not allowed to set $\cos(gt)\sin(gt)=0$ because it would result in a degenerate (in magnitude) eigenvalue. Observe that we have essentially two conditions (3.13), while we have three independent combination of parameters gt, ωt, and $\omega\tau$. We, therefore, have the possibility of an optimal distillation of the entangled state $|\Psi\rangle$, if the magnitudes of the other eigenvalues of V are made smaller than unity. The remaining eigenvalue of $\mathcal{N}$ under the conditions in (3.13) reads

$$\begin{aligned} &e^{-i\omega(t+\tau)}[e^{-i\omega\tau}\cos(gt)(\cos\varphi - i\sin\varphi\cos 2\theta) + \sin^2(gt)] \\ &\quad = e^{-i\omega(t+\tau)}[-\cos^2(gt) + \sin^2(gt)], \end{aligned} \tag{3.14}$$

and its absolute value cannot be made unity when $\cos(gt)\sin(gt)\neq 0$. On the other hand, matrix $\mathcal{M}$ is expressed as

$$\mathcal{M}=\begin{pmatrix} e^{-2i\omega(t+\tau)}\cos^2(gt) & \mp e^{-i\omega t}\sin^2(gt) \\ \mp e^{-i\omega(t+2\tau)}\sin^2(gt) & \cos^2(gt)\end{pmatrix} \tag{3.15}$$

and the absolute values of the eigenvalues of this matrix cannot reach unity if $\cos\omega(t+\tau)\neq\pm 1$ and $\cos(gt)\sin(gt)\neq 0$. This means that, under these conditions on gt, ωt, and $\omega\tau$ satisfying the relation (3.13), an optimal purification (i.e., distillation) of the entangled state $(|\uparrow_A\downarrow_B\rangle + e^{i\omega(t+\tau)}|\downarrow_A\uparrow_B\rangle)/\sqrt{2}$ is possible. It is in fact easily shown that the left eigenstate of V belonging to the eigenvalue $\lambda_0=-e^{-3i\omega(t+\tau)}$ is expressed as

$$\langle\Phi| = \frac{1}{\sqrt{2}}(\langle\uparrow_A\downarrow_B| + e^{-i\chi}\langle\downarrow_A\uparrow_B|),\ \langle\Phi|\Psi\rangle = 1, \tag{3.16}$$

and therefore the yield $P^{(\tau)}(N)$ approaches asymptotically, as N becomes large, a finite value

$$P^{(\tau)}(\infty) = \frac{1}{2}[\langle\uparrow_A\downarrow_B| + e^{-i\chi}\langle\downarrow_A\uparrow_B|]\rho_{AB}(0)[|\uparrow_A\downarrow_B\rangle + e^{i\chi}|\downarrow_A\uparrow_B\rangle]. \tag{3.17}$$

This is nothing but the probability of finding the target entangled state $|\Psi\rangle=(|\uparrow_A\downarrow_B\rangle+e^{i\chi}|\downarrow_A\uparrow_B\rangle)/\sqrt{2}$ in the initial state $\rho_{AB}(0)$.

IV. ENTANGLEMENT DISTILLATION OF CAVITY MODES

In the previous section, the possibility of realizing an entanglement distillation is demonstrated for the three-qubit system $A+B+X$. The particular form of interaction (3.3b) is shown to be suitable for this purpose following the procedure (3.2). In this section, another application of the purification mechanism [3,5,6] is explored in a system composed of a two-level system (e.g., an atom) interacting with two single-mode cavities. The two cavities may be located at spatially distant places (or may be near and separated later) and we aim at extracting an entanglement between the two-cavity states by repeatedly bringing the two-level atom into interaction with them and then selecting a particular state of the atom by measurements.

The ideas of generating [8] and of transferring [9] entanglement in two-cavity system have already been proposed and studied in the context of the cavity quantum electrodynamics (CQED) [10], spectacularly developed over the last two decades both in the microwave [11] and optical [12] domains. Entanglement is generated from a properly prepared pure state in the former [8] and an initially prepared entanglement in one cavity is transformed into another entanglement between the two cavities in the latter [9], via successive interactions with a two-level atom. The atom plays the role of a "mediator" or "transformer" of entanglement. A similar, but more complicated role is sought for the atom in the present scheme, because its interactions with the cavities and the measurements of its state are expected to enable us to extract an entangled state, that is to produce an entanglement distillation, *irrespective of the initial states of the two cavities*.

For simplicity, suppose that the two cavities A and B are identical and their interaction with a two-level atom X is well described by the Jaynes-Cummings Hamiltonian [13]. Let a and b indicate the annihilation operators of the modes of the two cavities A and B, respectively. The free and interaction Hamiltonians are

$$H_0 = \frac{\omega}{2}(1+\sigma_3) + \omega a^\dagger a + \omega b^\dagger b, \tag{4.1a}$$

$$H'_{XA} = g_A(\sigma_+ a + \sigma_- a^\dagger), \quad H'_{XB} = g_B(\sigma_+ b + \sigma_- b^\dagger). \tag{4.1b}$$

A state where the atom X is in the up (down) state and the modes a and b are in the nth and mth levels, respectively, is denoted as $|\uparrow(\downarrow),n,m\rangle$ $(n,m=0,1,2,\ldots)$.

Since our purpose is to extract a pure state not in product form but entangled, it turns out that simple processes like (3.2) for the three-qubit system would not work. Indeed, because of the choice of the Jaynes-Cummings (rotating-wave) interactions (4.1b), the number operator $(1+\sigma_3)/2+a^\dagger a+b^\dagger b$ commutes with any of H_0, H'_{XA}, and H'_{XB}, and therefore any state of the two-cavity system of the form $|n,0\rangle$, which is a product state, is easily seen to be an eigenstate of the time evolution operator constructed analogously to (3.4). (If the down state of X is measured, product states $|0,m\rangle$ are found to be eigenstates of the relevant time evolution operator.) Thus a process different from (3.2) would be necessary for our purpose.

The above consideration would suggest that, with interaction given by (4.1b), it would be better to select after measurement a state of X different from the initial state. However, at the same time, we need a procedure that can be repeated many times within the present framework of the purification mechanism. Thus we choose a procedure that can be described schematically as

preparation in $|\downarrow\rangle$ $\rightarrow$ interaction between X and A for t_A
$\rightarrow$ free evolution for τ_A
$\rightarrow$ interaction between X and B for t_B
$\rightarrow$ free evolution for τ_B
$\rightarrow$ projection to $|\uparrow\rangle$
$\rightarrow$ free evolution for τ_B
$\rightarrow$ interaction between X and B for t_B
$\rightarrow$ free evolution for τ_A
$\rightarrow$ interaction between X and A for t_A
$\rightarrow$ projection to $|\downarrow\rangle$. (4.2)

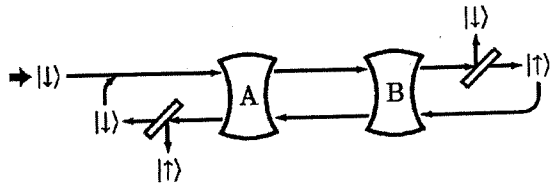

FIG. 2. A two-level atom X, prepared in $|\downarrow\rangle$, is brought to interaction with cavity modes a and b in the two cavities A and B successively, and its state is measured after the interactions. Atoms that are found in state $|\uparrow\rangle$ will be sent back to the cavities in the reversed order. The state of atom X is again measured, and if it is found in $|\downarrow\rangle$, the whole process is repeated; other events are discarded.

See also Fig. 2.

This is clearly a generalization of the purification process, "projection" $\rightarrow$ "time evolution" $\rightarrow$ "projection." Indeed, in the above scheme, "time evolution" is not meant in the usual sense, that is described by a total Hamiltonian. It is instead interrupted by another projection. However, the condition under which the purification mechanism does work is essentially the same as in the ordinary cases and all that we have to do here is to investigate the relevant evolution operator corresponding to the above process (4.2). It would be important to notice that the above choice of the initial and projected states for system X is not arbitrary. In fact, if it were prepared in the up state, a procedure analogous to that described before does not work. The vacuum state of the two cavities, which is a product state, would indeed turn out to be an eigenstate.

The relevant evolution for the above process (4.2) is represented by products of the time-evolution and projection operators and each of them is easily evaluated. The only nontrivial operators are

$$\begin{aligned} e^{-i(H_0+H'_{XA})t_A} = e^{-i\omega b^\dagger b t_A}\sum_{n=0}^{\infty} e^{-i(n+1)\omega t_A}(&\cos\varphi_A^{(n+1)}|\uparrow,n\rangle\langle\uparrow,n| - i\sin\varphi_A^{(n+1)}|\uparrow,n\rangle\langle\downarrow,n+1| \\ &- i\sin\varphi_A^{(n+1)}|\downarrow,n+1\rangle\langle\uparrow,n| + e^{i\omega t_A}\cos\varphi_A^{(n)}|\downarrow,n\rangle\langle\downarrow,n|) \end{aligned} \tag{4.3a}$$

and

$$\begin{aligned} e^{-i(H_0+H'_{XB})t_B} = e^{-i\omega a^\dagger a t_B}\sum_{m=0}^{\infty} e^{-i(m+1)\omega t_B}(&\cos\varphi_B^{(m+1)}|\uparrow,m\rangle\langle\uparrow,m| - i\sin\varphi_B^{(m+1)}|\uparrow,m\rangle\langle\downarrow,m+1| \\ &- i\sin\varphi_B^{(m+1)}|\downarrow,m+1\rangle\langle\uparrow,m| + e^{i\omega t_B}\cos\varphi_B^{(m)}|\downarrow,m\rangle\langle\downarrow,m|), \end{aligned} \tag{4.3b}$$

where angles $\varphi_A^{(n)}$ and $\varphi_B^{(m)}$ are defined as

$$\varphi_A^{(n)} \equiv g_A t_A\sqrt{n}, \quad \varphi_B^{(m)} \equiv g_B t_B\sqrt{m}. \tag{4.4}$$

It is an elementary task to evaluate in this case the relevant evolution operator V_c, analogously to (2.5),

$$V_c \equiv \langle\downarrow|e^{-i(H_0+H'_{XA})t_A}e^{-iH_0\tau_A}e^{-i(H_0+H'_{XB})t_B}e^{-iH_0\tau_B}|\uparrow\rangle\langle\uparrow|e^{-iH_0\tau_B}e^{-i(H_0+H'_{XB})t_B}e^{-iH_0\tau_A}e^{-i(H_0+H'_{XA})t_A}|\downarrow\rangle, \tag{4.5}$$

and its explicit expression reads

$$\begin{aligned} V_c = -\sum_{n,m=0}^{\infty} e^{-2i(n+m)\omega T}[&(\sin^2\varphi_A^{(n)}\cos^2\varphi_B^{(m+1)}+\cos^2\varphi_A^{(n)}\sin^2\varphi_B^{(m)})|n,m\rangle\langle n,m| \\ &+\sin\varphi_A^{(n+1)}\cos\varphi_A^{(n)}\sin\varphi_B^{(m)}\cos\varphi_B^{(m)}|n+1,m-1\rangle\langle n,m| \\ &+\sin\varphi_A^{(n)}\cos\varphi_A^{(n-1)}\sin\varphi_B^{(m+1)}\cos\varphi_B^{(m+1)}|n-1,m+1\rangle\langle n,m|], \end{aligned} \tag{4.6}$$

where $T \equiv t_A+\tau_A+t_B+\tau_B$.

It is manifest from (4.6) that in the product Hilbert space of the two cavities there are sectors of V_c within which the action of V_c is closed. These invariant sectors are characterized by the number $n+m$. We have $(n+m+1)$ states $\{|n+m,0\rangle,\ldots,|0,n+m\rangle\}$ for the $(n+m)$th sector. Notice that the singlet state (vacuum state) $|0,0\rangle$ $(n+m=0)$ belongs to zero eigenvalue of V_c and we need not consider it, for $V_c|0,0\rangle=0$. This is closely related to the choice of the initial state of X and is the reason why we must prepare X in the down state $|\downarrow\rangle$.

Let us turn our attention first to the doublet subspace $(n+m=1)$. The action of V_c on this subspace is easily read from (4.6) as

$$V_c\begin{pmatrix}|1,0\rangle\\|0,1\rangle\end{pmatrix} = -e^{-2i\omega T}\begin{pmatrix}\sin^2\varphi_A^{(1)}\cos^2\varphi_B^{(1)} & \sin\varphi_A^{(1)}\sin\varphi_B^{(1)}\cos\varphi_B^{(1)}\\ \sin\varphi_A^{(1)}\sin\varphi_B^{(1)}\cos\varphi_B^{(1)} & \sin^2\varphi_B^{(1)}\end{pmatrix}\begin{pmatrix}|1,0\rangle\\|0,1\rangle\end{pmatrix}. \tag{4.7}$$

Observe that the determinant of this matrix always vanishes, which means that one of the eigenvalues is zero and the other is given by the trace of the matrix $-e^{-2i\omega T}(\sin^2\varphi_A^{(1)}\cos^2\varphi_B^{(1)}+\sin^2\varphi_B^{(1)})$. Therefore we have a possibility of obtaining the largest (in magnitude) eigenvalue by adjusting the parameter g_At_A so that

$$\sin\varphi_A^{(1)} \equiv \sin(g_At_A) = \pm 1. \tag{4.8}$$

(The possibility $\cos\varphi_B^{(1)}=0$ would result, not in an entanglement distillation, but in a product-state purification.) In such a case, the above eigenvalue equation is simplified to

$$V_c\begin{pmatrix}|1,0\rangle\\|0,1\rangle\end{pmatrix} = \begin{pmatrix}\cos\varphi_B^{(1)} & \mp\sin\varphi_B^{(1)}\\ \pm\sin\varphi_B^{(1)} & \cos\varphi_B^{(1)}\end{pmatrix}\begin{pmatrix}-e^{-2i\omega T} & 0\\ 0 & 0\end{pmatrix} \times\begin{pmatrix}\cos\varphi_B^{(1)} & \pm\sin\varphi_B^{(1)}\\ \mp\sin\varphi_B^{(1)} & \cos\varphi_B^{(1)}\end{pmatrix}\begin{pmatrix}|1,0\rangle\\|0,1\rangle\end{pmatrix}, \tag{4.9}$$

from which it is clear that the entangled state $|\Psi_c^{(1)}\rangle = \cos\varphi_B^{(1)}|1,0\rangle \pm \sin\varphi_B^{(1)}|0,1\rangle$ can be extracted with the maximal probability by this setup. Notice that it still remains the freedom to adjust the value of $\varphi_B^{(1)}=g_Bt_B$.

The remaining task is to check whether there are other eigenstates of V_c belonging to eigenvalues with unit magnitude, under the condition (4.8). Consider the invariant sector characterized by $k=n+m>1$ that is composed of $k+1$ states $\{|k,0\rangle,\ldots,|0,k\rangle\}$. The action of V_c on this sector is represented by the following matrix [see (4.6)]:

$$V_c\begin{pmatrix}|k,0\rangle\\|k-1,1\rangle\\\vdots\\|2,k-2\rangle\\|1,k-1\rangle\\|0,k\rangle\end{pmatrix} = -e^{-2ik\omega T}\begin{pmatrix}c_k & d_k & \ldots & 0 & 0 & 0\\ d_k & c_{k-1} & \ldots & 0 & 0 & 0\\ \vdots & \vdots & \ddots & \vdots & \vdots & \vdots\\ 0 & 0 & \ldots & c_2 & d_2 & 0\\ 0 & 0 & \ldots & d_2 & c_1 & d_1\\ 0 & 0 & \ldots & 0 & d_1 & c_0\end{pmatrix} \times\begin{pmatrix}|k,0\rangle\\|k-1,1\rangle\\\vdots\\|2,k-2\rangle\\|1,k-1\rangle\\|0,k\rangle\end{pmatrix}, \tag{4.10}$$

where matrix elements c_j, d_j can be read from (4.6) as

$$c_j = \sin^2\varphi_A^{(j)}\cos^2\varphi_B^{(k-j+1)}+\cos^2\varphi_A^{(j)}\sin^2\varphi_B^{(k-j)}, \tag{4.11}$$

$$d_j = \sin\varphi_A^{(j)}\cos\varphi_A^{(j-1)}\sin\varphi_B^{(k-j+1)}\cos\varphi_B^{(k-j+1)}. \tag{4.12}$$

It is important to notice that the condition (4.8) implies that the element $d_2=\sin\varphi_A^{(2)}\cos\varphi_A^{(1)}\sin\varphi_B^{(k-1)}\cos\varphi_B^{(k-1)}$ vanishes, irrespective of $\varphi_B^{(k-1)}$, and thus the sector further splits into two subsectors $\{|k,0\rangle,\ldots,|2,k-2\rangle\}$ and $\{|1,k-1\rangle,|0,k\rangle\}$. Furthermore, it is easily seen that the entangled state in the latter subspace of the form $|\Psi_c^{(k)}\rangle=\cos\varphi_B^{(k)}|1,k-1\rangle \pm \sin\varphi_B^{(k)}|0,k\rangle$ has the eigenvalue $-e^{-2ik\omega T}$, while, as shown in the Appendix, no eigenstate in the former subspace $\{|k,0\rangle,\ldots,|2,k-2\rangle\}$ belongs to a unit (in magnitude) eigenvalue (if k is smaller than 9).

We have seen that there are, for any k sector, many entangled states $|\Psi_c^{(k)}\rangle = \cos\varphi_B^{(k)}|1,k-1\rangle \pm \sin\varphi_B^{(k)}|0,k\rangle$ ($k=1,2\ldots$) (that increase, in general, in higher k sectors) extracted with the optimal probabilities by the process (4.2). Repeated interactions of the two-level atom X in the cavities A and B and the prescribed measurements (projections) certainly bring us with a statistical (classical) mixture of these entangled states. The situation would not be considered completely satisfactory, since we would not be able to distill a single entangled state by the process (4.2). There is, however, a way out of this difficulty. We may prepare such an initial (mixed) state of $A+B$ that contains only those sectors with relatively small ks. Such a preparation of the initial state would effectively eliminate the possibility of obtaining other states than $|\Psi_c^{(k)}\rangle$ after performing the process (4.2). For example, we may consider the following preparation procedure, which is nothing but a purification process applied to cavity B. We send a two-level atom prepared in the down state $|\downarrow\rangle$ to cavity B. After its interaction, which is again assumed to be of the form (4.1b), with B, the atom is measured and only those events in which it is found in the state $|\downarrow\rangle$ are retained. This process is to be repeated many times and the resulting state of $A+B$, which will be used as the initial state for the following entanglement distillation process (4.2), is dominated by the state $\rho_{AB}(0) \sim \rho_A(0) \otimes |0\rangle\langle 0|$, since the vacuum state of system B is the unique eigenstate of the relevant evolution operator $\sim\langle\downarrow|e^{-iH'_{XB}t}|\downarrow\rangle$ belonging to eigenvalue unity if no fine tunings are made on the parameters. After having prepared the state $\rho_{AB}(0)$, we repeat the process (4.2) under the condition (4.8). We finally end up with the single entangled state $|\Psi_c^{(1)}\rangle$, because our initial state $\rho_{AB}(0)$ satisfies $\langle\Phi_c^{(k)}|\rho_{AB}(0)|\Phi_c^{(k)}\rangle = \langle\Psi_c^{(k)}|\rho_{AB}(0)|\Psi_c^{(k)}\rangle = 0$ for $k>1$, where $\langle\Phi_c^{(k)}|$ is the left eigenstate corresponding to $|\Psi_c^{(k)}\rangle$.

Concluding this section we wish to give typical values of relevant parameters under the aspect of the possibility of implementing our proposal in laboratory. We concentrate on the estimation of the total duration T of the experiment. To this end, we choose to be in the context of microwave CQED where both the geometrical arrangement of the experimental setup and the intensity of the atom-field coupling regime seem more favorable to our proposal. Let us first note that the typical atom-field coupling constant g (g_A or g_B) can be chosen in such a way that $g \sim 10^4 - 10^5\ \mathrm{s}^{-1}$ [14]. Moreover, the lifetime of a Rydberg atom is $\gtrsim 10^{-2}$ s [15]. As for the quality factor Q of the cavities currently used in laboratory, we quote typical values of the order of $10^8 - 10^{10}$ [14,15] corresponding to a cavity damping time 1 ms–1 s. Considering that in our case $t_A \sim t_B \sim g^{-1}$, the total duration T of the experiment may be estimated and turns out to be compatible with the entanglement distillation proposed in this section.

V. SUMMARY

In this paper, the idea of extracting entangled states among systems located at spatially separated places, irrespective of their initial states, has been proposed and applied to simple systems to show the potentiality of a measurement-based purification scheme [3]. The establishment of entanglement distillation relies on the successive interactions between the systems under consideration and the so-called "mediator" quantum system. In the first example, it is demonstrated that the entanglement between the two qubit states is possible via their interactions with another qubit, which plays the role of the entanglement mediator, with the maximal yield (optimal distillation). In the case of distillation of cavity-mode entanglement, however, a modification of the original simple scheme, that is, "interaction → measurement → interaction →···," is required and the modified procedure (4.2) turns out to result in the entangled state $|\Psi_c^{(1)}\rangle$, after an appropriate preparation of the initial state. We stress that there would also be the possibility of obtaining an entangled state not only in the lowest sector $k=1$ but also in the higher k sector, provided an appropriate initial state be prepared.

It would be worth stressing that in spite of such a modification required in the second example, the underlying notion is still the same: the action of a measurement (represented by a projection operator, for simplicity) causes an essential and critical dynamical change, not only in the system measured, but also in the others interacting with the former. Since the notion is so general, one can devise various applications of this scheme in many different situations. The examples explored in this paper are just two of them and further applications will be reported elsewhere.

Finally, we add some comments on the practical setup of our proposal. In both schemes reported in the previous sections, the entanglement mediator is an atom appropriately prepared before entering into interaction with the two subsystems to be entangled and subjected to a conditional measurement of its internal state at the end of the two successive coupling processes. We wish to stress that to realize in practice the required "many crosses" scheme one may synchronize the injection of the jth atom of the sequence into the process with the successful outcome of the internal state measurement of the $(j-1)$th one. This kind of experimental setup might be preferable to the conceptually simpler one based on the idea of using always the same atom, reversing its direction of motion at exit to reinject it into the process. Thus the representations in Figs. 1 and 2, as far as the aspect under scrutiny is concerned, have been reported only for the sake of simplicity.

ACKNOWLEDGMENTS

The authors (H.N., M.U., and K.Y.) acknowledge useful and helpful discussions with Professor I. Ohba. H.N. is grateful for the warm hospitality at Università di Palermo. This work is partly supported by a Grant for the 21st Century COE Program (Physics of Self-Organization Systems) at Waseda University and a Grant-in-Aid for Priority Areas Research (B) (No. 13135221), both from the Ministry of Education, Culture, Sports, Science and Technology, Japan, by a Grant-in-Aid for Scientific Research (C) (No. 14540280) from the Japan Society for the Promotion of Science, by a Waseda University Grant for Special Research Projects (No. 2002A-567), and by the bilateral Italian-Japanese project 15C1 on "Quantum Information and Computation" of the Italian Ministry for Foreign Affairs.

APPENDIX

In this appendix, a symmetric matrix of the form ($k \geqslant 2$)

$$\begin{pmatrix} c_k & d_k & 0 & \dots & 0 & 0 \\ d_k & c_{k-1} & d_{k-1} & \dots & 0 & 0 \\ 0 & d_{k-1} & c_{k-2} & \dots & 0 & 0 \\ \vdots & \vdots & \vdots & \ddots & \vdots & \vdots \\ 0 & 0 & 0 & \dots & c_3 & d_3 \\ 0 & 0 & 0 & \dots & d_3 & c_2 \end{pmatrix}, \tag{A1}$$

with the matrix elements [see Eqs. (4.11) and (4.12)]

$$c_j = \sin^2 \varphi_A^{(j)} \cos^2 \varphi_B^{(k-j+1)} + \cos^2 \varphi_A^{(j)} \sin^2 \varphi_B^{(k-j)}, \tag{A2a}$$

$$d_j = \sin \varphi_A^{(j)} \cos \varphi_A^{(j-1)} \sin \varphi_B^{(k-j+1)} \cos \varphi_B^{(k-j+1)}, \tag{A2b}$$

is investigated with particular attention to its eigenstates belonging to the eigenvalues with unit magnitudes. Since this matrix is real and symmetric, its eigenvalues are all real, and the eigenvalues of relevance in the framework of our procedure here are ± 1.

For the first possibility $+1$, let us consider the determinant I_i ($k \geqslant i \geqslant 2$) defined by

$$I_i \equiv \begin{vmatrix} c_i - 1 & d_i & 0 & \dots & 0 & 0 \\ d_i & c_{i-1} - 1 & d_{i-1} & \dots & 0 & 0 \\ 0 & d_{i-1} & c_{i-2} - 1 & \dots & 0 & 0 \\ \vdots & \vdots & \vdots & \ddots & \vdots & \vdots \\ 0 & 0 & 0 & \dots & c_3 - 1 & d_3 \\ 0 & 0 & 0 & \dots & d_3 & c_2 - 1 \end{vmatrix}. \tag{A3}$$

It is easy to see that the particular form of I_i and the definitions of c_j and d_j in Eq. (A2) lead to a recursion relation

$$\begin{aligned} &I_i + \cos^2 \varphi_A^{(i)} \cos^2 \varphi_B^{(k-i)} I_{i-1} \\ &\quad = -\sin^2 \varphi_A^{(i)} \sin^2 \varphi_B^{(k-i+1)} (I_{i-1} + \cos^2 \varphi_A^{(i-1)} \cos^2 \varphi_B^{(k-i+1)} I_{i-2}) \end{aligned} \tag{A4}$$

for $k \geqslant i \geqslant 4$. This is further reduced to

$$\begin{aligned} I_i &= -\cos^2 \varphi_A^{(i)} \cos^2 \varphi_B^{(k-i)} I_{i-1} \\ &\quad + (-1)^{i-1} \prod_{j=1}^{i-1} \sin^2 \varphi_A^{(j+1)} \sin^2 \varphi_B^{(k-j)} \quad (k \geqslant i \geqslant 2). \end{aligned} \tag{A5}$$

If we set $I_i \equiv (-1)^{i+1} P_i$, then P_i is found to be positive semidefinite and to satisfy

$$P_i = \cos^2 \varphi_A^{(i)} \cos^2 \varphi_B^{(k-i)} P_{i-1} + \prod_{j=1}^{i-1} \sin^2 \varphi_A^{(j+1)} \sin^2 \varphi_B^{(k-j)}. \tag{A6}$$

This relation is easily solved, to yield the explicit form of $I_k = (-1)^{k+1} P_k$ with

$$\begin{aligned} P_k &= \cos^2 \varphi_A^{(2)} \cdots \cos^2 \varphi_A^{(k)} \cos^2 \varphi_B^{(1)} \cdots \cos^2 \varphi_B^{(k-2)} \\ &\quad + \sum_{n=2}^{k-1} \sin^2 \varphi_A^{(2)} \cdots \sin^2 \varphi_A^{(n)} \cos^2 \varphi_A^{(n+1)} \cdots \cos^2 \varphi_A^{(k)} \\ &\quad \times \cos^2 \varphi_B^{(1)} \cdots \cos^2 \varphi_B^{(k-n-1)} \sin^2 \varphi_B^{(k-n+1)} \cdots \sin^2 \varphi_B^{(k-1)} \\ &\quad + \sin^2 \varphi_A^{(2)} \cdots \sin^2 \varphi_A^{(k)} \sin^2 \varphi_B^{(1)} \cdots \sin^2 \varphi_B^{(k-1)}. \end{aligned} \tag{A7}$$

Since each term in Eq. (A7) has the same sign as the others, vanishing of I_k, which is nothing but the condition for the matrix (A1) to possess eigenstates that belong to eigenvalue unity, is equivalent to that of each term. This means that there are k conditions for three parameters $g_A t_A$, $g_B t_B$, and k and it seems impossible to have a vanishing I_k in general, unless most of the conditions are simultaneously satisfied. If we choose a particular value for $g_A t_A$, say $g_A t_A = \pi/2$ as in (4.8), however, all I_k with $k \geqslant 9$ vanish because each term in Eq. (A7) contains either $\sin^2 \varphi_A^{(4)}$ or $\cos^2 \varphi_A^{(9)}$, each of which vanishes.

On the other hand, the matrix (A1) is shown to have no eigenstate belonging to the eigenvalue -1. Consider the following determinant:

$$J_i \equiv \begin{vmatrix} c_i + 1 & d_i & 0 & \dots & 0 & 0 \\ d_i & c_{i-1} + 1 & d_{i-1} & \dots & 0 & 0 \\ 0 & d_{i-1} & c_{i-2} + 1 & \dots & 0 & 0 \\ \vdots & \vdots & \vdots & \ddots & \vdots & \vdots \\ 0 & 0 & 0 & \dots & c_3 + 1 & d_3 \\ 0 & 0 & 0 & \dots & d_3 & c_2 + 1 \end{vmatrix}, \tag{A8}$$

where c_j and d_j are again given in (A2). Since $c_j > 0$, $d_j^2 < 1$, and therefore $J_2 = c_2 + 1 > 0$ and $J_3 = (c_3+1)(c_2+1) - d_3^2 > 0$, let us assume that all J_ℓ's are positive definite for ℓ up to $i-1$. Then it follows that

$$\begin{aligned} J_i &= (c_i + 1) J_{i-1} - d_i^2 J_{i-2} > c_i J_{i-1} - d_i^2 J_{i-2} \\ &= \sin^2 \varphi_A^{(i)} \cos^2 \varphi_B^{(k-i+1)} (J_{i-1} - \cos^2 \varphi_A^{(i-1)} \sin^2 \varphi_B^{(k-i+1)} J_{i-2}) \\ &\quad + \cos^2 \varphi_A^{(i)} \sin^2 \varphi_B^{(k-i)} J_{i-1}. \end{aligned} \tag{A9}$$

This relation recursively yields the inequalities

$$\begin{aligned} &J_i - \cos^2 \varphi_A^{(i)} \sin^2 \varphi_B^{(k-i)} J_{i-1} \\ &\quad > \sin^2 \varphi_A^{(i)} \cos^2 \varphi_B^{(k-i+1)} (J_{i-1} - \cos^2 \varphi_A^{(i-1)} \sin^2 \varphi_B^{(k-i+1)} J_{i-2}) \\ &\quad > \sin^2 \varphi_A^{(i)} \cos^2 \varphi_B^{(k-i+1)} \cdots \sin^2 \varphi_A^{(4)} \cos^2 \varphi_B^{(k-3)} \\ &\quad \times (J_3 - \cos^2 \varphi_A^{(3)} \sin^2 \varphi_B^{(k-3)} J_2). \end{aligned} \tag{A10}$$

The last factor on the right-hand side is shown to be positive definite,

$$\begin{aligned} &J_3 - \cos^2 \varphi_A^{(3)} \sin^2 \varphi_B^{(k-3)} J_2 \\ &\quad > (\sin^2 \varphi_A^{(3)} \cos^2 \varphi_B^{(k-2)} + 1) J_2 - d_3^2 > 0, \end{aligned} \tag{A11}$$

which means that the quantity on the left-hand side in (A10) is positive definite. We conclude that J_i is positive definite and therefore J_k does not vanish, which completes the proof.

[1] C. H. Bennett, G. Brassard, S. Popescu, B. Schumacher, J. A. Smolin, and W. K. Wootters, Phys. Rev. Lett. **76**, 722 (1996); **78**, 2031(E) (1997); C. H. Bennett, D. P. DiVincenzo, J. A. Smolin, and W. K. Wootters, Phys. Rev. A **54**, 3824 (1996); J. I. Cirac, A. K. Ekert, and C. Macchiavello, Phys. Rev. Lett. **82**, 4344 (1999).

[2] For reviews, see *The Physics of Quantum Information*, edited by D. Bouwmeester, A. Ekert, and A. Zeilinger (Springer, Heidelberg, 2000); A. Galindo and M. A. Martín-Delgado, Rev. Mod. Phys. **74**, 347 (2002), and references therein.

[3] H. Nakazato, T. Takazawa, and K. Yuasa, Phys. Rev. Lett. **90**, 060401 (2003); K. Yuasa, H. Nakazato, and T. Takazawa, J. Phys. Soc. Jpn. **72** Suppl. C, 34 (2003).

[4] In this respect, the present scheme seems to be closely related to the so-called quantum Zeno effect, though the mechanism is quite different, as has been pointed out in Ref. [3]. As for the quantum Zeno effect, see, for example, B. Misra and E. C. G. Sudarshan, J. Math. Phys. **18**, 756 (1977); K. Kraus, Found. Phys. **11**, 547 (1981); H. Nakazato, M. Namiki, and S. Pascazio, Int. J. Mod. Phys. B **10**, 247 (1996); D. Home and M. A. B. Whitaker, Ann. Phys. (N.Y.) **258**, 237 (1997); P. Facchi and S. Pascazio, in *Progress in Optics*, edited by E. Wolf (Elsevier, Amsterdam, 2001), Vol. 42, p. 147.

[5] K. Yuasa, H. Nakazato, and M. Unoki, J. Mod. Opt. **51**, 1005 (2004); H. Nakazato, M. Unoki, and K. Yuasa, Phys. Rev. A **70**, 012303 (2004).

[6] L.-A. Wu, D. A. Lidar, and S. Schneider, Phys. Rev. A **70**, 032322 (2004).

[7] For reviews, see C. H. Bennett and D. P. DiVincenzo, Nature (London) **404**, 247 (2000); M. A. Nielsen and I. L. Chuang, *Quantum Computation and Quantum Information* (Cambridge University Press, Cambridge, U.K., 2000), and references therein.

[8] P. Meystre, in *Progress in Optics*, edited by E. Wolf (Elsevier Science, New York, 1992), Vol. 30, p. 261; J. A. Bergou and M. Hillery, Phys. Rev. A **55**, 4585 (1997); A. Messina, Eur. Phys. J. D **18**, 379 (2002); D. E. Browne and M. B. Plenio, Phys. Rev. A **67**, 012325 (2003).

[9] A. Napoli, A. Messina, and G. Compagno, Fortschr. Phys. **51**, 81 (2003).

[10] H. Mabuchi and A. Doherty, Science **298**, 1372 (2002).

[11] E. Hagley, X. Maître, G. Nogues, C. Wunderlich, M. Brune, J. M. Raimond, and S. Haroche, Phys. Rev. Lett. **79**, 1 (1997); M. Weidinger, B. T. H. Varcoe, R. Heerlein, and H. Walther, *ibid.* **82**, 3795 (1999); A. Rauschenbeutel, G. Nogues, S. Osnaghi, P. Bertet, M. Brune, J. M. Raimond, and S. Haroche, *ibid.* **83**, 5166 (1999); J. M. Raimond, M. Brune, and S. Haroche, Rev. Mod. Phys. **73**, 565 (2001).

[12] R. J. Thompson, G. Rempe, and H. J. Kimble, Phys. Rev. Lett. **68**, 1132 (1992); C. J. Hood, T. W. Lynn, A. C. Doherty, A. S. Parkins, and H. J. Kimble, Science **287**, 1447 (2000).

[13] E. T. Jaynes and F. W. Cummings, Proc. IEEE **51**, 89 (1963); see also M. O. Scully and H. Walther, Phys. Rev. A **39**, 5229 (1989).

[14] H. Walther, in *Quantum Communication, Computing, and Measurement 3*, edited by P. Tombesi and O. Hirota (Kluwer Academic/Plenum, New York, 2001), p. 463.

[15] S. Haroche, in *Fundamental Systems in Quantum Optics*, edited by J. Dalibard, J.-M. Raimond, and J. Zinn-Justin (North-Holland, Amsterdam, 1992).

PHYSICAL REVIEW A **71**, 022302 (2005)

Control of decoherence: Analysis and comparison of three different strategies

P. Facchi,[1] S. Tasaki,[2] S. Pascazio,[1] H. Nakazato,[3] A. Tokuse,[2] and D. A. Lidar[4]
[1]*Dipartimento di Fisica, Università di Bari and Istituto Nazionale di Fisica Nucleare, Sezione di Bari, I-70126 Bari, Italy*
[2]*Department of Applied Physics and Advanced Institute for Complex Systems, Waseda University, Tokyo 169-8555, Japan*
[3]*Department of Physics, Waseda University, Tokyo 169-8555, Japan*
[4]*Chemical Physics Theory Group, Chemistry Department and Center for Quantum Information and Quantum Control, University of Toronto, 80 St. George Street, Toronto, Ontario, Canada M5S 3H6*
(Received 29 March 2004; revised manuscript received 23 June 2004; published 8 February 2005)

We analyze and compare three different strategies, all aimed at controlling and eventually halting decoherence. The first strategy hinges upon the quantum Zeno effect, the second makes use of frequent unitary interruptions ("bang-bang" pulses and their generalization, quantum dynamical decoupling), and the third uses a strong, continuous coupling. Decoherence is shown to be suppressed only if the frequency N of the measurements or pulses is large enough or if the coupling K is sufficiently strong. Otherwise, if N or K is large, but not extremely large, all these control procedures accelerate decoherence. We investigate the problem in a general setting and then consider some practical examples, relevant for quantum computation.

DOI: 10.1103/PhysRevA.71.022302 PACS number(s): 03.67.Pp, 03.65.Xp, 03.65.Yz, 03.67.Lx

I. INTRODUCTION

Interactions with the environment deteriorate the purity of quantum states. This general phenomenon, known as decoherence [1], is a serious obstacle against the preservation of quantum superpositions and entanglement over long periods of time. Decoherence entails nonunitary evolutions, with serious consequences, like a loss of information and/or probability leakage toward the environment.

This issue is recently attracting much attention in view of interesting applications: for instance, the possibility of controlling and eventually halting decoherence is a key problem in quantum computation [2], where several computational states are simultaneously described by a single wave function and parallel information processing is carried out by unitary operations. In such a situation, efficient quantum algorithms need large scale computations, performed over (microscopically) long time spans [3].

A number of interesting schemes have been proposed during the last few years in order to counter the effects of decoherence. Among these, there are quantum error-correcting codes [4], schemes based on feedback or stochastic control [5], the use of decoherence-free subspaces and noiseless subsystems [6], and mechanisms based on frequent unitary "bang-bang" (BB) pulses and their generalization, quantum dynamical decoupling [7–11]. In this context, it was recently proposed [12] that the method of dynamical decoupling can be unified with the basic ideas underlying the quantum Zeno effect (QZE) [13,14] (for a review, see [15,16]). In particular, the decoherence-free subspace is one of the dynamically generated quantum Zeno subspaces [17], within which the dynamics is not trivial [18] and whose subtle mathematical aspects are still debated [14,19–23].

It is worth stressing that the "bang-bang" scheme is a well-established "classical" control method, typically used in engineering problems and in connection with spin-echo techniques; see, for instance, Ref. [24]. Its revival in quantum-information-related problems is only very recent. The key ingredient of BB and dynamical decoupling is to apply frequent (unitary) interruptions during the evolution of the system, in order to suppress the system-environment interaction. There is a manifest similarity with the QZE. It is, however, clear that the two procedures are physically equivalent, if one adheres to the commonly accepted interpretation of the QZE as a *bona fide* dynamical process, that can be completely explained in terms of *unitary* evolutions [25]. One should notice that this idea hinges upon a seminal remark by Wigner [26], who introduced in 1963 the notion of "spectral decomposition," namely, a dynamical process that associates a different wave packet with each eigenvalue of the observable to be measured. For example, the interesting proposal by Cook [27] and the subsequent experiment with Rabi oscillations [28] can be easily interpreted in fully dynamical terms when one observes that the "measurement" was realized as a dynamical process (optical pulse irradiation) [16,25,29].

Once this physical equivalence is appreciated, the next logical step is a natural one: after having analyzed and understood the consequences of frequent unitary pulses, one studies the effect of a strong (unitary) continuous coupling. The relationship between these two procedures can be made mathematically precise (see Sec. II) and is of interest in itself: if an external field or "apparatus" is coupled to the system in such a way that the state of the system is "monitored" in some sense [30–33], a Zeno-like dynamics takes place in the strong coupling limit and once again one can tailor decoherence-free subspaces [12]. This happens to be one of the most efficient and convenient control procedures, from a practical point of view.

The aim of this article is to investigate these different physical procedures (Zeno, BB dynamical decoupling, and continuous coupling) and compare their effects. We will study the dynamics generated by very frequent interruptions (projective measurements or unitary "kicks," yielding dynamical decoupling), or by very strong coupling, and investigate the possibility of designing decoherence-free subspaces. The method is general and can be applied to diverse situations of practical interest, such as atoms and ions in

cavities, organic molecules, quantum dots, and Josephson junctions [34–37].

Our main objective is to endeavor to understand whether it is possible to *control* decoherence [38–42]. Clearly, this requires a thorough understanding of the physical mechanisms that provoke decoherence and in general dissipative phenomena. One finds that very frequent kicks or measurements or very strong couplings can indeed control the evolution of the system and suppress decoherence: The physical mechanisms at the origin of this phenomenon are very close to the quantum Zeno effect. However, if the kicks or measurements are not extremely frequent or the coupling not extremely strong, both controls may *accelerate* decoherence. This extends the notion of the "inverse" quantum Zeno effect (IZE) [43,44] to a wider framework (not necessarily based on projection operators and nonunitary dynamics) and entails a deterioration of the performance of these schemes. We will analyze this effect in great detail and see that in order to avoid it, one must carefully design the control and study the time scales involved. Our analysis is of general validity; however, for the sake of definiteness, we will study in particular the control of thermal decoherence [45].

This article is organized as follows. In Sec. II we briefly review the main features of the different control procedures. Our analysis is based on a master equation which is derived in Sec. III, where the relevant time scales are emphasized and the general type of interaction specified. We then consider the case of thermal decoherence, discussing the Zeno control, the control via dynamical decoupling, and the control by means of a strong continuous coupling in Secs. IV, V, and VI, respectively. Some relevant examples are then considered in Sec. VII, where we focus on the primary role of the form factors of the interaction in order to compare the different control procedures. Section VIII is devoted to conclusions and perspectives. Four Appendixes A–D, containing detailed calculations that are omitted in the text, are added for clarity.

II. CONTROL PROCEDURES: GENERALITIES

Let the total system consist of a target system and a reservoir and its Hilbert space $\mathcal{H}_{\rm tot}=\mathcal{H}_S\otimes\mathcal{H}_B$ be expressed as the tensor product of the system Hilbert space $\mathcal{H}_S$ and the reservoir Hilbert space $\mathcal{H}_B$. The total Hamiltonian

$$H_{\rm tot}=H_0+H_{SB}=H_S\otimes \mathbb{1}_B+\mathbb{1}_S\otimes H_B+H_{SB} \tag{1}$$

is the sum of the system Hamiltonian $H_S\otimes\mathbb{1}_B$, the reservoir Hamiltonian $\mathbb{1}_S\otimes H_B$, and their interaction H_{SB}, which is responsible for decoherence; the operators $\mathbb{1}_S$ and $\mathbb{1}_B$ are the identity operators in the Hilbert spaces $\mathcal{H}_S$ and $\mathcal{H}_B$, respectively, and the operators H_S and H_B act on $\mathcal{H}_S$ and $\mathcal{H}_B$, respectively.

The dynamics of the total system is conveniently expressed in terms of the Liouville operator (Liouvillian) $\mathcal{L}_{\rm tot}$, defined by

$$\mathcal{L}_{\rm tot}\rho\equiv -i[H_{\rm tot},\rho]=-i(H_{\rm tot}\rho-\rho H_{\rm tot}), \tag{2}$$

where ρ is the density matrix. If the Hamiltonian is given by Eq. (1), the Liouvillian is accordingly decomposed into

$$\mathcal{L}_{\rm tot}=\mathcal{L}_0+\mathcal{L}_{SB}=\mathcal{L}_S+\mathcal{L}_B+\mathcal{L}_{SB}, \tag{3}$$

where the meaning of the symbols is obvious. We will not explicitly write the coupling constant λ multiplying the interaction Liouvillian $\mathcal{L}_{SB}$.

We focus on a proper subspace $\mathcal{H}_{\rm comp}\subset\mathcal{H}_S$, in which quantum computation is to be performed. For this reason we will look in detail at the case

$$\mathcal{H}_S=\mathcal{H}_{\rm comp}\oplus\mathcal{H}_{\rm orth}. \tag{4}$$

In particular, when we look at some concrete examples, in Sec. VII, the computation subspace will be a qubit, $\mathcal{H}_{\rm comp}=\mathbb{C}^2$.

Since, in general, the reservoir state is mixed, it is convenient to describe the time evolution in terms of density matrices. In the case of a quantum state manipulation, the initial state of the total system $\rho(0)$ is set to be a tensor product of the system initial state $\sigma(0)$ and a reservoir (usually equilibrium) state ρ_B,

$$\rho(0)=\sigma(0)\otimes\rho_B. \tag{5}$$

The derivation of the master equation from Eqs. (1)–(5) is given in Appendix A. The validity of the assumption (5), usually taken for granted, is discussed in Appendix B (see also [46]). The system state $\sigma(t)$ at time t is given by the partial trace of the state $\rho(t)$ of the whole system with respect to the reservoir degrees of freedom:

$$\sigma(t)\equiv {\rm tr}_B\rho(t). \tag{6}$$

When $\sigma(t)$ is not unitarily equivalent to $\sigma(0)$ for a given class of initial states, decoherence is said to occur. The purpose of the control is to suppress such decoherence. Note that, for the control of decoherence, it is not necessary to look at all possible states: rather, it is sufficient to consider only those initial states that are relevant to the quantum state manipulation in question.

A. Quantum Zeno control

We first look at the Zeno control, by adapting the argument of Ref. [17]. The control is obtained by performing frequent measurements of the system. The measurement is described by a projection superoperator $\hat{P}$ acting on the density matrix

$$\rho\to\hat{P}\rho\equiv\sum_n (P_n\otimes\mathbb{1}_B)\rho(P_n\otimes\mathbb{1}_B), \tag{7}$$

where $\{P_n\}$ is a set of orthogonal projection operators acting on $\mathcal{H}_S$. In the following, we restrict our analysis to a measuring apparatus that does not "select" the different outcomes (nonselective measurement) [47], with a complete set of projection operators $\Sigma_n P_n=\mathbb{1}_S$. The measurement is designed so that

$$\hat{P}H_{SB}=\sum_n (P_n\otimes\mathbb{1}_B)H_{SB}(P_n\otimes\mathbb{1}_B)=0. \tag{8}$$

In terms of the Liouvillian, this condition reads

$$\hat{P}\mathcal{L}_{SB}\hat{P}=0. \tag{9}$$

(We will see in the next subsection that a similar requirement is necessary for the BB control and for the control via a continuous coupling.) The Zeno control consists in performing repeated nonselective measurements at times $t=k\tau(k=0,1,2,\ldots)$ (we include an initial "state preparation" at $t=0$). Between successive measurements, the system evolves via H_{tot}. The density matrix after $N+1$ measurements, with an initial state $\rho(0)$, is given by

$$\rho(t)=\rho(N\tau)=(\hat{P}e^{\mathcal{L}_{\text{tot}}\tau}\hat{P})^N\rho(0). \tag{10}$$

We take the limit $\tau\to 0$ while keeping $t=N\tau$ constant and get

$$\rho(t)=\hat{P}[1+\hat{P}\mathcal{L}_{\text{tot}}\hat{P}\tau+O(\tau^2)]^{t/\tau}\rho(0)\overset{\tau\to 0}{\longrightarrow}\hat{P}e^{\hat{P}\mathcal{L}_{\text{tot}}\hat{P}t}\rho(0). \tag{11}$$

Equation (8) yields

$$\begin{aligned}\hat{P}\mathcal{L}_{\text{tot}}\hat{P}\rho&=-i\hat{P}[H_{\text{tot}},\hat{P}\rho]=-i\hat{P}[(\hat{P}H_{\text{tot}}),\rho]\\&=-i\hat{P}[H_S'\otimes\mathbb{1}_B+\mathbb{1}_S\otimes H_B,\rho],\end{aligned} \tag{12}$$

with $H_S'=\hat{P}H_S=\Sigma_n P_n H_S P_n$, whence

$$\hat{P}e^{\hat{P}\mathcal{L}_{\text{tot}}\hat{P}t}\rho(0)=\hat{P}e^{\mathcal{L}_{\text{tot}}'t}\rho(0)=\hat{P}[e^{-iH_{\text{tot}}'t}\rho(0)e^{iH_{\text{tot}}'t}], \tag{13}$$

where the controlled Hamiltonian H_{tot}' and Liouvillian $\mathcal{L}_{\text{tot}}'$ are given by

$$H_{\text{tot}}'\equiv\hat{P}H_{\text{tot}}=H_S'\otimes\mathbb{1}_B+\mathbb{1}_S\otimes H_B, \tag{14}$$

$$\mathcal{L}_{\text{tot}}'=\hat{P}\mathcal{L}_{\text{tot}}\hat{P}=\hat{P}\mathcal{L}_S\hat{P}+\mathcal{L}_B\hat{P}=\mathcal{L}_S'+\mathcal{L}_B\hat{P}, \tag{15}$$

Hence, as a result of infinitely frequent measurements, the system-reservoir coupling is eliminated and, thus, decoherence is halted. We notice the formation of invariant *Zeno subspaces* [17] : in the limit of very frequent measurements, the evolution is given by Eqs. (14) and (15) and transitions among different sectors of the Hilbert space become forbidden, yielding a superselection rule. The subspaces are defined by the superoperator $\hat{P}$ defining the measurement. The "decoherence-free" subspace is one of these Zeno subspaces.

We will assume for simplicity that $\hat{P}$ commutes with the system Liouvillian,

$$\hat{P}\mathcal{L}_S=\mathcal{L}_S\hat{P}, \tag{16}$$

i.e., $H_S'=\hat{P}H_S=H_S$, because our purpose is to control decoherence and we are not interested in a QZE over the system Hamiltonian H_S. The above assumption is equivalent to the following hypothesis on the Hamiltonian:

$$[P_n,H_S]=0,\quad\forall n. \tag{17}$$

In such a case

$$\mathcal{L}_{\text{tot}}'=(\mathcal{L}_S+\mathcal{L}_B)\hat{P}. \tag{18}$$

B. Control via quantum dynamical decoupling and "bang-bang" pulses

We now turn our attention to the so-called quantum dynamical decoupling [8–10], of which "bang-bang" pulses can be viewed as a particular case. The control of decoherence is achieved via a time-dependent *system* Hamiltonian $H_c(t)$:

$$H(t)=H_{\text{tot}}+H_c(t)\otimes\mathbb{1}_B, \tag{19}$$

where $H_c(t)$ is designed so that

$$U_c(t)\equiv\mathcal{T}\exp\left(-i\int_0^t H_c(s)ds\right) \tag{20}$$

($\mathcal{T}$ denotes time ordering) satisfies

$$U_c(t+\tau)=U_c(t), \tag{21}$$

$$\int_0^\tau dt[U_c^\dagger(t)\otimes\mathbb{1}_B]H_{SB}[U_c(t)\otimes\mathbb{1}_B]=0. \tag{22}$$

In the interaction picture in which $H_c(t)$ is unperturbed, the density matrix at time $t=N\tau$, with initial state $\rho(0)$, is given by $\rho(t)=U_{\text{tot}}(N\tau)\rho(0)U_{\text{tot}}^\dagger(N\tau)$ where

$$\begin{aligned}U_{\text{tot}}(N\tau)&=\mathcal{T}\exp\left(-i\int_0^{N\tau}\tilde{H}_{\text{tot}}(s)ds\right)\\&=\left[\mathcal{T}\exp\left(-i\int_0^{\tau}\tilde{H}_{\text{tot}}(s)ds\right)\right]^N\end{aligned} \tag{23}$$

and $\tilde{H}_{\text{tot}}(t)=[U_c^\dagger(t)\otimes\mathbb{1}_B]H_{\text{tot}}[U_c(t)\otimes\mathbb{1}_B]$. The second equality follows from the periodicity of $\tilde{H}_{\text{tot}}(t)$. A standard Magnus expansion of the time-ordered exponential [48] leads to

$$\mathcal{T}\exp\left(-i\int_0^\tau\tilde{H}_{\text{tot}}(s)ds\right)=e^{-i[\bar{H}^{(0)}+\bar{H}^{(1)}+\cdots]\tau}, \tag{24}$$

where $\bar{H}^{(0)}\equiv(1/\tau)\int_0^\tau\tilde{H}_{\text{tot}}(s)ds$ and the term $\bar{H}^{(j)}$ is of order τ^j $(j=1,2,\ldots)$. By assumption (22), one has

$$\bar{H}^{(0)}=H_S'\otimes\mathbb{1}_B+\mathbb{1}_S\otimes H_B=H_{\text{tot}}', \tag{25}$$

which is formally identical to Eq. (14), where $H_S'\equiv(1/\tau)\int_0^\tau dt\ U_c^\dagger(t)H_SU_c(t)=\int_0^1 dx\ U_c^\dagger(x\tau)H_SU_c(x\tau)$ is independent of τ because $U_c(t)$ is τ periodic by Eq. (21) and is always written as a function of t/τ: $U_c(t)=V(t/\tau)$. Therefore, in the limit $\tau\to 0$ while keeping $t=N\tau$ constant, one obtains

$$U_{\text{tot}}(t)=[1-iH_{\text{tot}}'\tau+O(\tau^2)]^{t/\tau}\overset{\tau\to 0}{\longrightarrow}e^{-iH_{\text{tot}}'t}=e^{-iH_S't}\otimes e^{-iH_Bt}. \tag{26}$$

In short, as a result of the infinitely fast control, the system-reservoir coupling is eliminated and, thus, decoherence is halted. As we shall see in a while, this is a consequence of the formation of invariant (Zeno) subspaces.

As is well known, dynamical decoupling is a generalization of the evolution obtained by acting on the system with "bang-bang" pulses [8]. In the latter, particular case, one applies during a time interval τ two *instantaneous* unitary operators U_k and $U_k^\dagger$ and gets [12]

$$H'_{\rm tot} = \hat{P}H_{\rm tot} = \sum_n (P_n \otimes \mathbb{1}_B)H_{\rm tot}(P_n \otimes \mathbb{1}_B) \tag{27}$$

[see Eq. (14)], where the projections P_n arise from the spectral decomposition

$$U_k = \sum_n e^{-i\lambda_n}P_n \quad (\lambda_n \neq \lambda_m \bmod 2\pi \text{ for } n \neq m). \tag{28}$$

Notice that the map $\hat{P}$ is in this case the projection onto the commutant

$$Z(U_k) = \{X | [X, U_k] = 0\}. \tag{29}$$

Equation (27) yields a convenient explicit expression of the effective Hamiltonian. As in the case discussed in the previous subsection, one observes the formation of invariant Zeno subspaces: transitions among different subspaces vanish in the $\tau \to 0$ limit, yielding a superselection rule. In this case, the subspaces are defined by Eqs. (27) and (28) and are nothing but the ergodic sectors of U_k.

By assuming again, as in Eqs. (16) and (17), that $\hat{P}H_S = H_S$ and that $\hat{P}H_{SB}=0$, as in Eqs. (8) and (9), we get the controlled evolution for $\tau \to 0$, given by

$$U_{\rm tot}(t) = e^{-iH'_{\rm tot}t} = e^{-iH_S t} \otimes e^{-iH_B t} \tag{30}$$

or, in terms of Liouvillians, by $e^{\mathcal{L}'_{\rm tot}t}$ with $\mathcal{L}'_{\rm tot} = \hat{P}\mathcal{L}_{\rm tot}\hat{P} = (\mathcal{L}_S + \mathcal{L}_B)\hat{P}$, exactly as in Eq. (18).

Moreover, in Ref. [12] it was shown that one can obtain the same result (27) by repeating a single "bang," i.e., by using a single instantaneous unitary operator U_k, *without* closing the group with $U_k^\dagger$. For simplicity, in the following we will always consider such a situation and will assume the commutation property (16). In such a case, the evolution is conveniently expressed in terms of the Liouvillian and density matrix,

$$\rho(t) = [e^{\mathcal{L}_k}e^{\mathcal{L}_{\rm tot}\tau}]^{t/\tau}\hat{P}\rho(0) \to e^{\mathcal{L}'_{\rm tot}t}\hat{P}\rho(0), \quad \tau \to 0, \tag{31}$$

where $\mathcal{L}_k$ is the Liouvillian corresponding to the evolution (28) and $\mathcal{L}'_{\rm tot}$ is given by Eq. (18). Note that the controlled Hamiltonians for bang-bang pulses, Eq. (27), and for the Zeno control, Eq. (14), coincide when the set of orthogonal projections (7) is chosen equal to the set (28) of eigenprojections of U_k, namely,

$$\mathcal{L}_k\hat{P} = 0, \quad (\hat{P}\mathbb{1}) = \mathbb{1}. \tag{32}$$

Therefore, the two controls are equivalent in the ideal (limiting) case [12]. However, throughout this article, by dynamical decoupling we will refer to a situation where the evolution is coherent (unitary), while by Zeno control to a situation where the evolution involves incoherent (nonunitary) processes, such as quantum measurements.

The index "k" in the above expressions stands for "kicks." In the following, we shall use the expressions "bang-bang" pulses and "kicks" interchangeably. The latter is reminiscent of quantum chaos [49]. In fact, there is an interesting link between quantum chaotic dynamics, quantum diffusion processes, and the (inverse) quantum Zeno effect [50]. We will not elaborate on this issue in the present article.

C. Control via a strong continuous coupling

The formulation in the preceding sections hinges upon instantaneous processes, which can be unitary or nonunitary. However, as explained in the Introduction, the basic features of the QZE can be obtained by making use of a continuous coupling, when the external system takes a sort of steady "gaze" at the system of interest. The mathematical formulation of this idea is contained in a theorem [17] on the (large-K) dynamical evolution governed by a *generic* Hamiltonian of the type

$$H_K = H_{\rm tot} + KH_c \otimes \mathbb{1}_B, \tag{33}$$

which again need not describe a *bona fide* measurement process: H_c can be viewed as an "additional" interaction Hamiltonian performing the "measurement" and K is a coupling constant.

Consider the time evolution operator

$$U_K(t) = \exp(-iH_K t). \tag{34}$$

In the infinitely strong measurement (infinitely quick detector) limit $K \to \infty$, the dominant contribution is $\exp(-iKH_c t)$. One therefore considers the limiting evolution operator

$$\mathcal{U}(t) = \lim_{K\to\infty} \exp(iKH_c t)U_K(t), \tag{35}$$

which can be shown to have the form

$$\mathcal{U}(t) = \exp(-iH'_{\rm tot}t), \tag{36}$$

where

$$H'_{\rm tot} = \hat{P}H_{\rm tot} = \sum_n (P_n \otimes \mathbb{1}_B)H_{\rm tot}(P_n \otimes \mathbb{1}_B), \tag{37}$$

P_n being the eigenprojection of H_c belonging to the eigenvalue η_n,

$$H_c = \sum_n \eta_n P_n \quad (\eta_n \neq \eta_m \text{ for } n \neq m). \tag{38}$$

By designing H_c so that $\hat{P}H_{SB}=0$, the system-reservoir coupling is eliminated and, thus, decoherence is halted. Equation (37), restricted to the system of interest, is formally identical to Eqs. (27) and (14).

In conclusion, the limiting evolution operator is

$$\begin{aligned} U_K(t) &\sim \exp(-iKH_c t)\mathcal{U}(t) \\ &= \exp\left[-iKt\sum_n \eta_n P_n \otimes 1_B - i\hat{P}H_{\rm tot}t\right]. \end{aligned} \tag{39}$$

The above statements can be proved by making use of the adiabatic theorem [51]. It is worth noting that the evolution in the strong coupling limit is known to force the system to "cling" to the eigenstates of the interaction [52]. In this sense, one expects the dynamics to be dominated by H_c for K large. The above theorem clarifies how the structure of H_c determines the features of the dynamics. Once again, as in the two previous subsections, one observes the formation of invariant Zeno subspaces, which are in this case the eigenspaces of the interaction (37) and (38): the block-diagonal structure of (39) is explicit. The links between the quantum

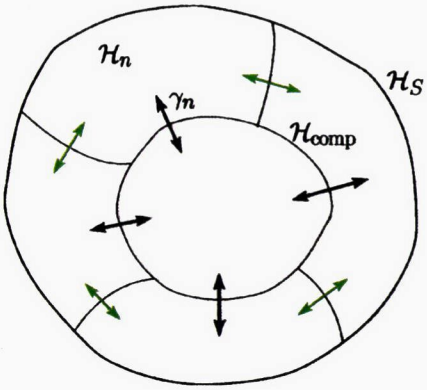

FIG. 1. The Zeno subspaces are formed when the frequency τ^{-1} of measurements or BB pulses or the strength K of the continuous coupling tends to ∞. The shaded region represents the "computational" subspace $\mathcal{H}_{\rm comp}\subset\mathcal{H}_S$ defined in Eq. (4). The transition rates γ_n depend on τ or K.

Zeno effect and the notion of "continuous coupling" to an external apparatus or environment has often been proposed in the literature of the last 25 years [30,31,33,53]. However, our interest here is focused on the gradual formation of the Zeno subspaces as K becomes increasingly large. In such a case, they are nothing but the adiabatic subspaces. In terms of the Liouvillian,

$$\rho(t) = e^{(K\mathcal{L}_c+\mathcal{L}_{\rm tot})t}\hat{P}\rho(0) \to e^{\mathcal{L}'_{\rm tot}t}\hat{P}\rho(0), \quad K\to\infty \tag{40}$$

[see (31)], where the notation is obvious, and

$$\mathcal{L}_c\hat{P} = 0, \quad (\hat{P}1) = 1 \tag{41}$$

[see (32)]. The Liouvillian $\mathcal{L}'_{\rm tot}=\hat{P}\mathcal{L}_{\rm tot}\hat{P}$ corresponds to $\hat{P}H_{\rm tot}=H'_{\rm tot}$ and, under the assumptions (16) and (9), is again given by (18).

D. Controlled evolution and Zeno subspaces

The three different procedures described in this section yield, by different physical mechanisms, the formation of invariant Zeno subspaces. This is shown in Fig. 1. If one of these invariant subspaces is the "computational" subspace $\mathcal{H}_{\rm comp}$ introduced in Eq. (4), the possibility arises of inhibiting decoherence in this subspace.

Of course, in the $\tau, K^{-1}\to 0$ limit, decoherence can be completely *halted*, according to Eqs. (13)–(15), (26), (27), (37), and (38). However, the objective of our study is to understand *how* the limit is attained and analyze the deviations from the ideal situation. This will be done by studying the transition rates γ_n between different subspaces and in particular their τ and K dependence (see Fig. 1). We shall see that in general this dependence can be complicated, leading to *enhancement* of decoherence in some cases and *suppression* in other cases. For this reason, the *physical* meaning of the expressions $\tau, K^{-1}\to 0$ in this section must be scrutinized with great care.

III. FREE DYNAMICS

A. The general case

We consider the time evolution when the initial state is factorized as in Eq. (5) (this hypothesis is discussed in Appendix B) and the reservoir equilibrium state has an inverse temperature β,

$$\rho_B = \frac{1}{Z}\exp(-\beta H_B) \quad (\mathcal{L}_B\rho_B = 0) \tag{42}$$

where $Z=\mathrm{tr}_B e^{-\beta H_B}$ is the normalization constant.

Assume that the interaction Hamiltonian H_{SB} in (1) can be written as [54]

$$H_{SB} = \sum_m (X_m\otimes A_m^\dagger + X_m^\dagger\otimes A_m), \tag{43}$$

where the X_m are the eigenoperators of the system Liouvillian, satisfying

$$\mathcal{L}_S X_m = i\omega_m X_m \quad (\omega_m\neq\omega_n \text{ for } m\neq n) \tag{44}$$

and A_m are the destruction operators of the bath,

$$A_m = A(g_m) = \int d^3k\, g_m^*(\boldsymbol{k})a(\boldsymbol{k}), \tag{45}$$

expressed in terms of bosonic operators $a(\boldsymbol{k})$, with form factors $g_m(\boldsymbol{k})$. We are specifying our analysis to three dimensions (although it is valid in any dimension). Incidentally, the form of the Hamiltonian (43) is of very general validity (and is not limited, as one might naively think, to dipolelike approximations): the only assumption made is that the coupling with the bath be linear, i.e., one is not considering terms of the type a^2, $a^{\dagger 2}$, etc., which would only be relevant for squeezed reservoirs. In practice, one determines the operators (44), then finds the bath operators in order to write the interaction in the form (43), and neglects nonlinear terms.

In Eq. (44) we will identify $\omega_{-m}=-\omega_m$ and will assume that $X_{-m}=X_m^\dagger$ and $g_m=g_{-m}$, which is equivalent to the hypothesis that the interaction Hamiltonian be the product of self-adjoint operators acting on the system and the bath, namely, $H_{SB}=\Sigma_i H_S^{(i)}\otimes H_B^{(i)}$, with $H_S^{(i)}$ and $H_B^{(i)}$ self-adjoint. Notice, therefore, that we are *not* making any rotating-wave approximation, and the interaction Hamiltonian H_{SB} (43) contains *both* rotating and counter-rotating terms.

Let us introduce the bare spectral density functions (form factors)

$$\kappa_m(\omega) = \int d^3k|g_m(\boldsymbol{k})|^2\delta(\omega_k-\omega), \tag{46}$$

$\kappa_m(\omega)=0$, for $\omega<0$, and the thermal spectral density functions $[N(\omega)=1/(e^{\beta\omega}-1)]$,

$$\kappa_m^\beta(\omega) = \kappa_m(\omega)[N(\omega)+1] + \kappa_m(-\omega)N(-\omega)$$
$$= \frac{1}{1-e^{-\beta\omega}}[\kappa_m(\omega)-\kappa_m(-\omega)], \tag{47}$$

which extend along the whole real axis due to the counter-rotating terms and satisfy the Kubo-Martin-Schwinger (KMS) symmetry [55]

$$\kappa_m^\beta(-\omega) = \frac{N(\omega)}{N(\omega)+1}\kappa_m^\beta(\omega) = \exp(-\beta\omega)\kappa_m^\beta(\omega). \quad (48)$$

Under the assumption that the bath is in a thermal state (42), in the Markov approximation the reduced state of the system (6) satisfies the master equation

$$\dot{\sigma}(t) = (\mathcal{L}_S + \mathcal{L})\sigma(t), \quad (49)$$

where, up to a renormalization of the free Liouvillian $\mathcal{L}_S$ by Lamb and Stark shift terms, $\mathcal{L}$ engenders the dissipation due to the interaction with the bath,

$$\mathcal{L}\sigma = \gamma_0\left(X_0\sigma X_0 - \frac{1}{2}\{X_0X_0,\sigma\}\right) + \sum_{m\geq 1}\gamma_m\left(X_m\sigma X_m^\dagger - \frac{1}{2}\{X_m^\dagger X_m,\sigma\}\right) + \sum_{m\geq 1}\gamma_{-m}\left(X_m^\dagger\sigma X_m - \frac{1}{2}\{X_mX_m^\dagger,\sigma\}\right), \quad (50)$$

and

$$\gamma_m = 2\pi\kappa_m^\beta(\omega_m). \quad (51)$$

The derivation of Eqs. (50) and (51), although well known, is given in Appendix A for self-consistency and in order to introduce the notation and techniques that will be used in the following.

It is useful to look at some concrete examples and scrutinize the modification of the form factor (46) due to the presence of the thermal bath. Let us focus, for the sake of clarity, on two particular Ohmic cases: an exponential form factor

$$\kappa_m^{(E)}(\omega) = g^2\omega\exp(-\omega/\Lambda)\theta(\omega) \quad (52)$$

and a polynomial form factor

$$\kappa_m^{(P)}(\omega) = g^2\frac{\omega}{[1+(\omega/\Lambda)^2]^n}\theta(\omega). \quad (53)$$

In the latter case, we focus on $n=2$, which is typical of quantum dots [36] (the case $n=4$ is also of interest, being the nonrelativistic form factor of the $2P$-$1S$ transition of the hydrogen atom [56,57]). In the above formulas, g is a coupling constant, Λ a cutoff, and θ the unit step function. In order to properly compare these two cases, we will require that the bandwidth be the same:

$$W = \frac{\int_{-\infty}^{\infty} d\omega|\omega|\kappa_m^{(E)}(\omega)}{\int_{-\infty}^{\infty} d\omega\,\kappa_m^{(E)}(\omega)} = \frac{\int_{-\infty}^{\infty} d\omega|\omega|\kappa_m^{(P)}(\omega)}{\int_{-\infty}^{\infty} d\omega\,\kappa_m^{(P)}(\omega)}, \quad (54)$$

where the inverse square root of the denominator

$$\left[\int_{-\infty}^{\infty} d\omega\,\kappa_m(\omega)\right]^{-1/2} \equiv \tau_Z \quad (55)$$

is the so-called Zeno time, characterizing the convexity of the survival probability at the origin [16,57,58]. Notice that a *finite* natural cutoff $\Lambda \simeq 8.498\times 10^{18}$ rad/s and a *finite* Zeno time $\tau_Z \simeq 3.593\times 10^{-15}$ s can also be computed for the hydrogen atom in vacuum [polynomial form factor (53) with $n=4$], as well as for atomic and molecular systems whose electronic wave functions are known. The condition (54) when $n=2$ yields the ratio $\Lambda_{\rm pol}/\Lambda_{\rm exp}=1.275$ between the cutoffs for the polynomial and exponential form factors, and $W=1.99\Lambda_{\rm exp}$. The two form factors are displayed in Fig. 2.

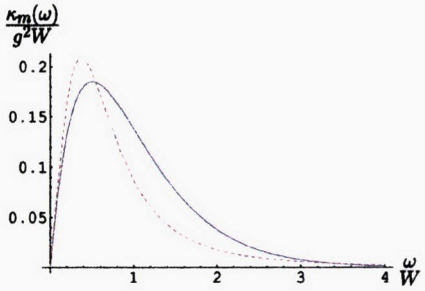

FIG. 2. The form factors at zero temperature, $\kappa_m(\omega)$ vs ω. Full line, exponential form factor (52), dashed line, polynomial form factor (53).

The thermal form factors (47) are displayed in Fig. 3 for two different temperatures. Three features are apparent. The form factor is an increasing function of the temperature β^{-1}. Its value at $\omega=0$ is $\kappa_m^\beta(0)=\kappa_m'(0^+)/\beta=g^2/\beta$, where the prime denotes the derivative. Moreover, its derivative reads $\kappa_m^{\beta\prime}(0^\pm)=\kappa_m'(0^+)/2\pm\kappa_m''(0^+)/(2\beta)$, whence it is continuous, $\kappa_m^{\beta\prime}(0)=g^2/2$, in the polynomial case [because $\kappa_m''(0^+)=0$], and discontinuous, $\kappa_m^{\beta\prime}(0^\pm)=g^2/2\mp g^2/(\beta\Lambda)$, in the exponential case; this is more apparent at higher temperatures. Finally, the support of the thermal form factors is no longer lower bounded, due to the effect of the counter-rotating terms.

B. Two-level system

A particular case of the above is the qubit Hamiltonian

$$H_{SB} = \sigma_z\otimes[A(g_0)+A^\dagger(g_0)] + \sigma_x\otimes[A(g_1)+A^\dagger(g_1)],$$

$$H_0 = \frac{\Omega}{2}\sigma_z. \quad (56)$$

This is of the form (43), when one identifies

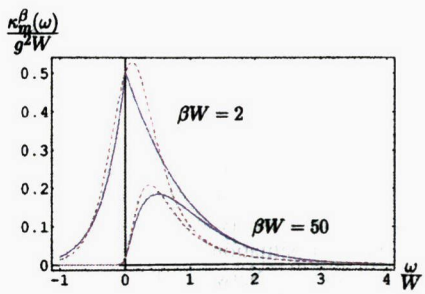

FIG. 3. The thermal form factors $\kappa_m^\beta(\omega)$ vs ω. Full lines, exponential form factors (47) and (52); dashed lines, polynomial form factors (47) and (53). The form factor is larger at higher temperature β^{-1}. Note the discontinuity of the derivative in the exponential case at $\omega=0$ (more apparent at higher temperature).

$$X_0 = \sigma_z, \quad X_{\pm 1} = \sigma_{\mp} = \frac{\sigma_x \mp i\sigma_y}{2},$$

$$\omega_{\pm 1} = \pm\Omega, \quad \omega_0 = 0, \tag{57}$$

hence

$$\mathcal{L}\rho = \gamma_0(\sigma_z\rho\sigma_z - \rho) + \gamma_{+1}\left(\sigma_-\rho\sigma_+ - \frac{1}{2}\{\sigma_+\sigma_-,\rho\}\right) + \gamma_{-1}\left(\sigma_+\rho\sigma_- - \frac{1}{2}\{\sigma_-\sigma_+,\rho\}\right), \tag{58}$$

with

$$\gamma_0 = 2\pi\kappa_0^\beta(0) = 2\pi\frac{\kappa_0'(0^+)}{\beta}, \quad \gamma_{\pm 1} = 2\pi\kappa_1^\beta(\pm\Omega), \tag{59}$$

where we used Eq. (47).

IV. QUANTUM ZENO CONTROL

Let us look at the quantum Zeno dynamics with a *finite* interval $\tau = t/N$ between measurements,

$$\rho(t) = [\hat{P}e^{\mathcal{L}_{\rm tot}\tau}\hat{P}]^{t/\tau}\rho(0), \tag{60}$$

where $\mathcal{L}_{\rm tot}$ and $\hat{P}$ are given by Eqs. (3) and (7), respectively. We will look at the subtle effects on the decay rate arising from the presence of the short-time quadratic (Zeno) region. Therefore the standard method [59] is not applicable to the present situation and the limit must be evaluated by a different technique. We only sketch the main steps in the derivation and give more details in Appendix C. Second-order perturbation in $\mathcal{L}_{SB}$ and the conditions (8) and (9) yield

$$\hat{P}e^{\mathcal{L}_{\rm tot}\tau}\hat{P} = \hat{P}e^{\mathcal{L}_0\tau}\mathcal{T}\exp\left(\int_0^\tau ds\mathcal{L}_{SB}(s)\right)\hat{P} \simeq e^{\mathcal{L}_0\tau}\hat{P}\left[\mathbb{1} + \int_0^\tau ds\mathcal{L}_{SB}(s) + \int_0^\tau ds\int_0^s ds_1\mathcal{L}_{SB}(s)\mathcal{L}_{SB}(s_1)\right]\hat{P}, \tag{61}$$

where $\mathcal{L}_{SB}(t) = e^{-\mathcal{L}_0 t}\mathcal{L}_{SB}e^{\mathcal{L}_0 t}$. In terms of the operator $\mathcal{G}_Z(\tau)$, defined as the solution of the operator equation

$$\int_0^\tau ds\, e^{-\mathcal{L}_0 s}\mathcal{G}_Z(\tau)e^{\mathcal{L}_0 s} = \hat{P}\int_0^\tau ds\int_0^s ds_1\mathcal{L}_{SB}(s)\mathcal{L}_{SB}(s_1)\hat{P} = \int_0^\tau ds\, e^{-\mathcal{L}_0 s}\left[\int_0^s ds_1\hat{P}\mathcal{L}_{SB}\mathcal{L}_{SB}(-s_1)\hat{P}\right]e^{\mathcal{L}_0 s}, \tag{62}$$

one obtains

$$[\hat{P}e^{\mathcal{L}_{\rm tot}\tau}\hat{P}]^{t/\tau} \simeq \left[\hat{P}e^{\mathcal{L}_0\tau}\mathcal{T}\exp\left(\int_0^\tau ds\, e^{-\mathcal{L}_0 s}\mathcal{G}_Z(\tau)e^{\mathcal{L}_0 s}\right)\hat{P}\right]^{t/\tau} = \hat{P}\exp\{[\mathcal{L}_0 + \mathcal{G}_Z(\tau)]t\}. \tag{63}$$

Under the assumption that the bath state can well be approximated by an equilibrium state at time t, the final reduced state $\sigma(t)$ is shown to satisfy the equation

$$\dot{\sigma}(t) = [\mathcal{L}_S + \mathcal{L}_Z(\tau)]\sigma(t), \tag{64}$$

with

$$\mathcal{L}_Z(\tau)\sigma = \mathrm{tr}_B\{\mathcal{G}_Z(\tau)\sigma\otimes\rho_B\}. \tag{65}$$

Note that $\mathcal{L}_Z(\tau)$ is the solution of the operator equation

$$\int_0^\tau dt\, e^{-\mathcal{L}_S t}\mathcal{L}_Z(\tau)e^{\mathcal{L}_S t} = \int_0^\tau dt\hat{P}\mathcal{L}(t)\hat{P} = \int_0^\tau dt\int_0^t ds\hat{P}\mathcal{K}_I(t,s)\hat{P}, \tag{66}$$

where

$$\mathcal{L}(t) = \int_0^t ds\, \mathcal{K}_I(t,s),$$

$$\mathcal{K}_I(t,s)\sigma = \mathrm{tr}_B\{\mathcal{L}_{SB}(t)\mathcal{L}_{SB}(s)\sigma\otimes\rho_B\} \tag{67}$$

[see Eqs. (A8) and (A9) in Appendix A]. The dissipative part of (65) is found to have the explicit form [analogous to Eq. (50)]

$$\mathcal{L}_Z(\tau)\sigma = \gamma_0^Z(\tau)\hat{P}\left(X_0\hat{P}\sigma X_0 - \frac{1}{2}\{X_0X_0,\hat{P}\sigma\}\right) + \sum_{m\geq 1}\gamma_m^Z(\tau)\hat{P}\left(X_m\hat{P}\sigma X_m^\dagger - \frac{1}{2}\{X_m^\dagger X_m,\hat{P}\sigma\}\right) + \sum_{m\geq 1}\gamma_{-m}^Z(\tau)\hat{P}\left(X_m^\dagger\hat{P}\sigma X_m - \frac{1}{2}\{X_mX_m^\dagger,\hat{P}\sigma\}\right), \tag{68}$$

where the controlled decay rates read

$$\gamma_m^Z(\tau) = \tau\int_{-\infty}^{\infty} d\omega\, \kappa_m^\beta(\omega)\mathrm{sinc}^2\left(\frac{\omega-\omega_m}{2}\tau\right), \tag{69}$$

with $\mathrm{sinc}(x) = \sin(x)/x$. This yields Zeno and inverse Zeno effects as τ is changed, as we will see in Sec. VII. The key issue, once again, is to understand *how small* τ should be in order to get suppression (control) of decoherence (QZE), rather than its enhancement (IZE).

V. CONTROL VIA DYNAMICAL DECOUPLING

We can now investigate the nonideal bang-bang control of decoherence. From Eq. (31), describing a BB control with a single kick [12],

$$\rho(t) = [e^{\mathcal{L}_k} e^{\mathcal{L}_{\rm tot}\tau}]^{t/\tau}\rho(0), \tag{70}$$

where $\mathcal{L}_{\rm tot}$ is again given by Eq. (3). As in the Zeno control, we consider here the case where τ is finite, so that the effects on the decay rate arising from the presence of a short-time quadratic (Zeno) region play a fundamental role. Once again, we only sketch the main steps in the derivation and give more details in Appendix D. Second-order perturbation in $\mathcal{L}_{SB}$ yields

$$\begin{aligned} e^{\mathcal{L}_k} e^{\mathcal{L}_{\rm tot}\tau} &= e^{\mathcal{L}_k} e^{\mathcal{L}_0\tau} \mathcal{T} \exp\left(\int_0^\tau ds \mathcal{L}_{SB}(s)\right) \\ &\simeq e^{\mathcal{L}_k} e^{\mathcal{L}_0\tau}\left[\mathbb{1} + \int_0^\tau ds\ \mathcal{L}_{SB}(s) \right. \\ &\quad \left. + \int_0^\tau ds \int_0^s ds_1\ \mathcal{L}_{SB}(s)\mathcal{L}_{SB}(s_1)\right], \end{aligned} \tag{71}$$

where $\mathcal{L}_{SB}(t) = e^{-\mathcal{L}_0 t}\mathcal{L}_{SB} e^{\mathcal{L}_0 t}$. In terms of the operators $\mathcal{F}_k(\tau)$ and $\mathcal{G}_k(\tau)$, defined as solutions of the operator equations

$$\int_0^\tau ds e^{-\mathcal{L}_\tau s}\mathcal{F}_k(\tau) e^{\mathcal{L}_\tau s} = \int_0^\tau ds \mathcal{L}_{SB}(s), \tag{72}$$

$$\begin{aligned} \int_0^\tau ds\ e^{-\mathcal{L}_\tau s}\mathcal{G}_k(\tau) e^{\mathcal{L}_\tau s} &= \int_0^\tau ds \int_0^s ds_1 [\mathcal{L}_{SB}(s)\mathcal{L}_{SB}(s_1) \\ &\quad - e^{-\mathcal{L}_\tau s}\mathcal{F}_k(\tau) e^{\mathcal{L}_\tau (s-s_1)}\mathcal{F}_k(\tau) e^{\mathcal{L}_\tau s_1}], \end{aligned} \tag{73}$$

with

$$\mathcal{L}_\tau = \frac{\mathcal{L}_k}{\tau} + \mathcal{L}_0, \tag{74}$$

one has

$$\begin{aligned} [e^{\mathcal{L}_k} e^{\mathcal{L}_{\rm tot}\tau}]^N &\simeq \left[e^{\mathcal{L}_\tau \tau} \mathcal{T} \exp\left(\int_0^\tau ds\ e^{-\mathcal{L}_\tau s}[\mathcal{F}_k(\tau) \right.\right. \\ &\quad \left.\left. + \mathcal{G}_k(\tau)] e^{\mathcal{L}_\tau s}\right)\right]^N \\ &= \exp\left\{\left[\frac{\mathcal{L}_k}{\tau} + \mathcal{L}_0 + \mathcal{F}_k(\tau) + \mathcal{G}_k(\tau)\right] t\right\}. \end{aligned} \tag{75}$$

With the aid of Eq. (75), the final reduced state $\sigma(t)$ satisfies the equation

$$\dot{\sigma}(t) = \left[\frac{\mathcal{L}_k}{\tau} + \mathcal{L}_S + \mathcal{L}_k(\tau)\right]\sigma(t) \tag{76}$$

with

$$\mathcal{L}_k(\tau)\sigma = {\rm tr}_B\{\mathcal{G}_k(\tau)\sigma \otimes \rho_B\}. \tag{77}$$

The dissipative part of Eq. (77) has the explicit form

$$\begin{aligned} \mathcal{L}_k(\tau)\sigma &= \gamma_0^k(\tau)\left[X_0(\tau)\sigma X_0(\tau) - \frac{1}{2}\{X_0(\tau)X_0(\tau),\sigma\}\right] \\ &\quad + \sum_{m\geq 1} \gamma_m^k(\tau)\left[X_m(\tau)\sigma X_m^\dagger(\tau) - \frac{1}{2}\{X_m^\dagger(\tau)X_m(\tau),\sigma\}\right] \\ &\quad + \sum_{m\geq 1} \gamma_{-m}^k(\tau)\left[X_m^\dagger(\tau)\sigma X_m(\tau) - \frac{1}{2}\{X_m(\tau)X_m^\dagger(\tau),\sigma\}\right], \end{aligned} \tag{78}$$

where, in analogy with Eq. (44), the $X_m(\tau)$ are the eigenoperators of the Liouvillian $\mathcal{L}_k/\tau + \mathcal{L}_S$, satisfying

$$\left(\frac{\mathcal{L}_k}{\tau} + \mathcal{L}_S\right) X_m(\tau) = i\omega_m(\tau) X_m(\tau) \tag{79}$$

($\omega_m \neq \omega_n$ for $m \neq n$) and the controlled decay rates read

$$\gamma_m^k(\tau) = 2\pi\kappa_m^\beta(\omega_m(\tau)) = 2\pi\kappa_m^\beta\left(\frac{2\pi m}{\tau} + O(1)\right). \tag{80}$$

Notice that the mechanism of decoherence suppression (80) is not fully determined by $\mathcal{L}_{\rm tot}$ and $\hat{P}$, in contrast to the Zeno case, and depends also on the details of the Liovillian $\mathcal{L}_k$ through $\omega_m(\tau)$. This is best clarified by explicitly looking at a particular case: let us consider the two-level system (56) with $g_0 = 0$ (spin-flip decoherence). We include an additional third level—that performs the control—and add to (56) the Hamiltonian (acting on $\mathcal{H}_S \oplus {\rm span}\{|M\rangle\}$)

$$H_M = -\frac{\Omega}{2}|M\rangle\langle M|, \tag{81}$$

so that $|M\rangle$ is degenerate with $|\downarrow\rangle$. The control consists of a sequence of 2π pulses [60] between $|\downarrow\rangle$ and $|M\rangle$, given by

$$U_k = \exp[-i\pi(|\downarrow\rangle\langle M| + |M\rangle\langle\downarrow|)] = P_\uparrow - P_{-1}, \tag{82}$$

where

$$P_\uparrow = |\uparrow\rangle\langle\uparrow|, \quad P_{-1} = P_\downarrow + P_M = |\downarrow\rangle\langle\downarrow| + |M\rangle\langle M|, \tag{83}$$

are the eigenprojections of U_k (belonging respectively to $e^{-i\lambda_\uparrow} = 1$ and $e^{-i\lambda_{-1}} = -1$) which define two Zeno subspaces. In the $\tau \to 0$ limit any decoherence between these two subspaces is suppressed. In fact, the total decay rate of the upper level reads [7,60]

$$\gamma_\uparrow^k(\tau) = \lim_{t\to\infty} t \int d\omega\ \kappa^\beta(\omega) {\rm sinc}^2\left[\frac{\omega - \Omega}{2} t\right] \tan^2\left[\frac{\omega - \Omega}{2}\tau\right] \tag{84}$$

and yields decoherence suppression for small τ. In addition, it is worth noting that the function multiplying the thermal form factor inside the integral can be explicitly evaluated and has the interesting limit

$$\lim_{t\to\infty} t\,\mathrm{sinc}^2\left(\frac{\omega t}{2}\right)\tan^2\left(\frac{\omega\tau}{2}\right) = \frac{2}{\pi}\sum_{j=0}^{\infty}\frac{1}{\left(j+\frac{1}{2}\right)^2}\left[\delta\left(\omega-\frac{2\pi}{\tau}(j+1/2)\right) + \delta\left(\omega+\frac{2\pi}{\tau}(j+1/2)\right)\right]. \tag{85}$$

The above limit is taken by keeping τ fixed—finite and nonvanishing—and $t=N\tau$, with N integer and even. By plugging Eq. (85) into Eq. (84) one gets

$$\gamma_{\uparrow}^{k}(\tau) = \frac{2}{\pi}\sum_{j=0}^{\infty}\frac{1}{(j+1/2)^2}\left[\kappa^{\beta}\left(\Omega+\frac{2\pi}{\tau}(j+1/2)\right) + \kappa^{\beta}\left(\Omega-\frac{2\pi}{\tau}(j+1/2)\right)\right], \tag{86}$$

which is a sum of suitably weighted terms of the form (80). This yields again control of decoherence as τ is varied, as we will see in Sec. VII. The key issue, once again, is to understand *how small* τ should be in order to get suppression of decoherence (control), rather than its enhancement. Equation (86) yields also a significant computational advantage, when compared to Eq. (84): for well-behaved form factors (without resonances) the first few terms already provide a good estimate of the controlled lifetime.

VI. CONTROL VIA A STRONG CONTINUOUS COUPLING

We can now analyze the last case, that of control by means of a strong continuous coupling. Since the control of decoherence is achieved by adding a control Hamiltonian KH_c acting on the Hilbert space $\mathcal{H}_S$, we begin with the study of the spectral properties of the new "system" Hamiltonian $H_S(K)\equiv H_S+KH_c$. By writing the spectral resolutions of H_S and H_c,

$$H_S=\sum_n E_n Q_n, \quad H_c=\sum_m \eta_m P_m, \tag{87}$$

with $\Sigma_n Q_n=\Sigma_m P_m=\mathbb{1}$, and by using the property (17) we see that $P_{mn}=P_m Q_n$ is a (finer) orthogonal resolution of the identity, i.e., $\Sigma_{m,n} P_{mn}=\mathbb{1}$, with $P_{mn}P_{m'n'}=\delta_{m,m'}\delta_{n,n'}P_{mn}$. Note that some P_{mn} can vanish. In particular $H_S(K)$ can be explicitly diagonalized,

$$H_S(K)=\sum_{m,n}(K\eta_m+E_n)P_{mn}, \quad P_{mn}=P_m Q_n. \tag{88}$$

Equations (87) and (88) directly translate in terms of the Liouvillian as

$$\mathcal{L}_S=-i\sum_n \omega_n\tilde{Q}_n, \quad \mathcal{L}_c=-i\sum_m \Omega_m\tilde{P}_m, \tag{89}$$

and

$$\mathcal{L}_S(K)=\mathcal{L}_S+K\mathcal{L}_c=-i\sum_{m,n}\omega_{mn}(K)\tilde{P}_{mn},$$

$$\omega_{mn}(K)=K\Omega_m+\omega_n, \quad \tilde{P}_{mn}=\tilde{P}_m\tilde{Q}_n. \tag{90}$$

The condition (8) for a complete control of decoherence, $\hat{P}H_{SB}=0$, leads to

$$0=\hat{P}H_{SB}=\sum_m P_m H_{SB} P_m=\tilde{P}_0 H_{SB}=\sum_n \tilde{P}_0\tilde{Q}_n H_{SB} = \sum_n \tilde{P}_{0n}H_{SB}, \tag{91}$$

whence

$$\tilde{P}_{0n}H_{SB}=0, \quad \forall\, n. \tag{92}$$

Therefore, by following exactly the same steps of Sec. III A, with $H_S(K)$ defined by Eq. (88) in place of H_S, one obtains that the dissipative part of the Liouvillian $\mathcal{L}_K$ governing the slow evolution of the reduced density matrix σ is given by

$$\mathcal{L}_K\sigma=\sum_{m\geq 1,n}\gamma_{mn}(K)\left[X_{mn}\sigma X_{mn}^{\dagger}-\frac{1}{2}\{X_{mn}^{\dagger}X_{mn},\sigma\}\right] + \sum_{m\geq 1,n}\gamma_{-m,n}(K)\left[X_{mn}^{\dagger}\sigma X_{mn}-\frac{1}{2}\{X_{mn}X_{mn}^{\dagger},\sigma\}\right], \tag{93}$$

where

$$X_{mn}\equiv\tilde{P}_m X_n, \tag{94}$$

with X_n given by Eqs. (43) and (44), and

$$\gamma_{mn}(K)=2\pi\kappa_n^{\beta}(\omega_{mn}(K)). \tag{95}$$

All terms with $m=0$ identically vanish due to Eq. (92). In the $K\to\infty$ limit, because the thermal form factor $\kappa_m^{\beta}(\omega)$ vanishes as $\omega\to\infty$ (cf. Fig. 2), one has

$$\gamma_{mn}(K)=2\pi\kappa_n^{\beta}(K\Omega_m+\omega_n)\sim 2\pi\kappa_n^{\beta}(K\Omega_m)\to 0. \tag{96}$$

Hence, in the $K\to+\infty$ limit, the dissipative part disappears, $\mathcal{L}_K\to 0$, or decoherence is suppressed, as expected.

It is interesting to observe that, when the condition (17) is not satisfied, the control via a strong continuous coupling needs an additional argument. In such a case, the control Hamiltonian H_c and the system Hamiltonian H_S cannot be simultaneously diagonalized, but (for a finite-dimensional $\mathcal{H}_S$), as a result of the analyticity of the eigenvalues and the corresponding eigenprojections of the Hermitian operator $H_S(K)/K=H_S/K+H_c$ with respect to the perturbation parameter $1/K$ [61], the eigenvalues $\omega_{mn}(K)$ of the new system Liouvillian $\mathcal{L}_S(K)=K\mathcal{L}_c+\mathcal{L}_S$ and the corresponding eigenprojections $\tilde{P}_{mn}(K)$ satisfy

$$\omega_{mn}(K)=K\Omega_m+\Omega_{mn}^{(1)}+O\left(\frac{1}{K}\right), \tag{97}$$

$$\tilde{P}_{mn}(K)=\tilde{P}_{mn}^{(0)}+\frac{1}{K}\tilde{P}_{mn}^{(1)}+O\left(\frac{1}{K^2}\right), \tag{98}$$

where $\Omega_{mn}^{(1)}$ and $\tilde{P}_{mn}^{(j)}$ $(j=0,1)$ do not depend on K. As in Eq. (92), one gets that $\tilde{P}_{0n}^{(0)}H_{SB}=0$, but this does not imply that

$\tilde{P}_{0n}(K)H_{SB}=0$. As a result, there appear dissipative terms which tend to 0 via a different mechanism from the one outlined above. This aspect will be discussed elsewhere, together with similar phenomena that occur also for the other two control mechanisms (BB and Zeno).

In general, as in the BB control but in contrast to the Zeno case, the mechanism of decoherence suppression (96) is not fully determined by H_S and depends on the details of the Hamiltonians H_S *and* H_c. Once again, this can be clarified by looking at a specific example: consider the two-level system (56) with $g_0=0$ (spin-flip decoherence). We add to (56) the Hamiltonian (acting on $\mathcal{H}_S \oplus \mathrm{span}\{|M\rangle\}$)

$$H_M = -\frac{\Omega}{2}|M\rangle\langle M| + KH_c,$$

$$H_c = |\downarrow\rangle\langle M| + |M\rangle\langle\downarrow| = P_+ - P_-, \tag{99}$$

where

$$P_\pm = \frac{(|\downarrow\rangle \pm |M\rangle)(\langle\downarrow| \pm \langle M|)}{2} \equiv |\pm\rangle\langle\pm|. \tag{100}$$

The third state $|M\rangle$ is now "continuously" coupled to state $|\downarrow\rangle$, $K\in\mathbb{R}$ being the strength of the coupling. As K is increased, state $|M\rangle$ performs a better "continuous observation" of $|\downarrow\rangle$, yielding the Zeno subspaces [16]. In terms of its eigenprojections, H_c reads [see Eq. (38)]

$$H_c = \eta_\uparrow P_\uparrow + \eta_- P_- + \eta_+ P_+, \tag{101}$$

with $P_\uparrow = |\uparrow\rangle\langle\uparrow|$ and $\eta_\uparrow = 0, \eta_\pm = \pm 1$. In the Zeno limit ($K\to\infty$) the subspaces $\mathcal{H}_\uparrow$, $\mathcal{H}_+$, and $\mathcal{H}_-$ decouple due to wildly oscillating phases $O(K)$. We get

$$\hat{P}H_{SB} = P_\uparrow H_{SB} P_\uparrow + P_- H_{SB} P_- + P_+ H_{SB} P_+ = 0. \tag{102}$$

Therefore in the limit $K\to\infty$, $\gamma_{\pm 1}=0$, and decoherence is halted.

We can diagonalize the new system Hamiltonian

$$H_S' = \frac{\Omega}{2}\sigma_z - \frac{\Omega}{2}|M\rangle\langle M| + KH_c$$
$$= \frac{\Omega}{2}P_\uparrow + \left(-\frac{\Omega}{2} + K\right)P_+ + \left(-\frac{\Omega}{2} - K\right)P_-. \tag{103}$$

The new system operators (57) become

$$X_\pm = P_\pm \sigma_x P_\uparrow = \frac{1}{\sqrt{2}}|\pm\rangle\langle\uparrow|, \quad X_0 = |-\rangle\langle +|,$$

$$\mathcal{L}_S' X_\pm = i(\Omega \mp K)X_\pm, \quad \mathcal{L}_S' X_0 = 2iKX_0, \tag{104}$$

and

$$H_{SB} = (X_+ + X_- + X_+^\dagger + X_-^\dagger) \otimes [A(g) + A^\dagger(g)]; \tag{105}$$

hence

$$\mathcal{L}_K\rho = \gamma_+(K)\left(X_+\rho X_+^\dagger - \frac{1}{2}\{X_+^\dagger X_+, \rho\}\right) + \gamma_-(K)\left(X_-\rho X_-^\dagger - \frac{1}{2}\{X_-^\dagger X_-, \rho\}\right) + \bar{\gamma}_+(K)\left(X_+^\dagger \rho X_+ - \frac{1}{2}\{X_+ X_+^\dagger, \rho\}\right) + \bar{\gamma}_-(K)\left(X_-^\dagger \rho X_- - \frac{1}{2}\{X_- X_-^\dagger, \rho\}\right), \tag{106}$$

where

$$\gamma_\pm(K) = 2\pi\kappa_1^\beta(\Omega \mp K), \quad \bar{\gamma}_\pm(K) = 2\pi\kappa_1^\beta(-\Omega \pm K). \tag{107}$$

For example, the decay rate out of state $|\uparrow\rangle$ reads (third article in [43])

$$\gamma_\uparrow(K) = \frac{\gamma_+(K) + \gamma_-(K)}{2} = \pi[\kappa_1^\beta(\Omega - K) + \kappa_1^\beta(\Omega + K)]. \tag{108}$$

VII. THE ROLE OF THE FORM FACTORS

We can now test the general scheme described in the previous sections by looking in detail at some particular cases. We will consider the two-level situation and compare the three control methods with both exponential (52) and polynomial form factors (53). We will concentrate on the transition between a regime in which decoherence is partially suppressed ("controlled") and a regime in which it is enhanced. We shall work in the high-temperature case, which is rather critical from an experimental point of view, because of temperature-induced transitions in two-level systems. We shall set $\Omega=0.01W$ and $\beta=50W^{-1}$, so that temperature $=\beta^{-1}=2\Omega$.

A. Quantum Zeno control

We first consider the Zeno control by projective measurements. Dissipation and decoherence are characterized by the decay rate (69):

$$\gamma^Z(\tau) = \tau\int_{-\infty}^{\infty} d\omega\ \kappa^\beta(\omega)\mathrm{sinc}^2\left(\frac{\omega-\Omega}{2}\tau\right) \sim \frac{\tau}{\tau_Z^2}, \tag{109}$$

for $\tau\to 0$, where τ_Z,

$$\tau_Z^{-2} = \int_{-\infty}^{\infty} d\omega\ \kappa^\beta(\omega) = \int_0^\infty d\omega\ \kappa(\omega)\coth\left(\frac{\beta\omega}{2}\right)$$
$$\overset{\beta\to\infty}{\sim} \int_0^\infty d\omega\ \kappa(\omega) + 2\int_0^\infty d\omega\ \kappa(\omega)\exp(-\beta\omega), \tag{110}$$

is the thermal Zeno time. (We dropped the subscript m for simplicity.) Observe that, by making use of the limit

$$\lim_{\tau\to\infty}\tau\ \mathrm{sinc}^2\left(\frac{\omega\tau}{2}\right) = 2\pi\delta(\omega), \tag{111}$$

one gets

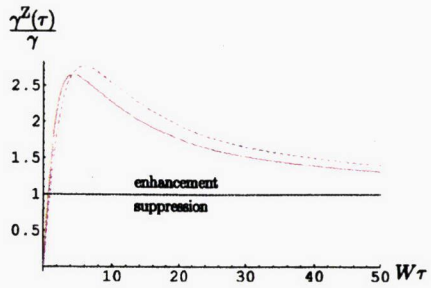

FIG. 4. Projective measurements: $\gamma^Z(\tau)/\gamma$ vs $W\tau$. Full line, exponential form factor (52); dashed line, polynomial form factor (53) with $n=2$.

$$\gamma^Z(\tau) \to \gamma, \quad \tau \to \infty, \tag{112}$$

where

$$\gamma = 2\pi\kappa^\beta(\Omega) \tag{113}$$

is the natural decay rate (51). The ratio $\gamma^Z(\tau)/\gamma$ is the key quantity: decoherence is suppressed if $\gamma^Z(\tau) < \gamma$, and it is enhanced otherwise. This ratio is shown in Fig. 4 as a function of τ [in units of W—the bandwidth defined in Eq. (54)]. The transition between these two regimes takes place at $\tau = \tau^*$, where τ^* is defined by the equation [44]

$$\gamma^Z(\tau^*) = \gamma^Z(\infty) = \gamma. \tag{114}$$

If τ^* belongs to the linear region (109) (which is our case and is true for sufficiently small energy Ω of the initial state), one gets

$$\tau^* \simeq \gamma\tau_Z^2 = 2\pi\frac{\kappa^\beta(\Omega)}{\int_{-\infty}^{\infty} d\omega\, \kappa^\beta(\omega)}. \tag{115}$$

The short-time region is displayed for clarity in Fig. 5.

It is useful to spend a few words on the physical meaning of the expressions $\tau \to 0$, $\beta \to \infty$ in the above (and following) formulas. Times and temperatures are to be compared with the bandwidth W (or frequency cutoff Λ). Times (temperatures) are "small" when $\tau \ll W^{-1}(\beta^{-1} \ll W)$. (But such temperatures can still be "high" if compared to Ω.) For example, when one considers short-time expansions in a Zeno context, the relevant time scale is τ^*, [44,58]: the expansion (109) is valid for $\tau \lesssim W^{-1}$ (and not $\tau \lesssim \tau_Z$, as is sometimes erroneously assumed).

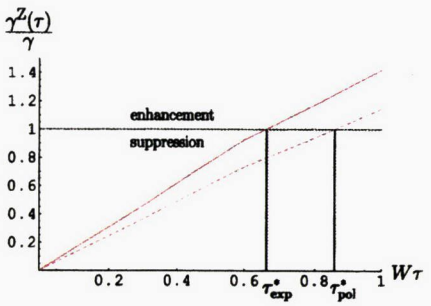

FIG. 5. Projective measurements: $\gamma^Z(\tau)/\gamma$ vs $W\tau$, for small τ. Full line, exponential form factor (52); dashed line, polynomial form factor (53) with $n=2$. τ^* (indicated) is defined by the equation $\gamma^Z(\tau^*)/\gamma = 1$. Decoherence is suppressed when $\gamma^Z(\tau) < \gamma$; it is enhanced otherwise.

B. "Bang-bang" control

We now discuss BB control. The decay rate is given by Eq. (86):

$$\begin{aligned}\gamma^k(\tau) &= \frac{2}{\pi}\sum_{j=0}^{\infty}\frac{1}{\left(j+\frac{1}{2}\right)^2}\left[\kappa^\beta\left(\Omega + \frac{\pi}{\tau}(2j+1)\right)\right.\\ &\quad\left.+\kappa^\beta\left(\Omega - \frac{\pi}{\tau}(2j+1)\right)\right]\\ &\overset{\tau\to 0}{\sim} \frac{2}{\pi}\sum_{j=0}^{\infty}\frac{1}{\left(j+\frac{1}{2}\right)^2}\kappa^\beta\left(\frac{\pi}{\tau}(2j+1)\right)\left(1+e^{-\beta(\pi/\tau)(2j+1)}\right)\\ &\sim \frac{2}{\pi}\sum_{j=0}^{\infty}\frac{1}{\left(j+\frac{1}{2}\right)^2}\kappa\left(\frac{\pi}{\tau}(2j+1)\right),\end{aligned} \tag{116}$$

where we made use of Eq. (48) in the first expansion and assumed that β is not too small (as compared to τ) in the second one. In the exponential case (52) one gets

$$\begin{aligned}\kappa^{(E)}\left(\frac{\pi}{\tau}(2j+1)\right) &= g^2\frac{\pi}{\tau}(2j+1)e^{-(\pi/\tau\Lambda)(2j+1)}\\ &= \kappa^{(E)}\left(\frac{\pi}{\tau}\right)(2j+1)e^{-2j(\pi/\tau\Lambda)},\end{aligned} \tag{117}$$

whence

$$\gamma^k(\tau) \sim \frac{8}{\pi}\kappa^{(E)}\left(\frac{\pi}{\tau}\right), \quad \tau \to 0, \tag{118}$$

while in the polynomial case (53) one gets

$$\begin{aligned}\kappa^{(P)}\left(\frac{\pi}{\tau}(2j+1)\right) &\sim g^2\frac{\Lambda}{[(\pi/\tau\Lambda)(2j+1)]^{2n-1}}\\ &\sim \kappa^{(P)}\left(\frac{\pi}{\tau}\right)\frac{1}{(2j+1)^{2n-1}},\end{aligned} \tag{119}$$

whence

$$\begin{aligned}\gamma^k(\tau) &\sim \frac{8}{\pi}\sum_{j=0}^{\infty}\frac{1}{(2j+1)^{2n+1}}\kappa^{(P)}\left(\frac{\pi}{\tau}\right)\\ &= \frac{8}{\pi}(1-2^{-2n-1})\zeta(2n+1)\kappa^{(P)}\left(\frac{\pi}{\tau}\right)\end{aligned} \tag{120}$$

for $\tau \to 0$, where $\zeta(x) = \sum_{k=1}^{\infty} k^{-x}$ is the Riemann zeta function.

On the other hand, in both cases,

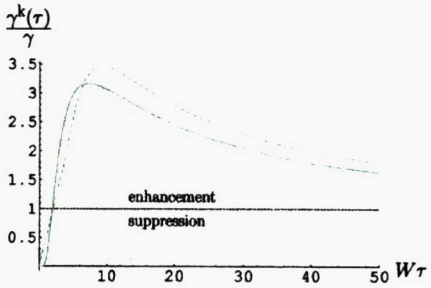

FIG. 6. BB kicks: $\gamma^k(\tau)/\gamma$ vs $W\tau$. Full line, exponential form factor (52); dashed line, polynomial form factor (53) with $n=2$.

$$\gamma^k(\tau) \to \frac{4}{\pi}\kappa^\beta(\Omega)\sum_{j=0}^{\infty}\frac{1}{\left(j+\frac{1}{2}\right)^2} = \gamma, \quad \tau \to \infty, \tag{121}$$

where we summed the series

$$\sum_{j=0}^{\infty}\frac{1}{\left(j+\frac{1}{2}\right)^2} = 4\sum_{j=0}^{\infty}\frac{1}{(2j+1)^2} = 3\zeta(2) = \frac{\pi^2}{2}. \tag{122}$$

The ratio $\gamma^k(\tau)/\gamma$ is shown in Fig. 6 as a function of τ. Once again, the transition between the two regimes takes place at $\tau=\tau^*$ where τ^* is defined by the equation

$$\gamma^k(\tau^*) = \gamma^k(\infty) = \gamma. \tag{123}$$

If τ^* is in the asymptotic region (118) one gets in the exponential case (52)

$$\kappa^{(E)}\left(\frac{\pi}{\tau^*}\right) \simeq \frac{\pi}{8}\gamma = \frac{\pi^2}{4}\kappa^\beta(\Omega), \tag{124}$$

which yields

$$\tau^* \simeq -\frac{\pi}{\Lambda}W_{-1}\left(-\frac{\pi}{8}\frac{\gamma}{g^2\Lambda}\right)^{-1} = -\frac{\pi}{\Lambda}W_{-1}\left(-\frac{\pi^2}{4}\frac{\kappa^\beta(\Omega)}{g^2\Lambda}\right)^{-1}, \tag{125}$$

where W is Lambert's W function [62], that is, the inverse of the function $f(W)=We^W$, and we have taken its -1 branch.

On the other hand, for the polynomial case (53) one gets from (120)

$$\kappa^{(P)}\left(\frac{\pi}{\tau^*}\right) \simeq \frac{\pi}{8(1-2^{-2n-1})\zeta(2n+1)}\gamma = \frac{\pi^2}{4(1-2^{-2n-1})\zeta(2n+1)}\kappa^\beta(\Omega) \tag{126}$$

and

$$\tau^* \simeq \frac{\pi}{\Lambda}\left(\frac{\pi}{8(1-2^{-2n-1})\zeta(2n+1)}\frac{\gamma}{g^2\Lambda}\right)^{1/(2n-1)} = \frac{3\pi}{\Lambda}\left(\frac{\pi^2}{4(1-2^{-2n-1})\zeta(2n+1)}\frac{\kappa^\beta(\Omega)}{g^2\Lambda}\right)^{1/(2n-1)}. \tag{127}$$

The short-time region is shown in Fig. 7. It is useful to observe that the results (124)–(127) bear an important dependence of τ^* on the "tail" of the form factor. This is to be sharply contrasted with the projective measurement situation (115), which yields a dependence of the transition time τ^* on the "global" features of the form factor. This difference is apparent if one compares Figs. 5 and 7 and shows that the latter method offers important advantages if one aims at inhibiting decoherence, because of the larger (and easier to attain) value of τ^*.

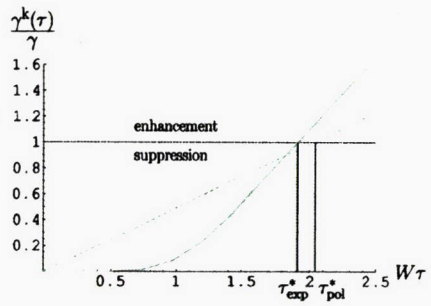

FIG. 7. BB kicks: $\gamma^k(\tau)/\gamma$ vs $W\tau$ for small τ. Full line, exponential form factor (52); dashed line, polynomial form factor (53) with $n=2$. Decoherence is suppressed when $\gamma^k(\tau)<\gamma$; it is enhanced otherwise.

C. Control by continuous coupling

Finally, we can look at continuous coupling. The time scale for decoherence is (108)

$$\begin{aligned}\gamma^c(K) &= \pi\int d\omega\, \kappa^\beta(\omega)[\delta(\omega-\Omega-K)+\delta(\omega-\Omega+K)] \\ &= \pi[\kappa^\beta(\Omega+K)+\kappa^\beta(\Omega-K)] \sim \pi\kappa(K)(1+e^{-\beta K}) \\ &\sim \pi\kappa(K),\end{aligned} \tag{128}$$

for $K\to\infty$. On the other hand,

$$\gamma^c(K) \to \gamma, \quad K \to 0. \tag{129}$$

Notice that the role of K in Eq. (128) and the role of $1/\tau$ in Eqs. (118) and (120) are equivalent (see also Appendix D). This yields a natural comparison [12] between different time scales (τ for measurements and kicks, $1/K$ for continuous coupling).

The ratio $\gamma^c(K)/\gamma$ is shown in Fig. 8 as a function of $2\pi/K$. The transition between these two regimes now takes place at $K=K^*$ where K^* is defined by the equation

$$\gamma^c(K^*) = \gamma^c(0) = \gamma. \tag{130}$$

If K^* is in the asymptotic region (128),

$$\kappa(K^*) \simeq \frac{\gamma}{\pi} = 2\kappa^\beta(\Omega). \tag{131}$$

For the exponential form factor (52) one gets

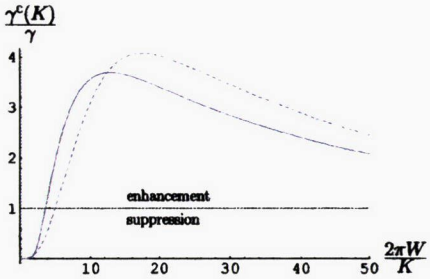

FIG. 8. Continuous coupling: $\gamma^c(K)/\gamma$ vs $2\pi W/K$. Full line, exponential form factor (52); dashed line, polynomial form factor (53) with $n=2$.

$$K^* \simeq -\Lambda W_{-1}\left(-\frac{1}{\pi}\frac{\gamma}{g^2\Lambda}\right) = -\Lambda W_{-1}\left(-2\frac{\kappa^\beta(\Omega)}{g^2\Lambda}\right), \tag{132}$$

while for the polynomial form factor (53) one gets

$$K^* \simeq \Lambda\left(\frac{1}{\pi}\frac{\gamma}{g^2\Lambda}\right)^{-1/(2n-1)} = \Lambda\left(2\frac{\kappa^\beta(\Omega)}{g^2\Lambda}\right)^{-1/(2n-1)}. \tag{133}$$

One observes a dependence of K^* on the tail of the form factor. The strong coupling region is shown in Fig. 9.

D. Comparison among the three control strategies

There is a clear difference between *bona fide* projective measurements and the other two cases, BB kicks and continuous coupling. In the former case Eqs. (114) and (115) yield a dependence of τ^* on the global features of the form factor (i.e., its integral). By contrast, Eqs. (124)–(127) and (131)–(133) "pick" some particular ("on-shell") value(s). This important difference, due to the different features of the evolution (nonunitary in the first case, unitary in the latter cases), is graphically displayed in Figs. 10 and 11, where the different mechanisms of control are compared. In Fig. 10, τ is "large" (in units of inverse bandwidth) and the three methods yield almost no control: one essentially reobtains the Fermi golden rule $\gamma=2\pi\kappa^\beta(\Omega)$, although in different ways. In Fig. 11, τ is "small" and the effective lifetime is sensibly modified, although by different mechanisms.

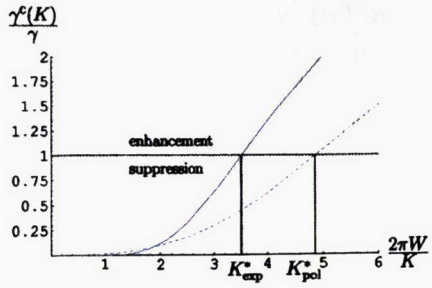

FIG. 9. Continuous coupling: $\gamma^c(K)/\gamma$ vs $2\pi W/K$ for large K. Full line, exponential form factor (52); dashed line, polynomial form factor (53) with $n=2$. Decoherence is suppressed when $\gamma^c(K)<\gamma$; it is enhanced otherwise.

The three control methods are graphically compared in Figs. 12 and 13. The different features discussed in Figs. 10 and 11 yield very different outputs, clearly apparent in Fig. 13, which can be important in practical applications: decoherence can be more easily halted by applying BB and/or continuous coupling strategies. These two methods yield values of τ^* (or K^*) that are easier to attain. However, this advantage has a price, because BB and continuous coupling yield a larger enhancement of decoherence for $\tau>\tau^*$, $K<K^*$. The two dynamical methods perform better only when $\tau\lesssim\tau^*$, $K\gtrsim K^*$. This is apparent in Fig. 12. We notice that a strict comparison between continuous coupling and the other two methods is difficult, as it would involve an analysis of numerical factors of order 1 in the definition of the relevant conversion factors between the frequency of interruptions τ and the coupling K [this factor has been sensibly—but arbitrarily—set equal to 2π in Figs. 12 and 13; see the sentence after Eq. (129) and Appendix D].

VIII. SUMMARY AND CONCLUDING REMARKS

We have analyzed and compared three control methods for combatting decoherence. The first is based on repeated

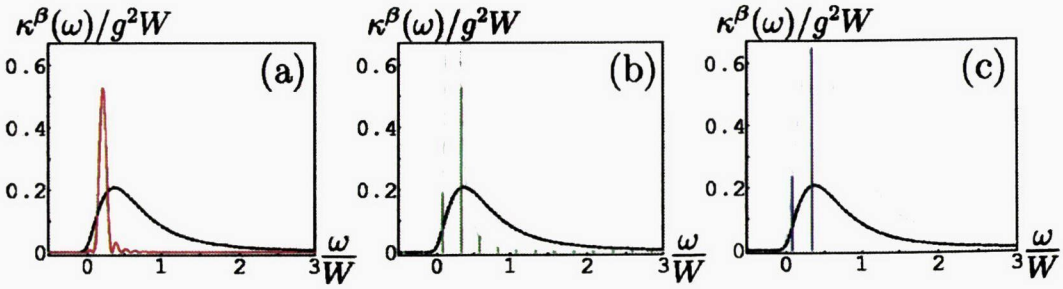

FIG. 10. Different features of the three control methods. Form factor (polynomial, $n=2$) $\kappa^\beta(\omega)$ (dashed line) and form factor modulated or multiplied by the control "response" function (full line) for (a) pulsed measurements, Eq. (109), with control response function $\tau\,\mathrm{sinc}^2[(\omega-\Omega)\tau/2]$ (here and in the other two cases, $\Omega=0.2W$); (b) BB kicks, Eq. (116), with control response function $(2/\pi)\Sigma_{j=0}^{\infty}(j+1/2)^{-2}[\delta(\omega-\Omega-(\pi/\tau)(2j+1))+\delta(\omega-\Omega+(\pi/\tau)(2j+1))]$ [see Eq. (85) and notice that the first two or three terms of the series yield an excellent approximation]; (c) continuous measurement, Eq. (128), with control response function $\pi[\delta(\omega-\Omega-K)+\delta(\omega-\Omega+K)]$. The gray line is a guide for the eye and interpolates $(2/\pi)(j+1/2)^{-2}\kappa^\beta(\omega)$ in (b) and $\pi\kappa^\beta(\omega)$ in (c). We set $\tau=2\pi/K=50W^{-1}$ (a "large" value): this yields in all cases a (controlled) decay rate that is very close to that obtained by the Fermi golden rule.

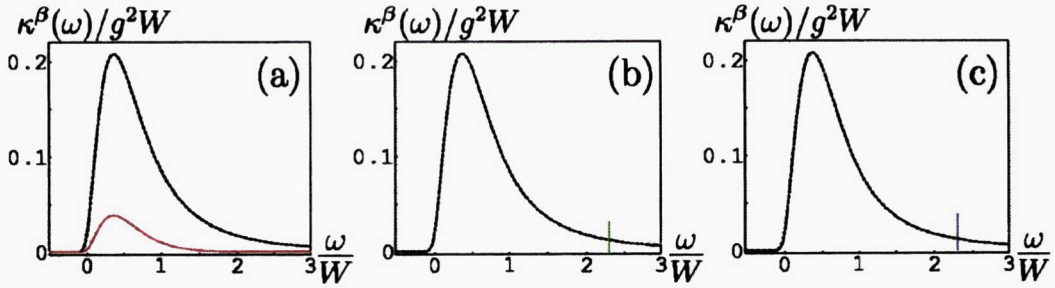

FIG. 11. Same as in Fig. 10, but for $\tau=2\pi/K=3W^{-1}$ (a "small" value): this yields a *bona fide* control of the decay rate (in this particular situation, decoherence is enhanced in the Zeno case and suppressed in the other two cases). (a) The control response function $\tau\,\mathrm{sinc}^2[(\omega-\Omega)\tau/2]$ is very broad and the effective lifetime depends on the "global" features of the form factor. (b) For small τ all the arguments of the δ functions in Eq. (85) tend to ∞: for well-behaved form factors (like that shown in the figure), only the *first* term contributes significantly; the controlled lifetime depends on the local features of the "tail" of the form factor. (c) For large K the arguments of the δ functions in Eq. (128) tend to $\pm\infty$ and the controlled lifetime depends again on the local features of the "tail" of the form factor.

quantum measurements (projection operators) and involves a description in terms of nonunitary processes. The second and third methods are both dynamical, as they can be described in terms of unitary evolutions. In all cases, decoherence can be halted by very rapidly or strongly driving or very frequently measuring the system state. However, if the frequency is not high enough or the coupling not strong enough, the controls may accelerate the decoherence process and deteriorate the performance of the quantum state manipulation. The acceleration of decoherence is analogous to the inverse Zeno effect, namely, the acceleration of the decay of an unstable state due to frequent measurements [43,44].

As a general rule, when one endeavors to control decoherence by suitably tailoring the coupling of the system of interest to another system (such as an external field, or a measuring apparatus), one should carefully look at the relevant time scales, as it is not true that repeated measurements or interruptions always lead to a suppression of decoherence.

It is convenient to summarize the main results obtained in this article in the particular case of a two-level system (qubit) with energy difference Ω. If the frequency τ^{-1} of measurements or BB kicks, or the strength K of the coupling tends to ∞, the two-dimensional (Zeno) subspace defining the qubit becomes isolated and decoherence is completely suppressed. However, if τ^{-1} and K are large, but not extremely large, the transition (decay) rates between the qubit subspace and the remaining sector of the Hilbert space display a complicated dependence on τ^{-1} and K, and decoherence can be suppressed or enhanced, depending on the situation.

At low temperatures $\beta^{-1}\ll\Omega\ll W$, where W is the bandwidth of the form factor of the interaction, the decay rates read, from Eqs. (109), (110), (118), (120), and (128),

$$\gamma^Z(\tau)\sim\frac{\tau}{\tau_Z^2},\quad \tau\to 0,$$

$$\gamma^k(\tau)\sim\frac{8}{\pi}\kappa\left(\frac{\pi}{\tau}\right),\quad \tau\to 0,$$

$$\gamma^c(K)\sim\pi\kappa(K),\quad K\to\infty, \tag{134}$$

where Z, k and c denote (Zeno) measurements, (BB) kicks, and continuous coupling, respectively, κ is the form factor, and $1/\tau_Z^2\simeq\int d\omega\,\kappa(\omega)$ the Zeno time (more accurate definitions were given in the preceding sections). As we have shown, there is a characteristic transition time τ^* (coupling K^*), such that one obtains

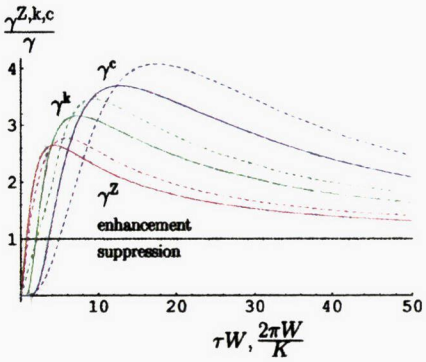

FIG. 12. Comparison among the three control methods. The graphs of Figs. 4, 6, and 8 are displayed together. BB kicks and continuous coupling are more effective than *bona fide* measurements for combatting decoherence, as the regime of "suppression" is reached for larger values of τ and K^{-1}.

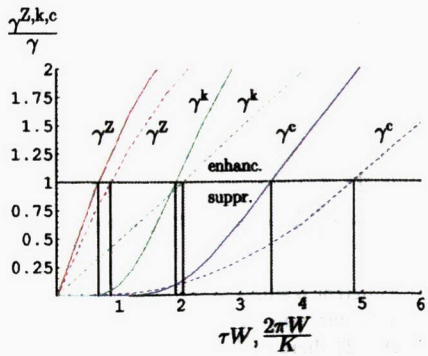

FIG. 13. Comparison among the three control methods: small times and strong coupling regions. The graphs of Figs. 5, 7, and 9 are displayed together.

$$\text{for } \tau < \tau^* \ (K > K^*)$$
$$\Rightarrow \text{decoherence suppression: } \gamma(\tau) < \gamma \ [\gamma(K) < \gamma],$$

$$\text{for } \tau > \tau^* \ (K < K^*)$$
$$\Rightarrow \text{decoherence enhancement: } \gamma(\tau) > \gamma \ [\gamma(K) > \gamma]. \tag{135}$$

Therefore, in order to obtain a suppression of decoherence, the interruptions (coupling) must be *very* frequent (strong). Notice, in this context, that both τ^* and $2\pi/K^*$ are not simply related to the inverse bandwidth $2\pi W^{-1}$: they can be in general (much) shorter. For instance, in the Ohmic polynomial case (53), one easily gets from Eqs. (54) and (134)

$$\tau_Z^* \simeq 2\pi W^{-1}\left(2(n-1)\alpha_n^2\frac{\Omega}{W}\right) \ll 2\pi W^{-1},$$

$$\tau_k^* \simeq 2\pi W^{-1}\frac{\alpha_n}{2}\left(\frac{\alpha_n \pi^2}{4}\frac{\Omega}{W}\right)^{1/(2n-1)} \ll 2\pi W^{-1},$$

$$K^* \simeq W\alpha_n^{-1}\left(\frac{2}{\alpha_n}\frac{W}{\Omega}\right)^{1/(2n-1)} \gg W, \tag{136}$$

where $\alpha_n = (\sqrt{\pi}/2)\Gamma(n-3/2)/\Gamma(n-1) \leq \pi/2$ is a coefficient of order 1 and n characterizes the polynomial falloff of the form factor (53). The above times and coupling may be (very) difficult to achieve in practice. In fact, we see here that the relevant time scale is not simply the inverse bandwidth $2\pi W^{-1}$, but can be much shorter if $\Omega \ll W$, as is typically the case. These conclusions, summarized here for the simple case of a qubit, are valid *in general*, when one aims at protecting from decoherence an N-dimensional subspace.

An important example that we have not explicitly analyzed in this article is the case of $1/f$ noise, and its suppression by means of techniques like those discussed here. There has recently been a surge of interest in this issue in quantum information processing devices, where such noise is often attributable to (but certainly not limited to) charge fluctuations in electrodes providing control voltages [63]. Several recent papers have dealt with suppression of this particular kind of noise via BB decoupling [41,60,64]. The "bottom-up" approach models $1/f$ noise as arising from a collection of bistable fluctuators [41,63,64]. The alternative is to treat $1/f$ noise as contributing a particular form factor [60,63]. We will pursue these ideas as a future topic of investigation, but we expect that the main results obtained in the present paper will be applicable to this case as well.

The results obtained in this paper are of general validity and bring to light the different features of the control procedures as well as the crucial role played by the form factor of the interaction. We do not expect any drastic change for different decoherence mechanisms and/or different physical systems. The only somewhat delicate issue, in our opinion, is to understand whether the system investigated can be consistently described by means of a set of discrete levels.

ACKNOWLEDGMENTS

This work is partly supported by the bilateral Italian-Japanese project 15C1 on "Quantum Information and Computation" of the Italian Ministry for Foreign Affairs, by a Grant-in-Aid for Scientific Research (C) from JSPS, by Grants-in-Aid for Scientific Research of Priority Areas "Control of Molecules in Intense Laser Fields" and for the 21st Century COE Program at Waseda University "Holistic Research and Education Center for Physics of Self-organization Systems" both from the Ministry of Education, Culture, Sports, Science and Technology of Japan. D.A.L. gratefully acknowledges financial support from NSERC, the Sloan Foundation, and the DARPA-QuIST program (managed by AFOSR under Agreement No. F49620-01-1-0468).

APPENDIX A

In this appendix we introduce notation and derive the master equation (49). We also set up the techniques that are necessary for the derivations of the "controlled" master equations given in the following appendixes. We will assume throughout our analysis that the characteristic time scales of quantum state manipulation in the space $\mathcal{H}_{\text{comp}}$ [see Eq. (4)] are much longer than any other time scales, so that the process is well described by the van Hove "$\lambda^2 t$" limit [55,59,65,66], where λ is the coupling constant between system and reservoir [see the comment after Eq. (3)]. For instance, if we take the time scale of quantum state manipulation to be of order λ^{-2} ($\sim$ to a Rabi period in $\mathcal{H}_{\text{comp}}$), then the other energies involved are at most $O(\lambda^0)$.

By following Gardiner and Zoller [54], the starting point is the decomposition of the Liouville equation with the aid of the projection operators

$$\mathcal{P}\rho = \text{tr}_B\{\rho\} \otimes \rho_B = \sigma \otimes \rho_B, \quad \mathcal{Q} = 1 - \mathcal{P}, \tag{A1}$$

where tr_B stands for the partial trace over the reservoir degrees of freedom and ρ_B is the equilibrium reservoir state (42). Note that $\mathcal{P}^2 = \mathcal{P}$ and $\mathcal{Q}^2 = \mathcal{Q}$. Moreover,

$$\mathcal{P}\mathcal{L}_S = \mathcal{L}_S\mathcal{P}, \quad \mathcal{P}\mathcal{L}_B = \mathcal{L}_B\mathcal{P} = 0, \tag{A2}$$

and we assume that

$$\mathcal{P}\mathcal{L}_{SB}\mathcal{P} = 0, \tag{A3}$$

which can always be satisfied by redefining the system Liouville operator $\mathcal{L}_S\rho \to \mathcal{L}_S\rho + \text{tr}_B\{\mathcal{L}_{SB}\rho\} \otimes \rho_B$ and the interaction Liouville operator $\mathcal{L}_{SB}\rho \to \mathcal{L}_{SB}\rho - \text{tr}_B\{\mathcal{L}_{SB}\rho\} \otimes \rho_B$.

The evolution in the interaction picture reads

$$\dot{\rho}_I(t) = \mathcal{L}_{SB}(t)\rho_I(t), \quad \mathcal{L}_{SB}(t) = e^{-\mathcal{L}_0 t}\mathcal{L}_{SB}e^{\mathcal{L}_0 t}, \tag{A4}$$

and by applying the projection (A1) together with Eq. (A3) one gets

$$\mathcal{P}\dot{\rho}_I(t) = \mathcal{P}\mathcal{L}_{SB}(t)\mathcal{Q}\rho_I(t),$$

$$\mathcal{Q}\dot{\rho}_I(t) = \mathcal{Q}\mathcal{L}_{SB}(t)\mathcal{P}\rho_I(t) + \mathcal{Q}\mathcal{L}_{SB}(t)\mathcal{Q}\rho_I(t). \tag{A5}$$

By formally integrating the second equation and plugging the result into the first one, one obtains to order λ^2

$$\mathcal{P}\dot{\rho}_I(t) = \int_0^t ds\ \mathcal{P}\mathcal{L}_{SB}(t)\mathcal{Q}\mathcal{L}_{SB}(s)\mathcal{P}\rho_I(s), \tag{A6}$$

where the initial condition (5), yielding $\mathcal{Q}\rho_I(0)=0$, was used. By using the definitions (A1) and the conditions (A2) and (A3), Eq. (A6) yields

$$\dot{\sigma}_I(t) = \int_0^t ds\ \mathcal{K}_I(t,s)\sigma_I(s), \tag{A7}$$

where

$$\mathcal{K}_I(t,s)\sigma = \mathrm{tr}_B\{\mathcal{L}_{SB}(t)\mathcal{L}_{SB}(s)\sigma\otimes\rho_B\}. \tag{A8}$$

By making use of the first Markov approximation $\sigma_I(s) \to \sigma_I(t)$ [54], which is motivated by the fact that the bath correlation kernel $\mathcal{K}_I(t,s)$ is different from zero only for $s \simeq t-\tau_c$ such that $\sigma_I(t-\tau_c)\simeq\sigma_I(t)$, one gets

$$\dot{\sigma}_I(t) = \mathcal{L}(t)\sigma_I(t), \quad \mathcal{L}(t) = \int_0^t ds\ \mathcal{K}_I(t,s). \tag{A9}$$

If the time t in Eqs. (A9) is much larger than the bath correlation time, $t \gg \tau_c$, one can safely replace the upper limit of integration with ∞, getting a Markovian equation with the time-independent Liouville operator $\mathcal{L}=\mathcal{L}(\infty)$.

We emphasize that this procedure can be rigorously justified in the (weak coupling) limit [65]

$$\mathcal{L} = \lim_{\lambda\to 0}\int_0^{t/\lambda^2} ds\ \mathcal{K}_I(t/\lambda^2,s), \tag{A10}$$

which physically corresponds to a time coarse-graining ansatz [67,68]. From Eqs. (A8) and (A10)) one gets (by suppressing, for simplicity, the subscript I for the operators in the interaction picture)

$$\begin{aligned}\mathcal{L}\sigma &= \lim_{\lambda\to 0}\mathrm{tr}_B\left\{e^{-\mathcal{L}_S t/\lambda^2}\left[\int_{-t/\lambda^2}^0 ds\ \mathcal{L}_{SB}\mathcal{L}_{SB}(s)\right]e^{\mathcal{L}_S t/\lambda^2}\sigma\otimes\rho_B\right\}\\ &= \mathrm{tr}_B\left\{\sum_\omega \tilde{Q}_\omega\left[\int_{-\infty}^0 ds\ \mathcal{L}_{SB}\mathcal{L}_{SB}(s)\right]\tilde{Q}_\omega\sigma\otimes\rho_B\right\},\end{aligned} \tag{A11}$$

where $\tilde{Q}_\omega$ are the eigenprojections of the Liouvillian $\mathcal{L}_S$,

$$\mathcal{L}_S = -i\sum_\omega \omega\tilde{Q}_\omega, \quad \sum_\omega \tilde{Q}_\omega = 1, \quad \tilde{Q}_\omega\tilde{Q}_{\omega'} = \delta_{\omega,\omega'}\tilde{Q}_\omega, \tag{A12}$$

and in the limit the off-diagonal terms $e^{i(\omega-\omega')t/\lambda^2}\tilde{Q}_\omega[\cdots]\tilde{Q}_{\omega'}$ vanish due to the Riemann-Lesbegue lemma. Notice that the superoperators $\tilde{Q}_\omega$ can be expressed in terms of the eigenprojections of the Hamiltonian H_S as

$$\tilde{Q}_\omega\rho = \sum_{\substack{m,n\\ E_m-E_n=\omega}} Q_m\rho Q_n, \quad H_S = \sum_n E_n Q_n. \tag{A13}$$

From a physical point of view, the result (A11) hinges upon a second-order perturbation expansion of the Liouvillian (3) in the interaction picture,

$$\begin{aligned}e^{-\mathcal{L}_0 t}e^{\mathcal{L}_{\mathrm{tot}}t} &= \mathcal{T}\exp\left(\int_0^t ds\ \mathcal{L}_{SB}(s)\right)\\ &\simeq \mathbb{1} + \int_0^t ds\ \mathcal{L}_{SB}(s) + \int_0^t ds\int_0^s ds_1\mathcal{L}_{SB}(s)\mathcal{L}_{SB}(s_1).\end{aligned} \tag{A14}$$

Indeed, the first-order term vanishes after the projection due to (A3), while the projected second-order term reads

$$\begin{aligned}&\mathrm{tr}_B\left\{\int_0^t ds\int_0^s ds_1\mathcal{L}_{SB}(s)\mathcal{L}_{SB}(s_1)\sigma\otimes\rho_B\right\}\\ &= \int_0^t ds\ \mathrm{tr}_B\left\{e^{-\mathcal{L}_S s}\left[\int_{-s}^0 ds_1\mathcal{L}_{SB}\mathcal{L}_{SB}(s_1)\right]e^{\mathcal{L}_S s}\rho\right\}\\ &\simeq \int_0^t ds\ \mathrm{tr}_B\left\{e^{-\mathcal{L}_S s}\left[\int_{-\infty}^0 ds_1\mathcal{L}_{SB}\mathcal{L}_{SB}(s_1)\right]e^{\mathcal{L}_S s}\rho\right\}\\ &\simeq t\ \mathrm{tr}_B\left\{\sum_\omega \tilde{Q}_\omega\left[\int_{-\infty}^0 ds\mathcal{L}_{SB}\mathcal{L}_{SB}(s)\right]\tilde{Q}_\omega\sigma\otimes\rho_B\right\} = \mathcal{L}t\ \sigma,\end{aligned} \tag{A15}$$

where $\rho=\sigma\otimes\rho_B$. In the second equality we considered times t much larger than the bath correlation time τ_c, so that the integration range can be extended from $(-s,0)$ to $(-\infty,0)$, while in the third equality we neglected the rapidly oscillating (compared with those responsible for decoherence) off-diagonal terms. By combining Eqs. (A15) and (A14) we finally get

$$\sigma_I(t) = \mathrm{tr}_B\{e^{-\mathcal{L}_0 t}e^{\mathcal{L}_{\mathrm{tot}}t}\sigma_I(0)\otimes\rho_B\} \simeq \exp(\mathcal{L}t)\sigma_I(0), \tag{A16}$$

which is nothing but (A9), when one substitutes $\mathcal{L}(t)\to\mathcal{L}(\infty)=\mathcal{L}$.

Some of these ideas and techniques, at different levels of rigor, have been investigated and applied in the literature of the last four decades [55,59,66].

Assume now that the interaction Hamiltonian H_{SB} has the form (43). In the interaction representation we get

$$H_{SB}(t) = e^{-\mathcal{L}_0 t}H_{SB} = \sum_m [X_m\otimes A_m^\dagger(t) + X_m^\dagger\otimes A_m(t)], \tag{A17}$$

where

$$A_m(t) = e^{i\omega_m t}e^{-\mathcal{L}_B t}A_m = \int d^3k\ g_m^*(\boldsymbol{k})e^{-i(\omega_k-\omega_m)t}a(\boldsymbol{k}). \tag{A18}$$

If the bath is in the thermal state (42) we obtain

$$\langle A_m^\dagger(t)A_m(s)\rangle = \int d^3k|g_m(\boldsymbol{k})|^2 N(\omega_k)e^{i(\omega_k-\omega_m)(t-s)}\langle A_m(t)A_m^\dagger(s)\rangle$$
$$= \int d^3k|g_m(\boldsymbol{k})|^2[N(\omega_k)+1]e^{-i(\omega_k-\omega_m)(t-s)}, \tag{A19}$$

and $\langle A_m(t)A_m(s)\rangle = \langle A_m^\dagger(t)A_m^\dagger(s)\rangle = 0$, with $N(\omega)=1/(e^{\beta\omega}-1)$. From Eq. (A11) we get

$$\mathcal{L}\sigma = \int_{-\infty}^{0} ds\, \mathrm{tr}_B\{\tilde{Q}_\omega \mathcal{L}_{SB}\mathcal{L}_{SB}(s)\tilde{Q}_\omega \sigma\otimes\rho_B\} \tag{A20}$$

and by using the property

$$\sum_\omega \tilde{Q}_\omega \mathcal{L}_1\mathcal{L}_2\tilde{Q}_\omega\rho = -\sum_\omega \tilde{Q}_\omega[H_1,[H_2,\tilde{Q}_\omega\rho]]$$
$$= -\sum_\omega [(\tilde{Q}_\omega H_1),[(\tilde{Q}_{-\omega}H_2),\rho]], \tag{A21}$$

which easily follows from the definition (A12), we get

$$\mathcal{L}\sigma = -\sum_\omega \int_{-\infty}^{0} ds\mathrm{tr}_B\{[(\tilde{Q}_\omega H_{SB}),[(\tilde{Q}_{-\omega}H_{SB}(s)),\sigma\otimes\rho_B]]\}. \tag{A22}$$

By using Eqs. (A13) and (43) one obtains

$$\tilde{Q}_{\omega_m}H_{SB} = H_{SB}^{(m)} = X_{-m}\otimes A_{-m}^\dagger + X_m^\dagger\otimes A_m, \tag{A23}$$

whence

$$\mathcal{L}\sigma = -\sum_m \int_{-\infty}^{0} ds\, \mathrm{tr}_B\{[H_{SB}^{(m)},[H_{SB}^{(-m)}(s),\sigma\otimes\rho_B]]\}$$
$$= -\sum_m \int_{-\infty}^{0} ds\, \mathrm{tr}_B\{[X_m^\dagger\otimes A_m,[X_m\otimes A_m^\dagger(s),\rho]]$$
$$+[X_{-m}\otimes A_{-m}^\dagger,[X_{-m}^\dagger\otimes A_{-m}(s),\rho]]\}, \tag{A24}$$

where $\rho=\sigma\otimes\rho_B$. Notice that in the second equality, terms containing two annihilation or creation operators identically vanish after taking the trace over the thermal state ρ_B and have been dropped. Equation (A24) can be put in the form [54]

$$\mathcal{L}\sigma = -i\sum_m [\delta_m X_m^\dagger X_m + \epsilon_m X_m X_m^\dagger,\sigma] + \sum_m K_m\left(X_m\sigma X_m^\dagger - \frac{1}{2}\{X_m^\dagger X_m,\sigma\}\right) + \sum_m G_m\left(X_m^\dagger\sigma X_m - \frac{1}{2}\{X_m X_m^\dagger,\sigma\}\right) \tag{A25}$$

with

$$\frac{1}{2}K_m - i\delta_m = \int_0^\infty dt\langle A_m(0)A_m^\dagger(t)\rangle,$$

$$\frac{1}{2}G_m - i\epsilon_m = \int_0^\infty dt\langle A_m^\dagger(0)A_m(t)\rangle. \tag{A26}$$

The first line in Eq. (A25) is just the renormalization of the free Liouvillian $\mathcal{L}_S$ by Lamb and Stark shift terms. The dissipative part is given by the second and third terms, which appear in the Lindblad form, so that $\mathrm{tr}\mathcal{L}\sigma=0$.

By identifying $\omega_{-m}=-\omega_m$, and assuming that $X_{-m}=X_m^\dagger$ and $g_m=g_{-m}$, the dissipative part of Eq. (A25) can now be rewritten as

$$\mathcal{L}\sigma = \gamma_0\left(X_0\sigma X_0 - \frac{1}{2}\{X_0X_0,\sigma\}\right) + \sum_{m\geq 1}\gamma_m\left(X_m\sigma X_m^\dagger - \frac{1}{2}\{X_m^\dagger X_m,\sigma\}\right) + \sum_{m\geq 1}\gamma_{-m}\left(X_m^\dagger\sigma X_m - \frac{1}{2}\{X_m X_m^\dagger,\sigma\}\right), \tag{A27}$$

where

$$\gamma_m = K_m + G_{-m}. \tag{A28}$$

Equation (A27) is the sought master equation (50) of the text.

By introducing the thermal spectral density functions (47) we explicitly get

$$K_m = 2\pi\kappa_m(\omega_m)[N(\omega_m)+1],$$
$$G_m = 2\pi\kappa_m(\omega_m)N(\omega_m), \tag{A29}$$

which by Eq. (A28) yield

$$\gamma_m = 2\,\mathrm{Re}\int_0^\infty dt[\langle A_m A_m^\dagger(t)\rangle + \langle A_{-m}^\dagger A_{-m}(t)\rangle] = 2\pi\kappa_m^\beta(\omega_m), \tag{A30}$$

which are the desired decay rates (51) of the text.

APPENDIX B

In this appendix, the assumption of the factorized form (5) of the initial density operator, which is usually taken for granted, is shown to be justified in the weak coupling (scaling) limit, provided ρ_B is mixing. We only outline the main derivation. Further details will be reported elsewhere [46].

Consider the initial-value problem

$$\frac{\partial}{\partial t}\rho = \mathcal{L}_{\mathrm{tot}}\rho = (\mathcal{L}_0+\lambda\mathcal{L}_{SB})\rho = (\mathcal{L}_S+\mathcal{L}_B+\lambda\mathcal{L}_{SB})\rho,$$
$$\rho(0)=\rho_0, \tag{B1}$$

where the dependence on the coupling constant λ of the interaction Liouvillian $\mathcal{L}_{SB}$ is made explicit. Notice that the initial density operator can be of any form and is *not* assumed here to be factorized as in (5). The projection operators $\mathcal{P}$ and $\mathcal{Q}$, defined in Eq. (A1), and the above Liouvillians $\mathcal{L}_S$, $\mathcal{L}_B$, and $\mathcal{L}_{SB}$ satisfy the same conditions (A2) and (A3). The projected density operators $\mathcal{P}\rho$ and $\mathcal{Q}\rho$ satisfy

$$\frac{\partial}{\partial t}\mathcal{P}\rho = \mathcal{L}_0\mathcal{P}\rho + \lambda\mathcal{P}\mathcal{L}_{SB}\mathcal{Q}\rho,$$

$$\frac{\partial}{\partial t}\mathcal{Q}\rho = (\mathcal{L}_0 + \lambda\mathcal{Q}\mathcal{L}_{SB}\mathcal{Q})\mathcal{Q}\rho + \lambda\mathcal{Q}\mathcal{L}_{SB}\mathcal{P}\rho, \tag{B2}$$

respectively. Following the same procedure as in Sec. III, we arrive at the following *exact* equation for the $\mathcal{P}$-projected operator in the interaction picture:

$$\frac{\partial}{\partial t}(e^{-\mathcal{L}_0 t}\mathcal{P}\rho) = \lambda e^{-\mathcal{L}_0 t}\mathcal{P}\mathcal{L}_{SB}e^{(\mathcal{L}_0+\lambda\mathcal{Q}\mathcal{L}_{SB}\mathcal{Q})t}\mathcal{Q}\rho_0 + \lambda^2\int_0^t dt' e^{-\mathcal{L}_0 t}\mathcal{P}\mathcal{L}_{SB}e^{(\mathcal{L}_0+\lambda\mathcal{Q}\mathcal{L}_{SB}\mathcal{Q})t'} \times \mathcal{L}_{SB}\mathcal{P}\rho(t-t'). \tag{B3}$$

Notice that the first term on the right-hand side represents the contribution arising from a possible initial correlation between the system and reservoir. We now show that this term dies out in the weak coupling (i.e., scaling) limit $\lambda \to 0$ with fixed $\tau \equiv \lambda^2 t$. For this purpose, define

$$\rho_I(\tau;\lambda) \equiv e^{-\mathcal{L}_0\tau/\lambda^2}\mathcal{P}\rho(\tau/\lambda^2), \tag{B4}$$

which satisfies

$$\dot{\rho}_I(\tau;\lambda) = \frac{1}{\lambda}e^{-\mathcal{L}_0\tau/\lambda^2}\mathcal{P}\mathcal{L}_{SB}e^{(\mathcal{L}_0+\lambda\mathcal{Q}\mathcal{L}_{SB}\mathcal{Q})\tau/\lambda^2}\mathcal{Q}\rho_0 + \int_0^{\tau/\lambda^2} dt' e^{-\mathcal{L}_0\tau/\lambda^2}\mathcal{P}\mathcal{L}_{SB}e^{(\mathcal{L}_0+\lambda\mathcal{Q}\mathcal{L}_{SB}\mathcal{Q})t'} \times \mathcal{L}_{SB}e^{\mathcal{L}_0(\tau/\lambda^2-t')}\mathcal{P}\rho_I(\tau-\lambda^2 t';\lambda). \tag{B5}$$

The first term vanishes in the $\lambda \to 0$ limit [46], since

$$\int_0^\infty d\tau\frac{1}{\lambda}e^{A\tau/\lambda^2}Y(\tau) = \lambda\int_0^\infty d\tau\, e^{A\tau}Y(\lambda^2\tau) \to 0, \tag{B6}$$

as $\lambda \to 0$, for any superoperator such that the integral $\int_0^\infty d\tau\, e^{A\tau}$ exists. This means that the contribution originating from the initial correlation between the system and reservoir disappears in the scaling limit and therefore we are allowed to start from an initial density matrix in the factorized form (5).

Finally, the dynamics of $\rho_I(\tau;0)$ is governed by

$$\dot{\rho}_I(\tau;0) = \sum_\omega \tilde{Q}_\omega\int_0^\infty dt'\mathcal{P}\mathcal{L}_{SB}(0)\mathcal{Q}\mathcal{L}_{SB}(-t')\tilde{Q}_\omega\rho_I(\tau;0) \tag{B7}$$

with the factorized initial condition (5), where the $\tilde{Q}_\omega$ are the eigenprojections of the Liouvillian $\mathcal{L}_S$ defined in (A12).

From a physical point of view, the factorization ansatz described in this appendix simply means that the "initial" correlations between the system and its environment are "forgotten" on a time scale of order λ^2. We also note that several authors have addressed the question of the modifications that arise when it is not permissible to assume initially separable system and environment, e.g., [69].

APPENDIX C

We derive Eq. (63). The first equality reads

$$[\hat{P}e^{\mathcal{L}_{\rm tot}\tau}\hat{P}]^{t/\tau} \simeq [\hat{P}V_Z(\tau)\hat{P}]^{t/\tau},$$

$$V_Z(\tau) = e^{\mathcal{L}_0\tau}\mathcal{T}\exp\left(\int_0^\tau ds\, e^{-\mathcal{L}_0 s}\mathcal{G}_Z(\tau)e^{\mathcal{L}_0 s}\right). \tag{C1}$$

Let us write $V_Z(\tau) = V(\tau,\tau)$, where

$$V(t,u) = e^{\mathcal{L}_0 t}\mathcal{T}\exp\left(\int_0^t ds\, e^{-\mathcal{L}_0 s}\mathcal{G}_Z(u)e^{\mathcal{L}_0 s}\right). \tag{C2}$$

By deriving with respect to t, we get

$$\partial_t V(t,u) = [\mathcal{L}_0 + \mathcal{G}_Z(u)]V(t,u), \tag{C3}$$

so that

$$V(t,u) = \exp\{[\mathcal{L}_0 + \mathcal{G}_Z(u)]t\}, \tag{C4}$$

where we used $V(0,u)=1$. As a consequence, $V_Z(\tau) = \exp\{[\mathcal{L}_0+\mathcal{G}_Z(\tau)]\tau\}$ and

$$[\hat{P}e^{\mathcal{L}_{\rm tot}\tau}\hat{P}]^{t/\tau} \simeq [\hat{P}\exp\{[\mathcal{L}_0+\mathcal{G}_Z(\tau)]\tau\}\hat{P}]^{t/\tau} = \hat{P}\exp\{[\mathcal{L}_0+\mathcal{G}_Z(\tau)]t\}, \tag{C5}$$

because $[\hat{P},\mathcal{L}_0]=[\hat{P},\mathcal{G}_Z]=0$. This is Eq. (63).

Let us now solve Eq. (65):

$$\int_0^\tau dt\, e^{-\mathcal{L}_S t}\mathcal{L}_Z(\tau)e^{\mathcal{L}_S t} = \int_0^\tau dt\hat{P}\mathcal{L}_I(t)\hat{P} = \int_0^\tau dt\int_0^t ds\hat{P}\mathcal{K}_I(t,s)\hat{P}. \tag{C6}$$

By using Eqs. (A8) and (A4),

$$\mathcal{K}_I(t,s)\sigma = \mathrm{tr}_B\{\mathcal{L}_{SB}(t)\mathcal{L}_{SB}(s)\sigma\otimes\rho_B\},$$

$$\mathcal{L}_{SB}(t) = e^{-(\mathcal{L}_S+\mathcal{L}_B)t}\mathcal{L}_{SB}e^{(\mathcal{L}_S+\mathcal{L}_B)t}, \tag{C7}$$

we get

$$\int_0^\tau dt\, e^{-\mathcal{L}_S t}\mathcal{L}_Z(\tau)e^{\mathcal{L}_S t}\sigma = \int_0^\tau dt\int_0^t ds\, \mathrm{tr}_B\{\hat{P}\mathcal{L}_{SB}(t)\mathcal{L}_{SB}(s)\hat{P}\sigma\otimes\rho_B\} = \int_0^\tau dt\, e^{-\mathcal{L}_S t}\int_{-t}^0 ds\, \mathrm{tr}_B\{\hat{P}\mathcal{L}_{SB}\mathcal{L}_{SB}(s)\hat{P}e^{\mathcal{L}_S t}\rho\}, \tag{C8}$$

where $\rho = \sigma\otimes\rho_B$. Let us rewrite the previous equation in terms of the eigenprojections $\tilde{Q}_\omega$ of $\mathcal{L}_S$ defined by (A12):

$$\sum_{\omega,\omega'}\int_0^\tau dt\, e^{i(\omega-\omega')t}\tilde{Q}_\omega\mathcal{L}_Z(\tau)\tilde{Q}_{\omega'}\sigma = \sum_{\omega,\omega'}\int_0^\tau dt\, e^{i(\omega-\omega')t} \times\int_{-t}^0 ds\, \mathrm{tr}_B\{\tilde{Q}_\omega\hat{P}\mathcal{L}_{SB}\mathcal{L}_{SB}(s)\hat{P}\tilde{Q}_{\omega'}\rho\}. \quad \text{(C9)}$$

Performing the first integral, we get

$$\tilde{Q}_\omega\mathcal{L}_Z(\tau)\tilde{Q}_{\omega'}\sigma = \frac{g((\omega-\omega')\tau)}{\tau}\int_0^\tau dt\, e^{i(\omega-\omega')t} \times\int_{-t}^0 ds\, \mathrm{tr}_B\{\tilde{Q}_\omega\hat{P}\mathcal{L}_{SB}\mathcal{L}_{SB}(s)\hat{P}\tilde{Q}_{\omega'}\rho\},$$

$$g(x) = \frac{ix}{e^{ix}-1}. \quad \text{(C10)}$$

Since $g(0)=1$, the diagonal terms yield

$$\tilde{Q}_\omega\mathcal{L}_Z(\tau)\tilde{Q}_\omega\sigma = \frac{1}{\tau}\int_0^\tau dt\int_{-t}^0 ds\, \mathrm{tr}_B\{\tilde{Q}_\omega\hat{P}\mathcal{L}_{SB}\mathcal{L}_{SB}(s)\hat{P}\tilde{Q}_\omega\rho\}. \quad \text{(C11)}$$

The off-diagonal terms do not contribute to the master equation, as explained in Appendix A, Eqs. (A10)–(A15).

By using the property (A21) and noting that $[\hat{P},\tilde{Q}_\omega]=0$ by Eq. (16), we get

$$\mathcal{L}_Z(\tau)\sigma = -\sum_\omega \frac{1}{\tau}\int_0^\tau dt\int_{-t}^0 ds \times \mathrm{tr}_B\{\hat{P}[(\tilde{Q}_\omega H_{SB}),[(\tilde{Q}_{-\omega}H_{SB}(s)),\hat{P}\rho]]\}, \quad \text{(C12)}$$

whence, by using Eq. (A23),

$$\begin{aligned}\mathcal{L}_Z(\tau)\sigma &= -\sum_m \frac{1}{\tau}\int_0^\tau dt\int_{-t}^0 ds\, \mathrm{tr}_B\{\hat{P}[H_{SB}^{(m)},[H_{SB}^{(-m)}(s),\hat{P}\rho]]\}\\ &= -\sum_m \frac{1}{\tau}\int_0^\tau dt\int_{-t}^0 ds \times \mathrm{tr}_B\{\hat{P}[X_m^\dagger\otimes A_m,[X_m\otimes A_m^\dagger(s),\hat{P}\rho]]\\ &\quad + \hat{P}[X_{-m}\otimes A_{-m}^\dagger,[X_{-m}^\dagger\otimes A_{-m}(s),\hat{P}\rho]]\}, \quad \text{(C13)}\end{aligned}$$

where, as in Eq. (A24), in the second equality we dropped terms containing two annihilation or creation operators. From Eq. (C13) we get Eq. (68) with

$$\gamma_m^Z(\tau) = \frac{2}{\tau}\mathrm{Re}\int_0^\tau dt\int_{-t}^0 ds[\langle A_m(0)A_m^\dagger(s)\rangle + \langle A_{-m}^\dagger(0)A_{-m}(s)\rangle]. \quad \text{(C14)}$$

By noticing that

$$\langle A_mA_m^\dagger(s)\rangle + \langle A_{-m}^\dagger A_{-m}(s)\rangle = \int_{-\infty}^\infty d\omega\, \kappa_m^\beta(\omega)e^{i(\omega-\omega_m)s}, \quad \text{(C15)}$$

we finally get

$$\gamma_m^Z(\tau) = \frac{2}{\tau}\int_{-\infty}^\infty d\omega\, \kappa_m^\beta(\omega)\frac{1-\cos(\omega-\omega_m)\tau}{(\omega-\omega_m)^2} = \tau\int_{-\infty}^\infty d\omega\, \kappa_m^\beta(\omega)\frac{\sin^2\left(\frac{\omega-\omega_m}{2}\tau\right)}{\left(\frac{\omega-\omega_m}{2}\tau\right)^2}, \quad \text{(C16)}$$

which is Eq. (69) of the text.

APPENDIX D

We derive Eqs. (78) and (80). We start from Eqs. (72) and (73):

$$\int_0^\tau ds\, e^{-\mathcal{L}_\tau s}\mathcal{F}_k(\tau)e^{\mathcal{L}_\tau s} = \int_0^\tau ds\, \mathcal{L}_{SB}(s), \quad \text{(D1)}$$

$$\int_0^\tau ds\, e^{-\mathcal{L}_\tau s}\mathcal{G}_k(\tau)e^{\mathcal{L}_\tau s} = \int_0^\tau ds\int_0^s ds_1[\mathcal{L}_{SB}(s)\mathcal{L}_{SB}(s_1) - e^{-\mathcal{L}_\tau s}\mathcal{F}_k(\tau)e^{\mathcal{L}_\tau(s-s_1)}\mathcal{F}_k(\tau)e^{\mathcal{L}_\tau s_1}], \quad \text{(D2)}$$

where $\mathcal{L}_\tau=\mathcal{L}_k/\tau+\mathcal{L}_0$, and by taking the trace over the bath we get

$$\int_0^\tau dt\, e^{-\mathcal{L}_S(\tau)}\mathcal{L}_k(\tau)e^{\mathcal{L}_S(\tau)}\sigma = \int_0^\tau dt\int_{-t}^0 ds\, \mathrm{tr}_B\{[e^{-\mathcal{L}_S t}\mathcal{L}_{SB}\mathcal{L}_{SB}(s) - e^{-\mathcal{L}_S(\tau)t}\mathcal{F}_k(\tau)e^{-\mathcal{L}_\tau s}\mathcal{F}_k(\tau)e^{\mathcal{L}_\tau s}e^{\mathcal{L}_S(\tau)t}]\rho\}, \quad \text{(D3)}$$

with $\rho=\sigma\otimes\rho_B$ and

$$\mathcal{L}_S(\tau) = \frac{\mathcal{L}_k}{\tau} + \mathcal{L}_S. \quad \text{(D4)}$$

Equation (D3) is similar to Eq. (C8) and, by projecting onto the eigenprojections $\tilde{P}_\omega(\tau)$ of $\mathcal{L}_S(\tau)$ and taking only the diagonal terms, one obtains Eq. (78). However, in order to compute the decay rates $\gamma_m^k(\tau)$ one can give an alternative, more physical derivation by elaborating on the technique of Ref. [12]. First notice that the BB dynamics (70) is generated by the time-dependent Hamiltonian

$$H(t/\tau) = H_{\mathrm{tot}} + H_k\delta_P(t/\tau), \delta_P(x) = \sum_{n\in\mathbb{Z}}\delta(x-n). \quad \text{(D5)}$$

In the enlarged Hilbert space $\mathcal{H}\otimes L^2(\mathbb{T})$ we can consider the (time-independent) Floquet Hamiltonian

$$H_{\mathrm{Floq}} = H(\theta) + \frac{1}{\tau}p_\theta = H_{\mathrm{tot}} + H_k\delta_P(\theta) + \frac{1}{\tau}p_\theta, \quad \text{(D6)}$$

where

$$\theta \in [-1/2, 1/2), \quad p_\theta = -i\partial_\theta, \quad [\theta, p_\theta] = i. \tag{D7}$$

We get

$$\dot{\theta} = -i[\theta, H_{\mathrm{Floq}}] = 1/\tau, \quad \theta(t) = t/\tau, \tag{D8}$$

whence $\forall A \in \mathcal{H}$,

$$\dot{A}(t) = -i[A(t), H_{\mathrm{Floq}}] = -i[A(t), H(t/\tau)], \tag{D9}$$

so that every observable in $\mathcal{H}$ evolves according to the original Hamiltonian (D5). The eigenvalue equation for p_θ reads

$$p_\theta|m\rangle = 2\pi m|m\rangle, \quad \langle\theta|m\rangle = e^{i2\pi m\theta}, \quad m \in \mathbb{Z}. \tag{D10}$$

The Hamiltonian (D6) in $\mathcal{H} \otimes L^2(\mathbb{T})$ represents a control by a strong continuous coupling, analogous to that discussed in Sec. VI, if one identifies $K = 1/\tau$ and $H_c = p_\theta$. Therefore, from Eqs. (97) and (D10) we obtain

$$\omega_{mn}(\tau) = \frac{1}{\tau}\Omega_m + \Omega_{mn}^{(1)} + O(\tau) = \frac{2\pi m}{\tau} + \Omega_{mn}^{(1)} + O(\tau), \tag{D11}$$

and from Eq. (95) we get

$$\gamma_{mn}^k(\tau) = 2\pi\kappa_n^\beta(\omega_{mn}(\tau)) = 2\pi\kappa_n^\beta\left(\frac{2\pi m}{\tau} + \Omega_{mn}^{(1)} + O(\tau)\right), \tag{D12}$$

which is Eq. (80) of the text.

[1] D. Giulini, E. Joos, C. Kiefer, J. Kupsch, I.-O. Stamatescu, and H.-D. Zeh, *Decoherence and the Appearance of a Classical World in Quantum Theory* (Springer, Berlin, 1996); M. Namiki, S. Pascazio, and H. Nakazato, *Decoherence and Quantum Measurements* (World Scientific, Singapore, 1997).

[2] A. Galindo and M. A. Martin-Delgado, Rev. Mod. Phys. **74**, 347 (2002); *The Physics of Quantum Information*, edited by D. Bouwmeester, A. Ekert, and A. Zeilinger (Springer, Berlin, 2000); M. A. Nielsen and I. L. Chuang, *Quantum Computation and Quantum Information* (Cambridge University Press, Cambridge, U.K., 2000).

[3] W. G. Unruh, Phys. Rev. A **51**, 992 (1995); see also I. L. Chuang, R. Laflamme, P. W. Shor, and W. H. Zurek, Science **270**, 1633 (1995).

[4] P. W. Shor, Phys. Rev. A **52**, R2493 (1995); A. R. Calderbank and P. W. Shor, *ibid.* **54**, 1098 (1996); A. Steane, Proc. R. Soc. London, Ser. A **452**, 2551 (1996); Phys. Rev. Lett. **77**, 793 (1996); for a review, see J. Preskill, in *Introduction to Quantum Computation and Information*, edited by H. K. Lo, S. Popescu, and T. P. Spiller (World Scientific, Singapore, 1999).

[5] S. Mancini and R. Bonifacio, Phys. Rev. A **64**, 042111 (2001); S. Mancini, D. Vitali, P. Tombesi, and R. Bonifacio, Europhys. Lett. **60**, 498 (2002); J. Opt. B: Quantum Semiclassical Opt. **4**, S300 (2002); H. Wiseman, S. Mancini, and J. Wang, Phys. Rev. A **66**, 013807 (2002).

[6] G. M. Palma, K. A. Suominen, and A. K. Ekert, Proc. R. Soc. London, Ser. A **452**, 567 (1996); L. M. Duan and G. C. Guo, Phys. Rev. Lett. **79**, 1953 (1997); P. Zanardi and M. Rasetti, *ibid.* **79**, 3306 (1997); D. A. Lidar, I. L. Chuang, and K. B. Whaley, *ibid.* **81**, 2594 (1998); E. Knill, R. Laflamme, and L. Viola, *ibid.* **84**, 2525 (2000). For a review, see D. A. Lidar and K. B Whaley, in *Irreversible Quantum Dynamics*, edited by F. Benatti and R. Floreanini, Lecture Notes in Physics Vol. 622 (Springer, Berlin, 2003), p. 83.

[7] L. Viola and S. Lloyd, Phys. Rev. A **58**, 2733 (1998).

[8] L. Viola, E. Knill, and S. Lloyd, Phys. Rev. Lett. **82**, 2417 (1999); **83**, 4888 (1999); **85**, 3520 (2000).

[9] P. Zanardi, Phys. Lett. A **258**, 77 (1999).

[10] D. Vitali and P. Tombesi, Phys. Rev. A **59**, 4178 (1999); **65**, 012305 (2001); C. Uchiyama and M. Aihara, *ibid.* **66**, 032313 (2002).

[11] M. S. Byrd and D. A. Lidar, Quantum Inf. Process. **1**, 19 (2002); Phys. Rev. A **67**, 012324 (2003).

[12] P. Facchi, D. A. Lidar, and S. Pascazio, Phys. Rev. A **69**, 032314 (2004).

[13] J. von Neumann, *Mathematical Foundation of Quantum Mechanics* (Princeton University Press, Princeton, NJ, 1955); A. Beskow and J. Nilsson, Ark. Fys. **34**, 561 (1967); L. A. Khalfin, JETP Lett. **8**, 65 (1968).

[14] B. Misra and E. C. G. Sudarshan, J. Math. Phys. **18**, 756 (1977).

[15] D. Home and M. A. B. Whitaker, Ann. Phys. (N.Y.) **258**, 237 (1997).

[16] P. Facchi and S. Pascazio, in *Progress in Optics*, edited E. Wolf (Elsevier, Amsterdam, 2001), Vol. 42, Chap. 3, p. 147.

[17] P. Facchi and S. Pascazio, Phys. Rev. Lett. **89**, 080401 (2002); in *The Physics of Communication*, Proceedings of the XXII Solvay Conference in Physics, edited by I. Antoniou, V. A. Sadovnichy, and H. Walther (World Scientific, Singapore, 2003) p. 251.

[18] P. Facchi, V. Gorini, G. Marmo, S. Pascazio, and E. C. G. Sudarshan, Phys. Lett. A **275**, 12 (2000); P. Facchi, S. Pascazio, A. Scardicchio, and L. S. Schulman, Phys. Rev. A **65**, 012108 (2002).

[19] C. N. Friedman, Indiana Univ. Math. J. **21**, 1001 (1972).

[20] K. Gustafson, in *Energy Storage and Redistribution in Molecules*, edited by J. Hinze (Plenum, New York, 1983), and Refs. [10,12] therein; K. Gustafson, e-print quant-ph/0203032.

[21] P. Exner and T. Ichinose, e-print math-ph/0302060.

[22] A. U. Schmidt, J. Phys. A **35**, 7817 (2002); **36**, 1135 (2003).

[23] B. Misra and A. Antoniou, in *The Physics of Communication* (Ref. [17]), p. 233.

[24] Y. Takahashi, M. J. Rabins, and D. M. Auslander, *Control and Dynamic Systems* (Addison-Wesley, Reading, MA, 1970); J. Macki and A. Strauss, *Introduction to Optimal Control Theory* (Springer-Verlag, New York, 1982); L. Lapidus and R. Luus, *Optimal Control of Engineering Processes* (Blaisdell Publishing, Waltham, MA, 1967).

[25] T. Petrosky, S. Tasaki, and I. Prigogine, Phys. Lett. A **151**, 109 (1990); Physica A **170**, 306 (1991); S. Pascazio and M.

Namiki, Phys. Rev. A **50**, 4582 (1994).
[26] E. P. Wigner, Am. J. Phys. **31**, 6 (1963).
[27] R. J. Cook, Phys. Scr., T **21**, 49 (1988).
[28] W. M. Itano, D. J. Heinzen, J. J. Bolinger, and D. J. Wineland, Phys. Rev. A **41**, 2295 (1990).
[29] A. Peres and A. Ron, Phys. Rev. A **42**, 5720 (1990); W. H. Itano, D. J. Heinzen, J. J. Bollinger, and D. J. Wineland, *ibid.* **43**, 5168 (1991); S. Inagaki, M. Namiki, and T. Tajiri, Phys. Lett. A **166**, 5 (1992); S. Pascazio, M. Namiki, G. Badurek, and H. Rauch, *ibid.* **179**, 155 (1993); Ph. Blanchard and A. Jadczyk, *ibid.* **183**, 272 (1993); T. P. Altenmüller and A. Schenzle, Phys. Rev. A **49**, 2016 (1994); J. I. Cirac, A. Schenzle, and P. Zoller, Europhys. Lett. **27**, 123 (1994); M. Berry, in *Fundamental Problems in Quantum Theory*, edited by D. M. Greenberger and A. Zeilinger, Annals of the N.Y. Academy of Sciences (New York Academy of Sciences, New York, 1995), Vol. 755), p. 303; A. Beige and G. Hegerfeldt, Phys. Rev. A **53**, 53 (1996); A. Luis and J. Peřina, Phys. Rev. Lett. **76**, 4340 (1996).
[30] M. Simonius, Phys. Rev. Lett. **40**, 980 (1978).
[31] R. A. Harris and L. Stodolsky, Phys. Lett. **116B**, 464 (1982).
[32] A. Peres, Am. J. Phys. **48**, 931 (1980).
[33] L. S. Schulman, Phys. Rev. A **57**, 1509 (1998).
[34] C. Monroe, D. M. Meekhof, B. E. King, W. M. Itano, and D. J. Wineland, Phys. Rev. Lett. **75**, 4714 (1995).
[35] R. J. Hughes *et al.*, Fortschr. Phys. **46**, 32 (1998); D. G. Cory *et al.*, *ibid.* **48**, 875 (2000); M. Lieven, K. Vandersypen, M. Steffen, G. Breyta, C. S. Yannoni, M. H. Sherwood, and I. L. Chuang, Nature (London) **414**, 883 (2001).
[36] L. Jacak, P. Hawrylak, and A. Wojs, *Quantum Dots* (Springer, Berlin, 1998); D. Steinbach *et al.*, Phys. Rev. B **60**, 12079 (1999).
[37] Y. Makhlin, G. Schön, and A. Shnirman, Rev. Mod. Phys. **73**, 357 (2001).
[38] T. Calarco, A. Datta, P. Fedichev, E. Pazy, and P. Zoller, Phys. Rev. A **68**, 012310 (2003).
[39] G. Falci, E. Paladino, and R. Fazio, in *Quantun Phenomena in Mesoscopic Systems*, Proceedings of the International School of Physics "Enrico Fermi," Course CLI, edited by, B. L. Altshuler and V. Tognetti (IOS Press, Amsterdam, 2004).
[40] E. Paladino, L. Faoro, G. Falci, and R. Fazio, Phys. Rev. Lett. **88**, 228304 (2002).
[41] G. Falci, A. D'Arrigo, A. Mastellone, and E. Paladino, Phys. Rev. A **70**, 040101(R) (2004).
[42] A. G. Kofman and G. Kurizki, Phys. Rev. Lett. **87**, 270405 (2001).
[43] A. M. Lane, Phys. Lett. **99A**, 359 (1983); W. C. Schieve, L. P. Horwitz, and J. Levitan, Phys. Lett. A **136**, 264 (1989); P. Facchi and S. Pascazio, Phys. Rev. A **62**, 023804 (2000); B. Elattari and S. A. Gurvitz, *ibid.* **62**, 032102 (2000); A. G. Kofman and G. Kurizki, Nature (London) **405**, 546 (2000); K. Koshino and A. Shimizu, Phys. Rev. A **67**, 042101 (2003).
[44] P. Facchi, H. Nakazato, and S. Pascazio, Phys. Rev. Lett. **86**, 2699 (2001).
[45] S. Tasaki, A. Tokuse, P. Facchi, and S. Pascazio, Int. J. Quantum Chem. **98**, 160 (2004).
[46] S. Tasaki *et al.* (unpublished).
[47] J. Schwinger, Proc. Natl. Acad. Sci. U.S.A. **45**, 1552 (1959); J. Schwinger, *Quantum Kinetics and Dynamics* (Benjamin, New York, 1970).
[48] R. M. Wilcox, J. Math. Phys. **8**, 962 (1967).
[49] G. Casati, B. V. Chirikov, J. Ford, and F. M. Izrailev, in *Stochastic Behaviour in Classical and Quantum Hamiltonian Systems*, edited by G. Casati and J. Ford, Lecture Notes in Physics Vol. 93 (Springer-Verlag, Berlin, 1979), p. 334; M. V. Berry, N. L. Balazs, M. Tabor, and A. Voros, Ann. Phys. (N.Y.) **122**, 26 (1979).
[50] B. Kaulakys and V. Gontis, Phys. Lett. **56A**, 1131 (1997); P. Facchi, S. Pascazio, and A. Scardicchio, Phys. Rev. Lett. **83**, 61 (1999); J. C. Flores, Phys. Rev. B **60**, 30 (1999); B. Kaulakys, Phys. Rev. B **62**, R16291 (2000); S. A. Gurvitz, Phys. Rev. Lett. **85**, 812 (2000); J. Gong and P. Brumer, *ibid.* **86**, 1741 (2001); A. Luis, J. Opt. B: Quantum Semiclassical Opt. **3**, 238 (2001).
[51] See, for instance, A. Messiah, *Quantum Mechanics* (Interscience, New York, 1961).
[52] M. Frasca, Phys. Rev. A **58**, 3439 (1998); Phys. Rev. B **68**, 165315 (2003).
[53] A. Venugopalan and R. Ghosh, Phys. Lett. A **204**, 11 (1995); M. P. Plenio, P. L. Knight, and R. C. Thompson, Opt. Commun. **123**, 278 (1996); M. V. Berry and S. Klein, J. Mod. Opt. **43**, 165 (1996); E. Mihokova, S. Pascazio, and L. S. Schulman, Phys. Rev. A **56**, 25 (1997); A. Luis and L. L. Sánchez–Soto, *ibid.* **57**, 781 (1998); K. Thun and J. Peřina, Phys. Lett. A **249**, 363 (1998); A. D. Panov, *ibid.* **260**, 441 (1999); J. Řeháček, J. Peřina, P. Facchi, S. Pascazio, and L. Mišta, Phys. Rev. A **62**, 013804 (2000); P. Facchi and S. Pascazio, *ibid.* **62**, 023804 (2000); B. Militello, A. Messina, and A. Napoli, Phys. Lett. A **286**, 369 (2001); A. Luis, Phys. Rev. A **64**, 032104 (2001).
[54] C. W. Gardiner and P. Zoller, *Quantum Noise* (Springer, Berlin, 2000).
[55] H. Spohn and J. L. Lebowitz, Adv. Chem. Phys. **38**, 109 (1979).
[56] V. B. Berestetskii, E. M. Lifshits, and L. P. Pitaevskii, *Quantum Electrodynamics*, Course of Theoretical Physics Vol. 4 (Pergamon Press, Oxford, 1982), Chap. 5; H. E. Moses, Lett. Nuovo Cimento Soc. Ital. Fis. **4**, 51 (1972); **4**, 54 (1972); Phys. Rev. A **8**, 1710 (1973); J. Seke, Physica A **203**, 269 (1994); **203**, 284 (1994).
[57] P. Facchi and S. Pascazio, Phys. Lett. A **241**, 139 (1998); Physica A **271**, 133 (1999).
[58] I. Antoniou, E. Karpov, G. Pronko, and E. Yarevsky, Phys. Rev. A **63**, 062110 (2001).
[59] L. van Hove, Physica (Amsterdam) **23**, 441 (1957); S. Nakajima, Prog. Theor. Phys. **20**, 948 (1958); I. Prigogine and P. Résibois, J. Chem. Phys. **27**, 629 (1961); R. Zwanzig, J. Chem. Phys. **33**, 1338 (1960); E. B. Davies, *Quantum Theory of Open Systems* (Academic Press, New York, 1976).
[60] G. S. Agarwal, M. O. Scully, and H. Walther, Phys. Rev. A **63**, 044101 (2001); M. O. Scully, S.-Y. Zhu, and M. S. Zubairy, Chaos, Solitons Fractals **16**, 403 (2003); K. Shiokawa and D. A. Lidar, Phys. Rev. A **69**, 030302(R) (2004).
[61] T. Kato, *Perturbation Theory for Linear Operators* (Springer, Berlin, 1980), Theorem 10.1.
[62] http://mathworld.wolfram.com/LambertsW-Function.html
[63] Y. M. Galperin, B. L. Altshuler, and D. V. Shantsev, e-print cond-mat/0312490; Y. Makhlin and A. Shnirman, e-print cond-mat/0308297.
[64] H. Gutmann, F. K. Wilhelm, W. M. Kaminsky, and S. Lloyd,

e-print cond-mat/0308107; L. Faoro and L. Viola, Phys. Rev. Lett. **92**, 117905 (2004).

[65] L. Accardi, Y. G. Lu, and I. Volovich, *Quantum Theory and Its Stochastic Limit* (Springer-Verlag, Berlin, 2002).

[66] G. Kimura, K. Yuasa, and K. Imafuku, Phys. Rev. A **63**, 022103 (2001); Phys. Rev. Lett. **89**, 140403 (2002).

[67] W. Pauli, in *Festschrift zum 60: Geburtstage A. Sommerfelds* (Hirzel, Leipzig, 1928), p. 30.

[68] D. A. Lidar, Z. Bihary, and K. B. Whaley, Chem. Phys. **268**, 35 (2001).

[69] P. Pechukas, Phys. Rev. Lett. **73**, 1060 (1994); R. Alicki, *ibid.* **75**, 3020 (1995); P. Pechukas, *ibid.* **75**, 3021 (1995); G. Lindblad, J. Phys. A **29**, 4197 (1996); P. Štelmachovič and V. Bužek, Phys. Rev. A **64**, 062106 (2001); K. M. Fonseca Romero, P. Talkner, and P. Hänggi, e-print quant-ph/0311077; D. M. Tong, Jing-Ling Chen, L. C. Kwek, and C. H. Oh, e-print quant-ph/0311091.

PHYSICAL REVIEW A **71**, 032102 (2005)

Steering distillation processes through quantum Zeno dynamics

B. Militello,[1] H. Nakazato,[2] and A. Messina[1]
[1]*INFM, MIUR, and Dipartimento di Scienze Fisiche ed Astronomiche dell'Università di Palermo, Via Archirafi, 36, I-90123 Palermo, Italy*
[2]*Department of Physics, Waseda University, Tokyo 169-8555, Japan*
(Received 18 April 2004; published 8 March 2005)

A quantum system in interaction with a repeatedly measured one undergoes a nonunitary time evolution and is pushed into a subspace substantially determined by the two-system coupling. The possibility of suitably modifying such an evolution through quantum Zeno dynamics (i.e., the generalized quantum Zeno effect) addressing the system toward an *a priori* decided target subspace is illustrated. Applications and their possible realizations in the context of trapped ions are also discussed.

DOI: 10.1103/PhysRevA.71.032102 PACS number(s): 03.65.Xp, 03.65.Ta, 32.80.Pj

I. INTRODUCTION

A distillation process, in its essence, is nothing but a systematic way of driving a system toward a state nonorthogonal to its initial condition. In some sense, thus, it often represents the realization of a projection operator. In recent years, efforts have been made to realize distillation procedures since they might be exploited to prepare and to control at one's will the state of a quantum system. In the field of quantum technology [1,2] covering such research areas as quantum computation, quantum information and quantum teleportation, it is usually assumed that a desired state, which is necessary to start a specific quantum manipulation, can be prepared in principle. In reality, however, it is not at all trivial and we have to specify explicitly how such a preparation is actually implemented. Various distillation processes have been proposed for this purpose so far [1,2].

Recently a general strategy of distillation specifically addressed to bipartite systems has been reported [3]. The key idea of this distillation process is to repeatedly measure a system (here called *master* and denoted by M) interacting with another one (here called *slave* and denoted by S) provoking a nonunitary evolution which forces the latter toward a subspace determined by the specific M-S coupling and by the results of the master measurements. It occurs with a probability that expresses the efficiency of the process.

Such a scheme for distillation shares some points with quantum nondemolition measurement (QND) methods [4,5], also based on the idea of repeatedly measuring a system in interaction with the one we want to observe. It is worth mentioning that, although the original scope of the QND was to measure observables (let us denote by A_S the generic one) related to the nonrepeatedly measured system (corresponding to the slave in the distillation scheme), the procedure (being nothing but a practical realization of a measurement on the slave) has the collateral effect of projecting the slave onto an eigenspace of the measured observable. Therefore, QND provides a way to generate quantum states through their *extraction* from the initial condition of the relevant physical system (i.e., the slave) [6–8]. Despite these similarities between distillation and QND, the formalism introduced in Ref. [3] allows one to bring to light all the potentialities of such a scheme overcoming restrictions present in the standard description of QND. Indeed, while in the quantum nondemolition measurement approach it is required that the analog of the M-S coupling should commute with the slave observable one is going to measure (a sufficient condition to realize a projection onto A_S subspaces), in distillation schemes a necessary and sufficient condition on the nonunitary operator describing the nonunitary dynamics above mentioned may be directly given in order to establish which subspace is going to be extracted, that is, distilled.

The interest in such a process is twofold. On the one hand, as already mentioned, it allows the realization of applications in the context of quantum state manipulation and in particular quantum state preparation. On the other hand, it is also interesting in fundamental physics, describing the behavior of a physical system when a part of it is repeatedly measured.

In this paper we analyze in depth the distillation process reported in [3], bringing to light the close connection between the final result of the distillation process and the master-slave interaction. In particular, neglecting any environment effect, we show that the survival probabilities of the slave states under the unitary evolution due to the M-S interaction are the crucial elements of this process. We shall prove that the higher is such a unitary survival probability, the higher is the probability that the relevant slave state is distilled by the process. On the basis of this observation, we demonstrate the possibility of steering distillation processes using mechanisms of control of survival probability relying on the generalized quantum Zeno effect, i.e., the quantum Zeno dynamics [9–12] recalled in the following.

In the next section, we recall the general statement of repeated measurement-based distillation following Ref. [3], and show applications in the specific case wherein the master is a two-level system. In the third section, we analyze the nature of the distillation and point out its connection with the survival probabilities related to the unitary evolution induced by the M-S interaction. In the same section, we recall the quantum Zeno dynamics and show how to use it for controlling such survival probabilities and hence for steering distillation. The realizations of some classes of projection operators in a harmonic-oscillator Hilbert space are reported in the case where the master is a few-level system. The realization of operators projecting in finite or infinite dimensional sub-

spaces corresponding to finite or infinite ranges of energy is described. In the final section, we discuss and show the possibility of realizing the method presented, in the context of trapped ions, and give some concluding remarks.

II. DISTILLATION PROCESSES

In this section, we analyze the behavior of a compound system when a part of it is repeatedly measured. It is easily understood that the measurements generally introduce nonunitary elements in the time evolution, and provoke the decay of a subset (subspace) of slave states when certain conditions are satisfied. In this circumstance, a projection operator onto a slave subspace is practically realized. The required conditions concern the spectrum of the nonunitary operator responsible for the evolution. As will be reported at the end of this section, in the case wherein the master is a two-level system, the relevant nonunitary operator is shown to be diagonalized and such conditions are explicitly examined. Moreover, it is necessary to analyze the relevant spectrum to determine the duration of the unitary interaction (i.e., the interval between adjacent measurements) and to individuate the classes of distillable subspaces.

A. General statement

Consider two interacting systems, referred to as *master* (M) and *slave* (S). Let $\{|\phi_k\rangle\}$ denote a basis of M, and $\{|\varphi_n\rangle\}$ indicate a basis of S. Let us denote by $\hat{U}(\tau)=e^{-i\hat{H}\tau}$ the time evolution operator ($\hbar=1$) for time τ, $\hat{H}$ being the compound system Hamiltonian.

Perform a measurement of the master state, and assume that the result is $|\phi_0\rangle$. Let the system evolve for time τ under $\hat{H}$, then perform another measurement of the master, and so on N times. Assume that at each step the master system is found in the state $|\phi_0\rangle$. In such a case, the compound system is subjected to a nonunitary time evolution characterized by the operator

$$\hat{W}^{(N)}(\tau) \equiv \mathcal{N}_N[|\phi_0\rangle\langle\phi_0|\hat{U}(\tau)]^N|\phi_0\rangle\langle\phi_0| = \mathcal{N}_N|\phi_0\rangle\langle\phi_0|[\hat{V}(\tau)]^N, \tag{1}$$

where

$$\hat{V}(\tau) \equiv \langle\phi_0|e^{-i\hat{H}\tau}|\phi_0\rangle \tag{2}$$

is a nonunitary operator describing the transformation that the slave state undergoes owing to both the time evolution $\hat{U}(\tau)$ and the projection following the successful measurement act on M. The normalization factor $\mathcal{N}_N$ takes into account the probability of finding M in the state $|\phi_0\rangle$ N times.

Let us solve the eigenvalue problem related to $\hat{V}(\tau)$. Since this operator is not Hermitian, generally its right and left eigenvalue problems have different solutions. Assume now that it is possible to *diagonalize* the operator $\hat{V}(\tau)$ in the standard way [13]

$$\hat{V}(\tau) = \sum_k \gamma_k \hat{P}_k, \tag{3}$$

where $\{\hat{P}_k\}$ are orthogonal projection operators satisfying the completeness relation $\Sigma_k \hat{P}_k = \hat{1}_S$, $\hat{1}_S$ being the slave identity operator, and γ_k are complex numbers having moduli in general not greater than 1. We shall denote also by $|\gamma_k, l\rangle$ the eigenstates corresponding to $\hat{P}_k$, l being indices spanning the eventually degenerate eigenspace, so that $\hat{P}_k = \Sigma_l |\gamma_k, l\rangle\langle\gamma_k, l|$.

Introducing $\gamma = \max_k\{|\gamma_k|\}$, one finds, for large enough N,

$$\hat{W}^{(N)}(\tau) \approx \aleph_N |\phi_0\rangle\langle\phi_0| \sum_{k:|\gamma_k|=\gamma} \gamma_k^N \hat{P}_k \tag{4}$$

which may also be cast in the form

$$\hat{W}^{(N)}(\tau) \approx \aleph_N |\phi_0\rangle\langle\phi_0| \gamma^N \hat{R}^N \hat{P}_{dist} \tag{5}$$

where $\hat{R} := \Sigma_{k:|\gamma_k|=\gamma}(\gamma_k/\gamma)\hat{P}_k$ (and hence $\hat{R}^N$) is a unitary operator acting on the distilled slave subspace corresponding to the projection operator

$$\hat{P}_{dist} := \sum_{k:|\gamma_k|=\gamma} \hat{P}_k. \tag{6}$$

If a unique eigenvalue of $\hat{V}(\tau)$ having modulus γ exists and in addition its eigenspace is nondegenerate, then the distillation procedure realizes just a single-state selection.

It deserves to be noted that the distillation is a conditional procedure in the sense that its success depends on N measurement results. More precisely, the master system (M), at each measurement act, should be always found in the state $|\phi_0\rangle$. Moreover, the procedure substantially realizes a projection operator; hence, if the process is successful, the would-be distilled states should be present in the initial slave state $\hat{\rho}_s$, where the initial state of the compound system is assumed to be $\hat{\rho}_s \otimes |\phi_0\rangle\langle\phi_0|$. The joint probability of finding the master system in its initial state $|\phi_0\rangle$ at each step ($\Pi_{k=1}^N \wp_k^{(M)}$, $\wp_k^{(M)}$ being the probability of finding the master in $|\phi_0\rangle$ at the kth measurement) tends, in the limit $N \to \infty$ and in the case $\gamma=1$, to the probability of finding the target subspace (i.e., the "distillate") into the initial slave state [17] (see the Appendix), that is,

$$\prod_{k=1}^N \wp_k^{(M)} \to \mathrm{Tr}_S\{\hat{\rho}_s \hat{P}_{dist}\}, \tag{7}$$

where Tr_S is the trace operation over the slave degrees of freedom.

The quantity in Eq. (7) expresses the efficiency of the distillation process, that is, the success probability of distillation. In connection with this point, it is worth remarking that in the case $\gamma=1$ the distillation may be thought of as a simulation of a measurement act on the slave. In fact, it projects the system onto a prefixed subspace with a probability given by the norm of the component of the slave state onto the distilled subspace.

Incidentally, Eq. (7) explains also the fact that QND may be used in many physical systems, for instance in trapped ions, both as a strategy for generating states and for measur-

ing slave state populations [6–8]. Indeed, on the one hand such processes project the system onto the distilled subspace with an efficiency given by Eq. (7) (state generation). On the other hand, the master is found in the state $|\phi_0\rangle$ all N times with a joint probability which (for large enough N) is equal to the population of the target subspace in the initial slave state, providing a way to measure such populations (population measurements).

B. A case of spin 1/2 as the master

In general, the eigenvalue problem of $\hat{V}(\tau)$ is not trivial, in the sense that the left and right problems are not adjoint to each other. As an example of solvable models, let us consider the case wherein the master is a two-level system (formally of spin $\frac{1}{2}$), while the slave is a harmonic oscillator. This is not just an academic example. Indeed, in the context of trapped ions, it is possible to realize a wide variety of such couplings provided the experimental setup is adequately adjusted. In fact, the actions of suitably tuned and polarized laser fields on the confined atom are responsible for specific vibronic couplings (vibronic, i.e., involving both the internal and center-of-mass motional degrees of freedom) of the form [14–16]

$$\hat{H}_v = \varepsilon\hat{\Omega}\hat{\sigma}_+ + \text{H.c.}, \tag{8}$$

where $\hat{\sigma}_+ = |+\rangle\langle -|$ ($\hat{\sigma}_- = |-\rangle\langle +|$) is the Pauli raising (lowering) operator, $|\pm\rangle$ being the internal ionic states, and ε is a positive coupling constant related to laser intensities and initial phases. The generic time-independent operator $\hat{\Omega}$ acts in the slave Hilbert space, and its specific form is determined once the specific nature of the master-slave interaction is given [17].

Assume that the master (M) is initially in the state $|+\rangle$, hence starting with the density operator

$$\hat{\rho} = \hat{\rho}_v \otimes |+\rangle\langle +|, \tag{9}$$

$\hat{\rho}_v$ being the initial slave state. Let the system evolve under the action of the Hamiltonian $\hat{H}_v$ (M-S interaction) for time τ, and then measure the internal ionic state. Assume the system is found in $|+\rangle$, and then let again the system evolve in accordance with $\hat{H}_v$ for another time τ, and measure the fermionic state finding it in $|+\rangle$, and so on N times.

Under these assumptions, the system undergoes the nonunitary evolution essentially described by the Nth power of the nonunitary operator

$$\hat{V}(\tau) \equiv \langle + |e^{-i\hat{H}_v\tau}| + \rangle = \cos(\varepsilon\tau\sqrt{\hat{\Omega}\hat{\Omega}^\dagger}). \tag{10}$$

Such an explicit expression provides a very useful insight for forecasting the result of a distillation based upon interactions of the form (8). Indeed, denoting by ω_k and $|\omega_k\rangle$ the eigenvalues and eigenstates of the operator $\hat{\Omega}\hat{\Omega}^\dagger$, it is possible to distill a class of eigenstates simply by adjusting the pulse area $\varepsilon\tau$. In fact, for large enough N, it turns out that

$$\cos^N(\varepsilon\tau\sqrt{\omega_k}) = (-1)^{l_k N} \quad \text{if } \varepsilon\tau\sqrt{\omega_k} = l_k\pi,$$

$$\cos^N(\varepsilon\tau\sqrt{\omega_k}) \approx 0 \quad \text{otherwise}, \tag{11}$$

and hence, choosing, for a prefixed $\overline{\omega}$, the pulse area $\varepsilon\tau$ such that for instance $\varepsilon\tau\sqrt{\overline{\omega}} = \pi$, it is possible to distill all those states belonging to integer-squared multiples of $\overline{\omega}$, and if no such eigenvalues exist, only the state corresponding to $\overline{\omega}$ is distilled.

In the context of trapped ions, this result may be used to realize a wide variety of applications concerning the generation of states whose Fock statistics involves only Fock states corresponding to perfect-square numbers, the generation of common eigenstates of energy and angular momentum, angular momentum Schrödinger cat states, and so on [17].

III. CONTROLLING DISTILLATION THROUGH QUANTUM ZENO EFFECT

In this section, we explain the connection between the final result of the distillation and the M-S interaction, showing that the distilled subspace is generated by those slave states which undergo unitary evolutions, in the time τ, characterized by the highest survival probability. On the basis of this fact, we propose to use quantum Zeno effect to control such survival probabilities. Moreover we show some applications, in particular the realization of what we call high-, low-, and bandpass bosonic filters, i.e., projection operators on subspaces whose states possess excitation numbers higher or lower than a quantity, or in a range.

A. Unitary vs nonunitary survival probability

Consider the *orthonormal* basis of the M-S system $|\gamma_k, l\rangle|\phi_j\rangle \equiv |\gamma_k, l\rangle \otimes |\phi_j\rangle$, and denote by $|\psi_{kl,j}(\tau)\rangle$ its evolution induced by $\hat{U}(\tau)$: $|\psi_{kl,j}(\tau)\rangle \equiv \hat{U}(\tau)|\gamma_k, l\rangle|\phi_j\rangle$. Therefore, the evolution operator may be cast in the form

$$\hat{U}(\tau) = \sum_{k,l,j} |\psi_{kl,j}(\tau)\rangle\langle\gamma_k, l|\langle\phi_j|. \tag{12}$$

Since $\hat{V}(\tau) \equiv \langle\phi_0|\hat{U}(\tau)|\phi_0\rangle = \Sigma_{k,l}\gamma_k|\gamma_k, l\rangle\langle\gamma_k, l|$, we obtain $\langle\phi_0|\psi_{kl,0}(\tau)\rangle = \gamma_k|\gamma_k, l\rangle$. This means that $\hat{U}(\tau)|\gamma_n, l\rangle|\phi_0\rangle = \sqrt{\wp_n(\tau)}e^{i\xi_n(\tau)}|\gamma_n, l\rangle \otimes |\phi_0\rangle + \Sigma_{j\neq 0}\Sigma_{m,q}c_{j,mq}(\tau)|\gamma_m, q\rangle \otimes |\phi_j\rangle$, $\wp_n(\tau)$ being the relevant survival probability related to γ_n through $\gamma_n = \sqrt{\wp_n(\tau)}e^{i\xi_n(\tau)}$. Therefore one immediately finds

$$\hat{V}(\tau) = \sum_{n,l} \sqrt{\wp_n(\tau)}e^{i\xi_n(\tau)}|\gamma_n, l\rangle\langle\gamma_n, l|. \tag{13}$$

Such a decomposition gives a precise physical meaning to the moduli of the eigenvalues of $\hat{V}(\tau)$ and shows that the distilled (preserved) slave states (corresponding to higher eigenvalue moduli) are those undergoing unitary evolutions (between two measurement acts) which do not induce (or induce smaller) abandon of the initial master states $|\phi_0\rangle$ in favor of the others $|\phi_j\rangle$, $j \neq 0$. In other words, in order to be distilled, the state $|\gamma_n, l\rangle|\phi_0\rangle$ should not undergo (or should undergo less than the other states) transitions to states with different master states $|\gamma_m, q\rangle|\phi_j\rangle$, $j \neq 0$. On the basis of this comment, each state $|\gamma_n, l\rangle$ may be thought of as a "channel" of probability loss, which may be opened or closed depend-

ing on the specific features of $\hat{U}(\tau)$. If the channel is closed the relevant state is preserved, otherwise it is going to be lost.

B. Quantum Zeno dynamics to control unitary survival probability: A toy model

The survival probability of a physical system undergoing a unitary time evolution may be changed using control mechanisms substantially relying on the dynamical quantum Zeno effect, i.e., quantum Zeno dynamics [9–11]. To better understand this fact, let us temporarily leave our original physical problem and consider a three-level system, assuming that its dynamics is governed by the tridiagonal Hamiltonian

$$\Xi_3 = \begin{pmatrix} 0 & \Omega & 0 \\ \Omega^* & 0 & \Lambda \\ 0 & \Lambda^* & 0 \end{pmatrix}, \tag{14}$$

Ω being the coupling constant between the ground state and the first excited state ($|g\rangle$ and $|e_1\rangle$, respectively), and Λ being the coupling constant between the first and the second excited levels ($|e_1\rangle$ and $\langle e_2\rangle$, respectively). We shall consider the dynamics in the regime $\Lambda=0$ as the *unperturbed* one, and it is straightforward to prove that it corresponds to Rabi oscillations between $|g\rangle$ and $|e_1\rangle$. The second excited state $|e_2\rangle$ is stationary. The introduction of the second coupling $\Lambda \neq 0$ gives rise to a modified regime, known as *Zeno dynamics*, such that for $|\Lambda| \gg |\Omega|$ the dynamics of the ground state is hindered. More in detail, assuming that the system starts in the state $|g\rangle$, the relevant survival probability is given by

$$\wp_g[\Xi_3,\tau] \equiv |\langle g|e^{-i\Xi_3\tau}|g\rangle|^2 = \left[\frac{|\Lambda|^2 + |\Omega|^2\cos(\omega\tau)}{|\Lambda|^2 + |\Omega|^2}\right]^2 \tag{15}$$

with $\omega = \sqrt{|\Omega|^2 + |\Lambda|^2}$.

Looking at this formula it is easy to see that in the regime $|\Lambda| \gg |\Omega|$, the probability approaches unity, $\wp_g \approx 1$, meaning that the unperturbed dynamics is hindered by the action of the Λ coupling which may be interpreted as a measurement coupling. Indeed the transitions from $|e_1\rangle$ to $|e_2\rangle$ produce in some sense a way to measure the population of level $|e_1\rangle$ [10–12], putting this behavior in the framework of quantum Zeno effect. Apart from philosophical and semantical discussions, the effect of the second (strong) coupling is to hinder the dynamics due to the first coupling.

The scheme may be generalized, assuming, for example, that a third excited level $|e_3\rangle$ coupled with the second exists, as expressed by the Hamiltonian

$$\Xi_4(\Omega,\Lambda,\Gamma) = \begin{pmatrix} 0 & \Omega & 0 & 0 \\ \Omega^* & 0 & \Lambda & 0 \\ 0 & \Lambda^* & 0 & \Gamma \\ 0 & 0 & \Gamma^* & 0 \end{pmatrix}. \tag{16}$$

It has been shown that, in the regime $|\Gamma| \gg |\Lambda|$, the hindering effect due to the Λ coupling is canceled [10,18]. In fact, we have

$$\wp_g[\Xi_4,\tau] \equiv |\langle g|e^{-i\Xi_4\tau}|g\rangle|^2 \approx \cos^2(|\Omega|\tau), \tag{17}$$

the unperturbed dynamics being restored.

Let us summarize this phenomenology. The four-level system under scrutiny performs Rabi oscillations between the two lowest states (those coupled by Ω) when $\Lambda=\Gamma=0$. Such a dynamical regime corresponds to the unperturbed time evolution. As Λ is made nonvanishing, the dynamics becomes more and more complicated until the condition $|\Lambda| \gg |\Omega|$ is reached. In such a situation, the dynamics of the lowest level is frozen, and this is just the continuous measurement quantum Zeno effect already recalled. Once Γ is also adjusted as a nonvanishing coupling constant, an unexpected phenomenon does happen: as $|\Gamma|$ grows up, the effect due to the strong coupling Λ between the second and the third levels becomes relatively weaker and weaker, up to the point, identified by the condition $|\Gamma| \gg |\Lambda|$, wherein the original Rabi oscillations are completely restored. In agreement with Refs. [10,18], one can interpret Λ and Γ couplings as "continuous" measurements so that it is possible to give the following *metaphorical* statement: "a watched pot never boils" ($|\Lambda| \gg \Omega$, $\Gamma=0$) but "a watched cook can freely watch a boiling pot" ($|\Lambda| \gg |\Omega|$, $|\Gamma| \gg |\Lambda|$) [10].

In passing, we mention the fact that the *hierarchical chain* of interactions in principle may be *extended* (with further rings), maintaining the same substantial features: the last ring of the chain is able to destroy the effects of the previous one depending on how the relevant coupling strengths compare to each other. For instance we could add a fifth level and a fourth coupling involving the fourth and fifth levels. In this way, we obtain a 5×5 tridiagonal matrix. In concomitance with an increase of the fourth coupling strength, the hindering of inhibition given by the third coupling (Γ) is hindered.

C. Low-, high-, and bandpass bosonic filters

Let us now come back to our original framework and consider the case when the master system is a three-level system and the slave is a harmonic oscillator. Assume that the unitary *M-S* evolution is induced by the Hamiltonian

$$\hat{H}_\Lambda = \Omega[f_p^{g1}(\hat{a}^\dagger\hat{a})\hat{a}^p|e_1\rangle\langle g| + \text{H.c.}] + \Lambda[f_q^{12}(\hat{a}^\dagger\hat{a})\hat{a}^q|e_2\rangle\langle e_1| + \text{H.c.}], \tag{18}$$

where p and q are integer numbers related to the specific choice of the laser frequencies (sidebands), Ω and Λ the (real) coupling constants, $\hat{a}$ the harmonic-oscillator annihilation operator (here the notation is such that $\hat{a}^{-s} \equiv \hat{a}^{\dagger s}$ for positive s), while $|g\rangle$, $|e_1\rangle$, and $|e_2\rangle$ are the three atomic states effectively involved in the dynamics. Finally the functions (assumed to be real, for notational simplicity) f_p^{g1} and f_q^{12} are introduced.

Consider the unitary evolution due to $\hat{H}_\Lambda$ in Eq. (18) in the special regime $\Lambda=0$ and $p=0$. Then the repeated detections of the atomic state $|g\rangle$ lead to the standard quantum nondemolition measurements, by which it is possible to extract, i.e., distill, a number state for instance in the context of trapped ions and cavity QED [6,7]. More in detail, denoting by $|n\rangle$ the harmonic-oscillator Fock states, the effective non-

unitary evolution operator acting upon the vibrational state is given by

$$\hat{V}_{\Lambda=0}(\tau) \equiv \langle g|e^{-i\hat{H}_{\Lambda=0}\tau}|g\rangle = \cos[\Omega f_0^{g1}(\hat{a}^\dagger\hat{a})\tau] = \sum_{n=0}^{\infty} \cos[\Omega f_0^{g1}(n)\tau]|n\rangle\langle n|. \tag{19}$$

Since in this case the Fock states are eigenstates of $\hat{V}(\tau)$, we have $|\gamma_n, l\rangle := |n\rangle$. It is possible to choose $\tau = \tau_{\bar{n}}$ such that $\Omega f_0^{g1}(\bar{n})\tau_{\bar{n}} = \pi$. Assuming that for $n \neq \bar{n}$, $f_0^{g1}(n)$ and $f_0^{g1}(\bar{n})$ are incommensurable, the eigenvector $|\bar{n}\rangle \otimes |g\rangle$, and *it only* is preserved by the distillation procedure ($|\cos[\Omega f_0^{g1}(\bar{n})\tau_{\bar{n}}]| = 1$), while all the others are partially destroyed at each master-state detection ($|\cos[\Omega f_p^{g1}(n)\tau_{\bar{n}}]| < 1$ for $n \neq \bar{n}$)). In the context of trapped ions a similar approach is used to realize quantum nondemolition measurements [6,7].

In the case of positive p ($p > 0$), it is possible to realize what is called a low-pass bosonic filter. In fact, one easily obtains

$$\hat{V}_{\Lambda=0}(\tau) = \sum_{n=0}^{p-1} |n\rangle\langle n| + \sum_{n=p}^{\infty} \cos[\Omega_n \tau]|n\rangle\langle n|, \tag{20}$$

with $\Omega_n \equiv \Omega f_p^{g1}(n-p)\sqrt{n!/(n-p)!}$. Unless $\Omega_n \tau = l\pi$ for any n and integer l, one realizes the projector $\Sigma_{n=0}^{p-1}|n\rangle\langle n|$ that filters those bosonic states characterized by excitation numbers lower than p. In the context of trapped ions, a strategy based on a coupling of the form in Eq. (18) with $p=1$ is used to realize the so-called resolved sideband cooling [6,14].

Consider now the effect of the freezing agent, i.e., assume that $\Lambda \neq 0$. In this case the total Hamiltonian $\hat{H}_\Lambda$ is substantially characterized by the three-dimensional invariant subspaces $\{|n\rangle \otimes |g\rangle, |n-p\rangle \otimes |e_1\rangle, |n-p-q\rangle \otimes |e_2\rangle\}$, wherein the operator may be represented as a 3×3 block of the form

$$\Xi_n = \begin{pmatrix} 0 & \Omega_n & 0 \\ \Omega_n^* & 0 & \Lambda_n \\ 0 & \Lambda_n^* & 0 \end{pmatrix}, \tag{21}$$

with $\Omega_n = \Omega f_p^{g1}(n-p)\sqrt{n!/(n-p)!}$ as before and $\Lambda_n = \Lambda f_q^{12}(n-p-q)\sqrt{(n-p)!/(n-p-q)!}$. Of course, depending on p and q, which are assumed to be non-negative here, there could exist also invariant doublets and singlets. For instance, in correspondence to $n-p<0$ there are singlets, while if $n-p \geqslant 0$ and $n-p-q<0$ there are doublets.

It is straightforward to evaluate the nonunitary operator $\hat{V}_\Lambda \equiv \langle g|e^{-i\hat{H}_\Lambda \tau}|g\rangle$. In particular, in the case $p=0$ (previously analyzed in the absence of a freezing agent) and positive q, we obtain

$$\hat{V}_\Lambda(\tau) = \sum_{n=0}^{q-1} \cos[\Omega f_0^{g1}(n)\tau]|n\rangle\langle n| + \sum_{n=q}^{\infty} \frac{|\Lambda_n|^2 + |\Omega_n|^2\cos(\omega_n\tau)}{|\Lambda_n|^2 + |\Omega_n|^2}|n\rangle\langle n| \tag{22}$$

with $\omega_n = \sqrt{|\Lambda_n|^2 + |\Omega_n|^2}$. The operator is diagonal in the Fock basis.

In the dynamical regime characterized by $\Lambda \gg \Omega$, $p=0$, if we assume that $f_q^{12}(n-q) \neq 0$ for all Fock states and that the functions f_0^g, f_q^{12} are of the same order, an inequality $|\Lambda_n| \gg |\Omega_n|$ holds $\forall n$. If the measurement interval τ is not fine tuned, i.e., $\tau \neq \tau_0^{(k)}, \tau_1^{(k)}, \ldots, \tau_{q-1}^{(k)}$, $\forall$ integer k, where $\tau_j^{(k)}$ satisfies $\Omega f_0^{g1}(j)\tau_j^{(k)} = k\pi$, all Fock states with an excitation number less than q are eliminated in the course of repeated measurements, hence realizing the projector $\hat{1} - \Sigma_{n=0}^{q-1}|n\rangle\langle n|$, that is, a high-pass filter:

$$[\hat{V}_\Lambda(\tau)]^N \xrightarrow{\text{large } N} \hat{1} - \sum_{n=0}^{q-1} |n\rangle\langle n|. \tag{23}$$

We mention that in principle also a bandpass filter is realizable by considering a four-level system as the master. In fact, the Hamiltonian

$$\hat{H}_{\Lambda,\Gamma} = \Omega[f_p^{g1}(\hat{a}^\dagger\hat{a})\hat{a}^p|e_1\rangle\langle g| + \text{H.c.}] + \Lambda[f_q^{12}(\hat{a}^\dagger\hat{a})\hat{a}^q|e_2\rangle\langle e_1| + \text{H.c.}] + \Gamma[f_r^{23}(\hat{a}^\dagger\hat{a})\hat{a}^r|e_3\rangle\langle e_2| + \text{H.c.}], \tag{24}$$

with $p=0$ and positive q and r, yields, for $|\Gamma| \gg |\Lambda| \gg |\Omega|$, the nonunitary operator

$$\hat{V}_{\Lambda,\Gamma}(\tau) \approx \sum_{n=0}^{q-1} \cos[\Omega f_0^{g1}(n)\tau]|n\rangle\langle n| + \sum_{n=q}^{q+r-1} \frac{|\Lambda_n|^2 + |\Omega_n|^2\cos(\omega_n\tau)}{|\Lambda_n|^2 + |\Omega_n|^2}|n\rangle\langle n| + \sum_{n=q+r}^{\infty} \cos[\Omega f_0^{g1}(n)\tau]|n\rangle\langle n|. \tag{25}$$

The third sum in Eq. (25) involves just $\cos[\Omega f_0^{g1}(n)\tau]$ because in the subspace generated by $\{|n\rangle, n=q+r, \ldots, \infty\}$ the unperturbed dynamics is restored due to the action of the third coupling Γ_n ($|\Gamma_n| \gg |\Lambda_n| \gg |\Omega_n|$). Such a condition holds only in the subspaces wherein the third coupling is *effective*, that is, for $n \geqslant q+r$; indeed otherwise $\Gamma_n = 0$.

Under the assumption

$$\tau \neq \tau_0^{(k)}, \tau_1^{(k)}, \ldots, \tau_{q-1}^{(k)}, \tau_{q+r}^{(k)}, \ldots, \tau_\infty^{(k)}, \tag{26}$$

we obtain a bandpass filter

$$[\hat{V}_{\Lambda,\Gamma}(\tau)]^N \xrightarrow{\text{large } N} \sum_{n=q}^{q+r-1} |n\rangle\langle n|. \tag{27}$$

Although the condition in Eq. (26) may seem too strong, it actually is not. In fact, taking account of the fact that in practical situations, for instance in trapped ions and in cavity QED, one deals with bosonic states with a finite

number of excitations, it would be sufficient to consider the condition up to a large but finite number $\bar{n}$: $\tau \neq \tau_0^{(k)}, \tau_1^{(k)}, \ldots, \tau_{q-1}^{(k)}, \tau_{q+r}^{(k)}, \ldots, \tau_{\bar{n}}^{(k)}$.

IV. APPLICATIONS IN TRAPPED IONS AND CONCLUDING REMARKS

Some of the applications reported in the previous sections may be realized in the context of trapped ions. As is well known, a time-dependent quadrupolar electric field is able to confine a charged particle, providing an effective quadratic potential that induces a harmonic motion [19,20]. When the confined particle is an ion, the complete result is a compound system possessing both fermionic and bosonic degrees of freedom, the first ones describing the internal motion of the electrons with respect to the atomic nucleus, the second ones describing the ion center-of-mass motion. In most of the experiments, only a few atomic states are really involved in the dynamics and a single vibrational mode is considered. Following Ref. [21], it is possible to realize an experimental setup which involves, in the dynamics, only the following three atomic levels of $^9Be^+$: $|g\rangle := |^2S_{1/2}, F=1, m_F=1\rangle$, $|e_1\rangle := |^2S_{1/2}, F=2, m_F=2\rangle$, $|e_2\rangle := |^2S_{1/2}, F=2, m_F=1\rangle$, using a magnetic field of 1 mT to obtain the useful level splittings $[\omega(e_2)-\omega(e_1) \approx 100$ MHz, $\omega(e_1)-\omega(g) \approx 1$ GHz$]$, and exploiting the auxiliary level $|^2P_{1/2}, F=2, m_F=2\rangle$ to realize Raman coupling schemes.

Consider now the action of two effective (i.e., implemented via Raman schemes) lasers, one tuned to the pth red sideband of the atomic transition $|g\rangle \to |e_1\rangle$, and the other to the qth red sideband of the atomic transition $|e_1\rangle \to |e_2\rangle$. The relevant interaction-picture Hamiltonian in the rotating wave approximation is given by [15,21]

$$\hat{H}_\Lambda = \Omega[f_p(\hat{a}^\dagger\hat{a}, \eta_1)\hat{a}^p|e_1\rangle\langle g| + \text{H.c.}] + \Lambda[f_q(\hat{a}^\dagger\hat{a}, \eta_2)\hat{a}^q|e_2\rangle\langle e_1| + \text{H.c.}], \tag{28}$$

where integers p and q are related to the specific choice of the laser frequencies (sidebands), the coupling constants Ω and Λ are proportional to the laser intensities, the relevant Lamb-Dicke parameters η_j $(j=1,2)$ express the ratio between the vibrational ground state oscillation amplitudes and the laser wavelengths, and $\hat{a}$ is the harmonic-oscillator annihilation operator (here the notation is the same as before). The functions f_p and f_q express nonlinear vibrational energy dependence of vibronic couplings [15],

$$f_s(\hat{a}^\dagger\hat{a}, \eta) \equiv e^{-\eta^2/2}\sum_{l=0}^{\infty}\frac{(i\eta)^{2l}}{l!(l+s)!}\hat{a}^{\dagger l}\hat{a}^l = e^{-\eta^2/2}\sum_{n=0}^{\infty}\frac{n!}{(n+s)!}L_n^{(s)}(\eta^2)|n\rangle\langle n|, \tag{29}$$

where $L_n^{(s)}(\eta^2)$ are Laguerre polynomials and are such that for very small Lamb-Dicke parameters [the so-called Lamb-Dicke limit (LDL)], they almost approach unity, while for larger values of η they exhibit a strong nonlinearity in the *variable* $\hat{a}^\dagger\hat{a}$, and possess some zeros. In the LDL, the condition $|\Lambda| \gg |\Omega|$ yields the inequality $|\Lambda_n| \gg |\Omega_n|$, making possible the realization of the high-pass filter.

In conclusion, in this paper we have addressed the general problem of how to project a quantum system in a prefixed subspace, or, in other words, we have described a way to realize the action of a projection operator. We have utilized the distillation approach based upon repeated measurements on a part of a bipartite system [3]. Moreover we have taken account of the possibility of exploiting the generalized quantum Zeno effect, or quantum Zeno dynamics, as a control mechanism of the two-subsystem-interaction determining the target subspace. Our main result is therefore that the presence of such a control mechanism transforms the original distillation process into a *driven distillation*. This allows the realization of what we have called high-, low-, and bandpass bosonic filters, that is, the realization of projection operators on subspaces whose states possess excitation numbers higher or lower than a quantity, or in a range, respectively.

Concerning the efficiency of the process, we stress the fact that the distillation here reported through all the applications considered (satisfying the condition $\gamma=1$) practically realizes (simulates) a measurement on the slave projecting the slave system onto a subspace with a probability, given by Eq. (7), which is just the probability of finding the target slave subspace in the initial slave state. Therefore, the efficiency of the procedure is not improved since it is intrinsically related to the initial condition of the system. Our analysis has indeed the merit of providing a more transparent understanding of the process, clarifying the relation with the survival probabilities, and hence the possibility of governing it.

We conclude by emphasizing that the method and the idea presented in this paper are general and exploitable in different physical contexts for both fundamental and technological research.

ACKNOWLEDGMENTS

This work is partly supported by the bilateral Italian-Japanese Project No. 15C1 on "Quantum Information and Computation"of the Italian Ministry for Foreign Affairs, by a Grant for the 21st Century COE Program (Physics of Self-Organization Systems) at Waseda University and a Grant-in-Aid for Priority Areas Research (B) (No. 13135221), both from the Ministry of Education, Culture, Sports, Science and Technology, Japan, and by a Grant-in-Aid for Scientific Research (C) (No. 14540280) from the Japan Society for the Promotion of Science. Moreover, the authors acknowledge partial support from Palermo University in the context of the bilateral agreement between Palermo University and Waseda University.

APPENDIX: EFFICIENCY

In this appendix we prove the limit expressed by Eq. (7). Assume that the system is prepared, for simplicity, in the pure state $|\psi_0\rangle = |\varphi\rangle|\phi_0\rangle$, $|\varphi\rangle$ being the initial slave state. The probability of finding the master system in $|\phi_0\rangle$ after the unitary M-S interaction is $\wp_1^{(M)} = \|\langle\phi_0|e^{-iH\tau}|\psi_0\rangle\|^2$

$=\|\hat{V}(\tau)|\varphi\rangle\|^2$, where $\|\cdot\|^2 \equiv |\langle\cdot|\cdot\rangle|^2$ denotes the relevant Hilbert space norm. The collapsed state is $|\psi_1\rangle=(1/\sqrt{\wp_1}) \times[\hat{V}(\tau)|\varphi\rangle]|\phi_0\rangle$. After the next unitary interaction and measurement one obtains $\wp_2^{(M)}=\|\langle\phi_0|e^{-i\hat{H}\tau}|\psi_1\rangle\|^2 =(1/\wp_1^{(M)})\|[\hat{V}^2(\tau)|\phi\rangle]\|^2$, and $|\psi_2\rangle=(1\sqrt{\wp_1^{(M)}\wp_2^{(M)}}) \times[\hat{V}^2(\tau)|\varphi\rangle]|\phi_0\rangle$.

In general the probability $\wp_n^{(M)}$ is given by

$$\wp_n^{(M)}=\frac{1}{\wp_0^{(M)}\wp_1^{(M)}\cdots\wp_{n-1}^{(M)}}\|\hat{V}^n(\tau)|\varphi\rangle\|^2 \tag{A1}$$

and the state $|\psi_n\rangle$ reads as

$$|\psi_n\rangle=\frac{1}{\sqrt{\wp_0^{(M)}\wp_1^{(M)}\cdots\wp_n^{(M)}}}\hat{V}^n|\varphi\rangle|\phi_0\rangle. \tag{A2}$$

From Eq. (A1) it follows that

$$\prod_{k=1}^{N}\wp_k^{(M)}=\wp_N^{(M)}\prod_{k=1}^{N-1}\wp_k^{(M)}=\|\hat{V}^N(\tau)|\varphi\rangle\|^2. \tag{A3}$$

Considering large enough N, corresponding to which $\hat{V}^N(\tau) \to \gamma^N\hat{R}^N\hat{P}_{\text{dist}}$ [compare with Eq. (5)], we easily obtain

$$\prod_{k=1}^{N}\wp_k^{(M)}\approx\gamma^N\|\hat{P}_{\text{dist}}|\varphi\rangle\|^2 \tag{A4}$$

which in the case $\gamma=1$ expresses the same content as that of Eq. (7).

The result is of course the same as Eq. (7) even if we start with a nonpure state.

[1] C. H. Bennett *et al.*, Phys. Rev. Lett. **76**, 722 (1996); **78**, 2031(E) (1997); Phys. Rev. A **54**, 3824 (1996); J. I. Cirac, A. K. Ekert, and C. Macchiavello, Phys. Rev. Lett. **82**, 4344 (1999). See also Refs. [2] and references therein.

[2] For reviews, see A. Galindo and M. A. Martin-Delgado, Rev. Mod. Phys. **74**, 347 (2002); *The Physics of Quantum Information*, edited by D. Bouwmeester, A. Ekert, and A. Zeilinger, (Springer, Berlin, 2000); M. A. Nielsen and I. L. Chuang, *Quantum Computation and Quantum Information* (Cambridge University Press, Cambridge, U.K., 2000).

[3] H. Nakazato, T. Takazawa, and K. Yuasa, Phys. Rev. Lett. **90**, 060401 (2003).

[4] V. B. Braginsky and F. Ya. Khalili, *Quantum Measurement* (Cambridge University Press, Cambridge, U. K., 1992).

[5] D. F. Walls and G. J. Milburn, *Quantum Optics* (Springer-Verlag, Berlin, 1994).

[6] R. L. de Matos Filho and W. Vogel, Phys. Rev. Lett. **76**, 4520 (1996).

[7] L. Davidovich *et al.*, Phys. Rev. A **54**, 5118 (1996).

[8] K. Wang *et al.*, Phys. Rev. A **63**, 043419 (2001).

[9] H. Nakazato, M. Namiki, and S. Pascazio, Int. J. Mod. Phys. B **10**, 247 (1996); D. Home and M. A. B. Whitaker, Ann. Phys. (N.Y.) **258**, 237 (1997).

[10] P. Facchi and S. Pascazio, Phys. Rev. Lett. **89**, 080401 (2002).

[11] P. Facchi and S. Pascazio, *Quantum Zeno and Inverse Quantum Zeno Effects*, Progress in Optics vol. 42, edited by E. Wolf (Elsevier, Amsterdam, 2001), p. 147.

[12] B. Militello, A. Messina, and A. Napoli, Phys. Lett. A **286**, 239 (2001).

[13] The most general case, in which the standard form (3) is no longer valid, owing to the presence of degenerate eigenvalues, is found in H. Nakazato, M. Unoki, and K. Yuasa, Phys. Rev. A **70**, 012303 (2004).

[14] D. J. Wineland *et al.*, J. Res. Natl. Inst. Stand. Technol. **103**, 259 (1998).

[15] W. Vogel and S. Wallentowitz, in *Coherence and Statistics of Photons and Atoms*, edited by Jan Perina (Wiley, New York, 2001).

[16] D. Leibfried *et al.*, Rev. Mod. Phys. **75**, 281 (2003).

[17] B. Militello and A. Messina, Phys. Rev. A **70**, 033408 (2004).

[18] B. Militello, A. Messina, and A. Napoli, Fortschr. Phys. **49**, 1041 (2001).

[19] P. K. Ghosh, *Ion Traps* (Clarendon Press, Oxford 1995).

[20] P. E. Toschek, in *New Trends in Atomic Physics*, edited by G. Grynberg and R. Stora (Elsevier, Amsterdam, 1984), p. 282.

[21] S. Maniscalco and A. Messina, Fortschr. Phys. **49**, 1027 (2001).

Optics and Spectroscopy, Vol. 99, No. 3, 2005, pp. 438–442. From Optika i Spektroskopiya, Vol. 99, No. 3, 2005, pp. 456–460.

PROBLEMS OF MEASUREMENTS IN QUANTUM OPTICS AND INFORMATICS

Governing Survival Probability to Distill Quantum States[1]

B. Militello*, A. Messina*, and H. Nakazato**

* *INFM, MIUR and Dipartimento di Scienze Fisiche ed Astronomiche dell'Università di Palermo, I-90123 Palermo, Italy*

** *Department of Physics, Waseda University, 169-8555 Tokyo, Japan*

Received October 19, 2004

Abstract—A quantum system interacting with a repeatedly measured one undergoes a nonunitary time evolution pushing it into some specific subspaces. We deeply investigate the origin of the relevant selection rule, bringing to the light its connection with the survival probability related with the two-system interaction. The possibility of inducing an effective dynamics in the distilled subspace just during the distillation process is demonstrated. © *2005 Pleiades Publishing, Inc.*

1. INTRODUCTION

In quantum mechanics, the ability to engineer nonclassical states plays an important role both in the field of applications and for analyzing fundamental aspects of the theory. Methods based upon unitary manipulations, widely used, for instance, in the context of trapped ions [1], are not always efficient enough and, moreover, are very dependent on and sensitive to the initial state. On the contrary, nonunitary processes are able to force the physical system toward a subspace of interest, in some cases, irrespectively of the initial condition [2]. In particular, when a part of a compound system is repeatedly measured, the remaining part, in interaction with the former, undergoes a nonunitary time evolution forcing the system toward a subspace (distillation process) in accordance with a suitable selection rule [2, 3]. This is strictly related with quantum nondemolition measurements [3]. In more detail, introducing the survival probability of a quantum state under the unitary evolution associated with the interaction between the two parts of the system, one can say that the nonunitary transformation preserves the subspace generated by those states exhibiting the highest survival probability in the unitary evolution between two measurement acts.

In this paper, we shall discuss how to govern such survival probabilities in order to direct the distillation toward a desired subspace. Moreover, we show that it is possible to induce an effective dynamics as a part of the distillation process itself.

The paper is organized as follows. In the next section, the effect of repeated measurements on a part of a compound system is reported. Distillation and the relevant selection rule are discussed. In the third section, we show how to govern the distillation through the quantum Zeno dynamics, while, in the fourth section, we report the induced effective dynamics. Finally, some concluding remarks are made.

[1] The text was submitted by the authors in English.

2. REPEATED MEASUREMENTS OF A PART OF A COMPOUND SYSTEM

Consider a compound physical system made of two parts, called the master, or M, and the slave, or S, in interaction with each other. Let us denote by $\hat{U}(\tau)$ the unitary evolution due to the master–slave interaction, and let the master be repeatedly measured and found always in the same state $|\Phi_0\rangle$. Assume, moreover, that the time interval between two measurement acts is constant, and denote it by τ. After N such measurements, the compound system evolves in accordance with the operator [2]

$$\hat{W}^{(N)}(\tau) \equiv \aleph_N[|\Phi_0\rangle\langle\Phi_0|\hat{U}(\tau)]^N|\Phi_0\rangle\langle\Phi_0|$$
$$= \aleph_N|\Phi_0\rangle\langle\Phi_0|[\hat{V}(\tau)]^N,$$

where we have introduced the nonunitary operator

$$\hat{V}(\tau) \equiv \langle\Phi_0|\hat{U}(\tau)|\Phi_0\rangle \quad (1)$$

acting on the slave Hilbert space. The quantity $\aleph_N$ is a suitable normalization constant introduced as a consequence of the repeated wave function collapses (projections). The evolution of the master is trivial, being nothing but the projection onto $|\Phi_0\rangle$. The nontrivial stepwise evolution of the slave is instead governed by the Nth power of $\hat{V}(\tau)$.

A. Distillation

Assuming that the spectral decomposition of the above nonunitary operator

$$\hat{V}(\tau) = \sum_k \gamma_k \hat{P}_k \quad (2)$$

is possible, γ_k and $\hat{P}_k$ being the generic eigenvalue and relevant eigenprojector, respectively, it easily turns out

that $\hat{V}^N(\tau)$, for large enough N, approaches, up to a unitary transformation, the projection operator onto the subspace generated by the eigenstates of $\hat{V}(\tau)$ corresponding to the eigenvalues with maximum modulus. In fact,

$$\hat{W}^{(N)}(\tau) \longrightarrow \aleph_N|\Phi_0\rangle\langle\Phi_0| \sum_{k:\,|\gamma_k|=\gamma} \gamma_k^N \hat{P}_k \equiv \aleph_N|\Phi_0\rangle\langle\Phi_0|\gamma^N e^{-i\hat{G}N\tau} \sum_{k:\,|\gamma_k|=\gamma} \hat{P}_k, \tag{3}$$

where $\gamma = \max_k\{|\gamma_k|\}$ and $\hat{G}$ is a Hermitian operator possessing nonvanishing matrix elements only in the "distilled" subspace $\hat{P}_{\text{dist}} \equiv \sum_{k:\,|\gamma_k|=\gamma} \hat{P}_k$, that is, $\hat{G} = \hat{P}_{\text{dist}}\hat{G}\hat{P}_{\text{dist}}$. Hence, the sketched process, where the master is repeatedly found in the state $|\Phi_0\rangle$ and is interacting with the slave, is a practical realization of a projection operator, up to a unitary transformation eventually approaching a trivial phase accumulation if the condition $\hat{G} \propto \hat{P}_{\text{dist}}$ is fulfilled. It is worth remarking that the procedure presented is a conditional one in the sense that it is based upon the success of the N measurement acts performed on the master. In more detail, it is possible to prove that such a probability of success (that is, the probability $\wp_N$ of finding M in $|\Phi_0\rangle$ in all N steps) for large enough N approaches the probability of finding the distilled subspace in the initial state, that is,

$$\wp_N \longrightarrow \mathrm{Tr}\{\hat{P}_{\text{dist}}\hat{\rho}_0\}, \tag{4}$$

$\hat{\rho}_0 \otimes |\Phi_0\rangle\langle\Phi_0|$ being the initial state of the compound system. Furthermore, we mention that the assumption of spectral decomposition given in Eq. (2) is crucial for our proposal and we shall consider only this case in the following.

B. The Selection Rule

It is possible to give a selection rule forecasting the surviving states at the end of the distillation processes. In fact, they are the eigenstates of $\hat{V}(\tau)$ whose corresponding eigenvalues have maximum modulus in the spectrum. Let us go through the physical meaning of such a condition. Denote by $|\gamma_k, l\rangle$ the eigenstates of $\hat{V}(\tau)$, l spanning the degenerate eigenspaces, so that $\hat{P}_k = \sum_{l=1}^{g_k} |\gamma_k, l\rangle\langle\gamma_k, l|$, g_k being the degeneracy of the eigenspace corresponding to γ_k. The unitary operator $\hat{U}(\tau)$ may be cast in the form

$$\hat{U}(\tau) = \sum_{m,k,l} |\Psi_{k,l}^m(\tau)\rangle\langle\gamma_k, l|\langle\Phi_m|, \tag{5}$$

where, by definition, $|\Psi_{k,l}^m(\tau)\rangle \equiv \hat{U}(\tau)|\gamma_k, l\rangle|\Phi_m\rangle$.

Generally, it reads

$$\hat{U}(\tau)|\gamma_k, l\rangle|\Phi_m\rangle = \sum_{m',k',l'} c_{m',k',l'}|\gamma_{k'}, l'\rangle|\Phi_{m'}\rangle. \tag{6}$$

Nevertheless, considering Eqs. (1), (2), and (5), one easily sees that

$$\langle\Phi_0|\Psi_{k,l}^{m=0}(\tau)\rangle = \gamma_k|\gamma_k, l\rangle, \tag{7}$$

from which it is straightforward to deduce

$$\hat{U}(\tau)|\gamma_k, l\rangle|\Phi_0\rangle = \gamma_k|\gamma_k, l\rangle|\Phi_0\rangle + \sum_{\substack{m\neq 0\\ k',l'}} c_{m,k',l'}|\gamma_{k'}, l'\rangle|\Phi_m\rangle. \tag{8}$$

This implies that $c_{m=0,k'\neq k,l'} = 0$, $\forall l'$ and $c_{m=0,k,l} = \gamma_k$. In words, Eq. (8) states that the eigenstates of $\hat{V}(\tau)$, $\{|\gamma_k, l\rangle\}$, are those slave states that possess the following property: if the state of the compound system has initially the form $|\gamma_k, l\rangle|\Phi_0\rangle$, then the total system evolves in such a way that the probability of finding the system in the state $|\gamma_{k'}, l'\rangle|\Phi_0\rangle$ with $k' \neq k$ or $l' \neq l$, after a time interval τ, exactly vanishes, while that relative to the state $|\gamma_{k'}, l'\rangle|\Phi_0\rangle$ is nonzero. In connection with this point, consider that the physical meaning of the generic eigenvalue γ_k is given by the fact that its modulus is nothing but the square root of the survival probability of the state $|\gamma_k, l\rangle|\Phi_0\rangle$ under the unitary evolution $\hat{U}(\tau)$ denoted by $\wp_{kl}(\tau) = |c_{m=0,k,l}|^2$. Finally, the phase of γ_k, denoted by $e^{i\xi_k}$, is the dynamic phase acquired during the time evolution.

Summarizing, the nonunitary operator acting upon the slave system may be cast in the form [4]

$$\hat{V}(\tau) = \sum_{k,l} \sqrt{\wp_k(\tau)}e^{i\xi_k(\tau)}|\gamma_k, l\rangle\langle\gamma_k, l|, \tag{9}$$

throwing a bridge between unitary and nonunitary survival probabilities. In fact, the distilled states are just those whose unitary survival probabilities related to $\hat{U}(\tau)$ are the largest. This is a crucial point of our further discussion, providing the key for inventing a strategy of distillation steering through the control of unitary survival probabilities.

3. GOVERNING SURVIVAL PROBABILITY

It is well known that the quantum Zeno effect is in general an effective tool for controlling survival probabilities [5]. In particular, we shall deal with the so-called quantum Zeno dynamics, wherein an interaction, which may be thought of as an "observation" [5], is

able to hinder the effect of another one. To better understand this point, let us analyze an interaction model between a three-level system and a harmonic oscillator. Let our three-level system versus harmonic oscillator interaction be given by [6]

$$\begin{aligned}\hat{H}_{\Omega,K} &= \Omega[f_p^{(1)}(\hat{a}^\dagger\hat{a})\hat{a}^p|g\rangle\langle e_1| + \text{h.c.}] \\ &+ K[f_q^{(2)}(\hat{a}^\dagger\hat{a})\hat{a}^q|e_1\rangle\langle e_2| + \text{h.c.}],\end{aligned} \tag{10}$$

p and q being positive integers; Ω and K, coupling strengths; $f_p^{(1)}$ and $f_q^{(2)}$, functions of the oscillator number operator $\hat{a}^\dagger\hat{a}$; and $|g\rangle$, $|e1\rangle$, and $|e2\rangle$, the three states of the system. It is easy to prove that the Hamiltonian possesses invariant triplets involving the states $\{|n, g\rangle, |n+p, e1\rangle, |n+p+q, e2\rangle\}$, where $|n, \sigma\rangle \equiv |n\rangle \otimes |\sigma\rangle$, $|n\rangle$ being a number state of the oscillator and $\sigma = g$, $e1$, $e2$. The Hamiltonian restricted in such a three-dimensional subspace is denoted by $\Xi_n(\hat{H}_{\Omega,K})$ and has a tridiagonal structure; i.e.,

$$\Xi_n(\hat{H}_{\Omega,K}) = \begin{pmatrix} 0 & \Omega_n & 0 \\ \Omega_n^* & 0 & K_n \\ 0 & K_n^* & 0 \end{pmatrix}, \tag{11}$$

where $\Omega_n = \Omega f_p^{(1)}(n)\sqrt{(n+p)!/n!}$, $K_n = K f_q^{(2)}(n+p)\sqrt{(n+p+q)!/(n+p)!}$.

Subspace by subspace, the interaction involving the levels $|e1\rangle$ and $|e2\rangle$ may be thought of as an observer [5] revealing the population of the level $|e1\rangle$ through transitions $|e1\rangle \longrightarrow |e2\rangle$. The stronger such an observation (that is, the matrix element K_n), the more the dynamics induced by the coupling between $|g\rangle$ and $|e1\rangle$ is hindered. In other words and apart from any philosophical interpretation addressing a coupling as an observation, K_n gives a control mechanism for the survival probability of the state $|n, g\rangle$. In fact, preparing the system in the state $|n, g\rangle$, the time evolution is such that [6]

$$\left|\langle n, g|e^{-i\hat{H}_{\Omega,K}\tau}|n, g\rangle\right|^2 = \left|\frac{|K_n|^2 + |\Omega_n|^2\cos(\omega_n\tau)}{|K_n|^2 + |\Omega_n|^2}\right|^2. \tag{12}$$

In particular, if $|\Omega_n| \ll |K_n|$, the state $|n, g\rangle$ approaches an eigenstate of $\hat{H}_{\Omega,K}$ and, hence, its evolution becomes more and more hindered. Indeed, its survival probability approaches unity. Hence, one has at one's disposal a mechanism of control of the survival probabilities.

Assume now that, at time interval τ, the three-level system is repeatedly measured and found in its ground state, $|g\rangle$. It is straightforward to find the relevant expression for the nonunitary operator acting on the harmonic oscillator Hilbert space

$$\begin{aligned}\hat{V}_{\Omega,K}(\tau) &\equiv \langle g|e^{-i\hat{H}_{\Omega,K}\tau}|g\rangle \\ &= \sum_{n=q}^{\infty}\frac{|K_n|^2 + |\Omega_n|^2\cos(\omega_n\tau)}{|K_n|^2 + |\Omega_n|^2}|n\rangle\langle n|\end{aligned} \tag{13}$$

with $\omega_n = \sqrt{|K_n|^2 + |\Omega_n|^2}$. In this case, all the numbers $\gamma_n = (|K_n|^2 + |\Omega_n|^2\cos(\omega_n\tau))/(|K_n|^2 + |\Omega_n|^2)$ are real providing $\xi_n = 0$, $\forall n$.

The ratio $|\Omega_n|/|K_n|$ may in principle be controlled subspace by subspace, determining which Fock states are preserved by the process. As two examples, consider the following cases. Suppose that, for some $\bar{n}$, it turns out $\Omega_{\bar{n}} \approx 0$, while, for all $n \neq \bar{n}$, $\Omega_n \neq 0$. In this case, the projector $|\bar{n}\rangle\langle\bar{n}|$ is substantially implemented, being $\gamma_{\bar{n}} > \gamma_n$, $\forall n \neq \bar{n}$. On the contrary, assume that $f_q^{(2)}(\bar{n}+p+q) = 0$, so that $K_{\bar{n}} = 0$ (see Eq. (11) and definitions immediately after). In the limit $K \gg \Omega$, in all subspaces except the nth, the condition $|K_n| \gg |\Omega_n|$ is fulfilled, providing the realization of an infinite-dimensional projector $\hat{1} - |\bar{n}\rangle\langle\bar{n}|$, since $\gamma_n \approx 1$ for $n \neq \bar{n}$ and $\gamma_{\bar{n}} \approx \cos\omega_{\bar{n}}\tau$ is generally smaller than unity.

4. INDUCING EFFECTIVE DYNAMICS IN THE DISTILLED SUBSPACE

Up to now, we have dealt with the control of survival probabilities and, hence, of the moduli of eigenvalues of $\hat{V}(\tau)$. In this section, we shall discuss the possibility that the distilled states acquire dynamic phases during the distillation process itself.

In the previous example, no phase is acquired because all $\hat{V}(\tau)$ eigenvalues are real. But consider now the following Hamiltonian:

$$\begin{aligned}\hat{H}_{\Omega,K} &= \omega_g(\hat{a}^\dagger\hat{a})|g\rangle\langle g| + \omega_{e1}(\hat{a}^\dagger\hat{a})|e1\rangle\langle e1| \\ &+ \omega_{e2}(\hat{a}^\dagger\hat{a})|e2\rangle\langle e2| + \Omega[f_p^{(1)}(\hat{a}^\dagger\hat{a})\hat{a}^p|g\rangle\langle e_1| + \text{h.c.}] \\ &+ K[f_q^{(2)}(\hat{a}^\dagger\hat{a})\hat{a}^q|e_1\rangle\langle e_2| + \text{h.c.}],\end{aligned} \tag{14}$$

ω_σ being three diagonal operators in the Fock basis and hence describing three n-dependent energy shifts $\Delta_n^{(\sigma)} \equiv \langle n|\omega_\sigma(\hat{a}^\dagger\hat{a})|n\rangle$, with $\sigma = g$, $e1$, $e2$. Such shifts appear in the generic three-dimensional Hamiltonian invariant block,

$$\Xi_n(\hat{H}_{\Omega,K}) = \begin{pmatrix} \Delta_n^{(g)} & \Omega_n & 0 \\ \Omega_n^* & \Delta_n^{(e1)} & K_n \\ 0 & K_n^* & \Delta_n^{(e2)} \end{pmatrix}. \tag{15}$$

As in the case of the previous section, the dynamics of each Fock state is closed within the three-dimensional invariant subspace and, moreover, involves phase shifts generally different Fock state by Fock state. Therefore, an effective dynamics in the distilled subspace just during the distillation process is indeed provided. Previously, in Eq. (3), such a circumstance was taken into account formally with the addition of the unitary transformation $e^{-i\hat{G}N\tau}$. As an example, consider the case $\Delta_n^{(e1)} = \Delta_n^{(e2)} = 0$. In such a situation, it is straightforward to get, with the help of the first-order perturbative approach, the formula

$$\hat{V}^N_{\Omega,K}(\tau) = \sum_{n:\left[\left|\frac{\Omega_n}{K_n}\right| \ll 1\right]} e^{-i\Delta_n^{(g)}N\tau}|n\rangle\langle n|, \tag{16}$$

provided $\Delta_n^{(g)} \ll |\Omega_n| \ll |K_n|$. The corresponding effective unitary dynamics in the distilled subspace is then generated by $\hat{G} = \hat{P}_{\text{dist}}\,\omega_g(\hat{a}^\dagger\hat{a})\hat{P}_{\text{dist}}$.

Such a result is strictly connected with the fact that, in the distilled subspace, the corrections to the moduli of the eigenvalues with respect to unity are of higher order in the infinitesimal quantities $\left|\Delta_n^{(g)}/\Omega_n\right|$ and $|\Omega_n/K_n|$ than the corrections to the corresponding phases. Hence, restricting our attention to the distilled subspace and retaining terms up to the order of the phase corrections, the $\hat{V}(\tau)$ eigenvalues may be thought of as just phase factors.

To better understand this point, it is instructive to consider the case $\Delta_n^{(g)} = \Delta_n^{(e2)} = 0$ and $\Delta_n^{(e1)} \ll |\Omega_n| \ll |K_n|$. In such a case, considering terms up to the second order in the two infinitesimal quantities $\left|\Delta_n^{(e1)}/\Omega_n\right|$ and $|\Omega_n/K_n|$, one obtains

$$\hat{V}^N_{\Omega,K}(\tau) = \sum_{n:\left[\left|\frac{\Omega_n}{K_n}\right| \ll 1\right]} |\gamma_n|^N e^{-iN\xi_n}|n\rangle\langle n|, \tag{17}$$

where

$$\begin{cases} |\gamma_n| = 1 + \left|\dfrac{\Omega_n}{K_n}\right|^2\left[\cos\dfrac{\Delta_n^{(e1)}\tau}{2}\cos(|K_n|\tau) - 1\right], \\ \xi_n = \left|\dfrac{\Omega_n}{K_n}\right|^2 \sin\dfrac{\Delta_n^{(e1)}\tau}{2}\cos(|K_n|\tau). \end{cases} \tag{18}$$

Differently from the previous situation, in this case both the correction to the moduli and that to the phases accumulated are second-order infinitesimals. Therefore, claiming well visible induced dynamics, i.e., appreciable phases, implies significant moduli corrections too. In particular, the states accumulating large enough phases are just those losing a nonnegligible amount of probability. Hence, we can assert that, in this situation, it is not possible to claim a unitary evolution in the distilled subspace.

5. DISCUSSION AND CONCLUSIONS

Summarizing, by repeatedly measuring a part of a compound system, it is possible to force the remaining part of the system toward pre-fixed subspaces. These elect subspaces correspond to the states possessing the highest survival probability related to the unitary evolution $\hat{U}(\tau)$ induced by the interaction between the two parts of the compound system. On the basis of such considerations, the result of the distillation process may be governed by exploiting the quantum Zeno dynamics in order to suitably adjust the survival probabilities related to the unitary evolution. Moreover, we have shown that it is possible to induce an effective dynamics during the distillation process, hence in principle performing simultaneously a projection into a subspace and a quantum state coherent manipulation. Concerning the realizability of the survival probability control, we mention that trapped ions provide a good platform for engineering such kinds of processes. In connection with our purpose, it is possible to consider an experimental setup involving in the dynamics only the three atomic levels [7] $|g\rangle := |^2S_{1/2}, F = 1, m_F = 1\rangle$, $|e_1\rangle := |^2S_{1/2}, F = 2, m_F = 2\rangle$, $|e_2\rangle := |^2S_{1/2}, F = 2, m_F = 1\rangle$, using a magnetic field of 1 mT to obtain a level splitting of about 100 MHz between the two excited levels and about 1 GHz between the ground and the first excited states. The auxiliary level $|^2P_{1/2}, F = 2, m_F = 2\rangle$ is exploited to realize Raman coupling schemes. Acting upon the system through two laser fields, one tuned to the atomic transition frequency between $|g\rangle$ and $|e1\rangle$ and the other to the frequency between $|e1\rangle$ and $|e2\rangle$, it is possible to realize the coupling in Eq. (10). The weak coupling between the trapped ion and its environment generally allows one to neglect decoherence for a long enough time, making realistic enough the previous discussion in this context. In conclusion, we mention our feeling that the method proposed in this paper for governing distillation processes and for eventually inducing effective dynamics in the meanwhile can be improved using the more general hierarchically controlled dynamics [8, 9] instead of the quantum Zeno dynamics, up to the point of distilling single quantum states practically at will.

ACKNOWLEDGMENTS

This work was partly supported by the bilateral Italian–Japanese project 15C1 on "Quantum Information and Computation" of the Italian Ministry for Foreign Affairs; by a grant for the 21st Century COE Program (Physics of Self-Organization Systems) at Waseda Uni-

versity and a Grant-in-Aid for Priority Areas Research (B) (no. 13135221), both from the Ministry of Education, Culture, Sports, Science and Technology, Japan; and by a Grant-in-Aid for Scientific Research (C) (no. 14540280) from the Japan Society for the Promotion of Science.

REFERENCES

1. D. Leibfried *et al.*, Rev. Mod. Phys. **75**, 281 (2003); W. Vogel and S. Wallentowitz, *Coherence and Statistics of Photons and Atoms*, Ed. by Jan Perina (Wiley, New York, 2001); D. J. Wineland *et al.*, J. Res. Natl. Inst. Stand. Technol. **103**, 259 (1998).
2. H. Nakazato, T. Takazawa, and K. Yuasa, Phys. Rev. Lett. **90**, 060401 (2003).
3. V. B. Braginsky and F. Ya. Khalili, *Quantum Measurement* (Cambridge University Press, 1992); D. F. Walls and G. J. Milburn, *Quantum Optics* (Springer-Verlag, Berlin, 1994); R. L. de Matos Filho and W. Vogel, Phys. Rev. Lett. **76**, 4520 (1996); L. Davidovich *et al.*, Phys. Rev. A **54**, 5118 (1996).
4. B. Militello, H. Nakazato, and A. Messina, Phys. Rev. A **71**, 032102 (2005).
5. P. Facchi and S. Pascazio, Prog. Opt. **42**, 147 (2001); H. Nakazato, M. Namiki, and S. Pascazio, Int. J. Mod. Phys. B **10**, 247 (1996); D. Home and M. A. B. Whitaker, Ann. Phys. **258**, 237 (1997); P. Facchi and S. Pascazio, Phys. Rev. Lett. **89**, 080 401 (2002).
6. B. Militello, A. Messina, and A. Napoli, Fortschr. Phys. **49**, 1041 (2001); Phys. Lett. A **286**, 239 (2001).
7. S. Maniscalco and A. Messina, Fortschr. Phys. **49**, 1027 (2001).
8. B. Militello, A. Messina, and A. Napoli, Fortschr. Phys. **49**, 1041 (2001).
9. P. Facchi and S. Pascazio, Phys. Rev. Lett. **89**, 080401 (2002).

Progress of Theoretical Physics, Vol. 114, No. 3, September 2005

A Simple Scheme to Entangle Distant Qubits from a Mixed State via an Entanglement Mediator

Kazuya YUASA*) and Hiromichi NAKAZATO**)

Department of Physics, Waseda University, Tokyo 169-8555, Japan

(Received November 29, 2004)

A simple scheme to prepare an entanglement between two separated qubits from a given mixed state is proposed. A single qubit (entanglement mediator) is repeatedly made to interact locally and consecutively with the two qubits through rotating-wave couplings and is then measured. It is shown that we need to repeat this kind of process only three times to establish a maximally entangled state directly from an arbitrary initial mixed state, with no need to prepare the state of the qubits in advance or to rearrange the setup step by step. Furthermore, the maximum yield realizable with this scheme is compatible with the maximum entanglement, provided that the coupling constants are properly tuned.

Entanglement is one of the peculiar concepts in quantum physics. It shows a nonlocal property of quantum mechanics, and is the essence of nonclassical phenomena. This concept is now regarded as a key to moving beyond classical ideas and plays a central role in the field of quantum information and computation.[1),2)] The peculiarity of entanglement reveals itself especially when it involves spatially separated systems. Nonlocality has been studied in such situations,[3)] and such an entanglement is of fundamental importance in quantum communication, for example, quantum teleportation.[1),2)]

Practically speaking, an important problem is how to prepare an entanglement between distant parties, and it has been studied for decades.[4)–8)] In particular, it is often required to prepare such an entanglement from a (naturally) given state, which is in general a mixed state. Entanglement distillation[2),9),10)] is therefore an important topic in this context.

A novel mechanism for driving a quantum system from an arbitrary mixed state to a pure state, which makes use of Zeno-like measurements,[11),12)] was discovered recently. This mechanism is that responsible for the following types of behavior: A series of repeated measurements applied to a quantum system can (asymptotically) drive a second system that interacts with the first one into a pure state, even if the second system is initially in an arbitrary mixed state.***) This provides us with useful procedures for preparing an entanglement between qubits, initialization

*) E-mail: yuasa@hep.phys.waseda.ac.jp

**) E-mail: hiromici@waseda.jp

***) Measurements play an important role in the scheme proposed in Refs. 11)–13), and in this regard, the mechanism discussed here seems to be closely related to the so-called quantum Zeno effect (QZE).[14)] But this mechanism is quite different, as pointed out in Ref. 11): In contrast to the fact that a small time interval between measurements is required in the QZE, the time intervals in the present scheme need not be small but, rather, are treated as parameters to be adjusted in such a manner to realize an efficient preparation of a pure state.

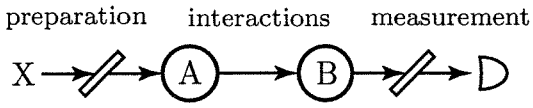

Fig. 1. A scheme for entanglement generation via successive interactions of an entanglement mediator X with qubits A and B.

of multiple qubits, etc.[12),13)] Furthermore, it has been extended in Ref. 15) to a scheme to establish an entanglement between *distant* systems, where measurements are repeated on an "entanglement mediator".

In this article, we point out that further improvement is possible for the scheme proposed in Ref. 15) in the case that a single qubit (entanglement mediator) interacts with each of the two (spatially separated) qubits, between which an entanglement is prepared, through a rotating-wave coupling, which is often discussed in the literature.[4)–7)] We show in the following that it is indeed possible to obtain a maximally entangled state from an arbitrary mixed state *without repeating measurements many times*, if the scheme presented in Ref. 15) is modified properly. In fact, it is found that we actually need only repeat the process (i.e., the interactions of the mediator with the qubits and the measurement of the mediator) three times. Furthermore, the maximum yield attainable in this scheme is shown to be compatible with the maximum entanglement.

We consider two qubits, A and B, which are spatially separated and do not directly interact with each other. In order to make them entangled, another two-level system (the entanglement mediator), X, prepared in a particular state is caused to interact with A and B successively and is measured (Fig. 1). Such entangling schemes are studied in Ref. 5), but there it is assumed that the initial states of the distant qubits A and B are prepared in specific pure states. What we show in the following is that no preparation is necessary for A and B. Indeed, a maximally entangled state can be obtained directly from a given (mixed) state *within the same (fixed) setup*, without introducing other resources or special tunings/arrangements for the initialization of the qubits.

It should be stressed here that the present scheme assumes the application of nonlocal operations of the qubits A and B indirectly through the operations applied to the mediator X, and hence, it is beyond the realm of the entanglement distillation discussed in Refs. 2), 9), 10), etc., which allow only local operations and classical communication.

We assume that the qubits A and B and the entanglement mediator X are two-level systems with a common energy gap Ω and that each qubit interacts separately with the mediator through a rotating-wave coupling. The free evolution of the three systems is hence described by the Hamiltonian*)

$$H_0 = \frac{\Omega}{2}(\sigma_3^{(\mathrm{A})} + \sigma_3^{(\mathrm{B})} + \sigma_3^{(\mathrm{X})}), \tag{1}$$

and while A (B) interacts with X for a time interval $\tau_{\mathrm{A(B)}}$, the total system evolves

*) In this article, we consider the idealized case in which the effect of dissipation is negligible.

according to the Hamiltonian

$$H_0 + H_{\mathrm{XA(B)}}, \tag{2}$$

with

$$H_{\mathrm{XA}} = g_{\mathrm{A}}(\sigma_+^{(\mathrm{X})}\sigma_-^{(\mathrm{A})} + \sigma_-^{(\mathrm{X})}\sigma_+^{(\mathrm{A})}), \tag{3a}$$

$$H_{\mathrm{XB}} = g_{\mathrm{B}}(\sigma_+^{(\mathrm{X})}\sigma_-^{(\mathrm{B})} + \sigma_-^{(\mathrm{X})}\sigma_+^{(\mathrm{B})}). \tag{3b}$$

Here, σ_i $(i = 1, 2, 3)$ are the Pauli operators, and $\sigma_\pm = (\sigma_1 \pm i\sigma_2)/2$ are the ladder operators. The coupling constant $g_{\mathrm{A(B)}}$ between the qubit A (B) and mediator X is assumed to be an adjustable parameter, *but it is fixed throughout the process* described in the following.

It is actually possible to initialize A and B in advance, as required in Ref. 5), without introducing additional resources in the above setup: One can transfer the pure state $|\uparrow\rangle$ of X (which is the eigenstate of the operator σ_3 with eigenvalue $+1$) to A (B) by applying the Hamiltonian (2) for an appropriate time interval $g_{\mathrm{A(B)}}\tau_{\mathrm{A(B)}} = \pi/2$, and the qubits are thereby prepared in the pure state $|\uparrow\uparrow\rangle_{\mathrm{AB}}$. Note, however, that special arrangements of the values of $g_{\mathrm{A}}\tau_{\mathrm{A}}$ and $g_{\mathrm{B}}\tau_{\mathrm{B}}$, which differ from those necessary for entangling qubits maximally, are required solely for this initialization. It is shown that, without rearranging these parameter values but, rather, fixing them throughout the entire process, we can prepare a maximally entangled state directly from a mixed state in the present scheme.

The idea for obtaining an entanglement from an arbitrary mixed state ϱ_{AB} is the following. An important point is that the excitation number of qubits

$$N = \frac{1+\sigma_3^{(\mathrm{A})}}{2} + \frac{1+\sigma_3^{(\mathrm{B})}}{2} + \frac{1+\sigma_3^{(\mathrm{X})}}{2} \tag{4}$$

is a constant of motion, due to the rotating-wave couplings in (3). We first prepare the mediator X in the state $|\uparrow\rangle_{\mathrm{X}}$*) and let it interact with the qubits A and B successively, through the interactions (3a) and (3b) for the time intervals τ_{A} and τ_{B}, respectively. After these consecutive interactions, the state of X is measured to see whether it has flipped down into the state $|\downarrow\rangle_{\mathrm{X}}$. If it has, we know that one and only one of the qubits has certainly flipped from $|\downarrow\rangle$ to $|\uparrow\rangle$, since the excitation number N given in (4) is conserved in this process. This process, that is, the preparation of X in the state $|\uparrow\rangle_{\mathrm{X}}$, the interactions between X and the two qubits A and B, and the projection to $|\downarrow\rangle_{\mathrm{X}}$, entails the following state changes of the initial state ϱ_{AB}:

$$\begin{aligned} |\uparrow\uparrow\rangle_{\mathrm{AB}} \quad & \longrightarrow \quad \text{disappearing}, \\ |\uparrow\downarrow\rangle_{\mathrm{AB}} \ \text{and} \ |\downarrow\uparrow\rangle_{\mathrm{AB}} \quad & \longrightarrow \quad |\uparrow\uparrow\rangle_{\mathrm{AB}}, \\ |\downarrow\downarrow\rangle_{\mathrm{AB}} \quad & \longrightarrow \quad |\uparrow\downarrow\rangle_{\mathrm{AB}} \ \text{or} \ |\downarrow\uparrow\rangle_{\mathrm{AB}}. \end{aligned} \tag{5a}$$

Note that the $|\uparrow\uparrow\rangle_{\mathrm{AB}}$ component of the initial state ϱ_{AB} is eliminated and the $|\downarrow\downarrow\rangle_{\mathrm{AB}}$ sector becomes vacant after the measurement (projection). Next, a second mediator

*) Such a preparation is not very difficult for a particular choice of X. For example, if X is a photon, as discussed below, one can easily prepare its polarization using a polarizer.

X prepared in the state $|\uparrow\rangle_{\mathrm{X}}$ is caused to interact with A and B (not necessarily in the same order as the first process), and it is subsequently confirmed again to be in the state $|\downarrow\rangle_{\mathrm{X}}$. In this second process too, it is possible that the state of only one of the qubits has flipped from $|\downarrow\rangle$ to $|\uparrow\rangle$, and the $|\uparrow\uparrow\rangle_{\mathrm{AB}}$ component has thus been eliminated:

$$\begin{aligned} |\uparrow\uparrow\rangle_{\mathrm{AB}} \quad &\longrightarrow \quad \text{disappearing}, \\ |\uparrow\downarrow\rangle_{\mathrm{AB}} \quad \text{and} \quad |\downarrow\uparrow\rangle_{\mathrm{AB}} \quad &\longrightarrow \quad |\uparrow\uparrow\rangle_{\mathrm{AB}}. \end{aligned} \tag{5b}$$

Now, only the $|\uparrow\uparrow\rangle_{\mathrm{AB}}$ sector is occupied. This was originally the $|\downarrow\downarrow\rangle_{\mathrm{AB}}$ component of the initial state ϱ_{AB}. That is, the state $|\downarrow\downarrow\rangle_{\mathrm{AB}}$ has been extracted from the initial state ϱ_{AB} in the form of $|\uparrow\uparrow\rangle_{\mathrm{AB}}$, and the qubits A and B have thus been driven to the pure state $|\uparrow\uparrow\rangle_{\mathrm{AB}}$ through these two processes. After this "purification", the third mediator X prepared in the state $|\downarrow\rangle_{\mathrm{X}}$ is caused to interact with A and B in a prescribed order, and the state $|\uparrow\rangle_{\mathrm{X}}$ is confirmed. This, in turn, flips one of the qubits (but we do not know which one) from $|\uparrow\rangle$ to $|\downarrow\rangle$,

$$|\uparrow\uparrow\rangle_{\mathrm{AB}} \quad \longrightarrow \quad |\uparrow\downarrow\rangle_{\mathrm{AB}} \quad \text{or} \quad |\downarrow\uparrow\rangle_{\mathrm{AB}}, \tag{5c}$$

and an entanglement between the distant qubits A and B results. Thus, an entanglement can be obtained from an arbitrary mixed state ϱ_{AB} after only three measurements, two for the purification and one for the creation of the entanglement. Also, note that this is done with a fixed parameter set, i.e., without readjusting the interaction strengths for the creation of the entanglement. Furthermore, there is no need to repeat these processes many times. Of course, we still need to optimize the processes in order to create an entanglement efficiently, as is clarified below.

There are several possible recipes for this entanglement preparation, because we have the freedom to choose the order in which the mediator X interacts with the qubits A and B for each process. Actually, there are essentially four combinations of such orders. (We can fix the order of the interactions with the mediator in the last process without loss of generality. Then, we are left with two choices for the first mediator, and two choices for the second.) The important point here is to understand which recipe (i.e., the combination of orders of the interactions) enables us to obtain a highly entangled state with a high yield. In the present scheme described in the preceding paragraph, every one of the three measurements applied to the entanglement mediators extracts the correct outcome, and they therefore produce an entangled state with certainty. This is due to the existence of the conserved quantity N given in (4), according to which all states are classified into four sectors with different values of N, namely $N = 0, 1, 2$, and 3, and to the combination of three measurements (projections), which only one of the sectors survives. However, we still need to clarify which combination of orders is the most efficient one, in the sense that the desired results are realized with high probability, and at the same time, a highly entangled state (i.e., a state whose concurrence[16)] is close to unity) is obtained.

It is elementary to confirm that the optimal preparation of a maximally entangled state is possible via the recipe presented in Fig. 2. In the situation depicted there, an appropriate choice of the parameters $g_{\mathrm{A}}\tau_{\mathrm{A}}$ and $g_{\mathrm{B}}\tau_{\mathrm{B}}$ enables us to obtain a

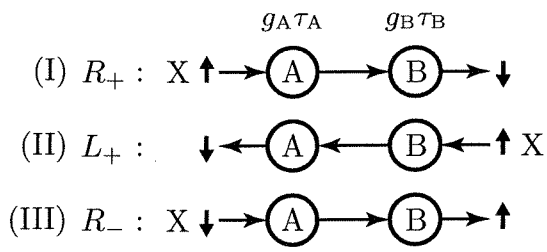

Fig. 2. A recipe for optimal entanglement preparation. The first mediator moves rightward (I), the second one moves leftward (II), and the last one moves rightward (III). (Here, "rightward" means that the interaction between X and A is followed by that between X and B, and "leftward" means that the order is opposite.) If the mediators are found to be in the states indicated in this figure, the processes (I)–(III), represented by the operators R_+, L_+, and R_-, respectively, extract a specific (entangled) state of the qubits A and B. The strength of the interaction between X and A (B) is fixed $g_{A(B)}\tau_{A(B)}$ throughout the processes (I)–(III).

maximally entangled state (with concurrence 1) with the maximum yield realizable in the present scheme. The mediator X is first allowed to travel rightward, that is, to interact with the qubit A and then B. If it is found to be in the state $|\downarrow\rangle_X$ after the interactions with A and B on the right, the state of A and B changes according to

$$\varrho_{AB} \to R_+\varrho_{AB}R_+^\dagger / \mathrm{Tr}_{AB}(R_+\varrho_{AB}R_+^\dagger), \tag{6}$$

where

$$\begin{aligned} R_+ &\equiv {}_X\langle\downarrow|e^{-iH_{XB}\tau_B}e^{-iH_{XA}\tau_A}|\uparrow\rangle_X \\ &= -i\left[s_A\,|\uparrow\rangle_A\langle\downarrow| \otimes \left(|\downarrow\rangle_B\langle\downarrow| + c_B\,|\uparrow\rangle_B\langle\uparrow|\right) + s_B\left(|\uparrow\rangle_A\langle\uparrow| + c_A\,|\downarrow\rangle_A\langle\downarrow|\right) \otimes |\uparrow\rangle_B\langle\downarrow|\right] \end{aligned} \tag{7}$$

in the interaction picture. (Here, $s_A \equiv \sin g_A\tau_A$, $c_A \equiv \cos g_A\tau_A$, etc.) The second and third mediators are translated leftward and rightward, as depicted in Fig. 2, and as a result, the state of the qubits A and B changes further. The relevant operators read

$$\begin{aligned} L_+ &\equiv {}_X\langle\downarrow|e^{-iH_{XA}\tau_A}e^{-iH_{XB}\tau_B}|\uparrow\rangle_X \\ &= -i\left[s_A\,|\uparrow\rangle_A\langle\downarrow| \otimes \left(|\uparrow\rangle_B\langle\uparrow| + c_B\,|\downarrow\rangle_B\langle\downarrow|\right) + s_B\left(|\downarrow\rangle_A\langle\downarrow| + c_A\,|\uparrow\rangle_A\langle\uparrow|\right) \otimes |\uparrow\rangle_B\langle\downarrow|\right] \end{aligned} \tag{8}$$

and

$$\begin{aligned} R_- &\equiv {}_X\langle\uparrow|e^{-iH_{XB}\tau_B}e^{-iH_{XA}\tau_A}|\downarrow\rangle_X \\ &= -i\left[s_A\,|\downarrow\rangle_A\langle\uparrow| \otimes \left(|\uparrow\rangle_B\langle\uparrow| + c_B\,|\downarrow\rangle_B\langle\downarrow|\right) + s_B\left(|\downarrow\rangle_A\langle\downarrow| + c_A\,|\uparrow\rangle_A\langle\uparrow|\right) \otimes |\downarrow\rangle_B\langle\uparrow|\right]. \end{aligned} \tag{9}$$

The sequence of these three processes thereby extracts a state of the qubits A and B as

$$\varrho_{AB} \to \tilde{\varrho}_{AB} = \mathcal{V}\varrho_{AB}\mathcal{V}^\dagger/P, \tag{10a}$$

with the operator

$$\mathcal{V} \equiv R_- L_+ R_+. \tag{10b}$$

Note that we retain only those events for which the correct states are observed on the mediators; other events are discarded. This is why the states (6) and (10) are renormalized, and the normalization constant,

$$P \equiv \mathrm{Tr}_{\mathrm{AB}}(\mathcal{V}\varrho_{\mathrm{AB}}\mathcal{V}^\dagger), \tag{11}$$

is the probability for the entire process depicted in Fig. 2 to be carried out successfully.

The operator $\mathcal{V}$ for this scenario reads

$$\mathcal{V} = 2i\,\mathrm{s_A}\,\mathrm{c_A}\,\mathrm{s_B}\left(\mathrm{c_A}\,\mathrm{s_B}\,|\uparrow\downarrow\rangle_{\mathrm{AB}} + \mathrm{s_A}\,|\downarrow\uparrow\rangle_{\mathrm{AB}}\right)\,{}_{\mathrm{AB}}\langle\downarrow\downarrow|, \tag{12}$$

which clearly shows that it extracts the $|\downarrow\downarrow\rangle_{\mathrm{AB}}$ component of the initial state ϱ_{AB} and converts it into the pure entangled state

$$|\Psi\rangle_{\mathrm{AB}} = \frac{1}{\sqrt{1-\mathrm{c_A^2}\,\mathrm{c_B^2}}}\left(\mathrm{c_A}\,\mathrm{s_B}\,|\uparrow\downarrow\rangle_{\mathrm{AB}} + \mathrm{s_A}\,|\downarrow\uparrow\rangle_{\mathrm{AB}}\right), \tag{13}$$

i.e.,

$$\varrho_{\mathrm{AB}} \to \tilde{\varrho}_{\mathrm{AB}} = |\Psi\rangle_{\mathrm{AB}}\langle\Psi|, \tag{14}$$

and the yield of this entangled state is given by

$$P = 4\,\mathrm{s_A^2}\,\mathrm{c_A^2}\,\mathrm{s_B^2}(1-\mathrm{c_A^2}\,\mathrm{c_B^2})\,{}_{\mathrm{AB}}\langle\downarrow\downarrow|\varrho_{\mathrm{AB}}|\downarrow\downarrow\rangle_{\mathrm{AB}}. \tag{15}$$

The concurrence[16] of the generated entangled state $|\Psi\rangle_{\mathrm{AB}}$ in (13) is readily estimated to be

$$C = \frac{2|\,\mathrm{s_A}\,\mathrm{c_A}\,\mathrm{s_B}\,|}{\mathrm{s_A^2}+\mathrm{c_A^2}\,\mathrm{s_B^2}}, \tag{16}$$

from which we see that C is unity if and only if the parameters $g_{\mathrm{A}}\tau_{\mathrm{A}}$ and $g_{\mathrm{B}}\tau_{\mathrm{B}}$ are adjusted to satisfy the condition

$$\tan^2 g_{\mathrm{A}}\tau_{\mathrm{A}} = \sin^2 g_{\mathrm{B}}\tau_{\mathrm{B}}; \tag{17}$$

i.e., a *maximally* entangled state can be generated by tuning the parameters properly. Furthermore, if they are tuned to satisfy

$$\tan^2 g_{\mathrm{A}}\tau_{\mathrm{A}} = \sin^2 g_{\mathrm{B}}\tau_{\mathrm{B}} = 1, \tag{18}$$

the maximally entangled state is obtained with yield $P = {}_{\mathrm{AB}}\langle\downarrow\downarrow|\varrho_{\mathrm{AB}}|\downarrow\downarrow\rangle_{\mathrm{AB}}$, which is the maximum realizable in the present scheme. This means that the entire component of $|\downarrow\downarrow\rangle_{\mathrm{AB}}$ contained in the initial state ϱ_{AB} is fully extracted and converted into the maximally entangled state $|\Psi\rangle_{\mathrm{AB}}$. Even from the *maximally mixed* state $\varrho_{\mathrm{AB}} = \mathbb{1}_{\mathrm{AB}}/4$, the maximally entangled state $|\Psi\rangle_{\mathrm{AB}}$ can be prepared with a nonvanishing yield, $P = 1/4$. The optimal preparation of the maximally entangled state

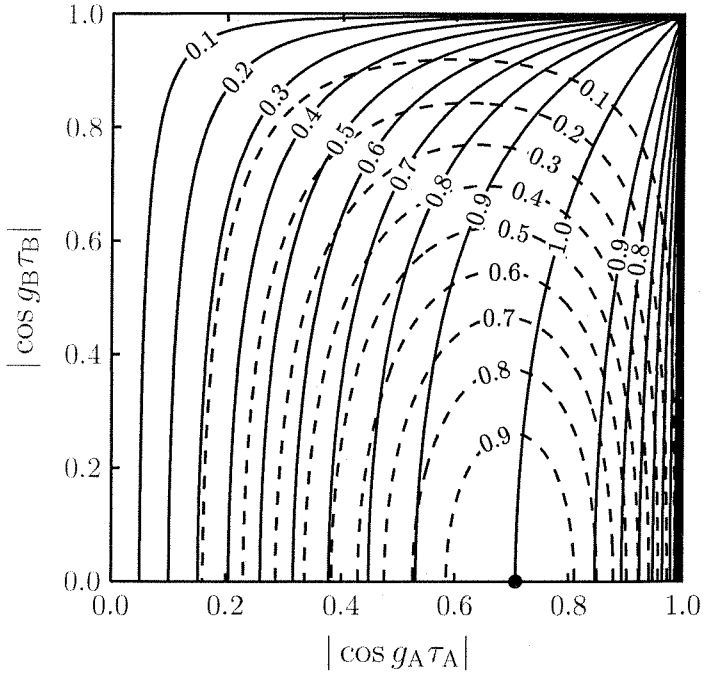

Fig. 3. Contour plots of the concurrence C (solid curves) and the yield P (divided by ${}_{AB}\langle\downarrow\downarrow|\varrho_{AB}|\downarrow\downarrow\rangle_{AB}$) (dashed curves) as functions of $g_A\tau_A$ and $g_B\tau_B$ for the preparation of the entangled state $|\Psi\rangle_{AB}$ through the processes depicted in Fig. 2. In this case, C and P are functions of $|\cos g_A\tau_A|$ and $|\cos g_B\tau_B|$. The optimal entanglement preparation with $C = 1$ and $P = {}_{AB}\langle\downarrow\downarrow|\varrho_{AB}|\downarrow\downarrow\rangle_{AB}$ is realized at the point $(|\cos g_A\tau_A|, |\cos g_B\tau_B|) = (1/\sqrt{2}, 0)$, indicated by the dot.

between the distant qubits with $C = 1$ and $P = {}_{AB}\langle\downarrow\downarrow|\varrho_{AB}|\downarrow\downarrow\rangle_{AB}$ is thus demonstrated to be possible through only three sequences of consecutive interactions of the mediator X with the qubits A and B. The parameter dependences of the concurrence C and the yield P are plotted in Fig. 3.

Similar analyses show that the combinations of the directions (i.e., the order of the interactions in each process) other than that depicted in Fig. 2 do not provide the optimal scheme, and the maximum concurrence and the maximum yield are not simultaneously realizable. Note again that the parameters $g_A\tau_A$ and $g_B\tau_B$ are fixed throughout all the processes. If it is allowed to vary these parameters step by step, more efficient schemes can be constructed. In particular, if the qubits A and B are initialized in the state $|\uparrow\uparrow\rangle_{AB}$ in advance, as described above, the first two steps in the present scheme are not necessary. The present scheme is, however, useful in such a situation that it is not easy to experimentally initialize the system, because it is still possible to prepare a maximally entangled state directly from a given mixed state, with a fixed setting. The scheme that is optimal in any given case depends on the actual experimental setups and experimental feasibility.

The present scheme makes use of the fact that the interactions given in (3) preserve the excitation number N given in (4). Such interactions are found in the literature in the context of quantum information and computation. For example,

generation of entanglement (from a specific pure state) was demonstrated in a cavity QED experiment,[4] in which a cavity mode plays a role similar to that of the mediator X, and the cavity-atom interaction preserves the excitation number of the atomic qubits and the cavity mode. For long-range entanglement, it is quite likely that a photon could act as the mediator X. In connection to this point, the interaction between a circularly-polarized photon and a Λ-type atom was recently proposed in this role.[17] Although this interaction, between a photon and an atom, is not precisely the interaction considered here, it also preserves the excitation number and is a potential system to be used in the experimental implementation of the present scheme. Applied to such systems, the present scheme would provide a method of entangling spatially separated qubits. With the goal of realizing such an experiment, we should clarify the effects of decoherence of the mediator X, which may travel a long distance between the qubits A and B, and other possible disturbances on the qubits during the process. Investigations of these points are now in progress.

Acknowledgements

The authors acknowledge helpful discussions with Professor I. Ohba. This work is partly supported by a Grant for the 21st Century COE Program at Waseda University and a Grant-in-Aid for Priority Areas Research (B) (No. 13135221), both from the Ministry of Education, Culture, Sports, Science and Technology, Japan, by a Grant-in-Aid for Scientific Research (C) (No. 14540280) from the Japan Society for the Promotion of Science, and by the bilateral Italian-Japanese project 15C1 on "Quantum Information and Computation" of the Italian Ministry for Foreign Affairs.

References

1) M. A. Nielsen and I. L. Chuang, *Quantum Computation and Quantum Information* (Cambridge University Press, Cambridge, 2000).
2) *The Physics of Quantum Information*, ed. D. Bouwmeester, A. Ekert and A. Zeilinger (Springer-Verlag, Heidelberg, 2000).
C. H. Bennett and D. P. DiVincenzo, Nature **404** (2000), 247.
A. Galindo and M. A. Martin-Delgado, Rev. Mod. Phys. **74** (2002), 347.
3) A. Peres, *Quantum Theory: Concepts and Methods* (Kluwer Academic Publishers, Dordrecht, 1995).
4) E. Hagley, X. Maître, G. Nogues, C. Wunderlich, M. Brune, J. M. Raimond and S. Haroche, Phys. Rev. Lett. **79** (1997), 1.
J. M. Raimond, M. Brune and S. Haroche, Rev. Mod. Phys. **73** (2001), 565.
5) J. A. Bergou and M. Hillery, Phys. Rev. A **55** (1997), 4585.
A. Messina, Eur. Phys. J. D **18** (2002), 379.
D. E. Browne and M. B. Plenio, Phys. Rev. A **67** (2003), 012325.
6) C. Cabrillo, J. I. Cirac, P. García-Fernández and P. Zoller, Phys. Rev. A **59** (1999), 1025.
L.-M. Duan, M. D. Lukin, J. I. Cirac and P. Zoller, Nature **414** (2001), 413.
D. E. Browne, M. B. Plenio and S. F. Huelga, Phys. Rev. Lett. **91** (2003), 067901.
7) X.-L. Feng, Z.-M. Zhang, X.-D. Li, S.-Q. Gong and Z.-Z. Xu, Phys. Rev. Lett. **90** (2003), 217902.
L.-M. Duan and H. J. Kimble, Phys. Rev. Lett. **90** (2003), 253601.
8) R. Ursin, T. Jennewein, M. Aspelmeyer, R. Kaltenbaek, M. Lindenthal, P. Walther and A. Zeilinger, Nature **430** (2004), 849.
9) C. H. Bennett, G. Brassard, S. Popescu, B. Schumacher, J. A. Smolin and W. K. Wootters, Phys. Rev. Lett. **76** (1996), 722 [Errata; **78** (1997), 2031].

C. H. Bennett, D. P. DiVincenzo, J. A. Smolin and W. K. Wootters, Phys. Rev. A **54** (1996), 3824.

10) T. Yamamoto, M. Koashi, Ş. K. Özdemir and N. Imoto, Nature **421** (2003), 343.
Z. Zhao, T. Yang, Y.-A. Chen, A.-N. Zhang and J.-W. Pan, Phys. Rev. Lett. **90** (2003), 207901.
A. Vaziri, J.-W. Pan, T. Jennewein, G. Weihs and A. Zeilinger, Phys. Rev. Lett. **91** (2003), 227902.
11) H. Nakazato, T. Takazawa and K. Yuasa, Phys. Rev. Lett. **90** (2003), 060401.
12) H. Nakazato, M. Unoki and K. Yuasa, Phys. Rev. A **70** (2004), 012303.
13) L.-A. Wu, D. A. Lidar, and S. Schneider, Phys. Rev. A **70** (2004), 032322.
14) See, for example, B. Misra and E. C. G. Sudarshan, J. Math. Phys. **18** (1977), 756.
H. Nakazato, M. Namiki and S. Pascazio, Int. J. Mod. Phys. B **10** (1996), 247.
D. Home and M. A. B. Whitaker, Ann. of Phys. **258** (1997), 237.
P. Facchi and S. Pascazio, in *Progress in Optics*, ed. E. Wolf (Elsevier, Amsterdam, 2001), Vol. 42, p. 147.
15) G. Compagno, A. Messina, H. Nakazato, A. Napoli, M. Unoki and K. Yuasa, Phys. Rev. A **70** (2004), 052316.
16) W. K. Wootters, Phys. Rev. Lett. **80** (1998), 2245.
17) W. Lange and H. J. Kimble, Phys. Rev. A **61** (2000), 063817.
J. Hong and H.-W. Lee, Phys. Rev. Lett. **89** (2002), 237901.
B. Sun, M. S. Chapman and L. You, Phys. Rev. A **69** (2004), 042316.

Available online at www.sciencedirect.com
SCIENCE DIRECT®
ELSEVIER
Physica E 29 (2005) 674–678
PHYSICA E
www.elsevier.com/locate/physe

Quantum entanglement formation by repeated spin blockade measurements in a spin field-effect transistor structure embedded with quantum dots

Kanji Yoh[a,b,*], Kazuya Yuasa[c], Hiromichi Nakazato[c]

[a]*Research Center for Integrated Quantum Electronics, Hokkaido University, Sapporo 060-8628, Japan*
[b]*CREST-JST, Kawaguchi-shi, Saitama 332-0012, Japan*
[c]*Department of Physics, Waseda University, Tokyo 169-8555, Japan*

Available online 2 August 2005

Abstract

We propose a method of operating a quantum state machine made of stacked quantum dots buried in adjacent to the channel of a spin field-effect transistor (FET) [S. Datta, B. Das, Appl. Phys. Lett. 56 (1990) 665; K. Yoh, et al., Proceedings of the 23rd International Conference on Physics of Semiconductors (ICPS) 2004; H. Ohno, K. Yoh et al., Jpn. J. Appl. Phys. 42 (2003) L87; K. Yoh, J. Konda, S. Shiina, N. Nishiguchi, Jpn. J. Appl. Phys. 36 (1997) 4134]. In this method, a spin blockade measurement extracts the quantum state of a nearest quantum dot through Coulomb blockade [K. Yoh, J. Konda, S. Shiina, N. Nishiguchi, Jpn. J. Appl. Phys. 36 (1997) 4134; K. Yoh, H. Kazama, Physica E 7 (2000) 440] of the adjacent channel conductance. Repeated quantum Zeno-like (QZ) measurements [H. Nakazato, et al., Phys. Rev. Lett. 90 (2003) 060401] of the spin blockade is shown to purify the quantum dot states within several repetitions. The growth constraints of the stacked InAs quantum dots are shown to provide an exchange interaction energy in the range of 0.01–1 meV [S. Itoh, et al., Jpn. J. Appl. Phys. 38 (1999) L917; A. Tackeuchi, et al., Jpn. J. Appl. Phys. 42 (2003) 4278]. We have verified that one can reach the fidelity of 90% by repeating the measurement twice, and that of 99.9% by repeating only eleven QZ measurements. Entangled states with two and three vertically stacked dots are achieved with the sampling frequency of the order of 100 MHz.

PACS: 03.67.Mn; 72.25.−b; 85.75.Hh; 73.23.Hk; 85.35.Gv

Keywords: Quantum dot; Spin transistor; Spin blockade; Quantum Zeno-like measurement; Qubit

*Corresponding author. Research Center for Integrated Quantum Electronics, Hokkaido University, Sapporo 060-8628, Japan.
E-mail address: KANJIYOH@aol.com (K. Yoh).

1386-9477/$ - see front matter
doi:10.1016/j.physe.2005.06.052

1. Introduction

A variety of methods [1–7] have been proposed [8–10] and a keen effort is paid to realize quantum bits in solid state device structures, particularly after the experimental demonstration of the factorization of 15 by an NMR quantum computer [11]. Essentially, we propose a quantum gate consisting of a spin field-effect transistor (FET) and vertically stacked quantum dots with self-assembled growth technique, whose small size, beyond lithography limits, enables one to perform quantum operations at reasonably high temperatures. In addition to the elevated operation temperature, the simplicity and the beauty of three terminal read/write operations is shown to enable one to form entangled states through repeated quantum measurements [5]. Here, we show how a quantum state is purified and an entangled state is achieved with reasonably high frequency compared to the spin relaxation time in quantum dots.

2. Device concept

As shown in Fig. 1, the proposed device is composed of a spin FET embedded with self-assembled InAs dots in the barrier layer adjacent to the spin channel. When the channel electrons are spin independent, the current (or channel conductance) exhibits maximum peaks each time an electron is added to the dot upon gate voltage scan. Suppose that we have one electron in the dot with a definite spin state, say, spin up. When channel electrons are spin polarized, the current (or channel conductance) exhibits either peaks or a monotonous increase, depending on the relative spin state between the existing electron in the dot and the impinging electron. When the spin state of both such electrons are the same, say, spin up, the second impinging electron ends up rejected from the dot because of the Pauli's exclusion principle (spin blockade) as schematically illustrated in Fig. 1. The heterostructure of the device for the case of a single quantum bit (qubit) is shown in Figs. 1 and 2. The experimental results for the Coulomb blockade were reported in Ref. [12].

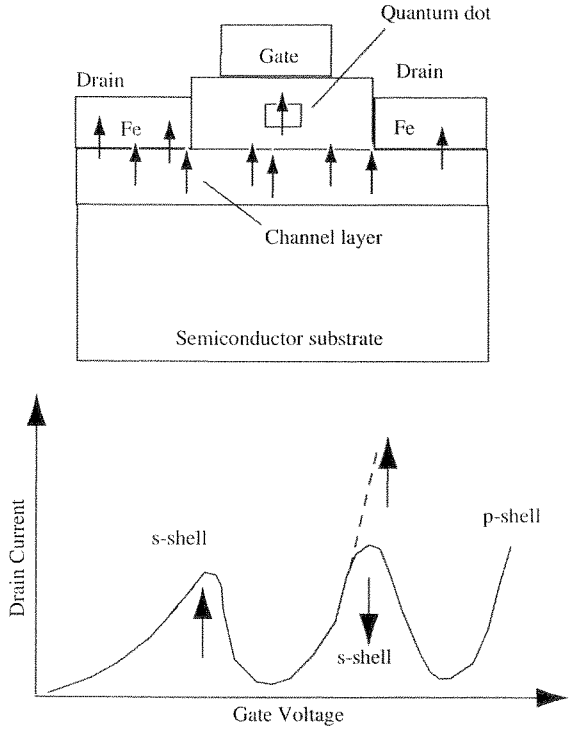

Fig. 1. Schematic spin-blockade transistor and its characteristic drain current. The first current peak indicates an electron (say, spin up) is injected into a dot. The second peak (solid line) denotes that the second electron was spin down. The dotted line would indicate that the current keeps on increasing because the second electron was blocked (spin blockade).

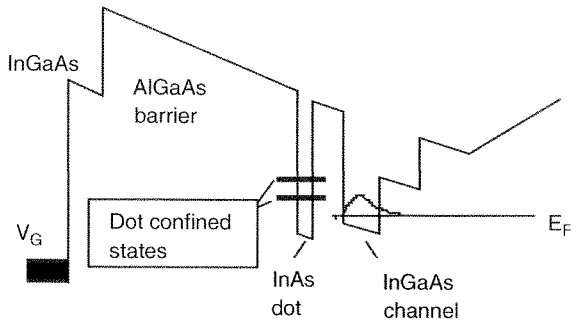

Fig. 2. Conduction band diagram of the heterostructure in the vicinity of the InAs dot and the transistor channel [4].

The current peak in Fig. 1 is caused by Coulomb blockade, as seen in experimental results of an FET/dot system [12], which is similar to the present proposal except that the ferromagnetic

electrodes are replaced by normal metals (Ti/Au). Because of this difference in the integrated spin FET and quantum dot system one can selectively fill the channel with spin polarized electrons. As a result, depending on the relative spin state between the electrons in the dot and in the channel, spin blockade is observed. In this way, one can achieve the charge to spin conversion. In the simplest situation, when the spin states in the dots are maximally randomized, the spin blockade measurements are done using the same spin state from the spin-polarized electron channel. If we repeat this measurement by applying a pulse sequence in the gate voltage, one can show that the initialization of the qubits is achieved through the exchange interaction of stacked quantum dots. This situation, a general extension of the quantum Zeno-like measurement [5,13,14] to a vertically stacked quantum dot system described above, is discussed more extensively in the next section. Furthermore, at the end of the next section, we will show that not only purification of the spin state but also the entangled state is possible to achieve by the repeated measurements. This procedure requires special treatment of the spin flip operation on an electron of the end of the stacked dots prior to the repeated measurements.

3. Quantum state initialization and entanglement

Exchange interaction between the electrons in adjacent dots determines the time evolution of each spin state. When spin blockade measurements are performed on vertically stacked dots by the methods described in the previous section, one can show that the randomly disordered dot system can be purified within a finite number of repeated measurements. The exchange interaction between dots is assumed to be limited to the nearest neighbors. First, we consider a two-dot system with an electron in a dot X, which is the nearest to the spin channel, and an electron in a dot A, which is stacked above dot X. Repeated measurements of X (spin states of an electron in a dot X) are shown to purify both X and A (spin states of an electron in a dot A) through exchange interaction. The interaction Hamiltonian is expressed as $H_{\text{int}} = g\sigma_X\sigma_A$, where g is the exchange interaction coefficient, and σ_X and σ_A are the electron spin Pauli operator for dots X and A, respectively. Fig. 3 describes how the Fidelity approaches unity as the state becomes purer by increasing the number of repetitions of the measurement. Here, the Fidelity is defined as

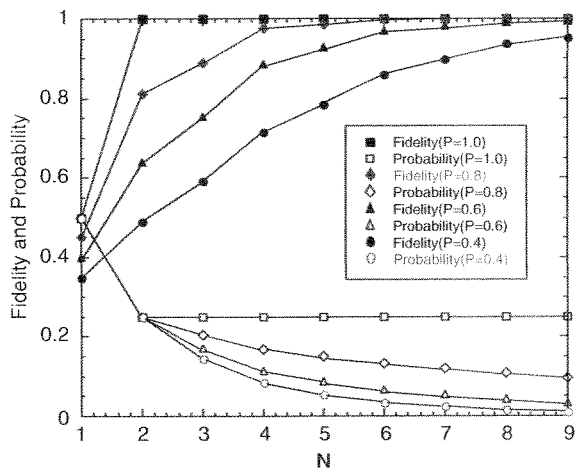

Fig. 3. Fidelity and the probability of the two-dot system to be in a pure state after N repeated measurements. The spin polarization of the channel is taken as a parameter P. Repeated measurements are seen to increase the fidelity, whereas the probability decreases unless the spin polarization is 100%.

$$F^{(\tau)}(N) \equiv {}_A\langle u_0|\rho_A^{(\tau)}(N)|u_0\rangle_A = {}_A\langle\uparrow|\rho_A^{(\tau)}(N)|\uparrow\rangle_A,$$

where $|u_0\rangle_A = |\uparrow\rangle_A$ is the target state and $\rho_A^{(\tau)}(N)$ is the reduced state of dot A after the successful confirmation of X to be in the state $|\uparrow\rangle_X$ for N repetition with the intervals of τ. In the same figure, we also plot the probability of finding the system to be purified after N repetitions with the intervals τ. More complex, but similar results can be obtained for three stacked qubits. In Fig. 3, the spin polarization probability of the channel (spin source) is changed as a parameter. One can see that even with a spin injection efficiency of 40%, which is our measured result in an Fe/InAs system [3,4], one can also initialize the qubit system with a certain probability. These results indicate that the initialization of the system might be greatly improved by improving the spin injection efficiency in the future. Now, let us examine the

minimum repetition number N to achieve high fidelity, as a function of the repetition period. The maximum repetition frequency is limited by the gate leakage current through the cut-off frequency f_T of the spin transistor structure. On the other hand, the total operation time is bound by the spin decoherence time in quantum dots [15]. Fig. 4 illustrates the minimum repetition number to achieve high fidelity (0.9 in this case) as a function of repetition period in the case of 2 qubits. In this case, the minima appears when the measurement period is a multiple of $\pi/2g$, where g denotes the exchange interaction factor. Let us define the characteristic time constant by $\tau_m = \pi/2g$. The minima of the purification period is expressed as $(1/4 + n/2)\pi/g$, with integer n. The exchange interaction of stacked self-assembled quantum dots, such as InAs dots in GaAs matrix, are estimated to range between 0.01 and 1 meV depending on the vertical separation of the dots. If we take 0.01 meV as g, then the characteristic time constant, τ_m, becomes 180 ps. So, if the period of gate voltage pulse is chosen to be 56 times τ_m, then we can achieve the initialization of 2 qubit system for 2 times and 11 times measurement with fidelity of 90% and 99.9%, respectively. The accuracy of the pulse frequency should be 100 MHz (1 ± 0.00044). The initialization time in this case becomes 90 and 495 ns for fidelity of 90% and 99.9%, respectively. It should be added that

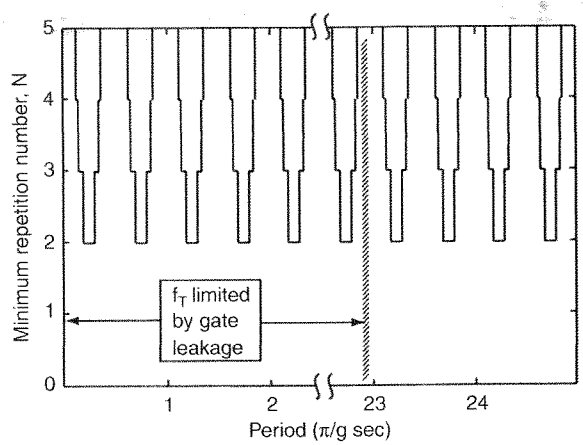

Fig. 4. Minimum repetition number to achieve high fidelity (0.9 in this case) as a function of the repetition period in the case of 2 qubits.

for the initialization scheme, we do not have to worry about the decoherence of spins in the dots, because the initialization process is a quantum Zeno-like measurement (QZM).

If we prepare an initial state like $|\downarrow\uparrow\rangle$, by flipping the first qubit spin by a π-pulse operation after a $|\uparrow\uparrow\rangle$ initialization, we can show that entangled states can be prepared. The time evolution of a 2 qubit system is shown in Fig. 5, where the entangled state $|\uparrow\downarrow\rangle + |\downarrow\uparrow\rangle$ periodically appears. One can indirectly verify the entangled states by repeating the measurements of the nearest dot (to the channel) with the period of $\pi/2g$ in order to verify $X = \downarrow$, while $X = \uparrow$ can be verified by adding the phase shift of $\pi/4g$ to the periodic $\pi/2g$ timing. Time evolution of the entangled states in Fig. 5 may be directly compared with experiments by statistically averaging the obtained spin states of X.

Again, due to the gate leakage problem associated with a high-frequency gate modulation, this verification scheme might be operated in every 56 multiple of τ_m. Because of the limited space, further discussion on the effect of the mismatch in the exchange interactions on the error rate in achieving the entanglement will be published elsewhere. The discussions on the sampling period

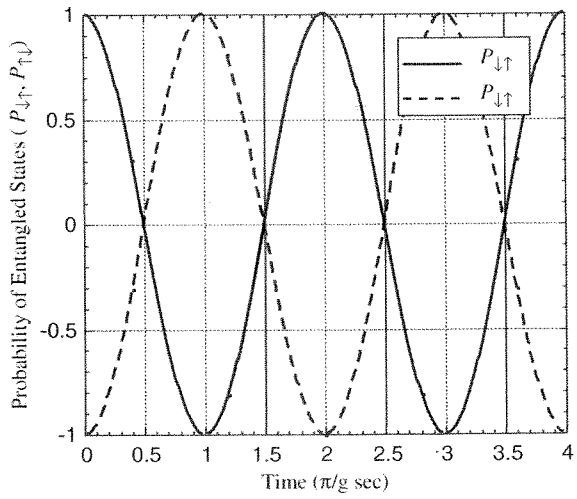

Fig. 5. Time evolution of the 2 qubit entangled states plotted as a function of normalized time. Complete entanglement can be verified by confirming the X state to be spin down at $t = (1/4 + n/2)\pi/g$, where n denotes an integer.

constraints initialization of the previous paragraph procedure also apply to the entanglement formation by QZM, because the quantum state evolution occurs by exchange interaction in both cases. QZM was shown to initialize and entangle the dot system with the sampling frequency of the order of 100 MHz. These estimations show the feasibility of initialization and entanglement of the qubit system composed of a spin transistor embedded with quantum dots. Higher frequency bounds are determined by the operation time necessary to complete quantum operations within a spin decoherence time. Finally, it should be noted that the maximum measurement frequency scales with the lateral device dimension.

4. Conclusions

We have proposed a method of operating a quantum state machine made of stacked quantum dots buried in adjacent to the channel of a spin field-effect transistor.

Extraction of a quantum state from a nearest quantum dot was shown to be achieved through Coulomb blockade of the adjacent channel conductance. Repeated quantum Zeno-like measurements (QZM) of the spin blockade is shown to purify the quantum dot states within several repetitions. The growth constraints of the stacked InAs quantum dots are shown to provide an exchange interaction energy in the range of 0.01–1 meV. We have verified that the fidelity of 90% is reached by repeating the measurements twice, and 99.9% is reached by repeating only 11 times of a QZM. Entangled states in the vertically stacked dots were shown to be achieved with the sampling frequency of the order of 100 MHz with the current nanotechnology.

References

[1] S. Datta, B. Das, Appl. Phys. Lett. 56 (1990) 665.
[2] K. Yoh, et al., Proceedings of the 23rd International Conference on Physics of Semiconductors (ICPS) 2004; H. Ohno, K. Yoh, et al., Jpn. J. Appl. Phys. 42 (2003) L87.
[3] K. Yoh, J. Konda, S. Shiina, N. Nishiguchi, Jpn. J. Appl. Phys. 36 (1997) 4134.
[4] K. Yoh, H. Kazama, Physica E 7 (2000) 440.
[5] H. Nakazato, et al., Phys. Rev. Lett. 90 (2003) 060401.
[6] S. Itoh, et al., Jpn. J. Appl. Phys. 38 (1999) L917.
[7] A. Tackeuchi, et al., Jpn. J. Appl. Phys. 42 (2003) 4278.
[8] Y. Nakamura, et al., Nature 398 (1999) 786.
[9] D. Loss, D.P. DiVicenzo, Phys. Rev. A 57 (1998) 120.
[10] B. Kane, Nature 393 (1998) 133.
[11] L.M.K. Vandersypen, Nature 414 (2001) 883.
[12] K. Yoh, H. Kazama, Physica E 6 (2000) 490.
[13] K. Yuasa, H. Nakazato, T. Takazawa, J. Phys. Soc. Japan 72 (Suppl. C) (2003) 34.
[14] H. Nakazato, M. Unoki, K. Yuasa, Phys. Rev. A 70 (2004) 012303.
[15] R. Hanson, et al., Phys. Rev. Lett. 91 (2003) 196802.